Role of Non-histone Chromatin Protein PC4 in Regulation of Autophagy and Tumorigenesis

A thesis submitted for the degree of

Doctor of Philosophy

By
Sweta Sikder

To
Molecular Biology and Genetics Unit,
Jawaharlal Nehru Centre for Advanced Scientific Research
(A Deemed University)
Jakkur P.O., Bangalore-560064, INDIA.

April, 2018

Declaration

I hereby declare that this thesis entitled “Non histone chromatin Chromatin Protein PC4 in Regulation of Autophagy and Tumorigenesis” is an authentic record of research work carried out by me under the supervision of Prof. Tapas K. Kundu at Molecular Biology and Genetics Unit, Jawaharlal Nehru Centre for Advanced Scientific Research, Bangalore, India and this work has not been submitted elsewhere for the award of any degree.

In keeping the general practice of reporting scientific observations, due acknowledgements have been made wherever the work is based on the finding of other investigators. Any omission which might have occurred by over sight or misjudgment is deeply regretted.

Sweta Sikder

Bangalore

Date

Acknowledgement

The work presented in this thesis would not have been possible without my close association with many people. I take this opportunity to extend my sincere gratitude and appreciation to all those who made this Ph.D thesis possible.

First and foremost, I would like to extend my sincere gratitude to my PhD supervisor, Prof Tapas K. Kundu for introducing me to this exciting field of science and for his dedicated help, advice, inspiration, encouragement and continuous support, throughout my Ph.D. His undying zeal to achieve better has been a source of inspiration and a guiding light throughout my PhD tenure. His constant enthusiasm and positivity to explore new arenas of research have been really intellectually enriching.

My special words of thanks should also go to Dr Ravi Manjithaya for his constant support, teaching and overwhelming enthusiasm. The work in Autophagy would not have been possible without his scientific inputs and fruitful discussions.

I express my heart-felt gratitude to Prof MRS Rao for his constant scientific interactions and educative discussions which has helped me to understand the world of "Chromatin Biology" in a larger perspective.

I am deeply grateful to my collaborators Dr Birendranath Banerjee from InDNA Life Sciences, Bhubaneswar; Dr Amit Dutt, ACTREC, Dr KS Gopinath, HCG,BIO and Prof Gautam Sethi, NUS.

I am grateful to all the faculties of MBGU and NSU, Prof Ranga Uday Kumar, Prof Anuranjan Anand, Prof Hemlatha Balaram,Prof Maneesha Inamdar, Prof Kaustav Sanyal, Prof Namita Surolia, Dr James Chelliah,, Dr Sheeba Basu for their very fruitful course work and the enriching scientific discussions I had throughout the span of my PhD thesis work.

I take this opportunity to thank all my teachers who have enlightened me and encouraged me to be in the scientific world. My gratitude extends to Dr Aditi Nag Chaudhari, Prof Dhrubajyoti Das, and Miss Shanti Gomes for their love, affection and encouragement.

Transcription and disease lab have been encouraging in terms of working and scientific culture; I am deeply indebted to all the past and present members for their help, encouragement and all the valuable scientific inputs. I thank Dr Sujata Kumari, whose scientific work I have carried out further; Dr Chandrima Das and Dr Kiran Batta for their valuable advice, Dr Parijat Senapati, and Dr Snehajyoti Chatterjee for helping me on my initial days in JNCASR. Dr Manoj Kumar for the help he has extended in terms of doing work. I am thankful to Surabhi Sudevan, Deepthi Sudarshan for the fun times we had in lab and in Bangalore. I thank all the Int –PhD students with whom I have worked Ms. Saheli Roy, Ms Swati Keshri, although for a short span of time but all of the experiences were very enriching,

I thank all my colleagues presently working in T and D for keeping up the scientific environment of the lab and helping me in the best possible way. I thank Dr. Amit K Behera, Dr. Stephanie Kaypee, Suchismita Dey, Arnab Bose, Siddharth Singh, Moumita Basu, Dr. Shrinka Sen, Dr Sourav Chatterjee, Pallabi Mustafi, Dr Sarmistha Sinha, Aditya Bhattacharya, Akash Singh, Smitha Mahadevan, Ila Joshi, and Vinay Rao.

This work would not have been possible without the helping hands of Mune Gowda, Sunil, Kruthi, Sallauddin. I thank them immensely for their timely help and support.

I am immensely grateful to all my friends and batchamtes in JNCASR who not only helped me in my scientific endeavours but also made me cherish some fond memories. I thank Sutanuka, Disha, Ronak, Piyush, Veena, Arun , Divyesh and Deboshree.

This acknowledement would not have been complete without thanking my friends, Parna, Santanu, Koyel, Dr Gopal for their constant support, encouragement and being such wonderful friends

I extend my heartfelt gratitude to my family my Mom and Dad and my very supporting brother for bestowing their love and faith on me. I am also indebted to my cute little nephew as his chraming words made my worst days to be full of sunshine.

Dedicated to the person who inspires me always

ShibDas Sikder

Table of Contents

Chapter 1: Introduction

This chapter introduces the basic concepts of ordered chromatin organization, chromatin dynamics, epigenetics and histone post-translational modifications. The chapter includes a brief review on chromatin organization and the role of non-histone proteins that regulate the dynamicity of the genome. This chapter further focuses on the signal dependent epigenetic language of chromatin and how it modulates several cellular functions and processes like autophagy and DNA damage repair. The chapter will present a comprehensible account of the discovery, functions and the regulation of the non-histone chromatin associated protein PC4

1.1. Chromatin dynamics

The ordered three dimensional organization of the eukaryotic genome in the confined space of the nucleus is important for the various functions of the cell and life processes. The huge genome of billion bases of DNA is orderly organized and enclosed in the eukaryotic cell nucleus with typical diameters in the range of 10 to 20 μm. This compaction of DNA is driven by small highly positively charged proteins called the **histones**, into a large nucleoprotein complex called **nucleosomes**. A nucleosome is formed by the wrapping of 145bp of DNA around a histone octamer. Several nucleosomes in turn associates with one another to form a higher order structure designated as the **chromatin** which further is organized into distinct entities known as chromosomes. The chromosomes are not randomly distributed in the nucleus, that occupy distinct spaced known as **"chromosome territories"** (Babu and Fullwood, 2015). This hierarchical organization of the chromatin poses a challenge regarding the accessibility of cis-regulatory elements such as promoters, enhancers and insulators to regulate transcription. The chromatin is organized in such a way that distant genomic elements can interact with a gene of interest which can influence its transcription. The chromatin forms "loops" which helps in bringing distant loci into a spatial proximity. These looped structures are formed with the help of other non-histone proteins and RNA which is closely associated with the core nucleosome structure of the chromatin (Bonev and Cavalli, 2016) (Figure 1.1).

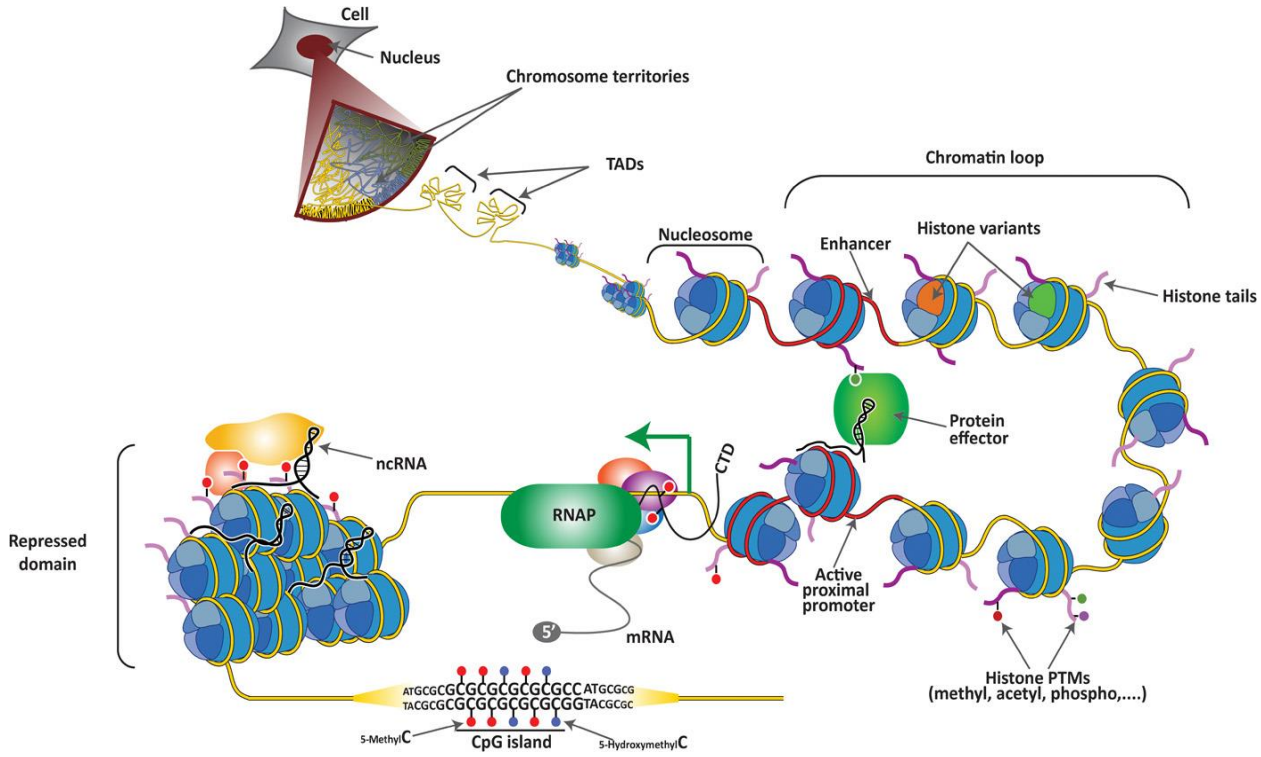

Figure. 1.1. Hierarchical organization of chromatin in mammalian cells. Individual chromosomes occupy a distinct region inside the nucleus denoted as chromosome territory. Chromosomes are packaged into structural units defined by the high frequency of chromatin interactions between their loci that are partitioned by sharp boundaries. These structural units are called topologically associating domains (TADs). Inside these domains, the enhancer elements and active proximal promoters (both depicted in red) form functional chromatin loops These loops are stabilized by protein effectors, noncoding RNAs (ncRNAs), and histone posttranslational modifications (PTMs). Presence of specific histone variants and PTMs on the histone tails distinguishes the enhancers and promoters from the rest of the genome sequence. During active transcription process, elongating RNA polymerase II (RNAP, marked in green) is phosphorylated at Ser5 and Ser2 on its C-terminal domain (CTD) and synthesizes mRNA. Transcriptionally silenced genomic regions form repressed chromatin domains stabilized by ncRNA and other non-histone protein complexes. The genome contains tracks of repetitive sequence at specific functional regions of the genome, including CpG islands (CGIs), in which cytosines can be modified (5-methylC and 5-hydroxymethylC). Adapted from (Aranda et al., 2015).

With the advent of chromosome capture methods such as 4C and HiC the importance of the chromatin loops gained importance suggesting it to be an important architectural design of the chromatin not any random event (Bonev and Cavalli, 2016). In the context of transcription, to attribute any activation or repressive effect on gene expression the regulatory DNA elements must be positioned in close spatial proximity to the susceptible genes. Enhancers positively promote transcription by providing binding sites to transcription factors that are able to communicate with the target genes often placed at a distance through the help of these chromatin loops. Most of the loops are placed in distinct domain like structures called as the tissue-invariant **topologically associating domains (TADs)** (Ea et al., 2015). TADs are not only domains where DNA contacts take place at a high frequency, but they also harbor distinct histone chromatin signatures and also lamina association. **Lamina associated domains (LADs)** are thus similar to TADs in having a high frequency of DNA-DNA interactions along with proteins and components of the lamina (Gonzalez-Sandoval and Gasser, 2016; Wright et al., 2016). The chromatin landscape of the TADs is highly variant. The transcriptionally active domains are associated with trimethylation of the lysines 4 and 36 of histone H3 (H3K4me3 and H3K36me3); while the repressed chromatin is divided into two kinds of domains, one linked to Polycomb group (PcG) proteins linked to trimethylation of the lysine 27 of histone H3 (H3K27me3) and the other associated to the HP1 and Su(var)3-9 heterochromatin proteins as well as to dimethylation of the lysine 9 of histone H3 (H3K9me2). The active domains consist of the euchromatin while the constitutive heterochromatin to HP1 domains and the facultative heterochromatin to PcG domains (Ea et al., 2015).

As mentioned in the figure above, the dynamicity and the organization of the chromatin are regulated by various factors. The canonical histones wrapped around by the DNA forms the basic unit structure. In addition to histone post translational modifications, histones exert their functions through their variants. Histone genes are present in multiple copies and their expression is strictly regulated at various levels. The canonical histones are synthesized only in S-phase in animals. Eukaryotic core histones have further evolved into additional paralogues, or variants, that function in multiple cellular processes, like transcription,

chromosome segregation and DNA repair (Talbert and Henikoff, 2010). While the synthesis and deposition of canonical histones in animals are coupled to DNA synthesis, incorporation of **histone variants** happens throughout the cell cycle and is independent of DNA synthesis. The replacement of canonical histones with the histone variants alters the composition and distribution of nucleosomes and also affects its interactions with the other DNA- binding proteins, like the chromatin remodelers and modifiers. For example the replacement of the canonical histone H3.1 by the highly similar variant H3.3 leads to repairing gaps in the chromatin landscape which result from that result from nucleosome disruption. H2A variants affect gene expression for instance H2A.Z and H2A.B are associated with transcription initiation while macroH2A in animals and H2A.W in plants are known to immobilize nucleosomes resulting in transcriptional silencing (Talbert and Henikoff, 2017). Thus the dynamicity and the organization of the eukaryotic genome is highly regulated and subjected to various modifications based on the external environment with the concerted activities of various factors.

1.2. Chromatin dynamics regulated by non-histone proteins

The binding of non-histone proteins is essential for the higher level organization of the chromatin as well as to maintain its dynamicity to mediate its several DNA templated functions. A number of studies in the recent past have revealed a family of chromosome associated non histone proteins which majorly functioned in the organization of the higher order structure of the eukaryotic genome (Holland, 2002). Structural maintenance class of proteins (SMC) are essential for chromosome condensation, sister chromatid cohesion and segregation. Besides their structural role the **SMC** proteins also possess conserved ATP motifs and harbor enzymatic properties. Non-histone proteins have greater roles other than just acting as structural scaffolds for the chromatin; they regulate several cellular events involving the hereditary material, including DNA replication, transcription, recombination and repair processes. Briefly, the enzyme DNA topoisomerases helps in resolving the tangles generated by the SMCs during chromosome condensation or during DNA replication, thus making it vital for the process of DNA replication. **Heterochromatin protein 1 α/β** (HP1) mediate heterochromatinization of genome frequently resulting in silencing of genes. Other

non-histone proteins, for example, the abundant high-mobility group (HMG) of proteins, regulate chromatin architecture by either DNA bending or by unfolding of the chromatin thereby helping in the process of transcription (Agresti and Bianchi, 2003; Gerlitz, 2010). Other chromosomal architectural proteins which play important roles in formation of transcriptionally inactive heterochromatin and thereby gene silencing are **PcG proteins including Polycomb Repressive Complex 1 (PRC1) and PRC2** (Aranda et al., 2015), **myeloid and erythroid nuclear termination stage-specific protein (MENT), MeCP2, and SIR** complex (Li and Reinberg, 2011). Adding to these group of proteins is the multifunctional **human transcriptional positive coactivator protein PC4** which forms an integral part of the chromatin inducing its compaction by directly interacting with the core histones (Das et al., 2006). Transient silencing of PC4 leads to an open chromatin conformation, altered epigenetic state and the expression of neuronal genes in non-neuronal cells (Das et al., 2010). Collectively, these studies reveal the critical role of the non-histone proteins in mediating chromatin compaction for the higher order chromatin structure formation as well as regulating its dynamicity to mediate gene expression. These chromatin interactions regulate several physiological processes inside the cell including differentiation, apoptosis, cell cycle, as well as DNA damage repair. Study of these non-histone chromatin associated proteins in terms of their regulation, function and maintenance of chromatin dynamics is of great importance in relevance to translational and clinical impact as their dysregulation could potentiate to alteration in chromatin interactions and thereby gene expression which could lead to altered cellular health and therefore pathophysiological conditions such as cancer (Babu and Fullwood, 2015).

1.3. Histone acetylation and transcription regulation

Transcription in eukaryotes is a highly orchestrated event with ordered recruitment of a set of factors which helps in reading the coding sequence of the genome. Transcription regulation is a complex set of events regulated by different factors. Along with the three different RNA polymerases (Polymerases I, II and III), general transcription initiation factors, gene specific transcription regulatory factors (activators or repressors), and coregulatory factors (coactivators and repressors) play important roles in the regulation of gene expression. These factors act through chromatin modifications facilitating the formation of preinitiation complex (Bártová et al., 2008). As discussed in Figure 1, besides the non-histone proteins, different histone modifications like lysine acetylation and methylation, serine phosphorylation and arginine methylation, play regulatory role in fine tuning gene expression by directly affecting transcriptional initiation, elongation or gene silencing. These milieu of diverse histone modifications can act in concert or individually bringing out the epigenetic language of the genome which acts as marks for mediating vital signal transduction pathways (Bannister and Kouzarides, 2011; Fischle et al., 2003). Among the histone modifications, **histone acetylation** has been closely associated with **transcriptional activation**. The histones majorly the amino termini lysines of H3 and H4 (e.g. H3K9, H3K14, H3K36, H4K8, H4K16,etc.) undergo dynamic acetylation–deacetylation modifications based on the different physiological conditions. The balance between these modifications is mediated through the large protein complexes having enzymatic activity such as **histone acetyltransferases (HATs)** and **histone deacetyltransferases (HDACs) (Figure 1.2.).** Histone acetyltransferases catalytically transfer an acetyl group from acetyl-CoA molecules to the lysine ε-amino groups on the N-terminal tails of histones. The acetylated histone tails are recognized by the bromodomains of various activating factors (transcription factors, chromatin remodelers) which help to modulate the chromatin template at the site of acetylation. Chromatin immunoprecipitation (X-Chip) studies using histone isotype-specific antisera has provided us with the knowledge of histone acetylation as a specific epigenetic mark for transcriptional activation (Struhl, 1998)(Eberharter and Becker, 2002). For example, acetylation on lysine 9 of histone H3 (H3K9Ac) in gene promoter or enhancer regions mediated by HAT enzymes (e.g., nuclear type A proteins, GCN5, p300/CBP and TAFII250)

is demarcated as a transcriptionally active chromatin (euchromatin). Removal of this acetyl group (deacetylation) by HDAC enzymes (e.g., nuclear class 1 proteins, HDAC 1, 2, 3 and 8) transforms the transcriptionally active form to transcriptionally inactive heterochromatin. In addition to histone acetylation, histone methylation also plays distinct role in determining gene expression. In a study in human CD4+ T cells, 20 histone methylations of lysine and arginine residues were mapped by using chromatin immunoprecipitation followed by sequencing (ChIP-seq) (Barski et al., 2007). It was observed that monomethylated H3K27, H3K9, H4K20, H3K79 and H2BK5 were linked to gene activation, while trimethylated H3K27, H3K9 and H3K79 were associated with gene repression. Thus the chromatin landscape is modulated by different histone modifications mediated by the interplay of epigenetic enzymes like histone demethylases, histone acetyltransferases, etc. to regulate gene expression. The HATs are mostly present in complexes which are recruited to the promoters of active genes which are mostly devoid of nucleosomes. Apart from promoters, operators and enhancers also determine the level of gene expression. As described earlier, the chromatin has to loop or bend to allow the enhancer bound activators to interact with the basal transcription machinery at the promoter to stimulate transcription. Transcription initiation is followed by elongation and termination which are also multifactorial dependent events and is highly regulated. Apart from basal transcription process there is activator dependent transcription which requires additional factors like coactivators or mediators other than the initiation factors. The Upstream Stimulatory Activity (USA) fraction isolated from human cells contain both positive cofactors (PC1, PC2, PC3/Dr2, PC4 and ACF) (Ge and Roeder, 1994; Kretzschmar et al., 1994); as well as negative cofactors that include Ada/Mot1NC1 and NC2 (Meisterernst et al., 1991).

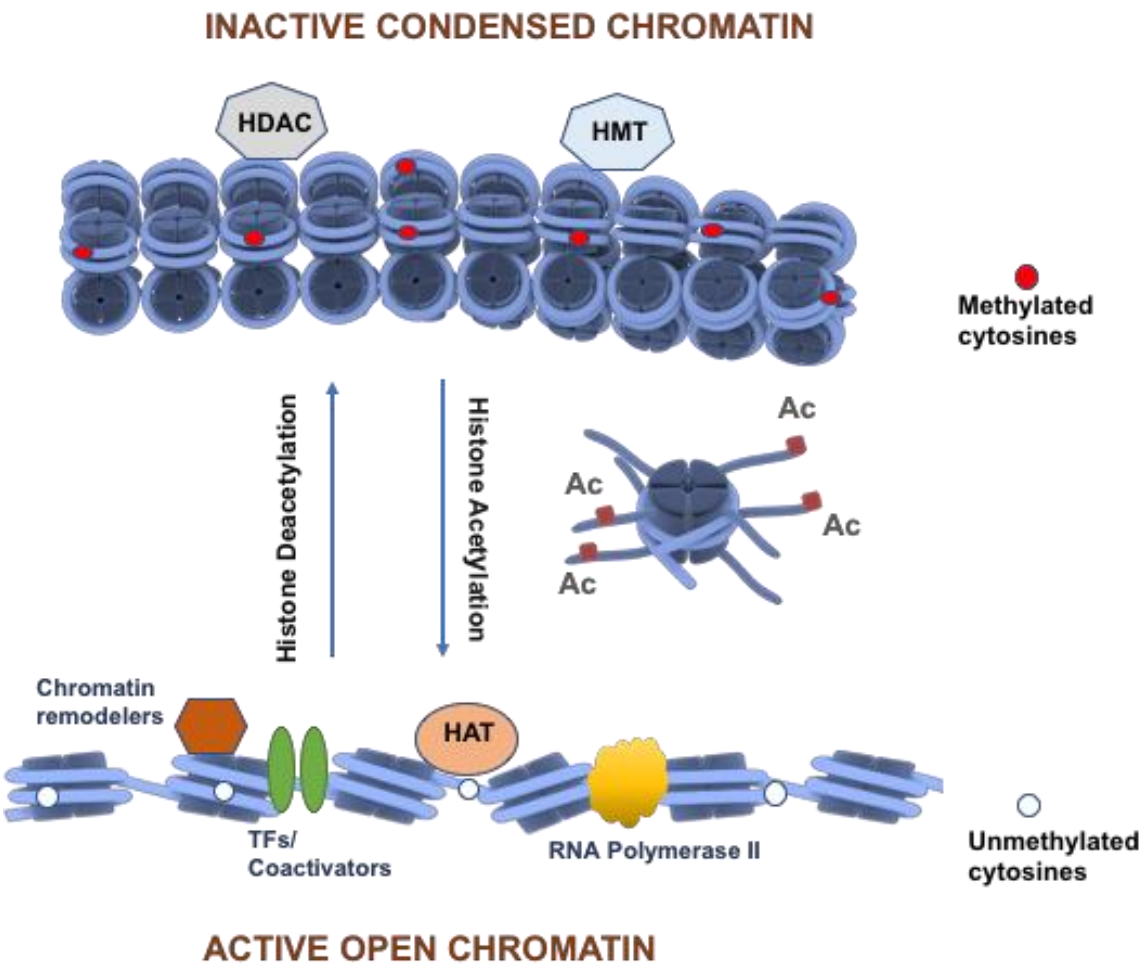

Figure 1.2. Histone acetylation as a switch from inactive to active chromatin state. Chromatin exists primarily into two structural states. An active, or open, euchromatin state in which the histone tails are acetylated by the Histone acetyltransferases (HATs). This acetylation loosens the chromatin structure, additionally chromatin remodelers modify the chromatin landscape by positioning the nucleosomes making it accessible for binding of the basal transcriptional complex and other activators of transcription. The other is the inactive, or condensed, heterochromatin state, where gene expression is inhibited. Methylation by Histone methyltransferase (HMT) and deacetylation by Histone deacetylase (HDAC) proteins condenses DNA around histones and thus, make DNA inaccessible for binding by RNA Pol II and other activators, leading to gene silencing.

1.4. Histone acetylation in regulation of cell physiology

Histone acetylation plays critical roles in cell physiological processes by modulating chromatin structure and gene expression. Differential pattern of histone acetylation has been observed during embryogenesis and development of various organisms. Histone acetylation generally functions in association with other epigenetic marks like histone methylation, phosphorylation to facilitate various cellular phenomena. During differentiation of embryonic stem cells there is a rapid decrease of H3K4 methylation, whereas the same pattern is observed for H3 acetylation during embryogenesis. During the process of differentiation the chromatin undergoes major changes in terms of its compaction; the heterochromatin mark H3K9 methylation is increased. Thus, the global transcription output in ES cells becomes more constrained upon differentiation, with concurrent decrease in histone H3 acetylation and H3K4 methylation. Furthermore the property of pluripotency can be reestablished in somatic cells by increasing the levels of histone H3 acetylation and H3K4 methylation (Bhaumik et al., 2007). Several reports have additionally investigated the interplay between cell lineage differentiation and global-histone acetylation. It has been observed that in differentiating chick myoblasts obtained upon treatment of immature chickens with estradiol leads to increased liver histone acetylation. Not only histone acetylation the role histone modifying enzymes particularly HATs and HDACs have been implicated in the process of development and growth. After implantation of the embryo in uterine wall, it grows rapidly until gastrulation period. During this developmental phase the gene expression is highly regulated in a spatial temporal manner by the concerted activities of chromatin modifying enzymes such as HATs and HDACs. Any mutations affecting the expression or function of these histone modifying activities lead to difficulty at or before embryo implantation, indicating a role for histone-modifying enzymes in regulation of specific gene expression during embryogenesis and development (Khan and Khan, 2010).

Histone acetylation also plays a significant role in the inactivation of the second X chromosome in the cells of female progeny. Patients carrying aberrant numbers of X chromosome exhibit incomplete deacetylation of all X chromosomes. The syndrome of fragile X chromosome thus provides another link between histone acetylation and human hereditary disorders(Brinkman et al., 2006). The process of DNA repair and genome

stability which requires faithful DNA replication, cell division, etc. also follows a distinct pattern of histone acetylation. Acetylation at Lysine56 of histone H3 is required for genome stability. Furthermore, acetylation of phospho-H2Ax is critical for DNA damage repair following exposure to ionizing radiation. These observations implicate the importance of histone acetylation at several steps of DNA repair (Masumoto et al., 2005). It is to be noted here that acetylation is not restricted to histones alone, but other non-histone substrates like transcription factors, chromosomal proteins, such as p53, E2F-1, MyoD, GATA-1, HMGI(Y), etc. Acetylation of these factors also plays essential roles in regulating gene expression and thereby cellular states. Inappropriate acetylation states of transcription factors or histones may therefore contribute to pathological conditions triggered by unbalanced enzymatic activities. Genes encoding histone acetylation modifies have been reported to be translocated, amplified, overexpressed, or point mutated in several types of cancer (Lu et al., 2015). Thus the regulated balance of histone acetylation and deacetylation is a major factor mediating cellular homoeostasis and maintaining a healthy cellular state.

1.5. Alteration of chromatin organization and gene expression by different stress

In addition to the ordered organization and maintenance of dynamicity by various factors, the chromatin of an eukaryotic cell needs to be safeguarded from various threats imposed both from intrinsic as well as extrinsic environment. Living organisms faces different kinds of abiotic and biotic stress during the process of life. The biotic stresses include fungal, bacterial and viral infection while the abiotic stresses include heat shock, salinity, pressure, radiation etc. To neutralize the effects of these hazards the eukaryotic cells have evolved precise multifaceted sensing mechanisms and signal transduction systems to provide dynamic and accurate response to stresses. Cellular stresses activate various intracellular signaling pathways which in turn regulate various aspects of cellular physiology. One of the major component of stress responses, besides alterations in metabolism, cell cycle progression, protein homeostasis, cytoskeletal organization, vesicular trafficking and modification of enzymatic activities is the change in gene expression (Smith and Workman, 2012). As discussed above, modulation of gene expression can be brought about by histones and chromatin proteins as a response to stress condition. Heat shock and oxidative stresses can

alter the binding status of histones onto the DNA through specific post translational modifications. Scientific literature suggests that several chromatin remodellers are recruited to promoters during stress responses. During osmotic stress in yeast, a dramatic change in the nucleosome organization of stress-responsive promoters is observed which is dependent on Hog1 and the RSC chromatin-remodeling complex (Mas et al., 2009). SWI/SNF has also been reported to bind at the promoters of stress responsive genes under adverse conditions, driving the transcriptional induction of target genes (Erkina et al., 2009). INO80 chromatin remodeling complex has also been implicated in stress response as its deficiency leads to prolonged expression of stress genes and an interruption of nucleosome reassembly at stress loci (Klopf et al., 2009). Along with chromatin remodelers, histone-modifying enzymes provide an additional means of modulating transcription. In yeast the Rpd3 histone deacetylase complex is recruited by Hog1 specifically at stress-activated promoters following stress(De Nadal et al., 2004). Likewise in D. melanogaster, DNA sequences that bind strongly the D. melanogaster Heat Shock Factor after an exposure to heat radiation, are demarcated by distinct chromatin marks, such as histone mono-ubiquitylation of H2B and H3K4 trimethylation. Certain conditions of stress also alter the localization or the enzymatic activity of chromatin modifying enzymes/remodelers which can also contribute to a change in chromatin dynamics and thereby gene expression pattern (Shivaswamy and Iyer, 2008). Thus it can be said conclusively that several chromatin-modifying complexes and histone modifications play decisive roles for transcription initiation on exposure to stress.

1.6. Autophagy a self-eating cellular process

Upon exposure to any intracellular or extracellular stress signal, cells counter these changes by altering gene expression which affect either their catabolic or anabolic pathways. Catabolism of cellular materials is mediated by two major pathways, the proteasome degradation pathway and autophagy. While the proteasome pathway is used majorly for protein degradation the autophagy pathway is a more universal one and degrades other macromolecules and damaged organelles. The term **'autophagy'** encompasses various types of processes, such as micro autophagy, macroautophagy, and chaperone-mediated autophagy (Codogno and Meijer, 2005). Autophagy is an evolutionary conserved mechanism in eukaryotic cells that engulfs cell's wastage, like damaged organelles, macromolecules, etc. through the formation of a double membraned vesicle called autophagosome. In mammalian cells, autophagosomes undergo a maturation process by fusing with endocytic compartments and lysosomes. In yeast genetic screens was carried out that identified a large number of genes involved in the process of autophagy usually referred to as ATG (Tsukada and Ohsumi, 1993) (Table 1.1). There are some core atg genes which are involved in autophagosome formation in both selective and non-selective autophagy summarized in the table below (Huang et al., 2017). The selectivity is conferred to the process by selectivity factors that act as a bridge between the cargo and autophagosome. The selective autophagy involves capture and degradation of specific cargo such as mitochondria (known as mitophagy), peroxisomes (pexophagy), ribosomes (ribophagy), protein aggregates (aggrephagy), pathogens (xenophagy), part of the nucleus (nucleophagy), endoplasmic reticulum (reticulophagy).

Yeast gene	Human ortholog	Function
ATG1	**ULK1,ULK2**	Serine-threonine kinase; induction/membrane recycling
ATG2	**C14orf103**	Peripheral membrane protein; retrograde ATG9 transport (from PAS)
ATG3	**hATG3**	E2-like; ATG8 conjugation
ATG4	**hATG4A (autophagin-2), hATG4B (autophagin-1), hATG4C(autophagin-3),hATG4 (autophagin-4)**	Cysteine protease; cleavage of ATG8
ATG5	**hATG5**	Conjugated to ATG12; formation/expansion
ATG6	**BECN1**	helps in PI3P synthesis; formation/expansion; often related to tumorigenesis
ATG7	**hATG7**	an E1-like enzyme for Atg12 and Atg 8 homologues
ATG8	**MAP1LC3A, MAP1LC3B, GABARAP,GABARAPL1**	Ubiquitin-like protein conjugated to PE; formation/expansion of autophagosomes
ATG9	**hATG9A,hATG9B**	Transmembrane protein shuttling between PAS and peripheral membranous structures (including mitochondria)
ATG10	**hATG10**	E2-like enzyme; ATG5-ATG12 conjugation
ATG11	**Unknown**	Cargo receptor/adaptor and anterograde (to PAS) ATG9 transport
ATG12	**hATG12**	Ubiquitin-like protein conjugated to ATG5; formation/expansion
ATG13	**Unknown**	Modulates ATG1 activity; formation/expansion
ATG14	**Unknown**	PI3P synthesis; formation/expansion
ATG15		Lipase-like; degradation of vesicle within vacuole
ATG16	**ATG16.1** **ATG16.2**	Forms homodimers and associates with ATG5-ATG12 complex; formation/expansion
ATG17	**Unknown**	Modulates ATG1 activity; regulate size of autophagosome
ATG18	**WIPI1, WIPI2**	PI(3,5)P2 binding protein involved in vacuole membrane recycling; PI3P binding protein involved in retrograde ATG9 recycling

Table 1.1. Autophagy genes and their functions: List of autophagy genes with their human ortholog are listed with each of their functions. (Adapted from Tanida et al., 2004 Murrow and Debnath, 2013).

In the mammalian system, the core autophagy pathway begins with the formation of an **isolation membrane (phagophore)** which comprises at least five molecular components : (1) the Atg1/unc-51-like kinase (ULK) complex; (2) the Beclin 1/ class III phosphatidylinositol 3-kinase (PI3K) complex; (3) two transmembrane proteins, Atg9 and vacuole membrane protein 1 (VMP1); (4) two ubiquitin-like protein (Atg12 and Atg8/LC3) conjugation systems; and (5) proteins that mediate fusion between **autophagosomes** and **lysosomes** (Yang and Klionsky, 2010) (Figure 1.3). This isolation membrane can be derived from various sources including the endoplasmic reticulum, the outer mitochondrial membrane or the plasma membrane. The ULK proteins (ULK1 and ULK2) play a key role in autophagy induction like their yeast Atg1. These proteins act downstream of the mammalian target of rapamycin (mTOR) complex 1 (mTORC1, a polyprotein complex that contains mTOR, Raptor, mLST8/GßL, Deptor and PRAS40. During nutrient rich conditions, mTORC1 is active and possesses kinase activity, forms a multiprotein complex that contains ULK1, Atg13, FIP200 and Atg101. During starvation conditions, mTORC1 is inactivated leading to its dissociation from the ULK complex. This brings about dephosphorylation of specific residues within ULK1 (or ULK2) and Atg13 (which are normally phosphorylated by mTORC1) rendering it active (Qin et al., 2010). ULK1/2 can also be positively regulated by directly interacting with the several subunits of the energy-sensing kinase, AMP-activated protein kinase (AMPK) (Alers et al., 2012). Although little is known about the exact molecular mechanism of how ULK1/2 activates downstream components of the autophagic machinery, it is shown to phosphorylate Ambra1, a component of the Beclin 1/Class III PI3K complex. The mTORC1 mediated regulation of autophagy is a tightly regulated circuitry consisting of various feedback loops, which makes it function like a that is either switched off (to inhibit autophagy at the level of ULK1/2) or on (to induce autophagy by ULK1/2 activation, as a result of a positive amplification loop).

The Beclin 1 core complex is another major affector protein complex which induces autophagy. It includes Beclin 1, Vps15, Vps34 and likely, Ambra1 (He and Levine, 2010). This complex allosterically activate the class III PI3K Vps34 to generate phosphatidylinositol-3-phosphate (PI3P) which allows the recruitment of other effectors such as the double FYVE domain-containing protein 1 (DFCP1) and WD-repeat protein

interacting with phosphoinositides (WIPI) family proteins to initiate the process of vesicle nucleation or autophagosome formation. Depending upon its interacting partners Beclin1 functions as an autophagy inducer or repressor. Atg14 (also called Atg14L or Barkor, for Beclin 1-associated autophagy-related key regulator) is a positive regulator of autophagy induction which is essential for PI3K activity. UVRAG (UV radiation resistance associated gene) competes with Atg14 for binding to Beclin 1 and may promote PI3K activity in a cell type-specific fashion, and through interactions with class C Vps/HOPS complexes, promotes autophagosome fusion with the late endosome/lysosome. Rubicon (RUN domain protein as Beclin 1 interacting and cysteine-rich containing), on the other hand negatively regulates autophagy (as well as endocytic trafficking) upon its interaction with Beclin 1/PI3K complexes (He and Levine, 2010). Thus the multiprotein Beclin1 complex through its different interacting partners relay intracellular or extracellular cues which directly affects the autophagy process. Cycling of the other core autophagy protein Atg9 between specific subcellular components might be crucial for providing lipids to the phagophore membrane. This cycling process of Atg9 requires Atg1/ULK1 and the kinase activity of Vps34 or involves the UVRAG/ Bif-1-containing Beclin 1 complex since Bif-1 transiently associates with Atg9 after starvation (Orsi et al., 2010).

Two distinct ubiquitin-like conjugation systems functions as a part of the vesicle elongation process. In the first pathway, Atg12 is covalently conjugated to Atg5, with the help of the E1-like enzyme Atg7 and the E2-like enzyme Atg10. This conjugate then forms a part of a complex by associating with Atg16 in a non-covalent fashion to form the multimeric Atg12-Atg5-Atg16. This multimeric complex possesses E3 ligase activity for LC3 (Yang and Klionsky, 2010). Conjugation of phosphatidylethanolamine (PE) to a glycine (Gly) residue of yeast Atg8/mammalian LC3 by the sequential action of the protease Atg4, the E1-like enzyme Atg7, and the E2-like enzyme Atg3 forms the crux of the second pathway. This conjugation converts the soluble form of LC3 (named LC3-I) to the autophagic vesicle-associated form, LC3-II (Tanida et al., 2004; Yang and Klionsky, 2010). This lipidated form of LC3 stably associates with the autophagosome membrane, making it a potent marker for detection of cellular autophagy (Barth et al., 2010). In the mammalian cell several proteins possesses an LC3-interacting region (LIR) which helps them to interact with LC3 (and its paralogs) serving as adaptors to target defined structures such as ubiquitinated proteins or

mitochondria to the autophagic machinery**.** The best studied among them are p62 (also known as sequestosome1, SQSTM1) and NBR1 (Neighbor of BRCA1), both of which recognize ubiquitinated proteins as well as BNIP3L, which binds to mitochondrial membranes(Larsen et al., 2010; Lazarou et al., 2015). The regulation of these autophagy adaptors is not yet understood but they provide an essential key to understand how specific stress stimuli trigger selective autophagy.

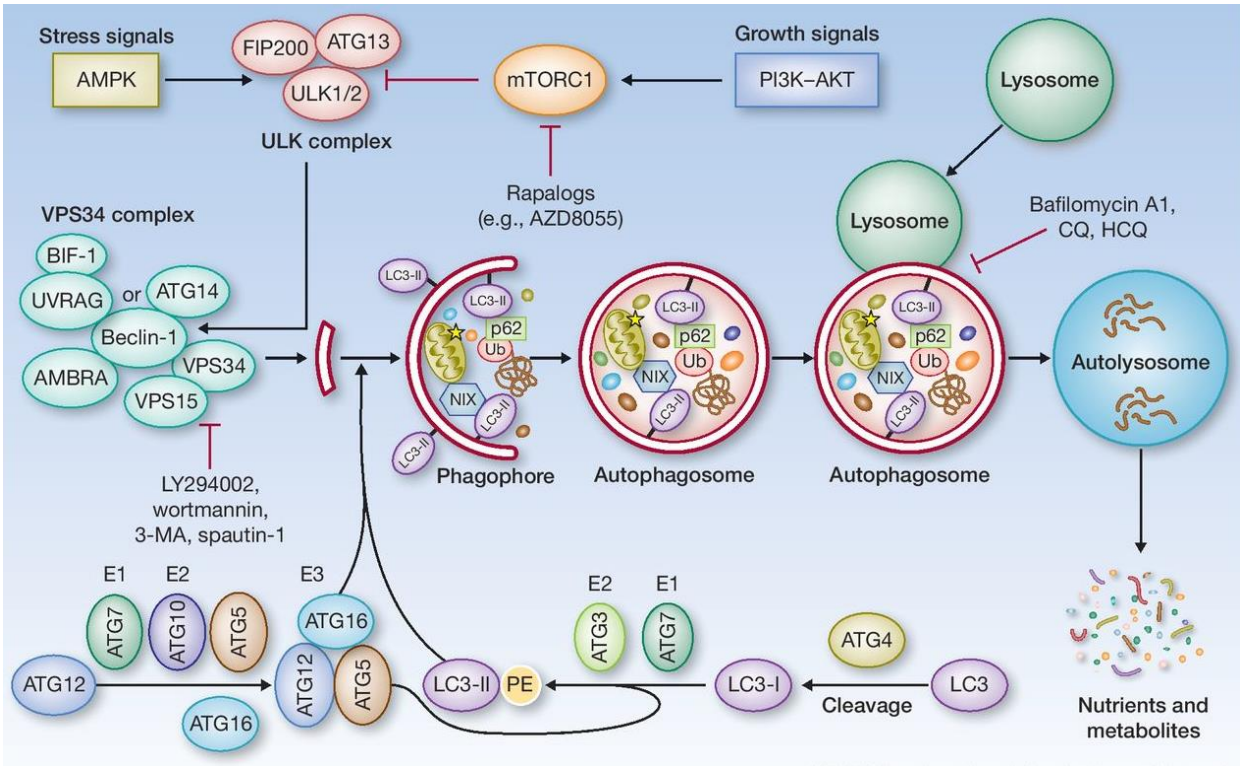

Figure 1.3. The autophagic process. Upon nutrient or growth factor deprived conditions, AMPK is activated with inhibition of mTOR leading to activation of ULK, which phosphorylates Beclin-1, leading to VPS34 activation and phagophore formation. ULK forms a complex with FIP200 and ATG13, whereas VPS34 function requires a regulatory subunit, VPS15 (p150), and Beclin-1, which further mediates the association of other regulatory factors such as AMBRA, ATG14, UVRAG, and BIF- 1. Multiple ATG proteins such as ATG5 and ATG7 constitute two "ubiquitin-like conjugation systems" that catalyze the formation of phosphatidylethanolamine (PE)-conjugated LC3 (LC3-II) and direct its proper incorporation into the phagophore membrane, where it serves as docking site of adaptor proteins (and bound cargos). The closure of an elongated phagophore marks the formation of a mature autophagosome, which eventually fuses with a lysosome, leading to cargo degradation and recycling of nutrients and metabolites. Ub, ubiquitin(Adapted from Cicchini et al., 2015).

1.7. Autophagy: A mechanism of cellular defense

The process of autophagy is an adaptive response to provide energy and nutrients to cells during starvation conditions. In yeast, autophagy is activated in response to changes in the extracellular milieu. Depending upon the stimulus, autophagy can degrade cytoplasmic contents non-specifically or can target the degradation of specific cellular components (Murrow and Debnath, 2013). The degradation products, like amino acids and other basic building blocks, are recycled back to the cytoplasm and are used up by the cell (Rabinowitz JD, White E, 2010). The cellular biosynthetic capacity and ATP levels are maintained during periods of stress through the autophagic pathway. It helps in regulating the ATP levels by supplying amino acids for de novo protein synthesis and providing substrates for the tricarboxylic acid (TCA) cycle, such as amino acids and free fatty acids. Following starvation, autophagy is upregulated in almost all tissues in mice. Mice devoid of the essential core autophagy genes ATGs Atg5 or Atg7 have decreased plasma and tissue amino acid concentrations which prove detrimental for their survival soon after their birth. This might be due to nutrient deprivation during the neonatal starvation period due to lack of autophagy (Kuma et al., 2004). Even in mammalian cell culture system, inhibition of autophagy by RNA interference (RNAi)-mediated Atg7 depletion or treatment with the autophagy inhibitors 3-methyladenine (3-MA) or chloroquine (CQ) leads to cell death signifying that the catabolic function of autophagy might mediate cytoprotection. The process of self-eating does not protect cells indefinitely but rather it helps the cells to survive extreme conditions of stress if the adverse conditions are resolved in a timely manner. Thus autophagy acts as a salvage mechanism which helps in the sustenance of the cell by providing basic components to sustain core metabolic functions during starvation or stress.

The stress-induced autophagy is regulated primarily at two critical nodes; by the **mammalian target of rapamycin (mTOR)** and **AMP activated protein kinase (AMPK)**. Here the AMPK signalling cascade is described (Figure 1.3). AMPK acts as a sensing kinase responding to low intracellular energy conditions through the levels of AMP to ATP. Under conditions of high AMP/ATP ratio, AMPK phosphorylates ULK1 thereby activating it and subsequently inhibiting mTOR complex1 (mTORC1) via phosphorylation of Raptor. Thus

both AMPK and mTOR also control cell growth and metabolism, coupling autophagy to these processes.

The HIF-1 (Hypoxia inducible) factor 1 (HIF-1) signaling is another major pathway which regulates autophagy under the conditions of hypoxia. HIF-1 directly affects the transcription of the BH3-only protein BNIP3, which is essential for induction of autophagy. It binds directly to autophagy thus alleviating the inhibitory interaction between Bcl-2 and Beclin 1 (the mammalian ortholog of yeast Atg6 (You et al., 2015; Zhou et al., 2009). Interestingly, a host of autophagy genes was identified as direct p53 target genes. While the autophagy program is regulated predominantly by p53, the p53 family members, p63 and p73 contribute to activation of this autophagy gene network. Induction of autophagy genes in response to p53 activation is associated with enhanced autophagy in diverse settings and depends on p53 transcriptional activity. While p53-induced autophagy does not affect cell cycle arrest in response to DNA damage, it is important for both robust p53-dependent apoptosis triggered by DNA damage and transformation suppression by p53. Reported studies highlight an intimate connection between p53 and autophagy through a vast transcriptional network and indicate that autophagy contributes to p53-dependent apoptosis. Interestingly, p53, induced by various cellular stresses plays dual roles in autophagy activation. The cytosolic p53 also has transcription independent functions, and cytosolic p53 inhibits autophagy (detailed molecular mechanism not known). The consequences of this balance between the pro- and anti-autophagic roles of p53 are however not well understood (Levine and Abrams, 2008).

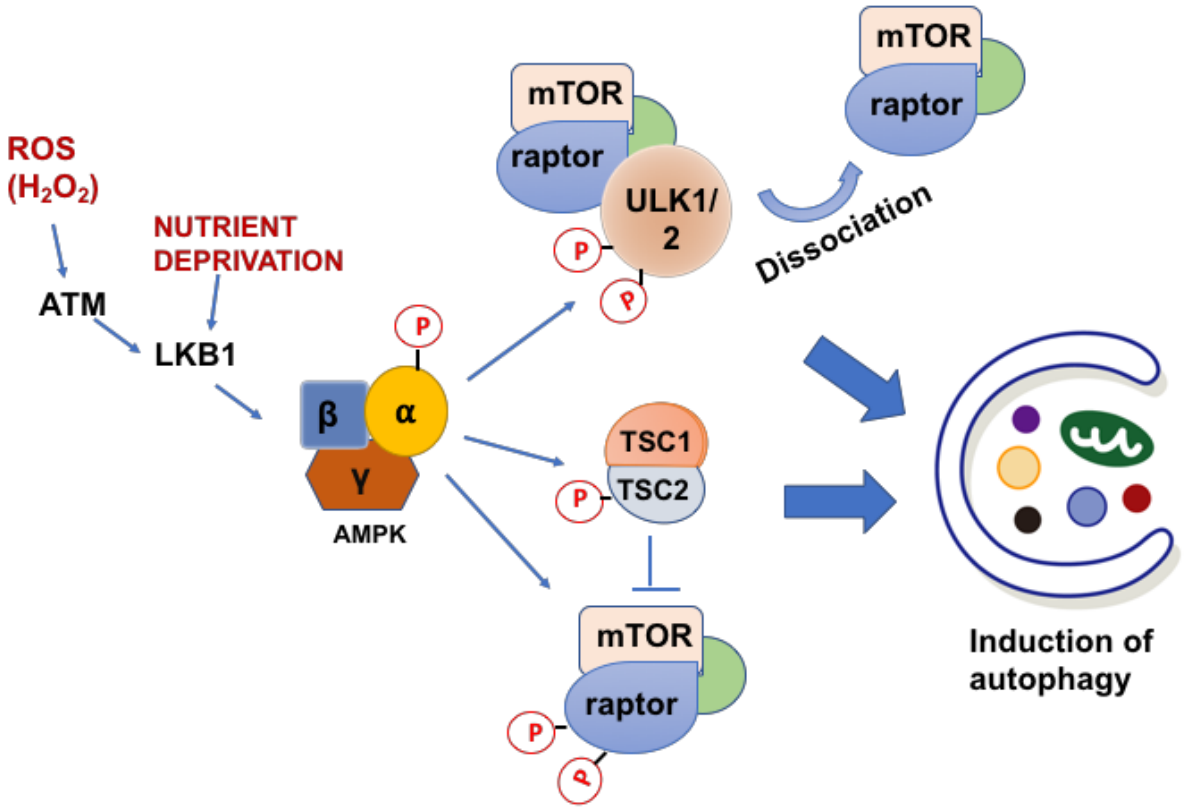

Figure 1.3. AMPK signaling pathway in autophagy: AMPK activates autophagy at various steps by directly phosphorylating different protein substrates involved in its initiation phases. Upon conditions of nutrient stress or through Reactive oxygen species (ROS) AMPK is activated. Upon nutrient rich conditions or in the absence of oxidative stress , AMPK is inactive and mTORC1 is active. The active mTORC1 phosphorylates Ulk1 on Ser 757 to prevent Ulk1 interaction with and activation by AMPK. When cellular energy level is limited, AMPK is activated and mTORC1 is inhibited by AMPK through the phosphorylation of TSC2 and Raptor. Phosphorylation of Ser 757 is decreased, and subsequently Ulk1 can interact with and be phosphorylated by AMPK on Ser 317 and Ser 777. The AMPK-phosphorylated Ulk1 is active and then initiates autophagy Figure adapted from (Alers et al., 2012; Qin et al., 2010).

1.8. Epigenetic regulation of autophagy

As discussed in the earlier sections, macroautophagy is a major pathway of self-digestion which is critical for maintaining cellular homeostasis and longevity. The regulation of autophagy is a growing interest as it unravels many unanswered questions regarding its selectivity and misregulation in various pathogenic conditions. Autophagy is a cytosolic event which requires an arsenal of cytosolic core and effector proteins for its functioning. However, recent advances reveal that the nucleus might play an important role in its regulation through its diverse histone post translational modifications (Füllgrabe et al., 2014**).** A network of diverse epigenetic modifiers like miRNAs (Liang and Yang, 2014) and histone modifications in association with transcription factors relay a highly intricate cellular signalling which influences or regulates whether autophagy leads to cell survival or cell death. Although the role of transcription factors, HATs and HDACs were known for a long time to be regulators of autophagy, their functions were only limited to the cytoplasmic interactions with autophagy-related proteins. Recent studies throws light on their nuclear impact which regulates autophagy at the transcriptional level (Füllgrabe et al., 2014). The effect of histone modifications in the adaptive response of autophagy acts in three tiers. During a rapid autophagic response, in addition to the post-translational modification of cytosolic proteins a battery of transcription factors upregulate the expression of autophagy protein encoding genes through the active histone marks (H3R17me2, H3K9Ac,etc.) (Shin et al., 2016). However, after prolonged exposure to autophagic stimuli, there is a global change observed in the histone modification pattern helping it to act as a negative regulatory feedback loop. The global downregulation of active histone marks prevents the transactivation of autophagy genes by several transcription factors, thus acting as a mechanism to prevent lethality in cells caused by sustained high level of autophagy. The global chromatin silencing by histone modifications (H4K16Ac) (Füllgrabe et al., 2014), and also by miRNAs might also help in energy conservation during times of prolonged starvation. Thus chromatin dynamics modulated by the interplay of several histone and non-histone factors articulately regulate the process of autophagy thus critically maintaining the cellular homeostasis and heath.

Transcription Factors		
Name	**Core autophagy genes regulated at the transcriptional level**	**Effect on Autophagy**
ATF4	ATG5, BH3-only LC3 and ULK1	Enhanced autophagy
ATF5	mTOR	Suppressed autophagy
β-catenin	SQSTM1	Suppressed autophagy
C/EBPβ	BNIP3, LC3 and ULK1	Enhanced autophagy
CHOP	ATG5 and LC3	Enhanced autophagy
E2F1	ATG5, BNIP3, LC3 and ULK1	Enhanced autophagy
FOXO1	ATG5, ATG12, ATG14, BECN1, BNIP3, LC3, and VPS34	Enhanced autophagy
FOXO3	ATG5, BH3-only LC3 and ULK1	Enhanced autophagy or suppressed autophagy
GATA1	LC3	Enhanced autophagy
HIF1	BNIP3	Enhanced autophagy
JUN	BECN1 and LC3	Enhanced autophagy
NF-κB	BCL2, BECN1, BNIP3 and SQSTM1	Enhanced autophagy or suppressed autophagy
p53	ATG2, ATG4, ATG7, ATG10, BCL2, BH3-only, ULK1 and UVRAG	In the cytosol: suppressed autophagy In the nucleus: enhanced autophagy
p63	ATG3, ATG4, ATG5, ATG7, ATG9, ATG10, BECN1, LC3 and ULK1	Enhanced autophagy
p73	ATG5, ATG7 and UVRAG	Enhanced autophagy
SOX2	ATG10	Enhanced autophagy
SREBP2	LC3, ATG4B and ATG4D	Enhanced autophagy
STAT1	ATG12 and BECN1	Suppressed autophagy
STAT3	ATG3, BCL2 and BNIP3	Suppressed autophagy
TFEB	ATG4, ATG9, BCL2, LC3, SQSTM1, UVRAG and WIPI	Enhanced autophagy
ZKSCAN3	*LC3*, *ULK1* and *WIP1*	Suppressed autophagy

Table 1.3. Regulation of autophagy at transcriptional level. Different transcription factors regulate autophagy through the differential expression of the target genes (Füllgrabe et al., 2014; Hu et al., 2016; You et al., 2015).

Histone Modifications		
Histone mark	**Epigenetic Enzyme**	**Effect on Autophagy**
H3R17me2	CARM1	Enhanced autophagy
H3K27me3	EZH2	Suppressed autophagy
H3K9me2	G9a	Suppressed autophagy
H4K16Ac	hMOF	Suppressed autophagy
H3K56Ac	EP300/KAT3B/p300 and KAT2A/GCN5	Suppressed autophagy
H4K20me	SETD8 and SUV420	Enhanced autophagy
H2BK120ub	RNF20–RNF40	Suppressed autophagy
miRNA		
Autophagy Target genes	**miRNA**	
RB1CC1	miR-10a	
ULK1	miR-20a and miR-106b	
ULK2	miR-885-3p	
ATG9	miR-34a	
ATG14	miR-195	
BCL2	miR-15,miR-16,miR-21,miR-24-2, miR-195, miR-196b, miR-204, miR-205 and miR-365-2	
BECN1	miR-30a, miR-30d,miR-376b and miR-519a	
UVRAG	miR-374a and miR-630	
ATG4	miR-101 and miR-376b	
ATG5	miR-30a,miR-30d,miR-180a and miR-374a	
ATG7	miR-17 and miR-375	
ATG10	miR-519a	
ATG12	miR-30d and miR-630	
ATG16	miR-519a and miR-885-3p	
BNIP3	miR-145 and miR-210	
LC3	miR-204	
SQSTM1	miR-17,miR-20,miR-93 and miR-106	
ATG2	miR-30d and miR-130a	
ATG9	miR-34a	

Table 1.4. Epigenetic regulation of autophagy. Table summarizing the effect of different histone modifications as well as the role of miRNAs in the process of autophagy (Easwaran and Baylin, 2010)(Baek and Kim, 2017; Bánréti et al., 2013; Füllgrabe et al., 2014; Wei et al., 2015).

1.9. Autophagy in cancer

Autophagy being a master prosurvival mechanism of the mammalian cells against various stresses like starvation, accumulation of damaged and unwanted intracellular protein and organelle has been implicated in various physiological processes such as development, anti-aging, elimination of microorganisms, cell death, tumor suppression, and antigen presentation (Murrow and Debnath, 2013). In mammals, autophagy has been implicated in either the pathogenesis or response to a wide variety of diseases, including neurodegenerative disease, chronic bacterial and viral infections, atherosclerosis, and cancer. As the basic molecular pathways and also various epigenetic regulatory mechanisms for autophagy are being elucidated, the relationship of autophagy to the pathogenesis of various disease states is gaining importance (Kundu., et.al, 2008). (Duve (2007). In tumorigenesis, autophagy acts as a two-way sword with respect to tumorigenesis. In cancer cells, autophagy possesses both tumor-promoting (Figure 1.4) and tumor-suppressing properties, which depend on the stage of cancer progression. During the initiation of cancer, autophagy-mediated elimination of altered cytosolic constituents, such as aggregated proteins or damaged organelles, prevents cells from further DNA damage and genomic instability (Mathew R, et. al, 2007, Bhutia SK, et.al, 2013). Autophagy can act as a cell death mechanism in cancer cells with apoptotic defect. Autophagy can also facilitate oncogene-induced senescence or protect tumors against necrosis and inflammation, thus promoting tumor growth. Once the cancer has formed, autophagy can contribute to tumour progression by allowing tumor cells to survive in stressful conditions (Yunyan Gu, et.al, 2015). Unlimited proliferation, a hallmark of cancer, demands high levels of nutrients and oxygen. When the blood supply is insufficient, cancer cells encounter metabolic stress and can induce autophagy, which allows them to survive (Liang C, et.al, 2006). Beclin 1 interacts with UV-irradiation-resistance-associated gene (UVRAG) to form core complexes that induce autophagy. Reports suggest siRNA knockdown of Beclin 1 or UVRAG can increase radiation-induced DNA double strand breaks (DSBs), shown by pATM and γH2Ax, and promote colorectal cancer cell death. Beclin 1 and UVRAG confer protection against radiation-induced DNA DSBs and may maintain centrosome stability in established tumor cells. (Paglin S, et.al, 2001). Paglin et al. first identified the formation of acidic vacuoles in neoplastic epithelial cells exposed to IR.

(Liang C. et.al, 2006). Liang et al. using Hela cells suggested that radiation induces autophagy, evident through increase of LC3-II/LC3-I ratio. There have been other reports showing an autophagy increase in the crypt cells of the murine small intestine 7 days after the exposure to gamma-radiation. There have been reports on how the process of autophagy tends to promote metastasis during advanced cancer stages by supporting ECM detached metastatic cell survival and colonization at a distant site and by inducing metastatic cells to enter dormancy if they fail to establish a contact with the ECM in the new environment. Autophagy induced by hypoxia inducible factor-1α (HIF-1α) has been reported to promote epithelial to mesenchymal transition. (Hoare et al., 2011)

In addition to the above mechanisms, autophagy helps in rendering resistance property to the cancer cells. Established cancer cells grow under great metabolic stress due to the high energy demands of rapidly growing tumor cells. This cellular environment induces autophagy which provides an alternative source of energy and metabolites to these cells. (Onodera and Oshumi, 2005; Degenhardt et al., 2006; Jones and Thompson, 2009; Rosenfeldt and Ryan, 2009; Rabinowitz and White, 2010). Furthermore, autophagy has also been reported to be induced through various cancer therapies, leading to chemo resistance and cancer cell survival (Chen and Karantza- Wadsworth, 2009; White and DiPaola, 2009). Inhibition of autophagy by various pharmacological inhibitors like treatment with 3-methyladenine (3-MA, a PI3K III inhibitor), Bafilomycin A (a specific inhibitor of vacuolar-type H+-ATPase), chloroquine (CQ) or hydroxychloroquine (HCQ) (lysosomotropic agents that impair fusion between autophagosomes and lysosomes), or by genetic deletion of autophagy related genes, such as ATG5, ATG6 and ATG7 resulted in the sensitization of these cancer cells (Table 1.5.). Thus autophagy inhibition sensitized cancer cells to various therapies like genotoxic chemo- and radio-therapy, hormonal therapy and receptor tyrosine kinase inhibition (Chen et al., 2010). These studies reveal the major therapeutic role of autophagy in treating cancer cells especially in terms of chemo and radio resistance. In this present study we elaborate the role of autophagy in Breast Cancer, one of the most deadliest cancer affecting women. Reports suggest that autophagy is differentially expressed during the progression of Breast cancer which further makes the functional re of autophagy in Breast Cancer manifestation enigmatic.

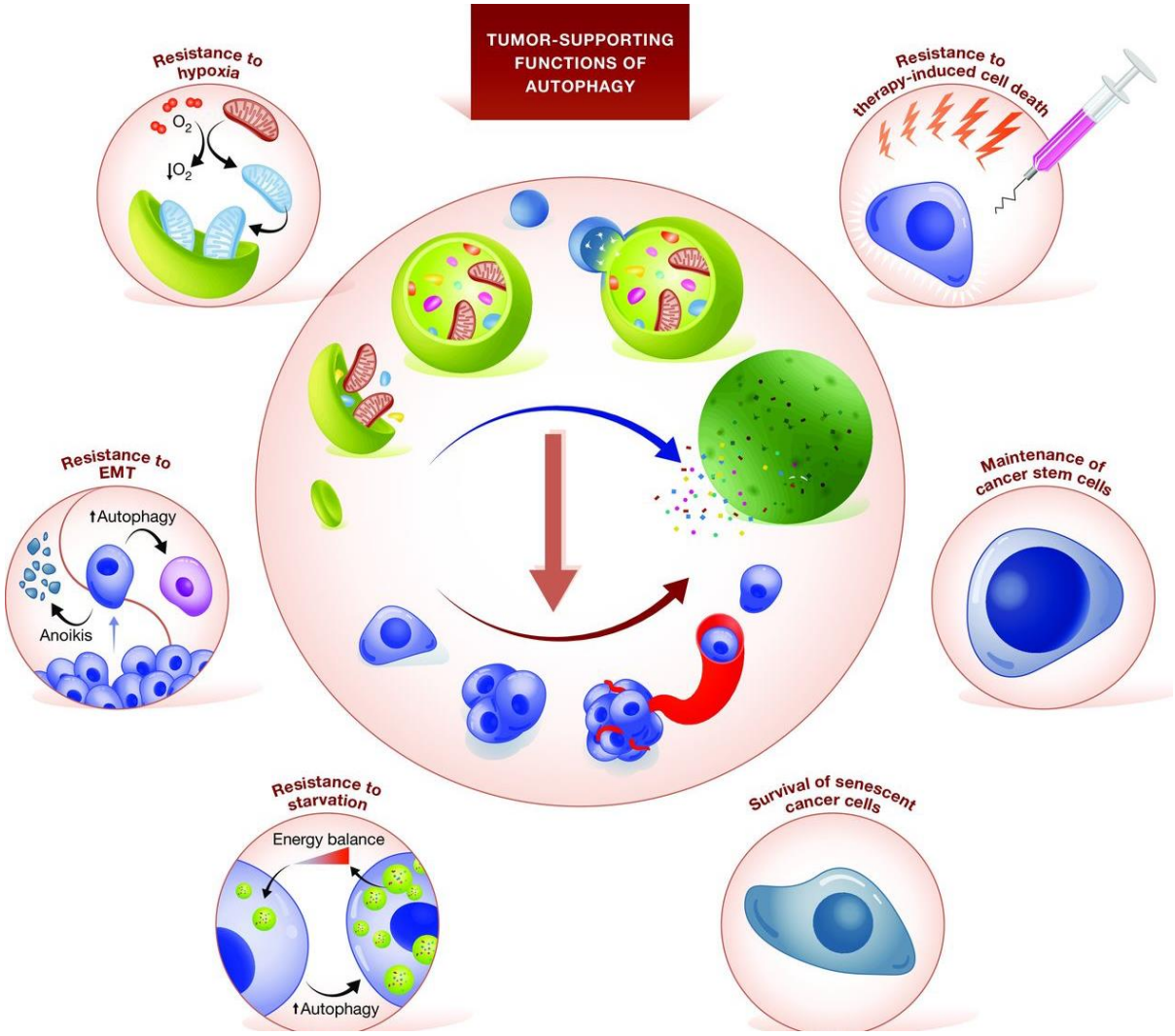

Figure 1.4. Functions of autophagy in promoting tumor formation and its progression. Once malignant transformation has occurred, autophagy is believed to facilitate tumor progression and resistance to therapy. Such tumor-supporting functions reflects the ability of autophagy to: (1) improve the resistance of cancer cells to endogenous conditions that normally provoke cell death, such as the detachment from the basal membrane, hypoxia and nutrient deprivation; (2) render transformed cells less sensitive to therapy-induced cell death; (3) sustain the survival of cancer cells that enter a state of dormancy or senescence in response to therapy; and (4) ensure the maintenance of the cancer stem cell compartment. EMT, epithelial-to-mesenchymal transition. Figure adapted from (Galluzzi et al., 2015)

Cancer Type	Treatment	Cell death by autophagy inhibition		
		Early Step	**Late Step**	**siRNAs**
Breast Cancer	γ-radiation			Beclin 1, ATG3, ATG4b, ATG4c, ATG5, ATG12
	Tamoxifen	3-MA		ATG5, Beclin 1, ATG7
	Bortezomib			LC3, HDAC6, ATF4
	Trastuzumab	3-MA	Baf	LC3
	Sulforaphane		Baf	
Colorectal Cancer	Bortezomib			Beclin1
	γ-radiation			Beclin 1, ATG5, ATG7,UVRAG
	5-FU	3-MA		ATG7
	Sulforaphane	3-MA		
Glioma	Temozolomide		Baf	
	4-HPR	3-MA	Baf	
	γ-radiation	3-MA	Baf	Beclin 1, ATG5
	Imatinib		Baf	
Multiple Myeloma	Bortezomib		Baf	
Prostate cancer	Androgen deprivation ADI-PEG20 (Arginine Deaminase)	3-MA		Beclin1
	Saracatinib (Src kinase)	3-MA	CQ	
Skin cancer	Cisplatin	3-MA		ATG5
Lymphoma	Tamoxifen		CQ	ATG5
Gastric cancer	Quercetin		CQ	ATG5, Beclin1

Table 1.5. Autophagy inhibitors in different cancers. Preclinical studies with autophagy small molecular inhibitors as well as inhibition of genes by siRNA treatment for cancer treatment. Inhibition of autophagy in these cancer cells results in rapid cell death (Chen et al., 2015; Choi, 2012; Hoare et al., 2011; Li et al., 2013; Maycotte, 2014).

1.10. Breast Cancer

Breast cancer is the most common non cutaneous cancer affecting women all around the world. Owing to the heterogeneity of the tumor, it poses a persistent concern in the field of diagnosis and therapeutics. Through the development of imaging techniques, detection of Breast Cancer at an early stage has been able to decrease the mortality rate and the disease burden to some extent in the general population. However the advancement of this disease to higher stages and also the occurrence of radiation and chemotherapy resistant tumors make it a deadly disease till date. Development of malignant tumor in breast tissues, mainly the lobules and ducts responsible for milk production results in breast tumor. Though a lot of research has highlighted the molecular pathway and gene expression pattern in breast tumors, yet the exact cause of breast cancer in most patients still remains an enigma. There are several risk factors associated with its development including age, a family history, obesity, alcohol consumption, estrogen exposure, and mutation in susceptibility genes, particularly BRCA1 and BRCA2. Women carrying germline mutation at BRCA1 or BRCA2 are considered to be at an high risk of developing Breast Carcinoma. BRCA1 and BRCA2, located on chromosomes 17 and 13, respectively are inherited in an autosomal dominant fashion with high penetrance , thus increasing the incidence of BRCA-associated cancers in affected families (King, 2003). The role of BRCA1 is predominantly in DNA damage repair response, thus the progression and generation of BRCA associated breast tumor relies on a disrupted DNA repair phenomenon (Hartman and Ford, 2003). Women possessing the BRCA mutation carries a 40% to 85% estimated lifetime risk of developing breast cancer, as well as ovarian cancer and other primary cancers.

Breast Cancers are mostly epithelial in origin and are categorized as carcinomas. Although arising from the same organ (breast), breast carcinomas are considered as a heterogeneous disease comprising of a wide array of cancer subtypes that varies both in microscopic appearance and biologic behavior as well as molecular signatures. Ductal carcinoma in situ (DCIS) occurs by the proliferation of malignant epithelial cells enclosed within the mammary ducts. They are identified by their distinct cytological features and abnormal growth pattern. Invasive Ductal carcinoma (IDC) differs from The key difference between DCIS and invasive ductal carcinoma (IDC) also known as the infiltrating ductal carcinoma, is that in

case of DCIS the malignant cells are still contained by the basement membrane of the ducts whereas in IDC the cells have invaded through the breast tissue, blood vessels, and lymphatics of the breast to the distant regional lymph nodes or, in later stages, throughout the body. IDC s are classified majorly into three grades, according to the stages of differentiation , grade 1 being well differentiated while grade 3 being poorly differentiated with solid nests of neoplastic cells, no gland formation, nuclear atypia, and a substantial amount of mitotic activity. Most of the IDC express the hormone receptors, estrogen and progesterone and are therefore susceptible to hormone mediated therapy. 15%-20% of the IDCs express as HER2, which attributes an aggressive behavior characteristic of these tumors. The second most common type of invasive carcinomas is the Infiltrating lobular carcinoma (ILC). It mostly occurs in older women, histologically is better differentiated, and is positive for estrogen receptor. It is often found to metastasize to different parts such as bone marrow, cerebrospinal fluid and leptomeninges, gastrointestinal tract, ovary, serosal surfaces, and uterus (resembles low-grade stromal sarcoma). These carcinomas occur mostly by a lack of cellular cohesion due to mutation or loss of function of E-cadherin. There are several less prevalent histologic types of breast cancer, which are summarized in the table below (Table 1.6.).

Invasive cancer	Occurrence	Tumor characteristics	Prognosis/metastasis
IDC	50-75%	Hard tumor texture Tumor appearance is irregular and speculated Cell features vary DCIS often present	Depends on stage and grade
ILC	15-55%	Normal, slightly firm, or hard tumor texture Cells most often appear in single file order Tumors are most often ER (+) and HER2 (-)	Metastases different from IDC Prognosis similar to IDC
Tubular Carcinoma	1-5%	Tumor is small and not palpable Forms tube-like structures and is usually HER2 (-) and ER (+)	Rare metastasis to lymph nodes, Prognosis better than IDC
Medullary Carcinoma	<1%	Soft tumor with sheet-like cells Tumors are usually triple negative	Prevalent in younger women and BRCA1 mutation carriers
Colloidal Carcinoma	<1%	Usually soft and nonpalpable tumor with cells surrounded by excess mucin Tumor often ER (+) and HER2 (-)	Rarer in young women Unlikely spread to lymph nodes
Invasive papillary carcinoma		Soft tumor with finger-like projections	More common in postmenopausal women Generally good prognosis

Table 1.6. Histological features of Breast Cancer. Different types of invasive Breast Carcinomas with their characteristic features and fate of prognosis have been listed (Klevos et al., 2017)**.**

1.11. Genomic instability and cancer: Focus on Breast Cancer

The eukaryotic cell utilizes several infallible mechanisms to safeguard its genome. Systematic organization of the chromatin with the help of histones and non-histone proteins provide the first amour to the genetic material. Cells maintain their genomic integrity through modulation of the chromatin by various factors, as described in the previous sections or through the regulation of catabolic pathways like autophagy, and DNA repair pathways. Disruption of this regulated safeguard mechanisms might result in genomic instability and cause tumorigenesis. The genome of tumor cells is highly unstable. The genomic instability confers advantages to the highly proliferating tumor cell population by shortening of cell cycle and/or bypassing various intracellular and immunological control systems. Genomic instability can be defined by small structure variations as increased frequencies of base pair mutation, (microsatellite instability) (MSI), or by significant structure variation such as chromosome number or structure changes, which is referred to as chromosome instability (CIN) (Karantza-Wadsworth et al., 2007), Roschke and Kirsch 2010). Microsatellite instability has been commonly observed in many solid malignancies. Chromosomal instability can result from an increased rate of chromosome missegregation in mitosis which causes an incorrect chromosome number and/or abnormal chromosome structure (Rao et al. 2009). Thus proper segregation of chromosomes during mitosis is crucial for maintaining genomic stability, any failure in this process either leads to cell death or malignant transformation. This segregation of chromosomes is carried out by different chromatin associated proteins as mentioned in the table before, thus signifying their crucial role in maintaining cellular homeostasis (Artandi and De Pinho, 2000). Any misregulation could culminate into tumor formation. Telomere function is also critical for maintaining genome instability. Hyper proliferation of cells (hyperplasia) during early stages of cancer progression can lead (in the normal absence of telomerase expression) to telomere abrasion, which could further enhance the process of chromosome fusion and breakage-fusion-bridge (BFB) cycles resulting in complicated, unbalanced chromosome rearrangements. Upon studying the genomic landscape of various tumors, it is found that there are numerous gains

and losses, and recurrent DNA amplifications (with presumptive oncogene driver) at 8p12 (FGFR1), 8q24 (MYC), 11q13 (CCND1), and 17q12 (ERBB2), etc. associated with breast tumor . In situ hybridization studies on breast cancer samples reveal the role of telomere abrasion in the transition from ductal hyperplasia to ductal carcinoma in situ (DCIS; a precursor lesion) (Chin et al., 2004).

Breast cancer is a heterogeneous disease characterized by its range of biological and clinical behaviors. This diversity is echoed in the morphologic and molecular variation through a range of histologic features which consequently act as the molecular pathologic markers useful for diagnosis and treatment (Subramaniam and Isaacs, 2005). For instance, estrogen receptor (ER)/progesterone receptor (PR) positivity defines a subset of tumor which can be treated by hormone modulation therapy (e.g. tamoxifen and aromatase inhibitors). Likewise, ERBB2 (HER2) amplification or overexpression classifies a definite subset which can be targeted through antagonists (e.g. trastuzumab). Tumors that fail to show positivity in ER, PR and HER2 amplification ("triple negative") fail to respond to the above mentioned therapeutics and are thus classified as tumors with poor prognosis (Reis-Filho and Tutt, 2008; Podo et al., 2010). Recent evidences from genome-scale analysis and in particular microarray-based gene-expression profiling, has helped in the molecular classification of breast cancer diversity. Expression patterns of "intrinsic" genes (more variant between than within tumors) have demarcated at least six molecular subtypes (Perou et al., 2000; Sorlie et al., 2001; Hennessy et al., 2009). Although luminal subtypes A and B both expressed markers of the luminal epithelial layer of normal breast ducts (e.g. keratins 8/18) and were found to be ER-positive, luminal B tumors were shown to be more proliferative and had less favorable prognosis. Amplification and overexpression of ERBB2 (HER2) and neighboring genes at 17q12-q21 is associated with the ERBB2 positive subtype. A basal-like subtype exhibits markers of the basal epithelial layer of normal breast ducts (e.g. keratins 5/6). They are generally triple negative for ER, PR and HER2, and carry an unfavorable prognosis. The "normal-like", "claudin low" is also included in the triple-negative class of breast tumors (Hennessy et al., 2009). It is intriguing to speculate on the origins of different molecular subtypes of a single carcinoma (Polyak, 2007; Stingl and Caldas, 2007). The different subtypes might arise as a result of distinct somatic DNA alterations which consequently

influences the altered gene expression and cell phenotype. Thus characterization of breast cancer genomes and their underlying genome instability has gained significant importance.

1.12. MiRNAs as modulators of gene expression: Role in Breast Cancer

Among the different factors which regulate chromatin dynamics and thereby gene expression miRNAs, forms a subclass of the non-coding RNA, which are critical regulators of gene expression. MicroRNAs are evolutionary conserved small group of RNA molecules encoded by about 1% of the genome in most species. Since the discovery of lin-4, there has been extensive study of this kind of single-stranded RNA particularly due to its ability to modulate gene expression by various methods. A primary microRNA is transcribed mainly by the RNA polymerase II (some by RNA polymerase III), either from the intron of a coding-gene or from the intergenic region like other regular mRNA. The pri-miRNA undergoes several processing(capping, polyadenylation, etc.) by various enzymes or functional proteins, such as Drosha, Exportin 5, and Dicer, to yield the functional mature microRNA after being spliced from its precursor form (Catalanotto et al., 2016). These tiny mature miRNA molecules of bodies of about 22 nucleotides regulate gene expression post transcriptionally by binding to their target mRNAs in an incomplete base-pairing manner, particularly in their untranslated regions, causing degradation of the mRNA by forming the RNA-induced silencing complex. Since the miRNA-mRNA binding do not require high complementarity for regulation, a single miRNA may target up to several hundred mRNAs. Thus any change in the expression of a single miRNA can bring a magnanimous effect by altering the levels of multitude of transcripts, which in turn can affect multiple cellular pathways, including cancer (Rehman Kayani et al., 2011) .

Microarray based studies in cancer cells and tumours reveal aberrant expression of several miRNAs particularly in breast, prostrate, thyroid and gastric cancers. To predict the outcome or prognosis of a specific type of cancer by the expression pattern of a particular miRNA is complicated due to the genetic diversity of tumors, and in cell lines derived from different tumors. A single miRNA can exhibit both oncogenic function in some types of cancers whereas can act as a tumor suppressor in other cancers. In breast cancer particularly, due to its heterogeneity and molecular subtypes, various miRNAs have been shown to be deleted or to exhibit downregulated or upregulated expression. Aberrant expression of miRNAs has

been related to several cancer-related genes thus inducing the process of cancer initiation, progression, metastasis or drug resistance. Certain miRNAs upon upregulation mediates cancer or tumour progression, termed as oncomiRs while other group of miRNAs show tumour suppressive functions and are found to be often downregulated in cancer cells. This class of miRNAs are referred to as tumor suppressor miRNAs. In the table below (Table 1.7), is listed a few miRNAs with their target genes, either overexpressed or downregulated in Breast cancer depending on their oncogenic/tumor suppressive property.

Oncogenic miRNAs associated with Breast Cancer		
MicroRNA(family)	**Identified Target**	**Function/Pathway**
miR-21	TPM1, PDCD4, TIMP3, PTEN	Cancer metastasis
miR-155	FOXO3a, SOCS1, caspase-3, TP53INP1	Cell proliferation and apoptosis
miR-182	RECK, MIM, FOXO1	Cell invasion
miR-10b	HOXD10, Tiam1	Cell invasion, migration
miR-27a	HOXO1, ZBTB10	Cell viability, angiogenesis
miR-9	E-cadherin	Cell motility and invasiveness, angiogenesis
miR-22	TET family	EMT
miR-181a	Bim	EMT, cancer metastasis
miR-373, miR-520c	CD44	Cell migration and invasion
miR-375	RASD1	Cell proliferation
miR-221/222	TRPS1, ADIPOR1, p27Kip1	Cancer metastasis, tumor growth, EMT
miR-632	DNAJB6	Cancer metastasis
miR-7, miR-218	HoxB3	Cell cycle, colony formation
miR-374a	WIF1, PTEN, WNT5A	Cancer metastasis

Tumor Suppressive miRNAs associated with Breast Cancer		
MicroRNA(family)	**Identified Target**	**Function/Pathway**
let-7 family	H-Ras, HMGA2, PAK1, DIAPH2, RDX, ITGB8	Tumor initiation, cell differentiation and metastasis, cell stemness maintenance
miR-145	IRS-1, ER-α, RTKN, MUC1, OCT4, N-Ras, VEGF-A	Tumor growth, cell differentiation, invasion and metastasis, angiogenesis
miR-200 family	ZEB1, ZEB2, HER3, Sec23a, SIRT1	EMT, tumor growth and metastasis
miR-335	SOX4, tenascin C, ER-α, IGF1, RSP1, ID4	Tumor migration and invasion, cell viability and apoptosis
miR-126	IGFBP2, MERTK, PITPNC1	Metastatic angiogenesis
miR-146a/b	IL-1-RSK, NFRSF-6	Cancer metastasis
miR-30 family	Ubc9, TWF1, Vimentin, KRAS, MTDH	CSC self-renewal, cell apoptosis, EMT
miR17-20 cluster	Cyclin D1	Cell proliferation
miR-26b	SLC7A11	Cell apoptosis
miR-290	Arid4b	Cell apoptosis
miR-27b	CYP1B1	Tumor growth
miR-31	Integrin-α5, radixin, RhoA, WAVE3, PRKCE	Cancer metastasis, cell apoptosis
miR-101	Stathmin1,Janus kinase 2 (Jak2),EZH2	Apoptosis, cancer metastasis
miR-125a/b	HER2, HER3	Cell invasion
miR-203	SNAI2	EMT, cell invasion
miR-224	CDC42, CXCR4	Cancer metastasis
miR-20b	HIF-1, STAT3	Angiogenesis
miR-206	Cyclin D2	Cell proliferation

Table 1.7. Expression of miRNAs in Breast Cancer. The table summarizes the miRNAs reported to be either upregulated (OncomiRs) or downregulated (tumor suppressor miRNAs) in Breast Cancer with their target genes and the pathway it affects.

1.13. miR29 family: Role in Cancer

The miR29 family in human consists of three mature miRNAs, hsa-miR-29a, has-miR-29b-1, hsa-miR-29b-2, and hsa-miR-29c. miR-29b-1 and miR-29b-2 which bear identical mature sequences, are together referred to as miR-29b. This group of miRNAs is highly conserved in their mature sequence across different species. Mature miR-29s share identical sequences at nucleotide positions 2–7, which form their seed region. Since the seed regions are responsible for binding to the protein coding genes, the target genes for the miR29 family often overlap. The genomic localization of these miR29 family genes however is distributed in two chromosomes. In humans, the gene encoding the precursors of miR-29b-1 and miR-29a is located on chr. 7q32.3 in human, whereas the gene encoding miR-29b-2 and miR-29c is on chr. 1q32.2 (Kriegel et al., 2012). Like other miRNAs, miR29 is transcribed by RNA pol II. Experimental evidence suggests that there are several transcription factors which regulate its expression, thereby indirectly modulating the expression of its mRNA targets. Transcription profiling of miRNA expression across tumor tissues or cancer cell lines reveal downregulation of miR-29 in the majority of cancers while being upregulated in very few of them. This differential expression of miR-29 and their potential oncogenic or tumor-suppressive functions have been extensively investigated in various types of cancers (Yan et al., 2015).

miR-29 was found to be downregulated in many solid tumors and hematologic neoplasms. In the respiratory system, miR-29 expressed at a lower level in lung cancer tissue when compared with that in normal lung tissue. In Non-small cell lung cancers the entire miR29 family was downregulated (miR-29a, miR-29b, and miR-29c) (Fabbri et al., 2007). In the nervous system too, miR-29 expressed at low levels in neoplasms such as glioblastomas (and neuroblastoma. MiR-29a was reported to induce osteoblastic cell apoptosis by silencing Bcl-2 and Mcl-1 and inducing E2F1 and E2F3 expression (Yan et al., 2015). Although miR29 was majorly downregulated in most cancers it was found to be upregulated in Breast cancer tumor tissues and serum of patients mediating cell invasion and chemotherapy resistance (Wang et al., 2011; Zhong et al., 2013). This upregulation of miR29 family was also observed several rare diseases such as malignant pleural mesothelioma and diffuse large B lymphoma. Thus the expression pattern of miR29 holds importance especially in the context

of the physiological state of the cell, the cancer cell type and also on the diverse mRNA targets which in turns regulates several cellular pathways. The target genes play a decisive role to determine the fate of the tumor, either its development, progression or its inhibition.

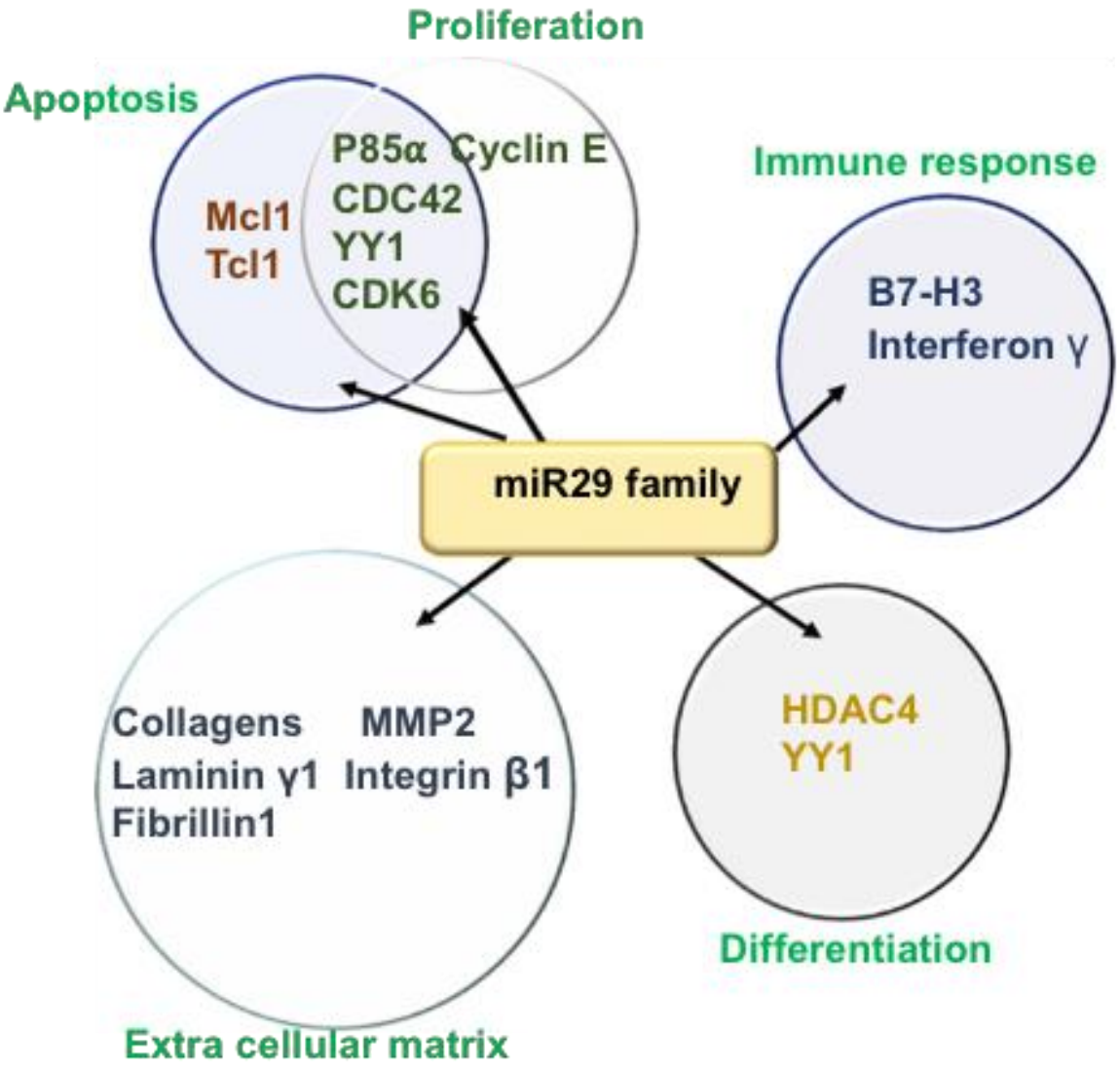

Figure 1.5. Diverse role of miR29. Several cellular processes and genes that have been reported to be targeted by miR-29s.The pathways regulated by the genes are denoted in green.

1.14. Chromatin dynamics during DNA damage: Role of histone acetyltransferase KAT5 Tip60.

As discussed earlier, the dynamicity of the chromatin structure is regulated by several factors including small RNAs like miRNAs. This dynamic structure of the chromatin is critical for almost all DNA templated processes like gene transcription, DNA replication and also DNA damage repair (Hauer and Gasser, 2017; Schneider and Grosschedl, 2007). The ATP-dependent remodeling complexes and the histone-modifying enzymes are the major two classes of enzymes known to play a critical role in the DNA damage response pathway. While the chromatin remodellers modulate the chromatin structure by the deposition or eviction of histones in an ATP dependent fashion, the histone modifying enzymes modifies the histones through the post translational modifications, thereby altering the chromatin landscape. One of the most critical enzyme involved in the DNA damage repair pathway is KAT5 (Tip60) acetyltransferase which is part of the evolutionarily conserved multi-subunit NuA4 complex. Scientific evidences suggest that this acetyltransferase plays a critical role in DNA damage repair pathway through both transcription-dependent and transcription-independent mechanisms (Ikura et al., 2000; Squatrito et al., 2006). The acetyltransferase activity of KAT5 (Tip60) is required for the activation of ATM (an important kinase) which is involved in the phosphorylation of several DNA damage response proteins, such as nbs1, p53, chk2 and SMC1. Considering the role of Tip60 in maintaining genome integrity and cellular homeostasis, it has been reported to express aberrantly in various cancers including prostate, breast and colorectal cancer. These findings suggest that Tip60 might affect the efficiency of DNA damage repair pathway and also in the progression of cancers (Bassi et al., 2016; Sapountzi et al., 2006).

Among the different kinds of DNA damage, double strand breaks appear to be the most deadly one. The cell has designed two pathways to counteract this damage mainly by Non homologous end joining repair (NHEJ) and the Homologous Recombination repair pathway (HR). Tip60 is recruited at the DNA damage site at double strand breaks in the genome signifying its role in the repair pathway. It acetylates ATM protein kinase which is activated upon ionizing radiation in mammalian cells. Upon DNA damage, ATM undergoes rapid autophosphorylation on ser1981 converting it to an active form. The acetylation of ATM by

KAT5 Tip60 is necessary for its activation and the ATM-dependent phosphorylation of H2AX, p53 and ChK2. Thus the HAT activity of Tip60 is crucial for ATM activation, a key step for DNA repair. It is thus very important that Tip60 is recruited at the DNA damage sites and acetylate ATM. Further understanding of this phenomenon revealed that the chromo-domain of Tip60 specifically bind to the histone H3 trimethylated lysine 9 (H3K9me3) (Sun et al., 2009). This direct binding of Tip60 to H3K9me3 at double strand breaks acts as an allosteric regulator and activates the Tip60 acetyltransferase activity during DNA repair. Additionally access to H3K9me3 by Tip60 is dependent on the DNA damage induced release of HP1β (heterochromatin protein 1β) from H3K9me3. Upon DNA damage HP1β gets quickly phosphorylated by casein kinase 2 (CK2). This phosphorylated HP1β then disassociates from H3K9me3 allowing Tip60 to interact with H3K9me3 (Dinant and Luijsterburg, 2009; Sapountzi et al., 2006). Additionally, the Mre11-Rad50-Nbs1 (MRN) complex facilitates the binding of Tip60 to the proper site in H3K9me3 (Figure 1.6)

The activation of Tip60 thus follows a novel mechanism involving direct interaction between methylated histones and Tip60's chromodomain, signifying the importance of chromatin structure in DSB repair. This suggest that any alterations in the global histone methylation patterns would affect the activity of KAT5 (Tip60) and thereby its regulation of DNA repair pathway.

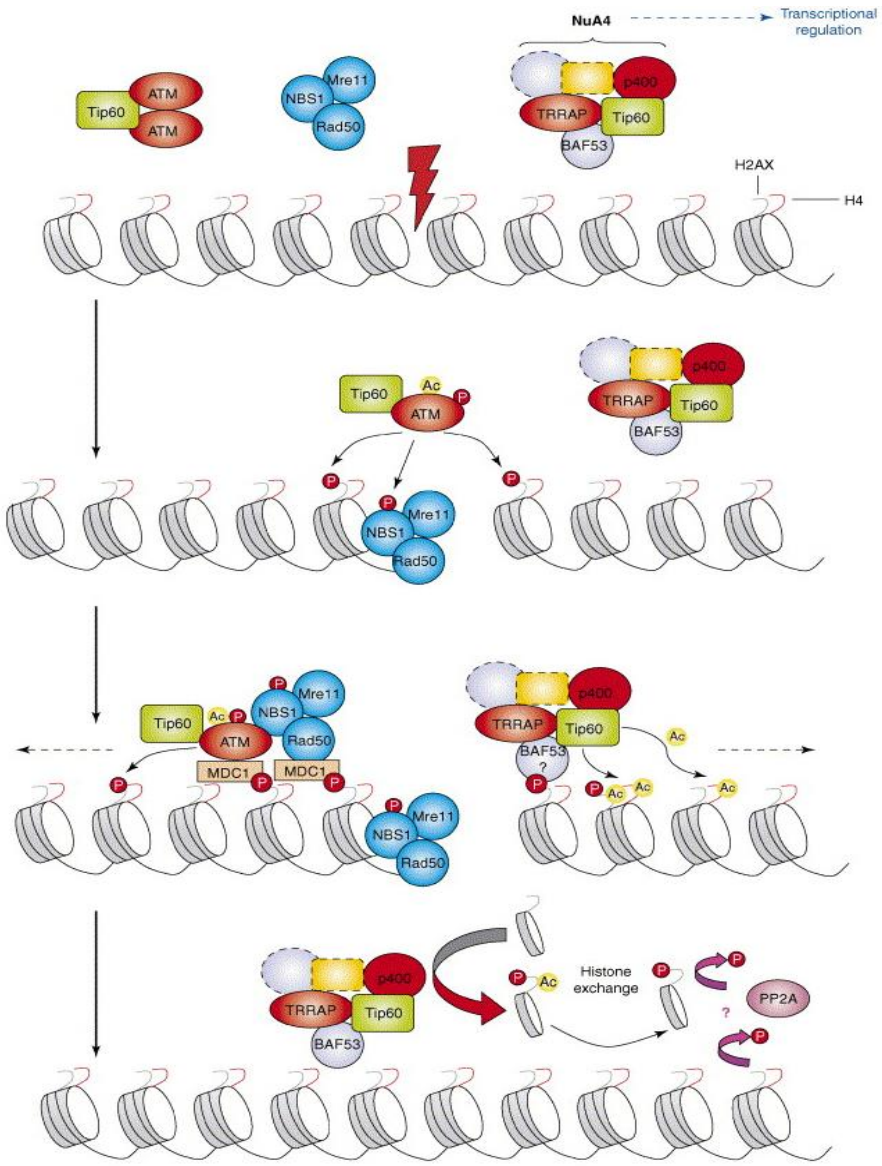

Figure 1.6. Putative model depicting the role of Tip60 in DNA damage repair pathway. Upon the formation of a DSB, the MRN complex (Mre11–Rad50–NBS1) is rapidly recruited to the damaged site and recruits ATM. Tip60 is thought to acetylate ATM, which subsequently autophosphorylates, although the relationship between MRN and Tip60 in ATM activation remains unclear. ATM, in turn, phosphorylates many different substrates (additional ATM molecules, NBS1, H2AX, p53 and others). Phosphorylated H2AX (or γ-H2AX) acts as a docking platform to engage MDC1 and other DDR proteins to spread the signal further downstream from the DSB. The Tip60-containing NuA4 complex might also recognize γ-H2AX, possibly through the BAF53 subunit, facilitating Tip60-mediated acetylation of histone H4 and of γ-H2AX itself. Figure adapted from (Squatrito et al., 2006).

1.15. Multifunctional Human non-histone Chromatin protein, PC4:

Human positive coactivator 4 (PC4) is a multifunctional non-histone chromatin associated protein which was isolated from Upstream Stimulatory Activity fraction (USA). It is a 14 kDa highly abundant nuclear protein involved in several cellular functions. This 127 amino acid long protein has a highly unstructured N-terminal domain (1-62) and a highly structured C-terminal domain (62-127) (Brandsen et al., 1997). A stretch of a Lysine rich domain (LYS) separates the two serine rich acidic at the N-terminus of the protein. PC4 contains a dimerization region and a single-stranded DNA-binding domain (ssDBD) in its C-terminal half. This ssDBD domain facilitates the binding of PC4 with high affinity to melted dsDNA or ssDNA. (Werten et al., 1998).

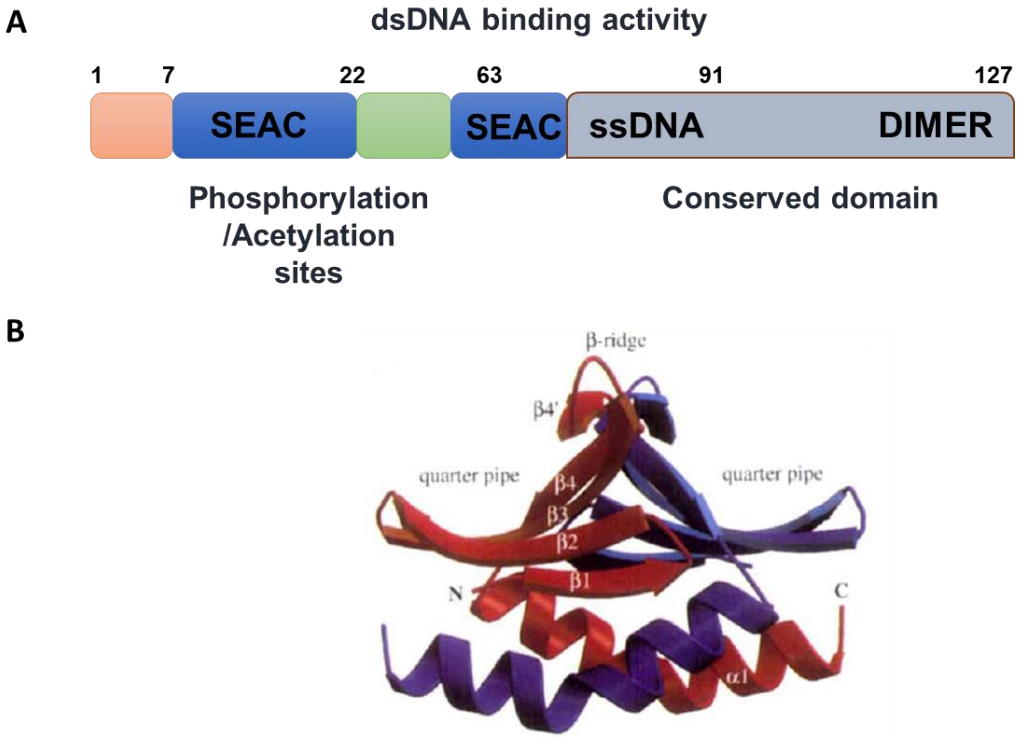

Figure 1.7. Model of the structure of Positive co activator domain wise (A) Schematic Representation of the different regions of Human Positive co activator 4 PC4 indicating each of their function; Figure adapted from S Debnath, et.al, 2011. (B) Ribbon diagram of the $PC4_{CTD}$ dimer with monomers shown in pink and blue Figure adapted from Brandsen, et al, 1997.

Although PC4 was a discovered as a transcriptional coactivator which enhances activator dependent RNA polII mediated transcription, studies over the years have revealed various cellular functions of PC4 its role in other DNA-templated processes like replication, repair, chromatin organization, neurogenesis and in cancers (Figure 1.8). In the context of the present study we here focus majorly on the role of PC4 as a genome organization maintaining genome stability and its role in oncogenesis.

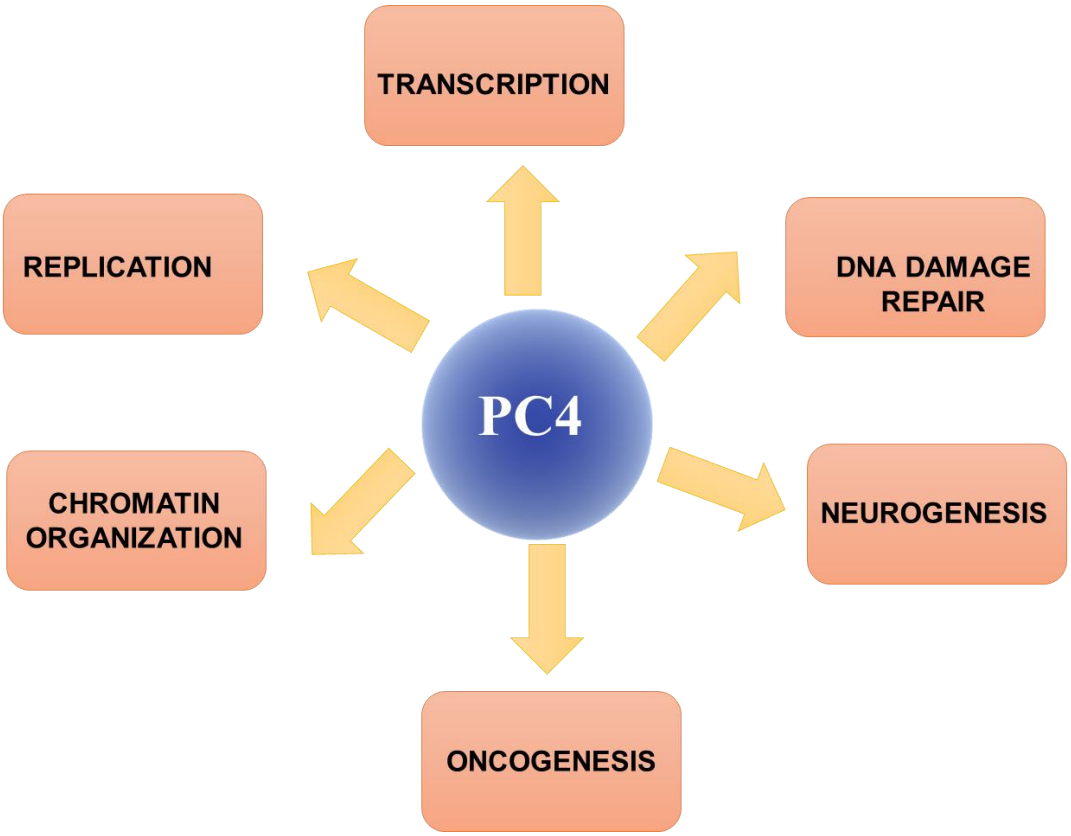

Figure 1.8. Multifunctional non histone chromatin associated protein PC4. The schematic diagram summarizes the major cellular processes regulated by PC4.

PC4 as a transcriptional coactivator:

PC4 acts as a general transcriptional coactivator that can interact with transcriptional activators like VP16, Tat, CTF1, NFκβ, Sp1, BRCA1, SMYD3 and AP2 and bring about activator dependent transcription(Ge and Roeder, 1994; Kannan and Tainsky, 1999; Liao et al., 2011). PC4 binds to free DNA or DNA bound to TFIIA and TBP complex but not with TBP alone. It binds to the promoter in conjunction with TFIID and TFIIA and brings about the activator dependent transcription. Repression of basal transcription initiation by PC4 in absence of TAFs and TFIIH has also been reported (Werten et al., 1998). This transcriptional repression was relieved by the ERCC3 helicase activity of TFIIH (Fukuda et al., 2004). Thus PC4 plays dual role of both stimulating basal transcription as well as it can inhibit transcription through its ssDNA-binding activity as mentioned above. The function of PC4 is not only restricted to RNA PolII transcription but it also plays a pivotal role in RNAPIII mediated transcription termination and reinitiation (Wang and Roeder, 1998). Thus the differential DNA binding property of PC4 determines its inhibitory or activation role in context of transcription.

PC4 as a chromatin organizer:

Earlier studies from our laboratory establish the role of PC4 in chromatin compaction. PC4 was found to be tethered to the chromatin and was present in the nucleosomal fraction. It was broadly distributed on metaphase chromosome except the centromeric region and remains attached to the chromatin throughout the cell cycle. PC4 is also shown to directly interact with core histones preferably histone H3 and H2B in vitro. This interaction with the histones brings about its chromatin condensation ability (Das et al., 2006). Detailed analysis of the interaction showed that the globular domain of histone H3 or H2B is the preferential docking site of PC4. PC4 folds the chromatin into a very distinct type of higher-ordered globular structure unlike that of the linker histone H1-induced folded fiber. siRNA mediated knockdown of PC4 resulted in the opening up of chromatin , alters gene expression pattern and also lead to G2/M cell cycle arrest (Das et al., 2010). Furthermore PC4 might form complexes with other hetrochromatinizing protein or non-coding RNA to bring about the genome wide compaction of the DNA.

PC4 in the maintenance of genome stability:

The yeast homologs of PC4 (SUB1) as well as PC4 have been shown to protect DNA from oxidative stress. This study gave a clue that PC4 might play greater roles beyond transcription process. PC4 is known to be recruited at the site of double strand DNA breaks soon after exposure to DNA damage conditions (Mortusewicz et al., 2008). Later studies in the field shows that it is involved both in the process of Non-homologous end joining as well as HR repair pathway by directly interacting with the repair proteins like Ku80, XPG, XRCC4, etc (Batta et al., 2009; Mortusewicz et al., 2016). Deletion of Sub1 results in elevated mutagenesis caused by cytosine deamination, particularly at gene promoters, suggesting genome protector role of Sub1(Wang et al., 2004). A very recent study shows that Sub1/PC4 can bind to G-quadruplex DNA in vitro(Garavís and Calvo, 2017) and thereby suppressing the process of genome instability. It is interesting to note that all these functions of PC4 in mediating DNA repair and genome stability is brought about through its ssDNA binding domain. Mutations at this domain of PC4 fail to function in the DNA repair pathway.

Post translational modifications of PC4:

Post translational modifications of PC4 play a major role in determining its function. The two extensively studied modifications are phosphorylation and acetylation. Phosphorylation of PC4 is mediated by CKII at seven predicted phosphorylation sites in its N terminal domain (Ge et al., 1994). It can also be phosphorylated by TFIIH and TAFII250 subunit of TFIID in the PIC complex. Phosphorylation of PC4 negatively regulates its transcriptional coactivator function (Ge et al., 1994). Recent study from our laboratory suggests that PC4 is a substrate for Aurora A and B kinase (Dhanasekaran et al., 2016). This phosphorylation in turn activates the kinase which then functions to carry out several mitotic events. Deficiency in phosphorylation by Aurora kinases results in various cell cycle defects. Thus apart from the transcriptional coactivator function, phosphorylation of PC4 by different kinases mediates its different physiological functions. Acetylation of PC4 results in antagonistic behavior of PC4 to its phosphorylation. Acetylation of PC4 is brought about by p300 which enhances the double strand DNA binding ability of PC4 while phosphorylation abolishes it(Kumar et al., 2001).The role of p300 mediated acetylation of PC4 might be further relevant to its transcriptional coactivation property. PC4 is known to interact with p53 and helps in its

transactivation property. This role of PC4-p53 interaction and regulation of p53 resposnive gene expression is further elevated by the acetylation of PC4 by p300 (Banerjee et al., 2004; Batta and Kundu, 2007).

PC4 in cancer:

SUB1 interacts with a multitude of transcription factors such as VP16, GAL4, AP2, HIV-TAT, P53 and SMYD3 thus modulating their expression and regulating a repertoire of genes. Dysregulation of this protein thus might mediate the expression of a completely different cascade of genes leading to pathophysiological state such as cancer. Studies indicate that SUB1 is overexpressed in multiple cancer types such as non-small cell lung cancer, lymphangiogenesis, lung adenocarcinoma, astrocytoma, prostate cancer (Chakravarthi et al., 2016; Chen et al., 2014; Kim et al., 2015; Tao et al., 2015). Overexpression of PC4 elevated the levels VEGF-C, VEGF-D and VEGFR-3 during the development of lymphangiogenesis and lymphatic metastasis in lung adenocarcinoma. PC4 also acts as a transcriptional coactivator for SMYD3 thus regulating the expression of SMYD3-mediated transactivation of growth/invasion-stimulatory genes in cancer cells.

Despite being overexpressed in majority of cancers, its putative tumour suppressor role cannot be overlooked. It interacts with AP2 α and inhibits AP2 transcriptional interference in *ras* transformed cell line. (Kannan and Tainsky, 1999). Its ability to interact and enhance the function of p53, a tumor suppressor protein, in vivo can also be interpreted as tumour suppressor activity of PC4. (Banerjee et al, 2004).Not only does the interaction of PC4 and p53 is critical for PC4-mediated activation of p53, but also the DNA bending ability of PC4 significantly contributes in the enhancement of DNA binding of p53 to its cognate sites. Thus the role of PC4 in mediating oncogenesis primarily lies in the cancer cell type, the expression pattern of PC4 and the repertoire of genes expressed in the particular cellular context.

1.16. Rationale of the study

Dynamic alteration of the chromatin organization is the fundamental driving force in the process of life. As discussed in the previous sections of this chapter, there are a multitude of factors which regulate the dynamicity of the chromatin. There are several highly abundant nuclear proteins which are not the component of core nucleosomes but dynamically interact with the chromatin fiber and thereby plays pivotal role in the process of chromatin condensation and decondensation. The non-histone chromatin associated protein PC4, is one such protein which is known to be closely associated with nucleosomes and condenses the chromatin fibre (Das et al., 2006). Earlier work from our laboratory suggests that in absence of PC4 the chromatin undergoes decondensation (Das et al., 2010). More recently, our laboratory has found that PC4 is absolutely essential protein critical for life. PC4 knockout is found to be embryonically lethal. However knocking out PC4 specifically in brain leads to defects in neurogenesis and memory extinction process (Swaminathan et al., 2016).

These findings collectively encouraged us to investigate the fundamental physiological role of PC4 in the cellular context so that the molecular pathway could be deciphered. Besides elucidating the physiological role of PC4, it is also important to investigate its role under pathophysiological role. PC4 is known to aberrantly express in multiple cancer types. It also interacts with tumor suppressor such as AP2 α and p53 (Banerjee et al., 2004; Kannan and Tainsky, 1999), thus signifying critical role in the process of oncogenesis. Besides being a transcriptional co-activator , and aiding in DNA replication it facilitates both non homologous end joining repair (NHEJ) as well as homologous recombination (HR) repair pathway (Batta et al., 2009; Mortusewicz et al., 2016). In this study we make an attempt to understand the role of PC4 in context of genome integrity and cancer progression in greater detail. Thus considering this background information the objectives of this study are made.

1.17. Objectives of the study

- **Understanding the physiological Role of Chromatin Protein PC4 in cellular survivability:** In this study we elucidate the role of PC4 in the cellular context through the knockdown approach by establishing as stable PC4 knockdown HEK293 cell line. The objective of this study is to characterize the role of PC4 in the context of genome organization, gene expression and cellular survivability.

- **To determine the State of PC4 Expression in Breast cancer and its possible mechanism of regulation**: Unlike many other cancers, PC4 was found to be downregulated in 65% Breast cancer patient samples. The second part of the study, aims to understand the regulation of PC4 expression and its consequences in Breast cancer manifestation.

- **To elucidate the role of Post translational modification (acetylation) of PC4 in genomic stability:** PC4 is an important factor responsible for DNA repair pathways and genome stability. In this objective we aim to understand the physiological consequence of acetylation of PC4 by the DNA damage responsive acetyltransferase Tip60.

Chapter 2: Materials and methods

This chapter presents a brief overview of the materials and experimental procedures used in this study.

2.1. General Methods

2.1.1. Preparation of competent cells

To prepare bacterial *E. coli* strains: BL21 (DE3), Rosetta(DE3)pLysS, DH5α, XL1-Blue, XL10-Gold cells were first streaked on Luria broth (10 gm/l tryptone, 5 gm/l yeast extract, and 10 gm/l NaCl) + 1.5% agar culture plates from respective frozen glycerol stocks. The streaked plates were incubated ~12 hours at 37 °C. Inoculation of a single colony was done into 10 ml Luria Broth (LB) containing 10 mM MgCl2 and 10 mM MgSO4. The culture was then grown at 37 °C in an incubator shaker for 12-16 hours. From this primary culture, 1% inoculum was then inoculated into 100 ml of LB. The secondary culture was grown 37 °C in an incubator shaker till the OD600 reached 0.35-0.4 (mid log phase). The secondary culture was immediately chilled to 4 °C and pelleted at 3000g for 10 minutes at 4 °C. This pellet was then resuspended in 12 ml TFB1 (30 mM potassium acetate pH 7.5, 100 mM KCl, 10 mM $CaCl_2$, 15% glycerol) and incubated for 60-90 min at 4 °C. After the incubation, the cells were pelleted at 3000g for 10 minutes at 4 °C. The pellet was resuspended in TFB2 (10 mM Na-MOPS, pH 6.8, 10 mM KCl, 75 mM CaCl2, 15% glycerol), made aliquots and flash-frozen in liquid nitrogen.

2.1.2. Transformation of competent cells

For transformation of ~50 ng of purified plasmid DNA an aliquot of *E. coli* competent cells were thawed on ice and purified plasmid DNA was added. The competent cells in the presence of DNA were incubated for 25 minutes on ice; following this a heat shock at 42 °C was given for 90 seconds. The cells were then immediately chilled on ice for 5 minutes. LB was added to the cells and the cells were allowed to recover at 37 °C in and incubator shaker for around 45 minutes to 1 hour. The transformed cells were subsequently spread over an

LB-agar plate containing the appropriate selection antibiotic. The plated cells were then incubated at 37 °C for 12-16 hours

2.1.3. DNA purification

Plasmids amplified in DH5α, XL10-Gold or XL1-Blue, were isolated using the QIAprep Spin Miniprep Kit (Qiagen) as per the manufacturer's protocol. The quality and quantity of the DNA purified was checked on agarose gels and the NanoDrop 1000 (Thermo Scientific). PCR amplicons and restriction enzyme digested products were purified from agarose gels using the Sigma GenElute Gel Extraction Kit following the manufacturer‟s protocol. The purified DNA was quality check and quantification was done on the NanoDrop 1000 (Thermo Scientific) by measuring the absorbance at 260 nm of 1 µl of the DNA sample. A260 of the value 1 corresponds to 50 ng/µl.

2.1.4. Agarose gel electrophoresis

Agarose (Sigma) gels of the percentage 0.8-1.5% were prepared in 1X TBE (90 mM Tris-Borate and 2mM EDTA, pH 8.3), to separate nucleic acids (DNA/RNA) by size. The nucleic acid samples were prepared in 6X loading buffer (0.25% bromophenol blue, 0.25% xylene cyanol, 30 % glycerol) to a final concentration of 1X. The samples were loaded into the gel wells submerged in 1X TBE buffer. The gel was run at 5V/cm. The agarose gel was stained in 0.5 mg/ml Ethidium Bromide (EtBr) solution and destained in water. The EtBr stained DNA/RNA samples were visualized and imaged under a UV illuminator in the BIO-RAD Gel Documentation System.

2.1.5. SDS-polyacrylamide gel electrophoresis (SDS-PAGE)

Proteins, either recombinant or cell lysates, were resolved on 8-15% SDS-PAGE, depending on their molecular weight. The resolving portion of the gel was made by adding the required volume (depending on the desired gel %) of 30% solution of acrylamide/ bisacrylamide (29% acrylamide, 1% bisacrylamide), 0.375 M Tris-HCl pH 8.8, 0.1% sodium dodecyl sulphate (SDS), 0.1% ammonium persulphate (APS) and 0.04% TEMED (N,N,N‟,N‟-tetramethylethylenediamine). The stacking portion of the gel was made by adding 5%

acrylamide, 0.125 M Tris-HCl pH 6.8, 0.1% SDS, 0.1% APS and 0.1% TEMED. The protein samples were prepared in 5X SDS gel loading buffer (50 mM Tris-HCl pH 6.8, 2% SDS, 0.1% bromophenol blue, 10% glycerol, 1% β-mercaptoethanol) to a final concentration of 1X. The samples were boiled at 90 °C for 5-10 minutes and loaded into the wells of the gel, mounted on a vertical electrophoresis system (Mini-PROTEAN® Tetra Vertical Electrophoresis Cell, BIO-RAD). The gels were run electrophoresis buffer consisting of 25 mM Tris, 250 mM glycine pH 8.3, 0.1% SDS, at a constant voltage of 150V. The protein bands were stained with Coomassie Brilliant Blue (CBB) staining solution (40% methanol, 10% acetic acid, 0.25% CBB). Once the gels were stained the excess background staining was removed using destaining solution consisting of 40% methanol and 10% acetic acid. The gels were imaged and dried for storage. In order to successfully resolve the different forms of LC3B protein, the cell lysates were loaded on a 15% SDS PAGE and then electrophoresed for about 1.5 hours followed by western blotting with specific antibodies to identify the different forms.

2.1.6. Silver Staining

To detect proteins on a polyacrylamide gel with high sensitivity (in the nanogram range), silver staining of gels is preferred over CBB staining. The proteins are electrophoresed on a polyacrylamide gel followed by fixing in 40% methanol and 10% glacial acetic acid in water. The gel was allowed to fix for 2 hours to overnight. The gel was then rinsed thrice in 50% ethanol in water. The proteins were sensitized with 0.02% sodium thiosulfate for 2 minutes then rinsed in deionized water for a minute. The gel was then incubated with 0.1% silver nitrate for 20 minutes at room temperature. The gels were then rinsed thrice with deionized water. The gel was developed in freshly prepared 0.04% formalin/2% sodium carbonate (~4-20 minutes). The reaction was stopped in 1% glacial acetic acid. The gel was imaged and then stored in 1% glacial acetic acid.

2.2. Cloning

2.2.1 Cloning of miRNAs

The pre-miR sequences of miRNA 29a, 29b and 29c were cloned into pSUPER vector. The pSUPER RNAi system provides a mammalian expression vector that guides intracellular

synthesis of mature miRNAs from the precursor. The vector uses the polymerase-III H1-RNA gene promoter, as it produces a small RNA transcript lacking a polyadenosine tail and has a well-defined start of transcription and a termination signal consisting of five thymidines in a row (T5). Most important, the cleavage of the transcript at the termination site is after the second uridine, yielding a transcript resembling the ends of synthetic siRNAs, which also contain two 3' overhanging T or U nucleotides (nt). Forward and reverse oligonucleotide sequences of miR 29 family (Sigma) were obtained and these were then annealed. pSUPER vector was double digested with BglII and HindIII and then ligated with the respective annealed oligonucleotides. Ligation was carried out at room temperature for 8hrs. Plasmids were isolated from positive colonies obtained on LB Amp plates and they were digested with EcoRI and HindIII to confirm the clones by insert release (Figure 2.1). The clones were further confirmed by sequencing.

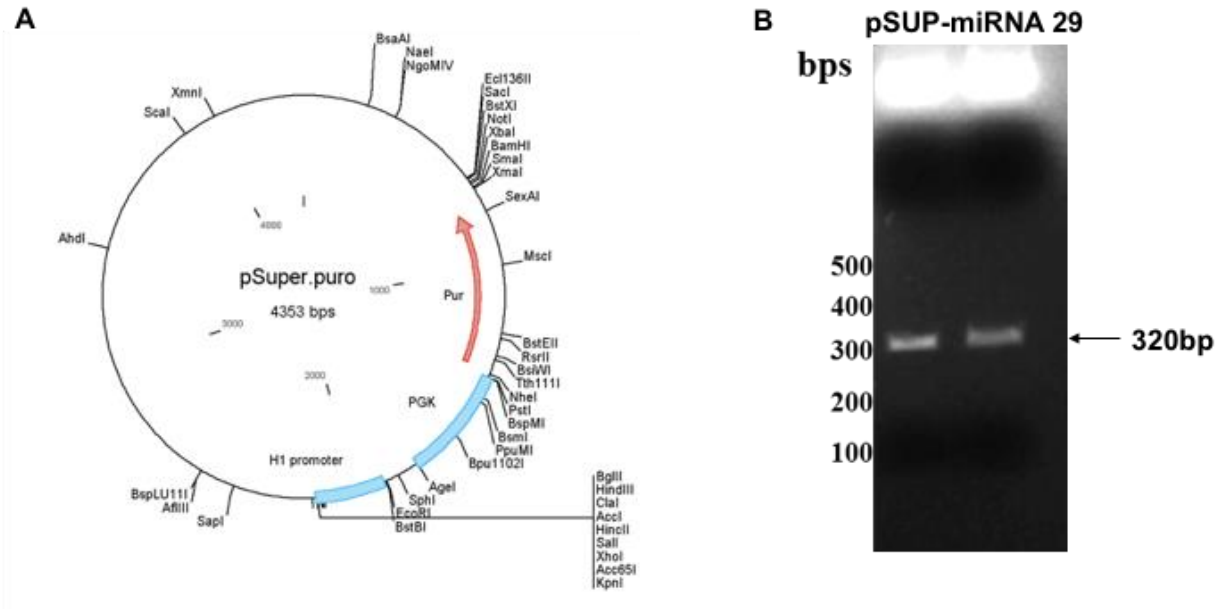

Figure 2.1. Cloning of pre-miRNA constructs into pSUPER Mammalian Expression Vector. (A) Vector Map of pSUPER Mammalian Expression Vector**.** Cloning of (B) miR29 into the pSUPER Mammalian Expression Vector. Clones were confirmed by double digestion with HindIII-HF and EcoRI-HF restriction enzymes (New England Biolabs) with an insert release of 320bp

2.2.2 Generation of acetylation site mutants (K-R) using PC4-His6 as a template in bacterial expressing vector:

Site directed mutagenesis technique was employed to create point mutations replacing lysines to arginine at sites acetylated by Tip60 obtained from the analysis of mass spectrometry as described previously. Quick Change II XL site directed mutagenesis kit (Agilent technologies) was used for this purpose. The schematic illustrating the protocol of site directed mutagenesis is shown in figure. Briefly mutagenic primers were designed and PCR was set up using these and taking 50ng of PC4-His_6 as the template DNA. PCR conditions were followed as given in the table below. The PCR product was incubated with DpnI for 1 hour at 37ºC to digest the original template DNA (wild type PC4-His_6).Transformation of the digested product was done in *E.coli* XL10 Gold Cells. Colonies were screened for the desired mutation and confirmed by sequencing (Figure 2.3).

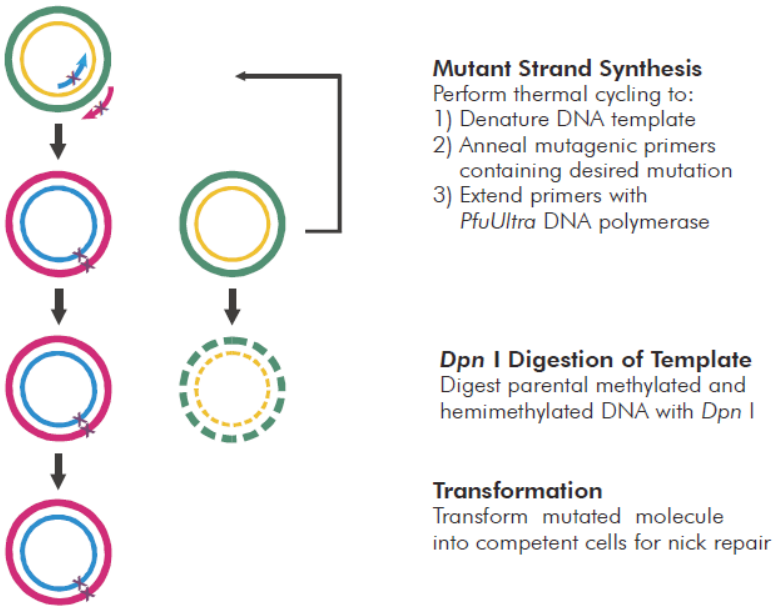

Figure 2.2. Overview of the site directed mutagenesis method (Adapted from QuickChange II X_L site directed mutagenes kit, Agilent Technologies)

Site	Forward Primer (5'-3')	Reverse Primer (5'-3')
K5R	ACCATGCCTAAATCAAGAGAACTTG TTTCTTCAAGCTCTTCTGGC	GCCAGAAGAGCTTGAAGAAACAAGTTC TCTTGATTTAGGCATGGT
K80R	5'GGTACGTTAGTGTTCGCGATTTTA AAGGCAGAGTGCTAATTGATAT	5'AATATCAATTAGCACTCTGCCTTTAAA ATCGCGAACACTAACGTACC
K101R	TGAAGGTGAAATGAAACCAGGAAGA AGAGGTATTTCTTTAAATCCA	TGGATTTAAAGAAATACCTCTTCTTCCT GGTTTCATTTCACCTTCA

Table No.1: Sequences of mutagenic primers used for SDM

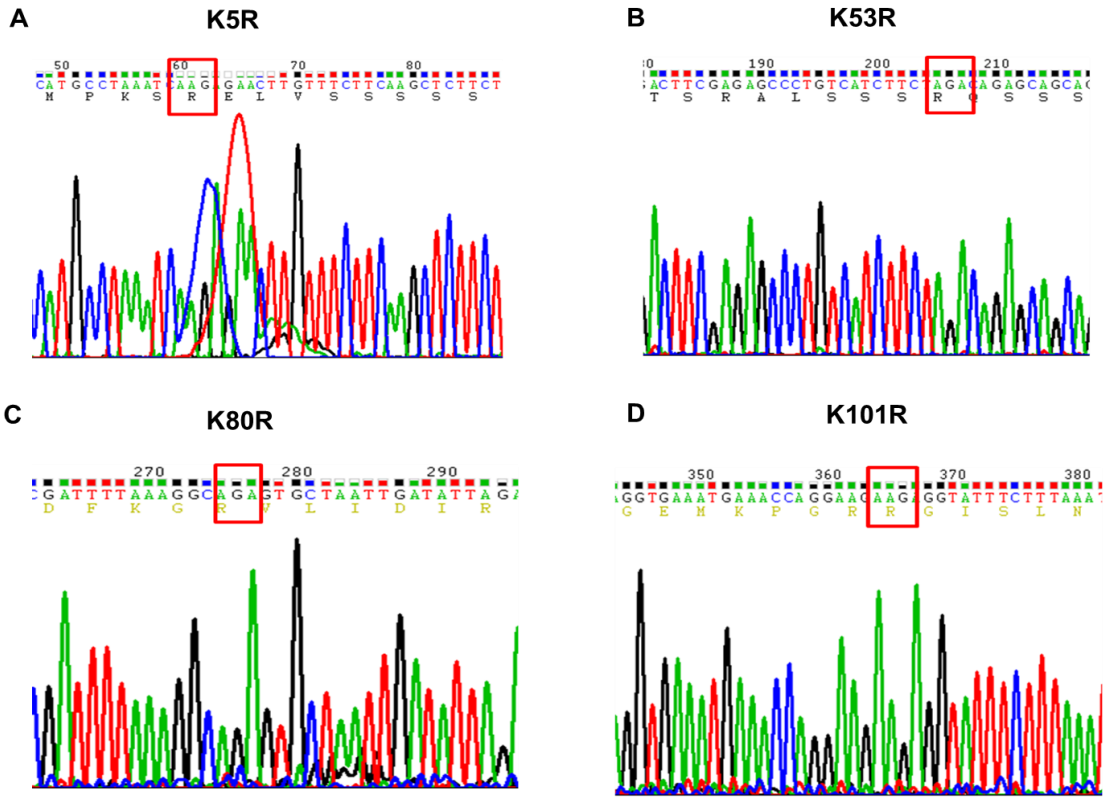

Figure 2.3. Introduction of single amino acid changes into wildtype PC4 construct in the in the pET22b bacterial expression plasmid. Chromatogram representation of all lysine mutants of PC4 generated through site directed mutagenesis. Red square indicates the altered codon to obtain mutant amino acid. The K53R mutant was generated previously in the laboratory (Kumari S, et.al, Kundu TK unpublished).

2.3. Cell culture

2.3.1. Mammalian cell culture

MCF7 (mammary gland carcinoma cells isolated from metastatic site: pleural effusion) and HEK293 (human embryonic kidney) cells were procured from American Type Culture Collection (ATCC) (Figure 2.4A,C). ZR751 cells, a human breast carcinoma cell line derived from the derived from metastatic site: ascites, was a kind gift from Dr. Amit Dutt (ACTREC, Mumbai, India) (Figure 2.4B). ZR751 cells were grown in RPMI-1640 media, MCF7 cells were grown in Minimum Essential Media (MEM) and HEK293 cells in Dulbecco's Modified Eagle's Media. Each of these media was supplemented with 2 mM glutamine, antibiotic solution (penicillin, streptomycin, amphotericin) and 10% fetal bovine serum (FBS). The cell stocks were stored in liquid nitrogen. The growth medium for MCF7 cells was also supplemented with 0.01 mg/ml human recombinant insulin in addition to the basic media requirements. To revive the cell lines, the stocks were quickly thawed in 37 °C waterbath, then the stocks were diluted 10 times in supplemented media containing 10% FBS (complete media). The cells were pelleted at 1000 rpm for 3 minutes at room temperature. The pelleted cells were resuspended in 5 ml of fresh complete media and seeded into a T25 flask (eppendorf). The cells were grown in a monolayer in complete media, with fresh media supplemented every 2-3 days. The cells were grown at 37 °C, 5% CO2 in a humidified incubator. When the cells reached a confluency of 80% they were passaged by removing the spent media. The cells were gently washed with 1X PBS (Hi-Media, cell culture grade) to ensure all the media was removed, following which 1 ml of 0.25% Trypsin-0.53 mM EDTA was added to the cells and incubated at 37 °C in the CO2 incubator till the cells detached from the flask polystyrene growth surface. The trypsinization process was stopped in fresh complete media. The cells were collected and pelleted at 1000 rpm for 3 minutes. The cells were pelleted in complete media, counted using a hemocytometer (Neubauer"s Chamber) and seeded for experiments in the desired numbers. For cell stock preparation, the cells were trypsinized and collected as mentioned before. The cells were then resuspended in freezing mixture (40% incomplete media, 50% FBS and 10% DMSO) for MCF7 cells (35% incomplete media, 50% FBS and 5% DMSO), distributed into cryovials and stored in -80 °C,

in cell freezing containers where the cell stocks freeze slowly (-1 °C/ min). After 24 hours the frozen stocks were then transferred to liquid nitrogen storage cylinders.

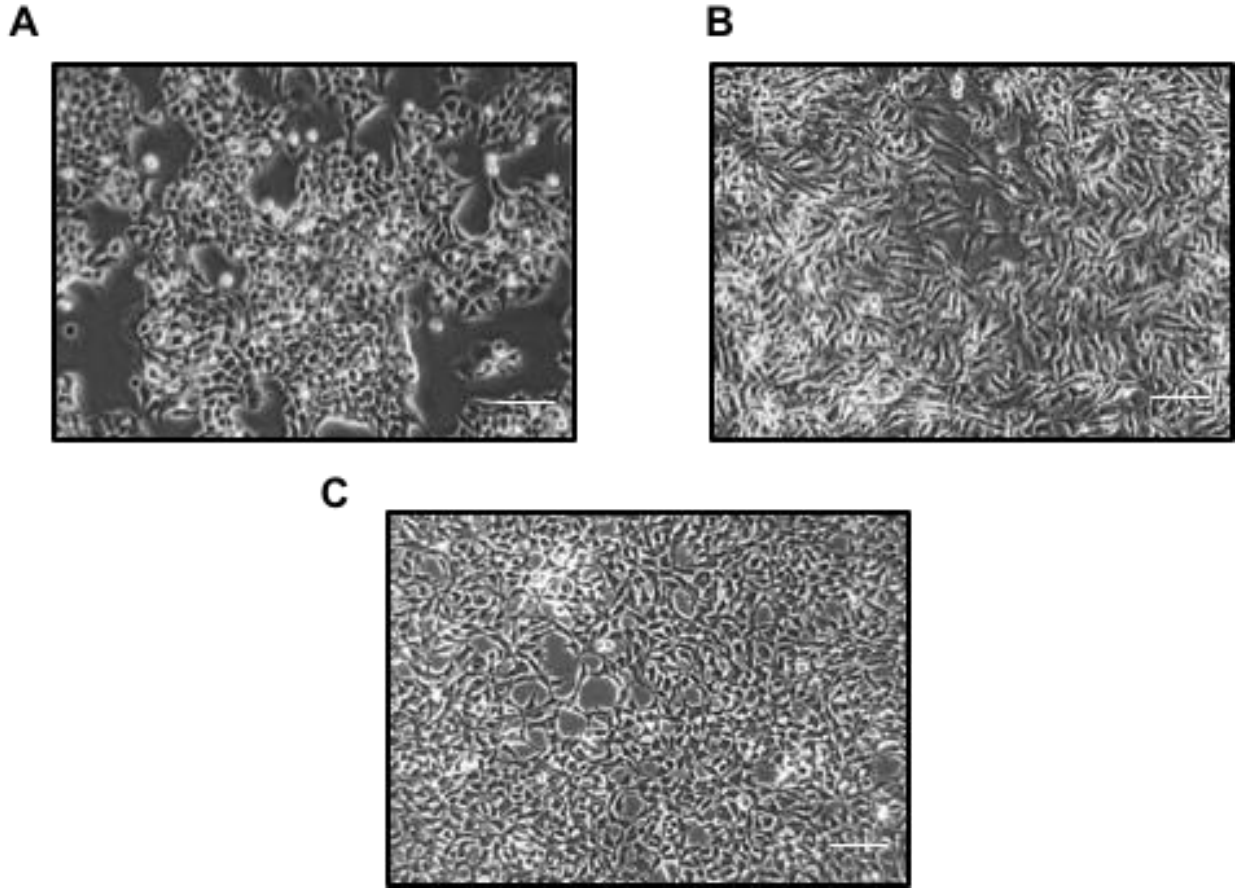

Figure 2.4. Morphological features of mammalian cells grown in a monolayer.
(A) MCF7, (B) ZR751, (C) HEK293 imaged at 10X magnification. Scale bar represents 100 µm.

2.3.2. Transfection

HEK293/MCF7/ZR751 cells were transfected with purified mammalian expression plasmids using the Lipofectamine2000 reagent (Invitrogen) as per the manufacturer's protocol. The DNA dissolved in incomplete media and Lipofectamine2000 in incomplete media were mixed in a 1:1 (v:v) ratio. The DNA-Lipofectamine complex was allowed to stand for 25 minutes before adding it to the cells in incomplete media. The incomplete media was replaced with fresh complete media after 6 hours post transfection

2.3.3. Generation of stable cell lines

2.3.3.1 Generation of PC4 Knockdown HEK293 cell line

HEK293 cells constitutively expressing shRNA (Clone ID: V3LHS_331786, Dharmacon pGIPZ shRNA; Mature sequence: TTTTCTGGAGCAACTTGCT) against the ORF of PC4 mRNA was established to make a PC4 knockdown cell line. This was generated using 10 µg pGIPZ lentiviral shRNAs targeting PC4 and helper plasmids (5 µg psPAX2, 1.5 µg pRSV-Rev, 3.5 µg pCMV-VSV-G). 10 µg of sh-plasmid was mixed with helper plasmids (5 µg psPAX2, 1.5 µg pRSV-Revs, 3.5 µg pCMV-VSV-G) and were co transfected into HEK293T cells using calcium phosphate method. 48 hours post transfection media containing assembled virus was collected and its titre was estimate (Figure 2.5 A). Desired cell line (here HEK293) was infected with 10^5 IU/ml virus. The rest of the virus aliquots were stored in -80°C. Infected cells were subjected to selection pressure 72 hours post transfection. Cells were fist sorted for positive GFP signals and the GFP sorted cells were grown in presence of 3 µg/ml puromycin for three passages to establish the cell line. To validate the extent of knockdown, PC4 levels were checked both at protein and mRNA level and compared against the wild type HEK293 cells.

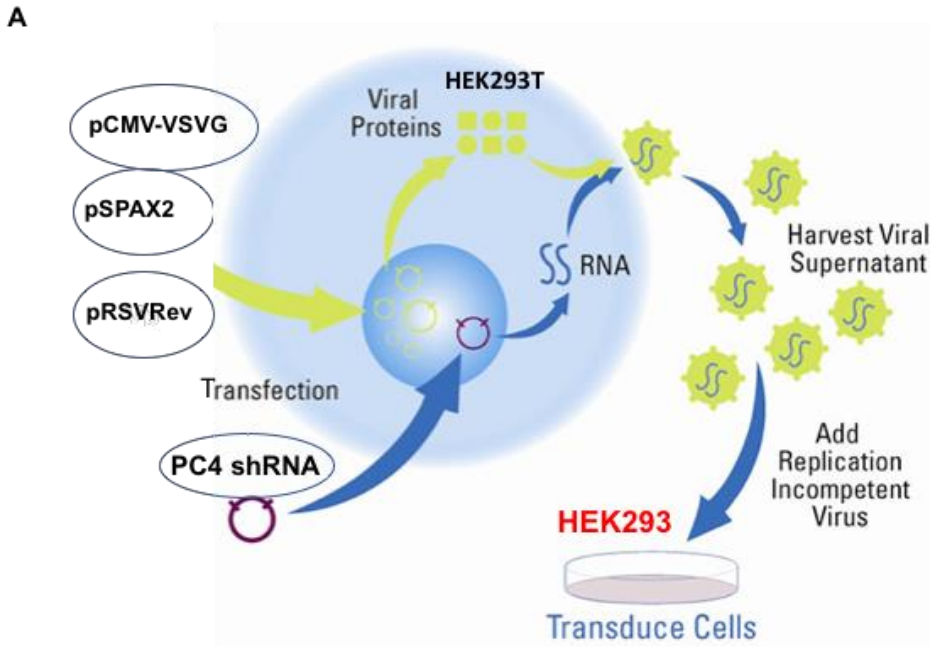

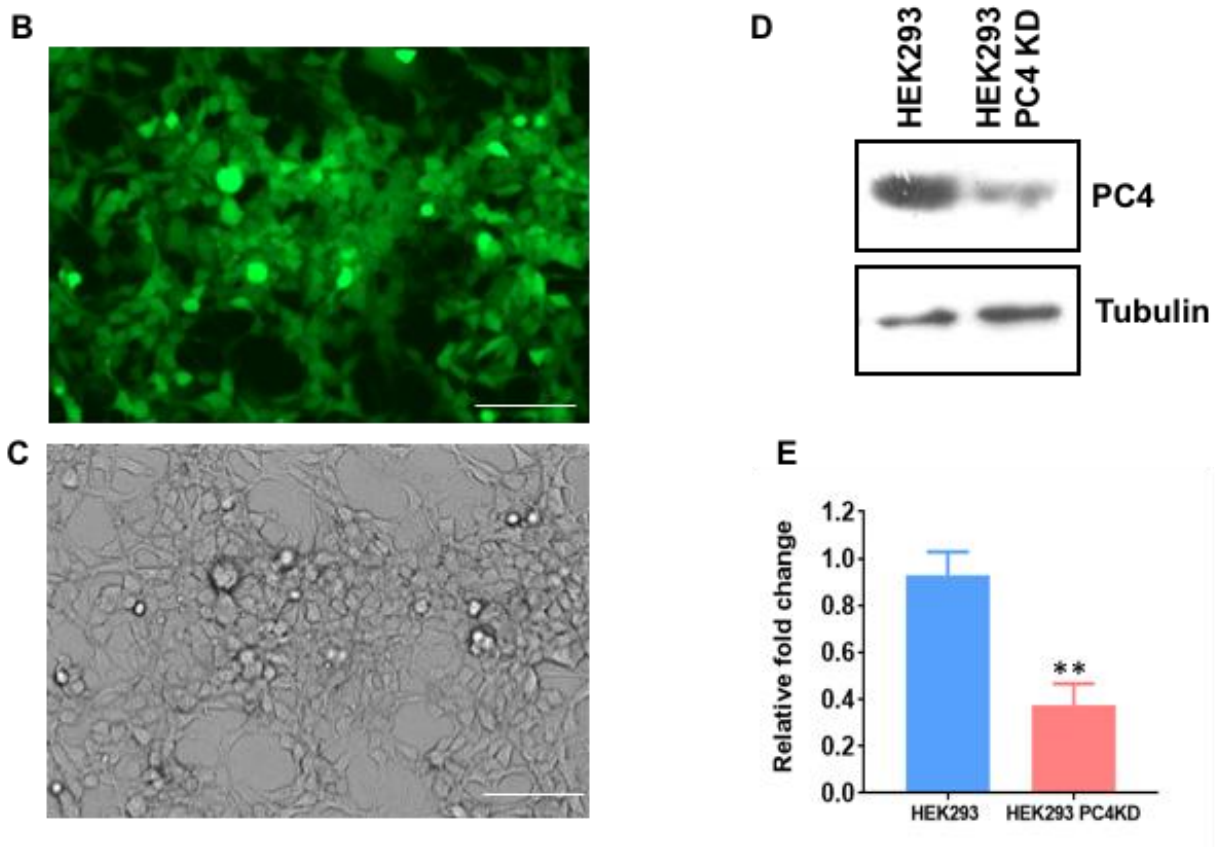

Figure 2.5. Establishment of HEK293 PC4 knockdown cells. (A) Schematic outline of the method used to establish the lentivirus mediated PC4 knockdown cells. (B) Cells which were transduced successfully with the pGIPZ PC4 targeting shRNA expressed GFP which were further sorted to establish the cell line. Microscopic image of GFP positive HEK293 cells transduced with shRNA after sorting captured through a fluorescent microscope. (C) Morphological features of HEK293 PC4knockdown cell line. (D) Western blot analysis for PC4 in normal HEK293 cells and stable shRNA harboring cells. Tubulin is used as a loading control. (D) PC4 gene expression analysis done from RNA extracted from the established PC4 knockdown cells.

2.3.3.2. Generation of PC4 Knockdown MCF7 cell line

MCF7 cells constitutively expressing shRNA (Clone ID: V3LHS_331786, Dharmacon pGIPZ shRNA; Mature sequence: TTTTCTGGAGCAACTTGCT) against the ORF of PC4 mRNA was established to make a PC4 knockdown cell line. To negate the effect of shRNA transduction a cell line expressing a non-silencing shRNA control was also established. The non-silencing control hairpin sequence is as follows: 22mer sense: ATCTCGCTTGGGCGAGAGTAAG 22mer antisense: CTTACTCTCGCCCAAGCGAGAG This sequence does not match any known mammalian genes (had at least 3 or more mismatches against any gene as determined via nucleotide alignment/BLAST of 22mer sense sequence). These cell lines were generated using the same scheme as depicted in Figure 2.5 A. Desired cell line (here MCF7) was infected with 10^5 IU/ml virus. Infected cells were subjected to selection pressure 72 hours post transfection. Cells were fist sorted for positive GFP signals and the GFP sorted cells were grown to establish the stable cell line. To validate the extent of knockdown, PC4 levels were checked at protein level and compared against the nonsilencing shRNA harboring MCF7 cells.

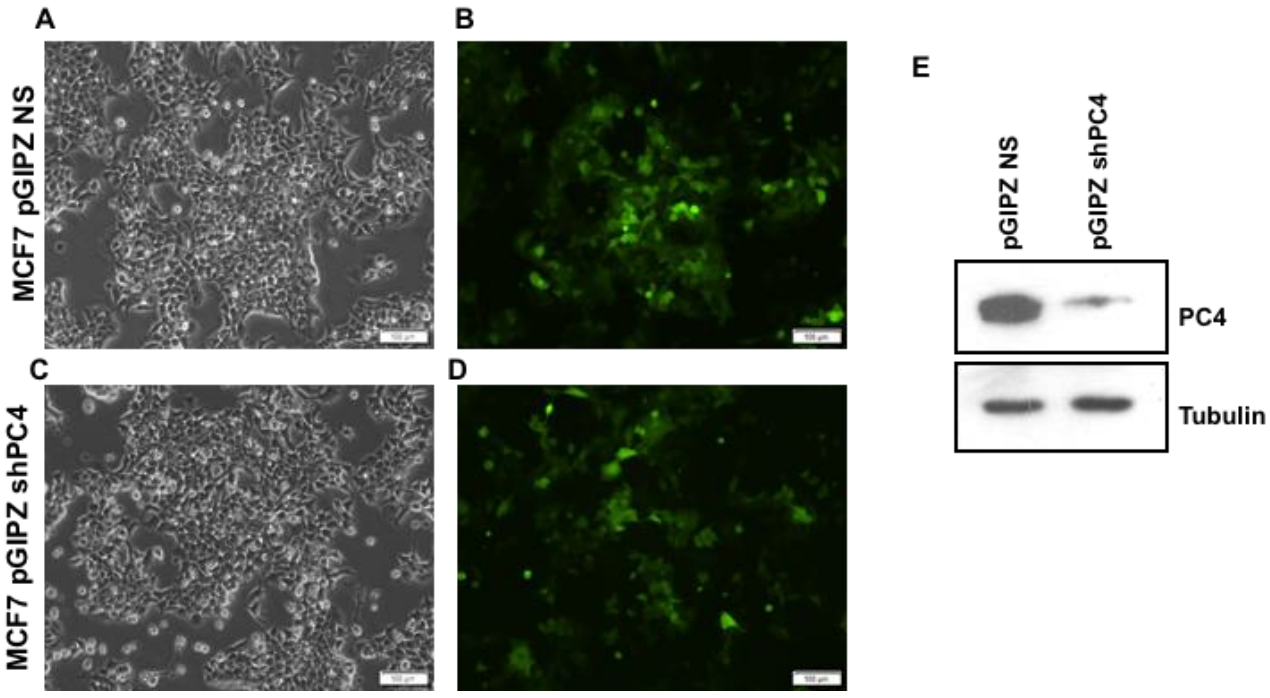

Figure 2.6. Establishment of MCF7 (Breast cancer) PC4 knockdown cells. Morphological features of MCF7 PC4knockdown cell line (sh-PC4) (C) and the non-silencing control cell line (A). Cells which were transduced successfully with the pGIPZ PC4 targeting/NS shRNA expressed GFP which were further sorted to establish the cell line. Microscopic image of GFP positive MCF7 cells transduced with (B) non-silencing (NS) shRNA or (D) shRNA targeting PC4 after sorting captured through a fluorescent microscope.). (E) Western blot analysis for PC4 in non-silencing shRNA MCF7 cells and stable PC4 shRNA harboring cells. Tubulin is used as a loading control.

2.4. Cell-based assays

2.4.1. Immunofluorescence

HEK293 or HEK293 PC4 knockdown cells were grown on poly-lysine coated cover slips at 37°C in a 5% CO2 incubator. The media was removed and the cell layer was washed in PBS to ensure all the media was removed. The cells were fixed in 4% para-formaldehyde for 10 minutes at room temperature. The cells were washed with PBS to remove the remnant PFA. The cells were then permeabilized in 0.5% Triton X-100. Cells were washed in PBS to remove the residual TritonX-100. The cells were blocked in blocking solution (5% FBS in PBS) at 37 °C for 45 minutes. The blocked cells were then incubated in primary antibody at the indicated dilution for 1-1.5 hours at room temperature on a reciprocal shaker. The cells were washed in washing buffer (1% FBS in PBS). The number of washes is standardized to remove any background (usually 2-3 washes). The cells were then incubated in Alexa-fluor conjugated secondary antibody corresponding to the primary antibody used, incubated at room temperature for 1 hour. Cells were washed in washing buffer. The nucleus was counter-stained with Hoechst 33258 (bis-benzamide (Sigma)), a fluorescent dye which emits blue fluorescence, for 10 minutes at room temperature (in the dark). Excess Hoechst stain was washed off with PBS. The cover slips were mounted (inverted) in 70% glycerol onto a microscope glass slide. The stained cells were visualized using Carl Zeiss confocal microscopes LSM 510 META or the LSM 880 with Airyscan.

2.4.2. Chromosome spreads and immunostaining

HEK293 cells and HEK293 PC4 knockdown cells were cultured as monolayers and treated with 0.03μg/ml of colchicine for 3 hours. Condensed metaphase chromosomes were spread by drop technique on a fresh clean slide after being treated with the hypotonic solution (75mM KCl) and fixing using 1ml of Carnoy's Fixative solution (Methanol: Glacial Acetic Acid 3:1). To stain the chromosomal DNA Hoechst 33258 (bis-benzamide (Sigma) was used.

2.4.3 Analysis of segregation defects (Binucleate Analysis)

Wild type and PC4 knockdown HEK293 were grown to 60% confluence and treated with 26μg/ml Cytochalasin B for 3hours in 37°C incubator with 5% CO_2. Cells were harvested by pipetting, washed once with 1X PBS and pellet was fixed in 1ml of Carnoy's Fixative (Methanol: Glacial Acetic Acid 3:1). Fixed cells can be kept at 4°C for storage. Fixed cells were gently agitated and slides were prepared by the slide drop technique using Pasteur pipette. Slides were air dried, stained with 1mM of DAPI (4',6-diamidino-2-phenylindole) and sealed with a coverslip. Imaging was carried out using Olympus BX-61 Fluorescence Microscope. Segregation defect was analyzed in terms of the number of anaphase bridges formed per 100 binucleates counted for both wild type and PC4 knockdown HEK293 and a graph was plotted using GraphPad Prism™.

2.4.4. FISH analysis of segregation defects

Wild type and PC4 knockdown HEK293 were grown to 60% confluence and both were treated with 26 μg/ml Cytochalasin B and 2.6% Colcemid for 3 hours in 37°C incubator with 5% CO_2. Cells treated with Colcemid were harvested for chromosome analysis and treated with 1ml of 0.54 % Potassium Chloride for 20 min at 37°C water bath. Pellet was then fixed in 1ml of Carnoy's Fixative (Methanol: Glacial Acetic Acid 3:1) and stored at 4°C. Cytochalasin B treated cells for binucleate analysis were harvested, washed, fixed in 1ml of (Methanol: Glacial Acetic Acid 3:1) and stored at 4°C. Slides for chromosomes and binucleates were prepared by the slide drop technique, air dried and aged in a dust free environment overnight. Fluorescence In- Situ Hybridization of Telomere PNA probe was performed with chromosomes and binucleates as per the protocol. Signal obtained was observed under Olympus BX 61 fluorescent microscope and quantified using ImageJ software. A graph was plotted in GraphPad Prism™ for the binucleate FISH in terms of the signal positivity in the daughter nuclei.

2.4.5. Total RNA extraction from cells

Total RNA was isolated from different cell lines using TRIzol reagent (Invitrogen) according to the manufacturer's protocol. To lyse the cells, appropriate volume of TRIzol is added to

the cells (1ml TRIzol per 10 cm2 growth area = 1 ml TRIzol per ~106 cells), incubated at room temperature for 2 minutes. The TRIzol lysate was collected in a DEPC-treated microfuge tube and chloroform was added (0.2 ml per 1 ml of TRIzol), mixed thoroughly and incubated at room temperature for 2-3 minutes. The lysate was centrifuged at 12000g for 10 minutes at 4 °C and the aqueous phase containing the RNA was collected. The RNA was precipitated with equal volumes of isopropanol incubated at room temperature for 10 minutes. The RNA was pelleted at 12000g for 10 minutes at 4 °C. The pellet was washed with 75% ethanol and centrifuged at 12000g for 5 minutes. The wash was discarded and the pellet was allowed to air-dry. Once the pellet was dried, it was dissolved in nuclease-free water. The RNA was quantified on a Nanodrop1000 Spectrophotometer wherein the A260 value for 1 corresponds to 40 ng/µl of RNA. The quality of the RNA was determined by the A260/A280 ratio, where a ratio of 2 is indicative of pure RNA. The integrity of the RNA was further checked on a 0.8 % non-denaturing agarose gel. Distinct bands corresponding to the 28S and 18S rRNA indicated that the RNA was not denatured (Figure). The purified RNA was stored at -80 °C.

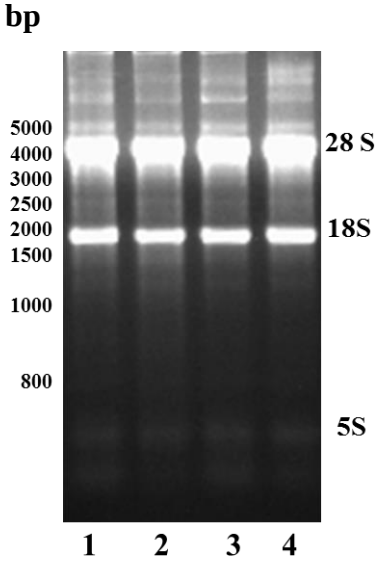

Figure 2.7. RNA purification profile: RNA profile from mammalian cells profile on a 1% non-denaturing agarose gel.

RNA extraction from patient samples

RNA from patient samples were either obtained paraffin embedded tissues or from solid tumors stored in RNA Later solution. For paraffin embedded tissues first deparaffinization was carried out by xylene method followed by Proteinase K digestion. For solid samples it was crushed using a sterile mortar and pestle using liquid nitrogen. The tissue homogenate was further processed by the Trizol method. To ensure efficient precipitation of the RNA the isopropanol step was done overnight. This was followed by ethanol wash and pellet was dried similarly and dissolved in water as given above.

2.4.6 cDNA synthesis

miRNA cDNA synthesis

For cDNA synthesis the NCODE VLO miRNA cDNA synthesis kit was used. The NCode™ VILO™ miRNA cDNA Synthesis Kit provide qualified reagents for the tailing of microRNAs (miRNAs) and other small RNAs in a total RNA population, synthesis of first-strand cDNA from the tailed RNA, and subsequent detection in real-time quantitative PCR (qPCR). These kits have been optimized for the detection and quantification of miRNA from 100 pg to 1 µg of total RNA, with the amount of starting material ranging as low as 10 pg. cDNAs were made from 400ng-1µg of RNA as per instruction in the manual at 37ºC for 1hour followed by heat inactivation at 90ºC for 10 minutes. cDNAs were stored at -20ºC for long time storage.

Gene	Primer sequence 5'-3'
ULK1 Fwd	GTCACACGCCACATAACAGA
ULK1 Rev	CCATCAAGGTGATGAGGAAGAA
ULK2 Fwd	CCCTCCCAAGTCTCATGTTTAG
ULK2 Rev	TCTGATGTGGTTTCCTCTGATG
GABARAPL1 Fwd	AGGACAGAGCTGTTGGATTG
GABARAPL1 Rev	CCTCCTGACCCATCTATGAAAC
GABARAPL2 Fwd	GTGAGGTAGGTGCGGTATTAAA
GABARAPL2 Rev	CATGATTGGCAGTTGGCATATT

AMPKalpha1 Fwd	GTCAAAGCCGACCCAATGATA
AMPKalpha1 Rev	CGTACACGCAAATAATAGGGGTT
AMPKalpha2 Fwd	CAGGCCATAAAGTGGCAGTTA
AMPKalpha2 Rev	AAAAGTCTGTCGGAGTGCTGA
DRAM1Fwd	GTCAGCCGCCTTCATTATCT
DRAM1Rev	CACTCTCTGGAGGTGTTGTTC
BECN1 Fwd	CCCGTGGAATGGAATGAGATTA
BECN1 Rev	CCGTAAGGAACAAGTCGGTATC
PTEN Fwd	TGTAATCAAGGCCAGTGCTAAA
PTEN Rev	AGCATCCACAGCAGGTATTATG
BAX Fwd	GGAGGAAGTCCAATGTCCAG
BAX Rev	GGGTTGTCGCCCTTTTCTAC
BCL2 Fwd	AGATGGAGCATGAATGGTACTG
BCL2 Rev	TCTGTGCTCAGCTTGGTATG
DNMT 3A Fwd	CAGACTCATGCAATAACCCTTTG
DNMT3A Rev	CACTTTCCCACACTCTGGATTA
DNMT 3B Fwd	GTGTGAAGCAAGGAGCTTAGA
DNMT3B Rev	CTGTCACTGCCTCTGAGTTTAG
PC4 Fwd	AGGTGAGACTTCGAGAGCCCTGT
PC4 Rev	TTCAGCTGGCTCCATTGTTCTGG
ACTIN Fwd	AGATGTGGATCAGCAAGCAGGAGT
ACTIN Rev	TCCTCGGCCACATTGTGAACTTTG
hsa-miR-29a	ACCATCTGAAATCGGTTAAAA
hsa-miR-29c	CACCATTTGAAATCGGTTAA
U6SnRNA	GGAACGCTTCACGAATTAA

Table No.2 List of Primers used.

mRNA cDNA synthesis

Before cDNA synthesis from the isolated total RNA, the RNA was treated with DNase I to eliminate any genomic DNA contamination. Approximately 10 µg RNA was added to 1X DNase I Reaction Buffer made up to a final volume of 100 µl. 2 U of RNase-free DNase I

was added to the reaction and incubated at 37 °C for 20 minutes. 5 mM EDTA was added to stop the reaction. The DNase I was heat inactivated at 75 °C for 10 minutes. 2 µg DNase I-treated RNA was used for the subsequent steps of cDNA synthesis and the remaining RNA was stored at 80 °C. For first strand cDNA synthesis, the RNA was added to a 10 µl reaction containing 1 mM dNTPs and 7 µM Oligo dT (Sigma, Catalog No. 04387). The reaction mixture was incubated for 10 minutes at 70 °C. The first strand cDNA synthesis was initiated by adding 2 µl of 10X M-MLV Reverse Transcriptase, 20 U of RNaseOUT (Invitrogen Catalog No. 10777019). The reaction was allowed to continue for another 50 minutes at 37 °C, followed by heat inactivation at 94 °C for 10 minutes. The cDNA synthesized was stored at -20 °C.

2.4.7. Real Time PCR analysis

1µl of respective cDNA was used in PCR reaction mix containing specific gene primers and 2X Syber Green mix (KAPA Biosystems). Sybr Green mix contains SYBR green I dye and required PCR reagents like dNTPs, DNA polymerase and compatible buffers. The first strand cDNA synthesized was used for Real-Time/ quantitative PCR (RT-PCR/ qPCR). To the 2X SYBR Green mastermix, specific primers (forward and reverse), cDNA and high ROX (for normalization) were added. The reaction was carried out in the StepOnePlus Real time PCR system. The data was analysed in StepOne software v2.3. PCR conditions were standardised for each set of gene primers used. Fold expression change was calculated using ΔΔCt method using either Actin or U6SnRNA (in case of miRNAs) gene primers for normalization. Sensitivity and specificity of the primers was ascertained by melt curve analysis. The sequences of the primers are given below. For miRNAs universal Reverse primer from the NCODE VLO cDNA synthesis kit (Invitrogen) was used.

2.4.8. Apoptosis analysis by Fluorescent activated cell sorting (FACS):

Annexin V-Cy3 Apoptosis Detection Kit (Sigma APOAC) (utilizes the sharp and bright Cy3 red fluorescence dye conjugated to Annexin V. Annexin V-Cy3 binding can be detected by flow cytometry (Ex = 488 or 543 nm; Em = 570 nm) using the phycoerythrin emission signal detector (usually FL2). Detection of apoptosis was carried out as suggested by manufacturer's kit protocol. Briefly, around 50,000 cells were washed twice with Annexin Binding buffer IV (100 mM HEPES/NaOH, pH 7.5, containing 1.4 M NaCl and 25 mM $CaCl_2$). Cells were dissolved in the buffer such that it is 10^6 cells/ml. 100 µl of cell suspension was taken to this 1.5µl of Dye was added. Incubated for 15 mins in dark and then added to 400 µl of Annexin Buffer. This is used for analysis.

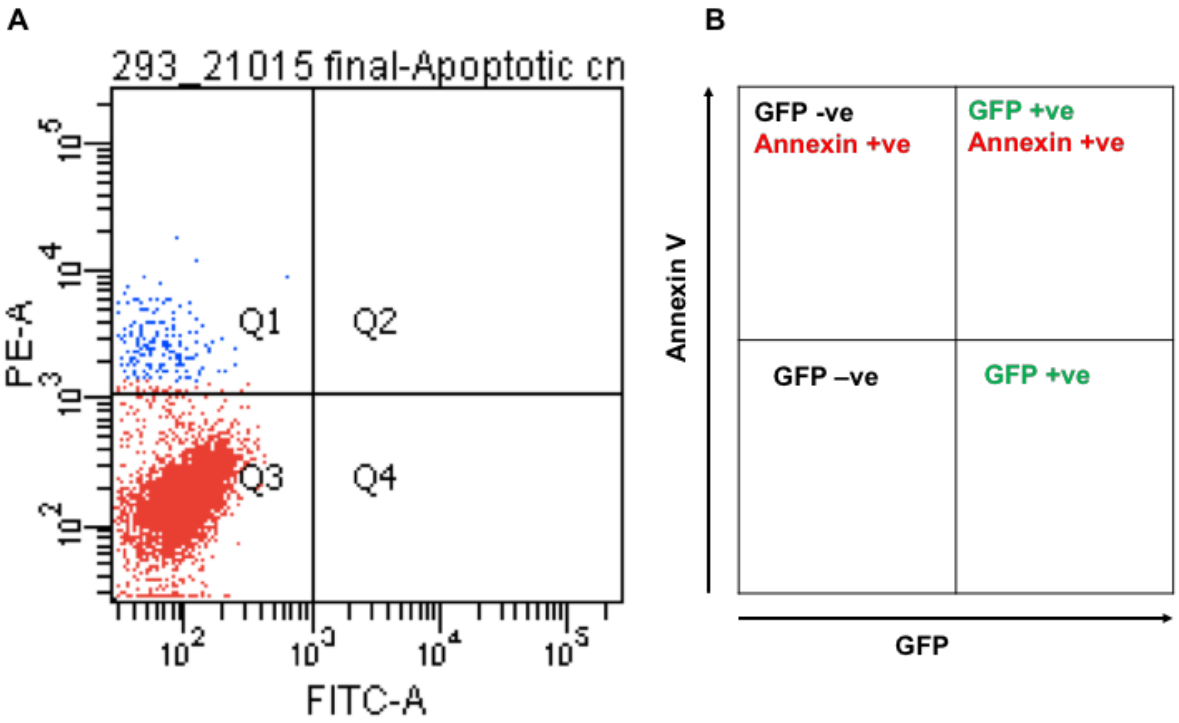

Figure 2.8. Apoptosis analysis using Annexin V staining: (A) Cells were heated at 90°C to induce apoptosis. A suspension of cells was made in 1:1ratio of live cells and the heat killed cells. Cells stained with Annexin V-Cy3 dye is represented along y axis while GFP to detect GFP positive cells were plotted along x axis. HEK293 cell suspension containing the dead cells was represented in Quadrant 1. (B) Representation and Interpretation of each quadrant in an apoptosis analysis.

For sorting 2 million cells were taken (100 ul suspensions containing 10^6 cells stained with 1.5 µl of Dye). Volume was made upto 2 ml using Annexin Buffer. Cells which stained positive for Annexin V were excluded and the live population collected in autoclaved PBS buffer after sorting.

2.4.9. Luciferase assay

Human Embryonic Kidney cells were maintained at 37°C in Dulbecco's modified Eagle's medium with 10% fetal bovine serum. Before transfection cells were seeded at 0.6–1*10^6 cells in 30-mm-diameter dishes. pMIR REPORT luciferase construct is used. The 3' UTR of the luciferase gene contains a multiple cloning site for insertion of predicted miRNA binding targets or other nucleotide sequences. By cloning a predicted miRNA target sequence into pMIR-REPORT, the luciferase reporter is subjected to regulation that mimics the miRNA target. The 3'UTR region of PC4 is cloned into the MCS region pMIR-REPORT luciferase vector. This luciferase vector was co transfected with miRNA expression vectors using lipofectamine (Invitrogen).The pMIR-β-gal construct was used as an internal control. Empty vector (pSUPER) was used as a control. Prior to transfection, the medium was replaced with fresh DMEM without FBS. The constructs and Lipofectamine was incubated for a period of 20mins to ensure Lipofectamine-DNA complex formation, as per the manufacturer's protocol. After 6hrs the medium was replaced by 10% FBS supplemented DMEM medium. Luciferase and β-galactosidase activities were measured 48h after the transfection with luciferase assay and β-galactosidase assay systems according to the procedure provided by manufacturer.

2.4.10. Micrococcal Nuclease assay

The HEK293 cells and HEK293 PC4 KD cells were grown in Dulbecco's minimal essential medium supplemented with 10% fetal bovine serum. The nuclei were prepared from packed cells (approximately from 30million cells)suspended in hypotonic buffer (10 mM Tris-HCl, 10 mM KCl, 15 mM MgCl2) followed by 10 min of incubation at 4°C. The nuclei were digested with micrococcal nuclease (MNase) (0.2 U/µl) for 0, 5, 10 and 15 min at room temperature in nuclei digestion buffer (10% glycerol, 10 mM Tris-HCl [pH 8], 3 mM CaCl2, 150 mM NaCl, 0.2 mM phenylmethylsulfonyl fluoride). MNase digestion was stopped by the addition of 10 mM EDTA, and the digested chromatin was then isolated by Phenol Chloroform method. DNA was estimated and 1µg was loaded in each lane.

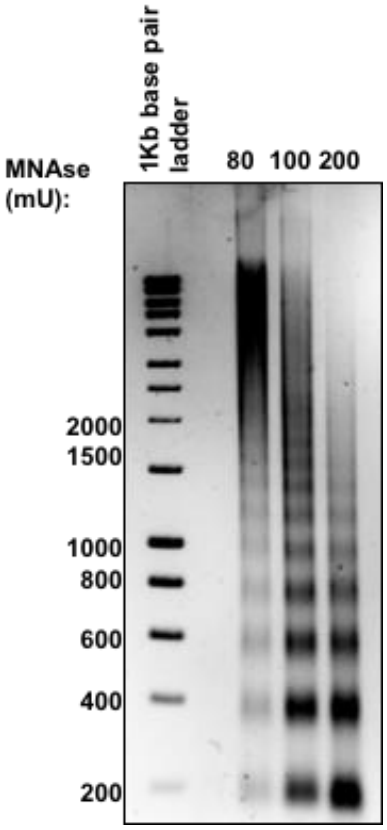

Figure 2.9. Micrococcal Nuclease digestion pattern of mammalian cells: Chromatin isolated from HEK293 cells were digested with increasing amount of micrococcal nuclease in miliunits.

2.4.11. Histone Extraction

Around 1 million HEK293 and HEK293 PC4 Knockdown cells were harvested and washed twice with ice-cold PBS (10 mL). PBS was supplemented with 5mM Sodium Butyrate to retain levels of histone acetylation. Cells were resuspended in Triton Extraction Buffer (TEB: PBS containing 0.5% Triton X 100 (v/v), 2mM phenylmethylsulfonyl fluoride (PMSF)) at a cell density of 107 cells/ml (5 mL). Cells were lysed on ice for 10 minutes with gentle stirring, followed by extraction with 0.2N HCl for 2hours in ice. The histones were then washed and TCA precipitated. The histone pellet was dissolved in appropriate volume of 50 mM TrisHCl pH 7.4 (typically 50 µL, scale with quantity of cellular source, increasing volume of the histone solution was seperated on 15% SDS/PAGE gel and stained with Coomassie Brilliant Blue solution to characterize concentration of the histones.

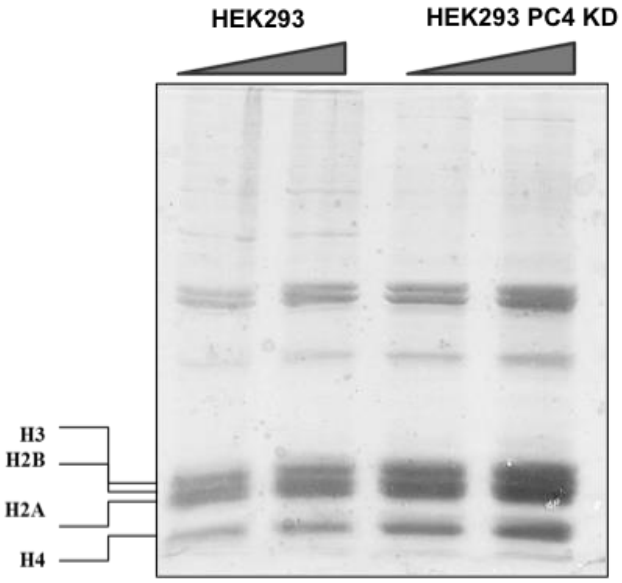

Figure 2.10. Histone Extraction profile: Histones extracted from HEK293 and HEK293 PC4 Knockdown cells were resolved in a 15% SDS PAGE. Increasing volume of the total histone extracted was loaded to estimate the concentration.

2.4.12. Chromatin Immunoprecipitation (ChIP)

Around 10 million cells were used for each ChIP. The cells are crosslinked in 1% formaldehyde. The crosslinking was quenched in 0.125M glycine. The cells were lysed in SDS buffer and the chromatin was sheared using Diagenode ChIP sonicator). 10% of the total lysate volume was kept aside as the input. The lysates were pre-cleared with BSA-blocked protein-G sepharose beads. 5-10 μg antibody was used in each ChIP. The antibody and BSA-blocked protein G sepharose beads were added the cleared lysates and incubated at 4 °C overnight. The beads were then washed to remove non-specific binding with buffers containing different salt concentrations. The DNA-protein complexes were eluted from the washed beads using SDS-sodium bicarbonate elution buffer. The eluates and input were decrosslinked at 65 °C for 4 hours. Proteinase K and RNase H were added to the decross-linked lysates to remove the proteins and RNA. The DNA was extracted using phenol:chloroform:isoamyl alcohol method. The DNA was precipitated at -20 °C, overnight, using sodium acetate, glycogen in 100% ethanol. The DNA pellet was washed in 70% ethanol and dissolved in nuclease-free water.

2.4.13. Small molecule inhibition of Autophagy

For the small molecule inhibition assays the cells were grown to 70% confluency and then treated with 10mM of 3-Methyl Adenine (10mM) (Sigma) and 50nM or 100nM Bafilomycin (Cayman Chemicals) for 2 hours.

2.4.14. Gamma Irradiation

HEK293 and PC4 knock down cells were seeded onto a 35mm dish and grown till 80% confluency. The dishes were exposed to different doses of radiation by setting the time in the irradiator (Blood Irradator-2000, Bl-2000), JNCASR, which has the rate of irradiation as 5.463 Grey units (Gy) per minute as follows:

- 1Gy-14seconds
- 2Gy-29seconds
- 3Gy-43seconds

After exposure to radiation, fresh media was given to the cells and incubated for 24hours at 37^0C in a 5% CO_2 supply and an 80% relative humidity of a CO_2 incubator. After 24hours of irradiation the cells were harvested and lysates were prepared for western blotting or seeded for clonogenic assay.

2.4.15. Clonogenic assay

Clonogenic assay was performed using 200 cells (single cell population) seeded in 100 mm tissue culture dishes 12 hours prior to gamma irradiation. Cells were subjected to different doses of irradiation namely 0, 1, 2, 3 Gy. Media was replaced with fresh complete media soon after the irradiation. Plate was kept in 37°C incubator with 5% CO_2 for 10 days to monitor colony formation. Colonies were stained with Crystal violet solution, counted in both the cases and surviving fraction was calculated as (No. of colonies at a particular dose/ No. of colonies at 0Gy)*100. For Clonogenic assay with autophagy inhibitors, cells were seeded onto a 35mm dish and grown till 70% confluency, cells were then pre-treated with autophagy inhibitors for 2 hours, prior to exposure to 2 Gy gamma irradiation. After exposure to radiation, fresh media was given to the cells and incubated for 24 hours at 37ºC in a 5% CO_2 supply and an 80% relative humidity of a CO_2 incubator. Cells which were pre-treated with autophagy inhibitors were also supplemented with fresh media containing the desired concentration of inhibitors after exposure to gamma irradiation. After 24 hours of irradiation, cells were trypsinized and then seeded for colony formation and then counted after 10 days as indicated above.

2.4.16. Matrigel invasion assay

MCF7 non silencing control cells as well as MCF7 PC4 knockdown cells were seeded onto BD BioCoat Matrigel matrix (Corning Life Sciences, Tewksbury, MA, USA) in the upper chamber of a 24-well culture plate at a confluency of 20,000 to 25,000 cells. The lower chamber containing respective medium was supplemented with 10% serum as a chemoattractant. After 12-16 hours, the noninvading cells and Matrigel matrix were gently removed with a cotton swab. Invasive cells located on

the lower side of the chamber were stained with 0.2% crystal violet in methanol, air-dried and photographed using an inverted microscope (× 4). For migration assays similar protocol was followed without the coating of the basement matrix. For quantitation at least 3 independent fields from each biological replicate was considered.

2.4.17. Comet Assay

The comet assay, or single cell gel electrophoresis assay (SCGE), is a common technique for measurement of DNA damage in individual cells. Under an electrophoretic field, damaged cellular DNA (containing fragments and strand breaks) is separated from intact DNA, yielding a classic "comet tail" shape under the microscope. Extent of DNA damage is usually visually estimated by comet tail measurement. The Cell Biolabs OxiSelect™ Comet Assay kit was used for simple evaluation of cellular DNA damage. First, individual cells (around 20,000 ZR751 cells, and ZR751 cells after 48 hours of transfection with Flag constructs of PC4 and mutant PC4) were mixed with molten agarose in 1:10 (v/v) ratio before application to the OxiSelect™ Comet Slide. These embedded cells are then treated with a lysis buffer (As instructed in the manufacture's protocol) and alkaline solution, which relaxes and denatures the DNA. Finally, the samples are electrophoresed (alkaline electrophoresis buffer) in a horizontal chamber to separate intact DNA from damaged fragments. Following electrophoresis, the samples are dried, stained with a DNA dye, and visualized by epifluorescence microscopy. Under these conditions, the damaged DNA (containing cleavage and strand breaks) will migrate further than intact DNA and produce a "comet tail" shape.

2.4.18. Transmission Electron Microscopy

2 million of HEK293 and sh-PC4 cells were harvested and suspended in 100µl of PBS solution. The cells were fixed in suspension with 4 % glutaraldehyde in 0.1 M cacodylate buffer (pH 7.3) after harvesting, overnight at 4°C. Cells were dehydrated with a graded series of ethanol, and embedded in epoxy resin. Then the areas containing cells were cut into ultrathin sections, stained and observed on transmission electron microscope Tecnai G2 F-30, a 300 Kv TEM / STEM equipped with a schottky field emission source and a point - point

resolution of 2.2. The processing of the samples and imaging were done in CMC Vellore Institute and IISc TEM facility respectively.

2.4.19. DNA Damage

Cells were exposed to different agents to mediate DNA damage. 10nM actinomycin treatment for 12 hours, as well as exposure to γ irradiation of 2 grey units followed by incubation for 6 hours could successfully create a DNA damaged condition in cells. The induction of DNA damage was assayed by immunofluorescence with γ-H2Ax antibody in the treated cells as compared to the untreated cells.

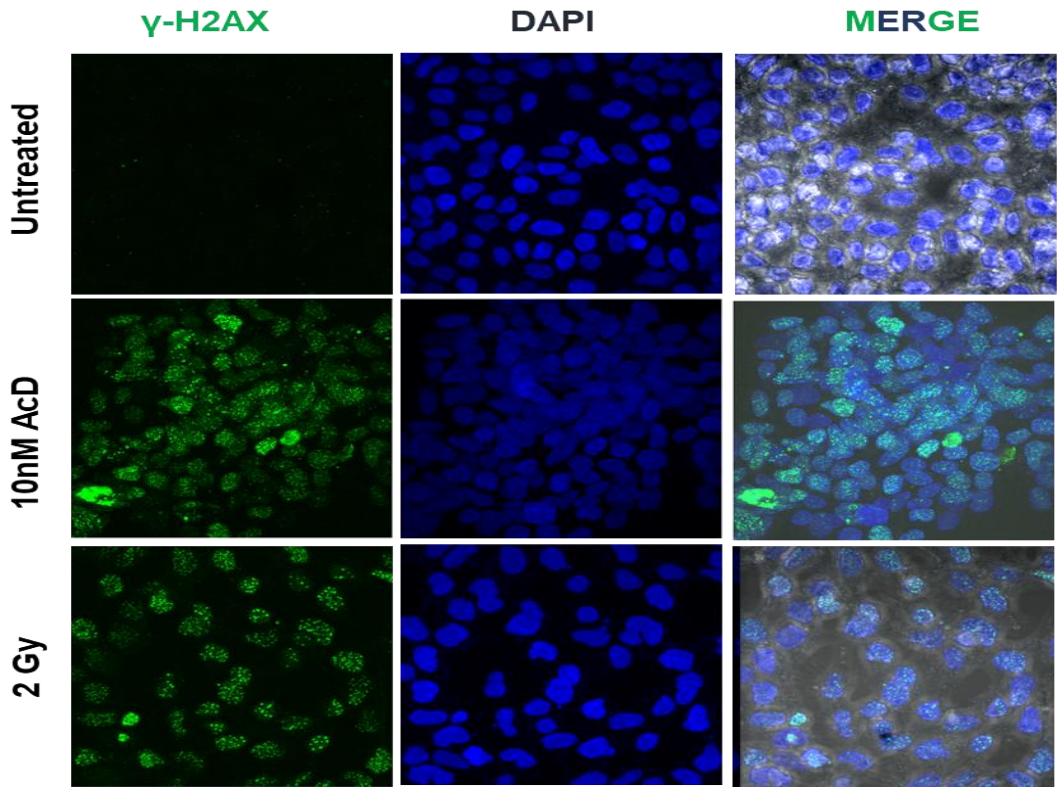

Figure 2.11. DNA damage conditions. HEK293 cells were treated either with AcD 10nM or exposed to 2Gy of Gamma radiation followed by immunofluorescence with γ-H2Ax antibody (a marker for double strand breaks or DNA damage in general).

2.5. Recombinant Protein Purification

2.5.1. Purification of bacterially expressed recombinant PC4 expression

E.coli BL21 cells were transformed with His PC4 expression vector. 100ml of LB medium containing 50µg/ml Kanamycin was inoculated from the transformed colony and grown overnight at 37ºC. This overnight culture was further inoculated into 900ml of Luria Bertani broth containing 50µg/ml Kanamycin and grown at 37ºC until the O.D. reaches 0.4(O.D. 600). The culture was then induced with 0.4mM IPTG for 3hrs at 37ºC. The culture was then harvested and then homogenized in homogenization buffer (20mM Tris-HCl, 20% Glycerol, 2mM PMSF, 20mM EDTA, 20mM Imidazole, 300mM KCl, 2mM βMe, 0.1% NP40) and then sonicated. Cleared lysate is obtained by centrifuging at 16,000 rpm at 4ºC for 30mins. The cleared lysate is then incubated with pre-equilibrated Ni-nitrilotriacetic acid beads (Novagen) at 4ºC for 3hrs. The beads are then washed with 10ml of wash buffer (20mM Tris-HCl, 20% Glycerol, 2mM PMSF, 20mM EDTA, 40mM Imidazole, 600mM KCl, 2mM βMe, 0.1% NP40) for 9 times. The beads are then loaded into a column and the protein was eluted out with elution buffer (20mM Tris-HCl, 20% Glycerol, 2mM PMSF, 20mM EDTA, 250mM Imidazole, 100mM KCl, 2mM βMe, 0.1% NP40). Elutions were collected in aliquots. The eluted proteins were further dialyzed against BC100buffer (20mM Tris-HCl, 20% Glycerol, 2mM PMSF, 20mM EDTA, 20mM Imidazole, 100mM KCl, 2mM βMe, 0.1% NP40) and snap freezed in liquid nitrogen and stored at -80ºC.

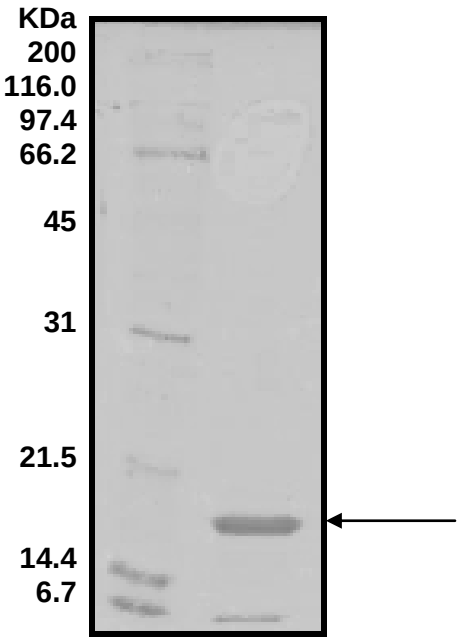

Figure 2.12. Purification of bacterial expressed His tagged PC4: Purification profile of recombinant His tagged PC4 from transformed bacterial culture. His tagged PC4 was purified through a Ni-NTA column. The arrow indicates the specific band for PC4 protein.

2.5.2. Purification of acetylation defective PC4 mutants

Acetylation site PC4 mutants were purified till homogeneity using Ni-NTA agarose column as described in the previous section. All proteins were dialyzed against BC100 buffer and snap freezed in liquid nitrogen and stored at -80ºC.

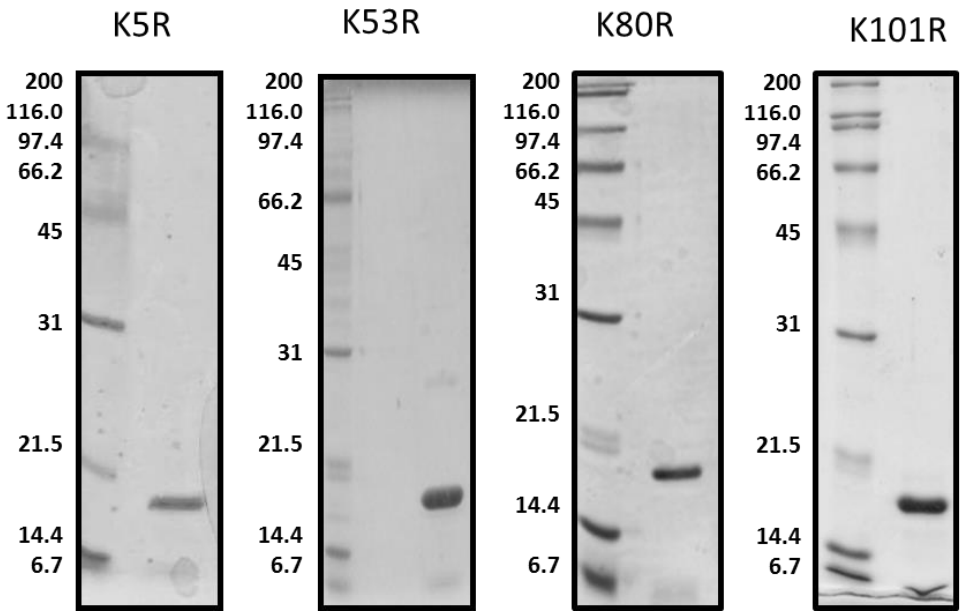

Figure 2.13. Purification of bacterial expressed His tagged mutant PC4: Purification profiles of recombinant His tagged PC4 mutants generated by site directed mutagenesis from transformed bacterial culture. His tagged PC4 was purified through a Ni-NTA column.Numbers denote KDa.

2.6. General Molecular Biology techniques

2.6.1. Western Blotting Analysis

Proteins electrophoresed on an SDS-PAGE were transferred onto nitrocellulose or PVDF membrane in transfer buffer (25 mM Tris, 192 mM glycine , 0.036 % SDS in 20 % methanol) by Semi-dry or Wet transfer method, followed by blocking in 5 % skimmed milk, the proteins of interest were detected with their corresponding primary antibodies. HRP-conjugated secondary antibodies (Genei) were used against the primary antibodies to give a chemiluminescent signal in the presence of SuperSignal West Pico Chemiluminescent Substrate (Thermo Scientific), which was captured on an X-ray film.

2.6.2. Dot-Blot/ Slot Blot Analysis

Proteins or 50ng of peptides were spotted onto nitrocellulose paper directly or using the BioRad Slot Blot apparatus. Following blocking in 5% skimmed milk, the proteins of interest

were detected with their respective primary antibodies. HRP-conjugated secondary antibodies (Genei) were used against the primary antibodies to give a chemiluminescent signal in the presence of SuperSignal West Pico Chemiluminescent Substrate (Thermo Scientific), which was captured on an X-ray film.

2.6.3. Immunohistochemistry Analysis

The breast cancer patient samples used in the study were collected from HCG Bangalore Institute of Oncology, Bangalore after obtaining Bioethics clearances from both institutes (HCG BIO and JNCASR). The samples were collected with prior consent from the patients. The tumor and adjacent normal tissue samples were fixed in 10% formalin for 24-48 hours. Then the tissue samples were dehydrated and embedded in paraffin blocks. 5 μ sections of the samples were made using a microtome (Leica). The tissue samples were stained with haematoxylin and counterstained with eosin. The regions with higher density of cells were marked and those regions where punctured from the tissue blocks with a 1 mm puncturing tool. The 1 mm sections were placed onto a tissue microarray precast block. One array can hold 20 pairs of tissue (normal and tumor) samples. Once the tissue microarray paraffin blocks were prepared, 5 μ sections of the samples were made and collected on silane-coated glass slides. The sections were fixed on the slides by incubating the slides at 45 °C on a hot plate for 24 hours. Before processing the samples for staining, the slides were kept at 65 °C to melt the paraffin. The paraffin was then removed in xylene, followed by dehydration of the samples in 100% alcohol and rehydration in water. Epitope retrieval was done in sodium citrate buffer by boiling for 10 minutes. Once cooled to room temperature, the sample slides were transferred to 0.9% H_2O_2 in methanol for 15 minutes to quench the endogenous peroxidases. The samples were blocked in 5% skimmed milk for 45 minutes and probed with primary antibody of interest. The Strept-Avidin Biotin (biotinylated secondary antibodies (anti-rabbit + anti- mouse) and HRP-conjugated streptavidin) kit from Dako was used. The immune-reactivity of the antigen was measured by intensity of the brown precipitate formed in the presence of the chromogen di-aminobenzidine tetrahydrochloride (DAB, Sigma) followed by counter staining with haemotoxylin. The staining was examined and imaged. Semi-quantitative analysis of the staining (H-scoring) was performed by assigning values between 0-3 (0 = no stain to 3= strong stain) per cell in a field (3 fields per sample) using the

ImageJ add-on IHC profiler (ref). H-score is calculated by the following formula: H-score= 0x % cells with no stain+ 1x % cells (low stain) + 2x % cells (moderate stain) + 3x % cells (strong stain), which can range from 0 to 300. Therefore higher the H-score corresponds to higher levels of protein.

2.6.4 In vitro Acetylation Assay

2.6.4.1. Filter Binding Assay

1µg of Histone H4 or Histone H3 was incubated with 1µl of Tip60 enzyme (1:5 diluted) or 1µl of p300 at 30ºC for 30 mins in 2X HAT buffer (1X composition: 50mM Tris-HCl pH 8.0, 10% glycerol, 1mM DTT, 1mM PMSF, 0.1mM EDTA), 10mM Na-butyrate and 1µl of 2.1 Ci/mmol of [^{3}H]-acetyl CoA. The reaction mixture was then spotted on a Phosphocellulose P-81 filter paper. The radioactive counts were recorded on a Wallac 1409 Liquid scintillation counter. The activity of Tip 60 and p300 assayed as is given below.

2.6.4.2. Gel Assay

HAT assays were performed using 500ng/1µg of Histone H3 or 500ng/1µg of recombinant PC4,or 500ng/1µg of p53 incubated in HAT assay buffer at 30ºC for 30mins with or without baculovirus expressed recombinant Tip60, 1µl of 3.3 Ci/mmol of ^{3}H-acetyl CoA and 10mM Na-butyrate. To visualize the radiolabeled acetylated protein, the reaction products were resolved electrophoretically on 12% SDS-polyacrylamidegel and subjected to fluorography. The gel was stained by coomassie to ascertain the presence of protein in equal amounts in each of the reaction and was later dehydrated in DMSO for 1 hr. Later the gel was incubated in scintillation fluid (PPO solution in DMSO) for 30 mins and then rehydrated in water for 2hrs. The gel was dried using a gel drier and exposed in an X-ray cassette using a film for 7days in -80 degree cooler. The film was later developed to get intensity profiles for each of the reaction.

2.6.4.3. Acetylation of PC4:

Mass acetylation of PC4 was carried out using 1µg of His-PC4. Reaction mixture containing 1µl of Tip60 (~ 30,000 Counts/µl), 2X HAT buffer, 10mM Na-Butyrate and 1.68mM acetyl-CoA was incubated at 30ºC for 30 mins, followed by replenishment with the enzyme and

Acetyl CoA every 1hr and then kept for 6-8hrs after the final replenishment. Mock acetylation reaction was also set up without the enzyme.

2.6.5. Mass spectrometric analysis of *in vitro* acetylated PC4

2.6.5.1. Preparation of the sample

1µg of PC4 was mass acetylated as given in the previous section. The acetylated sample was electrophoresed in a 12% SDS PAGE. The gel was silver stained by the following method. The specific band for PC4 was cut and dried and given for mass spectrometric analysis.

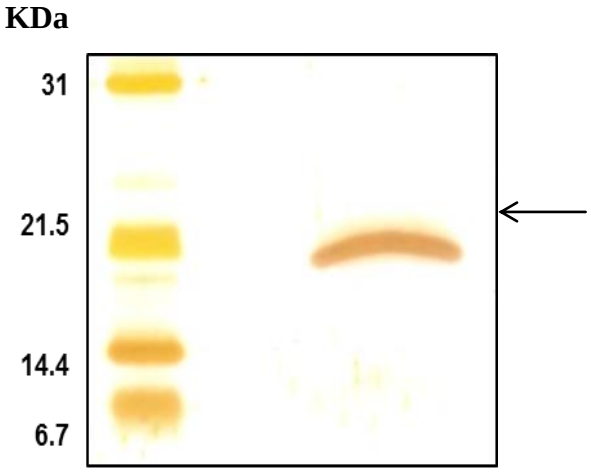

Figure 2.14. Silver staining of mass acetylated PC4 on a 12%SDS PAGE. The arrow indicates the specific band for PC4.

2.6.5.2 Mass spectrometric analysis of *in vitro* acetylated PC4

The mass spectrometric service of ITSI Biosciences, USA was availed to carry out the PTM analysis. In-gel digestion of the PC4 band was performed using trypsin as the enzyme. After trypsinization, peptides were transferred to another tube and two more extraction of peptides was done using 1:2 (v/v) 5 % Formic acid and acetonitrile. Eluates were dried down using a speed vac and reconstituted in 2% Acetonitrile with 0.1% Formic acid. Samples were then loaded onto a PicoFrit C18 nanospray column (New Objective) using a Thermo Scientific Surveyor Autosampler operated in the no waste injection mode. Peptides were eluted from

the column using a linear acetonitrile gradient from 2 to 30% acetonitrile over 90 minutes followed by high and low organic washes for another 20 minutes into an LTQ XL mass spectrometer (Thermo Scientific) via a nanospray source with the spray voltage set to 1.8kV and the ion transfer capillary set at 180 degrees Celsius. A data-dependent Top 5 method was used where a full MS scan from m/z 400-1500 was followed by MS/MS scans on the five most abundant ions and multistage activation was turned on for detecting acetylated peptides. Raw data files were searched using Proteome Discoverer 1.3 (Thermo Scientific) and the SEQUEST algorithm against the most recent species-specific database for Homo sapiens and custom database with the protein of interest from UniProt. Trypsin was the selected enzyme allowing for up to three missed cleavages per peptide; Carbamidomethyl Cysteine was used as a static modification, Acetylation on lysine and Oxidation of Methionine as a variable modification. Proteins were identified when two or more unique peptides had X-correlation scores greater than 1.5, 2.0, and 2.5 for respective charge states of +1, +2, and +3.

2.7. Generation of Polyclonal Antibody (PC4 K80Ac)

Polyclonal antibodies were generated by injecting the Keyhole Limpet Hemocyanin (KLH) coupled peptides in rabbits. New Zealand strains of rabbits were primed with an emulsion of the peptide-KLH conjugate in complete adjuvant. Before the priming, a few ml of blood was collected from the rabbit (control serum). Booster doses were given every 2-3 weeks till the serum showed sufficient strength and specificity against the target protein or modification. Major bleed of 15-20 ml was collected twice in the course of raising the antibody. Serum was separated from the collected blood and IgG was purified using Protein G sepharose beads. The IgG was eluted from the beads using 100 mM glycine, pH 3.0 and collected into tubes containing Tris-Cl buffer to neutralize the acidic pH of the elution buffer. The IgG purified was then dialyzed against 50% glycerol in PBS. A peptide was generated spanning K80Ac site in PC4 and was used to raise K80Ac specific polyclonal Ab of PC4. The peptide was KLH conjugated **KGK (ac) VLIDIREYWMDC.** The antibody was raised according to the scheme given below.

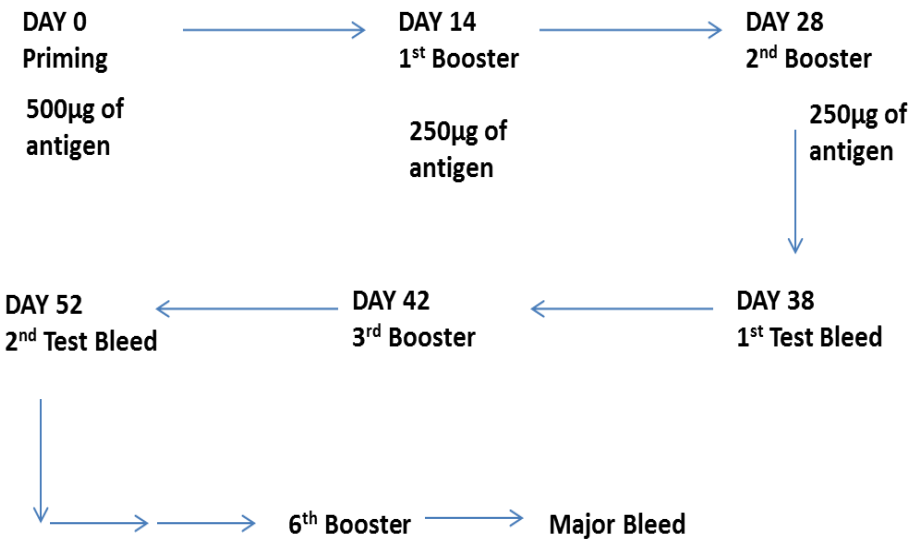

Figure 2.15. Scheme depicting the protocol for antibody raising: Detailed protocol of raising polyclonal Ac PC4 antibody.

The crude acetylation specific antibody was collected and stored in small aliquots in -20 degrees for further use. The antibody was characterized by western blotting analysis and immunofluorescence (Figure 2.16-2.18). The K80 site is located on the C-terminal domain of PC4 (Figure 2.16A). Acetylation of the site serves as a measure of Tip60 acetylated form of PC4. The antibody immuno-reacts strongly with the acetylated Tip60 acetylated PC4 but not with the acetylated form of K80R PC4.

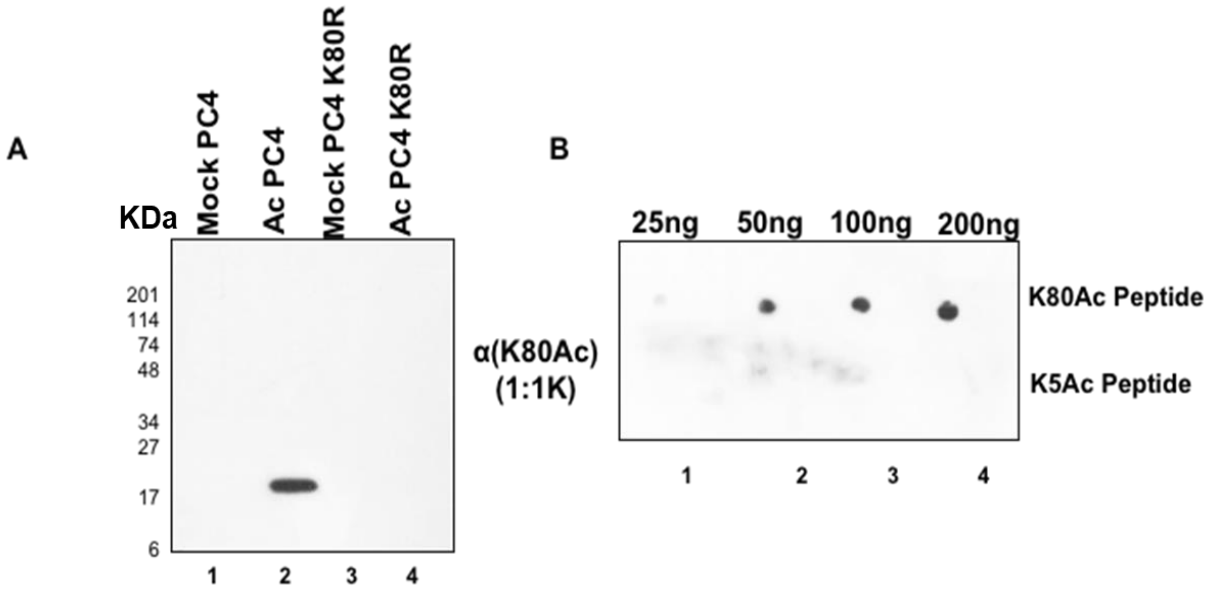

Figure 2.16. Characterization of anti-K80Ac PC4 antibody. (A) Western to determine the specificity of the antibody to recognize the Tip60 acetylated recombinant PC4 (lane 2) over the mock- acetylated PC4 (lane 3). The antibody is specific for K80 site as it failed to recognize the Tip60 acetylated PC4 which had a mutation at K80(K80R) (lane 4). (B) Dot blot to determine the specificity and sensitivity of the polyclonal anti-K80ac antibody (upper panel). To determine its cross reactivity it was used with another acetylated peptide spanning the K5 site of PC4.

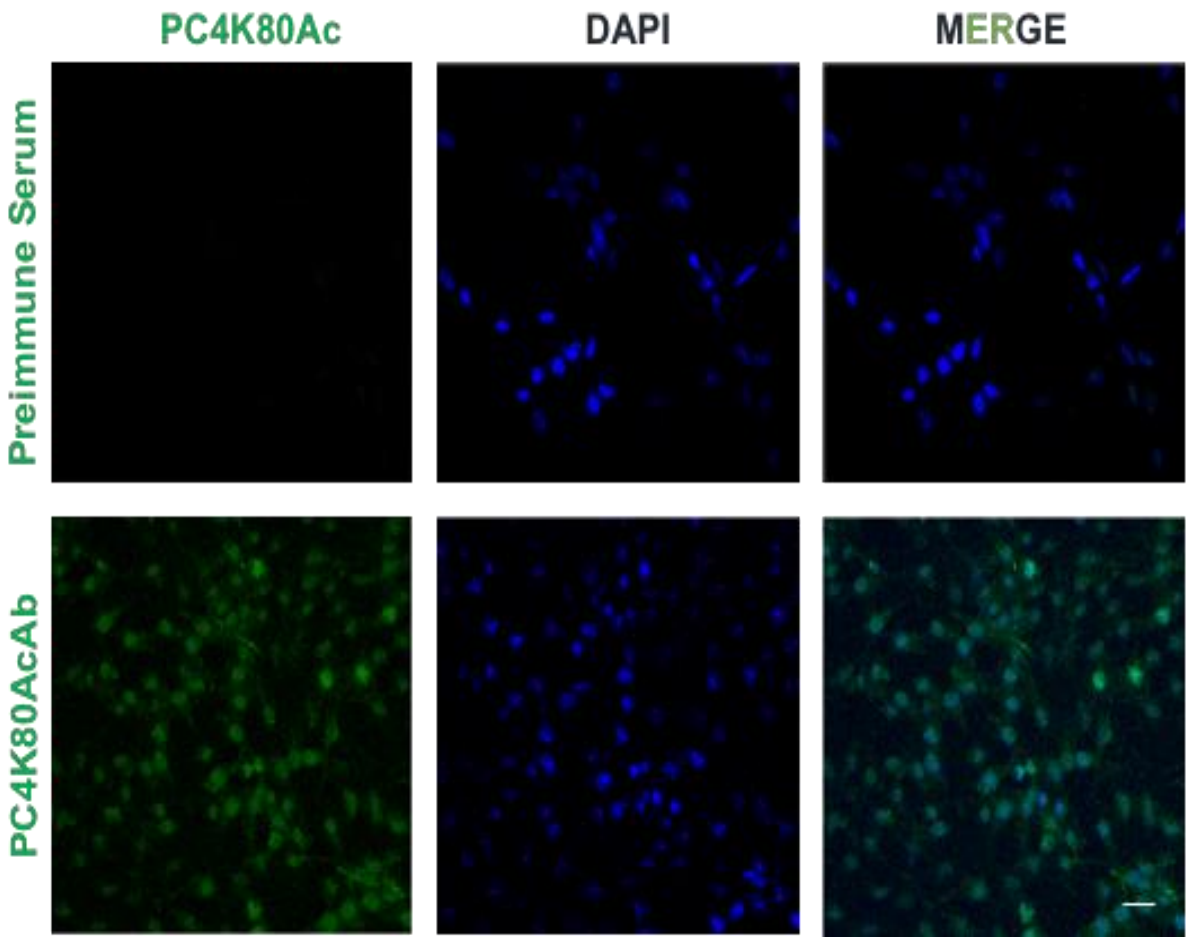

Figure 2.17: Characterization of anti-K80Ac PC4 antibody in cells. Immunofluorescence to detect the levels of acetylated PC4 using the anti-K80Ac PC4 antibody.

2.8. Gene Expression analysis

2.8.1. Prediction of miRNAs targeting PC4 3'UTR

The 3Kb long 3'UTR was analyzed to determine the presence of miRNA binding sites with the help of online prediction tools such as miRANDA and TargetScan

miRANDA (microRNA.org) follows a three step analysis to predict miRNAs. For the PC4 3'UTR analysis the search for miRNAs was done giving the SUB1 Huaman 3'UTR as the input. miRNA sequences from the database input are scanned against user-provided 3′ UTRs to check for Watson Crick matches. The free energy of each miRNA:mRNA target pair that exceeds a threshold matching score is calculated. Each target that has a predicted free energy below a threshold is then passed to the last step. Finally, conservation is used as a final filter. However, miRanda considers conservation of both binding site and position. Unlike most miRNA target predictors, miRanda considers matching along the entire miRNA sequence (Enright et al., 2003). It takes the seed region into account by weighting matches in the seed region more heavily. Matches are allowed to contain limited G-U wobble pairs and insertions or deletions (indels). Free energy is calculated by predicting the folding of the miRNA:mRNA hybrid using the Vienna package (Hofacker et al., 1994). Although this is a common method, it ignores any additional protein interaction, such as with the RNA-induced silencing complex (Enright et al., 2003). Based on these analysis miRSVR score is obtained based on the seed-site pairing, site context, free-energy, and conservation. A mirSVR cutoff of <= -1.2 is recommended to predict miRNAs.

Position 1977-1983 of SUB1 3' UTR **hsa-miR-29c**	**5' ...CAAUCUACUAACAGAUGGUGCUG...** **|||||||** **3' AUUGGCUAAAGUUUACCACGAU**	**mirSVR score** **-0.4186**
Position 1977-1983 of SUB1 3' UTR **hsa-miR-29a**	**5' ...CAAUCUACUAACAGAUGGUGCUG...** **||||||||||** **3' AUUGGCUAAAGUCUACCACGAU**	**-0.4186**
Position 1977-1983 of SUB1 3' UTR **hsa-miR-29b**	**5' ...CAAUCUACUAACAGAUGGUGCUG...** **|||||||** **3' UUGUGACUAAAGUUUACCACGAU**	**-0.4186**

Table No. 3. Prediction of PC4 3'UTR through miRANDA. miR29 family showed higher conservation and perfect Watson crick pairing, resulting in good miRSVR score.

TargetScan (Lewis et al., 2005; Grimson et al., 2007; Friedman et al., 2009; Garcia et al., 2011) ia another online prediction tool which allows the user to search by miRNA name, gene name, or from broadly conserved, conserved, or poorly conserved miRNA families across several species. The output screen ranks predicted targets by either the predicted efficacy of targeting (context+ scores) or the probability of conserved targeting (PCT). For conservation, the conservation of a 3′ UTR is first determined followed by analysis of a specific k-mer (8mer, 7mer-m8, or 7mer-1A). Since one 3′ UTR can contain multiple target sites, an aggregate PCT is provided. For each type of k-mer, the number is provided for that target and whether or not it is considered a conserved site or a poorly conserved site. Furthermore, there is a link to the 3′ UTR of the gene that demonstrates the conserved seed sequence (Friedman et al., 2009). The context+ score demonstrates the probability of a given target as being effectively targeted. Scoring for this feature was derived from experimental results. Several features are included when defining the score, such as 3′ compensatory pairing, local AU content, and position contribution (Grimson et al., 2007; Garcia et al., 2011).

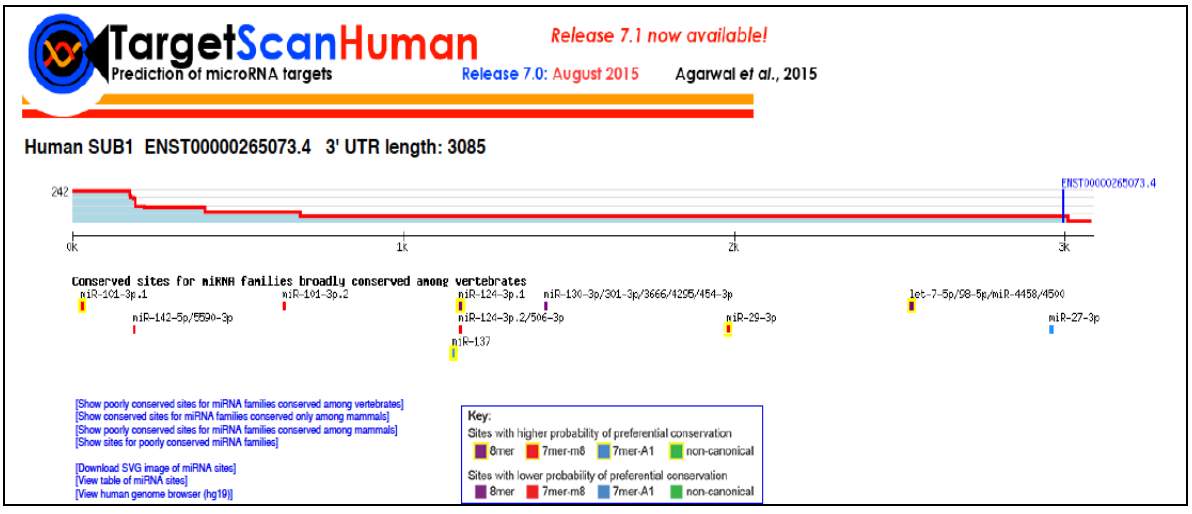

Figure 2.18: Analysis of the 3'UTR of PC4 through TargetScan Human 7.0: Analysis of the 3'UTR of PC4 shows a number of miRNAs predicted to bind to the 3'UTR at distinct regions. However among them miR29 showed greater number of base pairing with higher probability of preferential conservation.

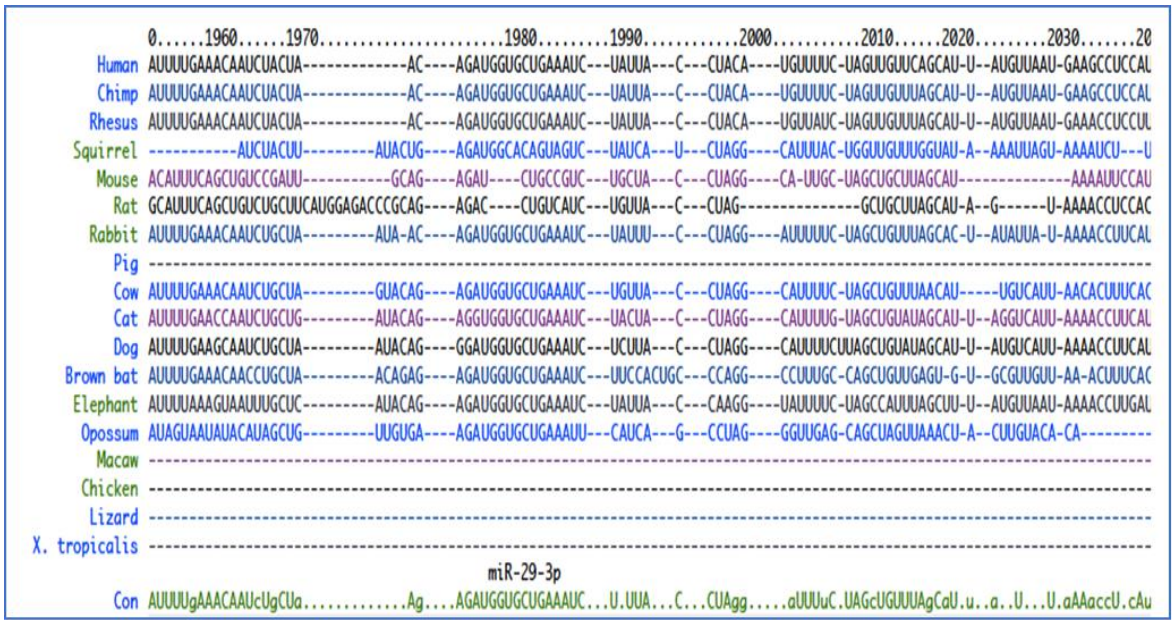

	Predicted consequential pairing of target region (top) And miRNA (bottom)	Site type	Context +++ score	Context +++ score percentile	Weighted Context +++ score	Conserved Branch length	P_{CT}
Position 1977-1983 of SUB1 3' UTR	5' ...CAAUCUACUAACAGAUGGUGCUG...	7mer-m8	-0.27	90	-0.05	3.694	0.76
hsa-miR-29a-3p	3' AUUGGCUAAAGUCUACCACGAU						
Position 1977-1983 of SUB1 3' UTR	5' ...CAAUCUACUAACAGAUGGUGCUG...	7mer-m8	-0.25	88	-0.05	3.694	0.76
hsa-miR-29b-3p	3' UUGUGACUAAAGUUUACCACGAU						
Position 1977-1983 of SUB1 3' UTR	5' ...CAAUCUACUAACAGAUGGUGCUG...	7mer-m8	-0.25	88	-0.05	3.694	0.76
hsa-miR-29c-3p	3' AUUGGCUAAAGUUUACCACGAU						

Context++ score and features that contribute to the context++ score are evaluated as in Agarwal et al., 2015.
Conserved branch lengths and P_{CT} are evaluated as in Friedman et al., 2008, with an expanded 84-species alignment as described in Agarwal et al., 2015.

Figure 2.19. Analysis of miR29 binding: Alignment of the miR29 binding site with PC4 3'UTR of different species to determine the conservation (Upper panel). Scoring of the binding of miR29a, 29b, 29c to the 3'UTR of PC4 based on the seed sequence matching and conservation(P_{CT} value)

2.8.2. Gene expression analysis from TCGA

The patient's clinical data for breast carcinoma were downloaded using TCGA assembler using GDC server. Downloaded data comprised of tumor pathologic and node pathologic information. The information obtained is summarized in Table no.4. TCGA RNA-seq data (including raw_read_count and scaled_estimate for each sample) for all primary tumor, metastatic tumor and matched normal samples were downloaded using TCGA assembler. Transcript per million values for each gene was obtained by multiplying scaled_estimate by 1 000 000. Boxplot was generated using R (https://cran.r-project.org/).Gene expression correlation analysis of PC4, and miR-29a/b/c using R programming language.

TCGA–Breast cancer transcriptome (BRCA) cohort		**1090**	
TCGA-BRCA cohort with PC4 and miR-29 expression data available		1069	
BRCA subtype	**N**	**Tumour Stage**	**N**
Luminal A	388	**I**	179
Luminal B	321	**II**	606
Her2	111	**III**	242
Basal	180	**IV**	20
Normal-like	69	**NA**	22
Total	1069	**Total**	1069

Table No. 4. Summary of the patient sample data obtained from TCGA database. N represents the number of patient samples.

Chapter 3: Role of Chromatin protein PC4 in cellular survivability and regulation of autophagy

This chapter describes the role of Human Positive Coactivator 4 PC4 in cellular survivability and regulation of autophagy with detailed experimental results. PC4 knockdown cells were shown to harbor several cellular defects like cell segregation, irregular chromosomal and nuclear shape etc. Despite these defects the property of cellular survivability of these cells was not compromised, rather PC4 knockdown cells showed greater proliferation rate and gamma irradiation resistance. This chapter focusses on these properties of PC4 depleted cells and also further demonstrates the molecular mechanism of its survival advantage upon stressful conditions possibly through the process of enhanced autophagy.

Background

The mammalian chromatin is a highly complex nucleoprotein structure efficiently organized by the histones, noncoding RNAs and the chromatin associated proteins. The chromatin associated proteins functions not only in the organization but also in the maintenance of the dynamicity of the chromatin thus rendering a functional genome. Human positive co activator 4 is a highly abundant nuclear protein which performs multiple cellular functions (Garavís and Calvo, 2017). Although discovered as a positive coactivator for activator dependent RNA polymerase II mediated transcription (Ge and Roeder, 1994; Kretzschmar et al., 1994) it was later found to be an integral part of the chromatin inducing chromatin compaction (Das et al., 2006). It is absolutely essential for life as PC4 knockout mice was found to be lethal in the early embryonic stage. Conditional knockout in brain resulted in defects in neurogenesis and also memory extinction process (Swaminathan et al., 2016). In this study, we make an attempt to establish the invivo role of Human positive coactivator 4 (PC4) by a cellular knockdown approach. PC4 being an important protein in mediating genome stability (Mortusewicz et al., 2016) and efficient and ordered chromatin organization, its depletion would lead to a drastic alteration in the phenotype of the cell.

Chromatin associated proteins often act as sensors of stress to efficiently safeguard the genetic material of the cell through the coordinate function of histone modifications and thereby an altered transcriptional output. Macro-autophagy (herein referred as only autophagy), a well conserved cellular self-eating process, is a lysosome dependent degradative pathway known to maintain the cellular homeostasis by getting rid of unwanted organelles, misfolded proteins and toxic aggregates (Alerting, 2007). Autophagy has a prosurvival role as it responds to stress such as starvation and genomic insult due to radiation. Several studies have highlighted the cytoprotective role of autophagy upon radiation stress in tumor cells (Bristol et al., 2013; Chakradeo et al., 2015). This role might be mediated by extensive crosstalk of the autophagy process and the apoptotic pathway. It has also been shown that autophagy protects tumor cells from injury and stressful environment by eliminating unwanted or non-functional organelles, controlling the production of reactive oxygen species and by the recycling of essential proteins required for repairing DNA lesions.

To gain an insight into the *invivo* functions of this multifunctional protein we established a lentivirus mediated PC4 knockdown cell line through the stable integration of PC4 specific shRNA in Human Embryonic kidney cells. This study is the detailed characterization of this PC4 knockdown cell line. Transient silencing of PC4 in Hela cells led to an open chromatin state and an altered gene network (Das et al., 2010). In this study we further correlated the open chromatin state and the altered gene network to the induction of a cellular process which balanced the cellular chaotic conditions and led to higher proliferation of the PC4 knockdown cells including its gamma irradiation resistance property. This study brings forth the role of chromatin proteins in mediating the organization of the chromatin, maintaining the epigenetic language of the cells and thereby preserving cellular homeostasis.

3.1. Knockdown of PC4 leads to altered nuclear architecture

Human Positive coactivator 4 PC4 is one of the most abundant proteins found in the nucleus of cell playing key roles in various cellular functions as is described in Chapter 1. To gain an insight into its *invivo* role in greater detail, a stable PC4 knockdown cell line was established using Human embryonic kidney cells. A specific shRNA (described in Chapter 2) targeting PC4 was delivered to HEK293 cells through lentivirus mediated transfection. PC4 being a chromatin organizer, it was important to look into the state of chromatin, the nuclear and cellular physiology of the cell in absence of PC4. HEK293 (Taken as control) and PC4 knockdown cells (sh-PC4) were subjected to transmission electron microscopy to examine the ultrastructures and visualize the organelles particularly the nucleus.PC4 knockdown cells were found to have highly deformed nuclei (Figure 3.1). The shape and size of the nuclei were found to be variable in the sh-PC4 (PC4 knockdown cells) (Figure 3.1. Right panel) in comparison to the round uniform shape in the wild type HEK293 (control) cells (Figure 3.1. Left panel). HEK293 wildtype cells also exhibited densely stained nuclei whereas the PC4 knockdown cells harbored lightly stained nuclei. PC4 is also known to induce heterochromatinization possibly through its interaction with histones and non-histone proteins, like HP1alpha. Transient silencing of PC4 in Hela cells altered the heterochromatin organization of the genome by decompacting the chromatin. (Das et.al, 2010) The lightly stained nuclei in the PC4 stable knockdown cells possibly indicates the loss of heterochromatin foci which were found to be present in the darkly stained nuclei of the wild type HEK293 cells. This observation thus reinforces the role of PC4 in chromatin compaction and also brings forth its critical role in maintenance of nuclear architecture. Interestingly, the micrographs also revealed accumulation of large number of double membraned vesicles around the nucleus of PC4 knockdown cells which was not found in the control wildtype HEK293 cells. The significance of the appearance of such structures specifically in the PC4 knockdown cells have been discussed in the later sections of this chapter.

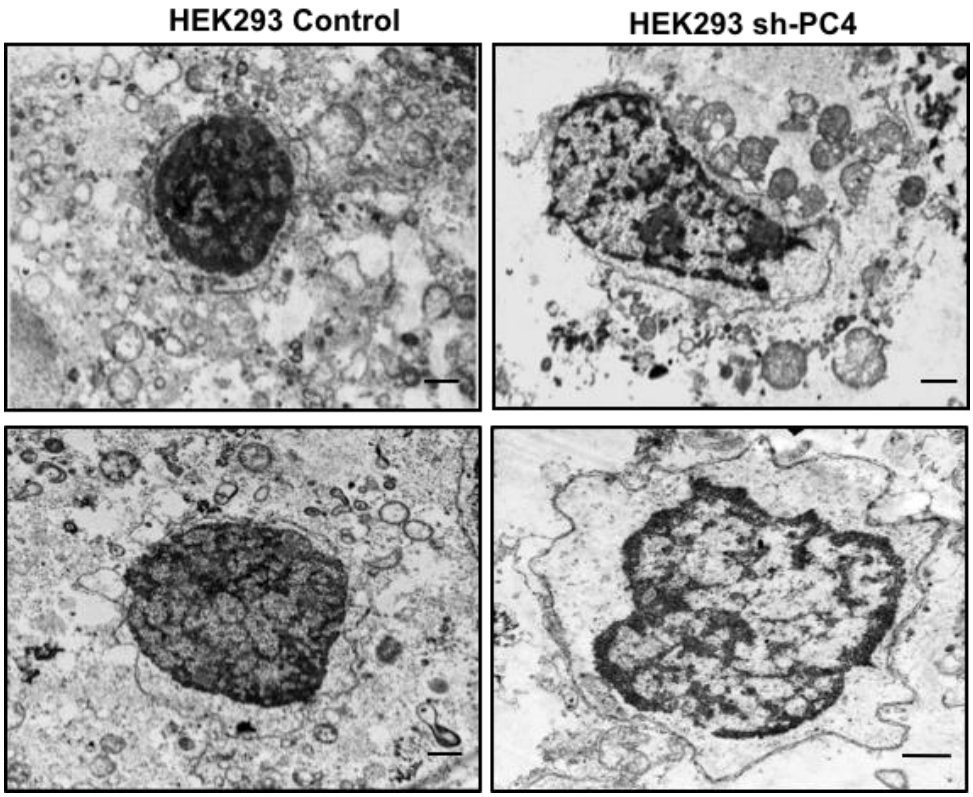

Figure 3.1. PC4 is critical for the maintenance of nuclear architecture of the cell. Ultrathin sections of HEK293 and HEK293 PC4 knockdown cells were visualized using transmission electron microscope. Electron micrographs showing abnormal nuclei in absence of PC4.The densely stained region in the nuceleus is the heterochromatin region. Right panel represnts fields of PC4 knockdown cells showing altered nuclear structures. Left hand panel represents fields from HEK293 cells with nucleus. Scale bar represents 1μm.

3.2. Absence of PC4 leads to defects in chromosomal morphology and cell segregation

As absence of PC4 altered the global nuclear architecture of the cells, the state of the chromosomes and their segregation pattern was further examined in the PC4 Knockdown cells. To analyze the morphology of the chromosomes, metaphase chromosome spreads were done both from the control as well as PC4 knockdown cells followed by Hoechst staining. Chromosomes from the PC4 knockdown cells (sh-PC4) failed to spread efficiently and appeared as clumped structures. The chromosomes of the PC4 depleted cells appeared fuzzy,

broader in diameter and did not have the typical shape of the metaphase chromosomes as found in the control cells (Figure 3.2.1)

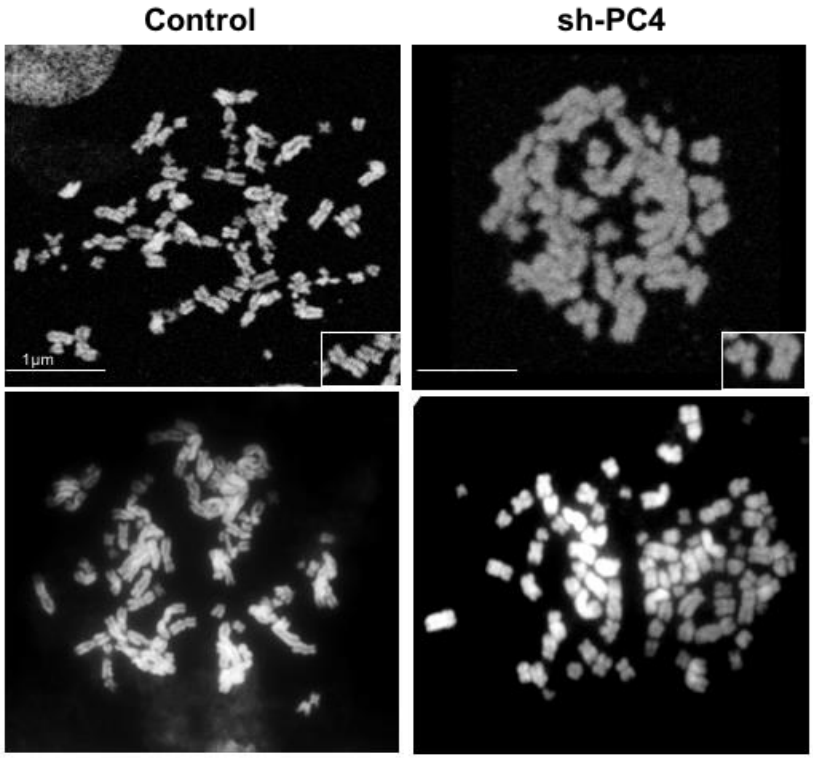

Figure 3.2.1. PC4 Knockdown alters the morphology of the chromosomes: Metaphase spreads from HEK293(control) and PC4 knockdown (sh-PC4) cells reveal abnormal chromosomal structures in PC4 knockdown (sh-PC4) cells. The upper panel represents metaphase spreads from control HEK293 cells, while the lower panel shows spreads from PC4 Knockdown cells (Different fields) Scale bar 1µm**.**

The presence of abnormal shaped and poorly spread metaphase chromosomes from PC4 knockdown cells prompted us to look into the segregation pattern in absence of PC4. For studying segregation pattern, we followed two approaches, **Binucleate analysis and Telomere PNA FISH**. Binucleate analysis was performed followed by nuclear staining with Hoechst. This nuclear analysis revealed presence of nucleoplasmic bridges between two dividing nuclei in the PC4 knockdown cells (sh-PC4) (Figure 3.2.2.A). Control cells showed very few number of such ultrafine structures as compared to the PC4 knockdown cells (Figure 3.2.2 B). Anaphase bridges are formed as a result of unfaithful segregation of

daughter nuclei during the late mitotic or anaphase stage. The presence of higher number of anaphase bridges in cells which were devoid of PC4 signifies the role of PC4 cells in cell segregation process.

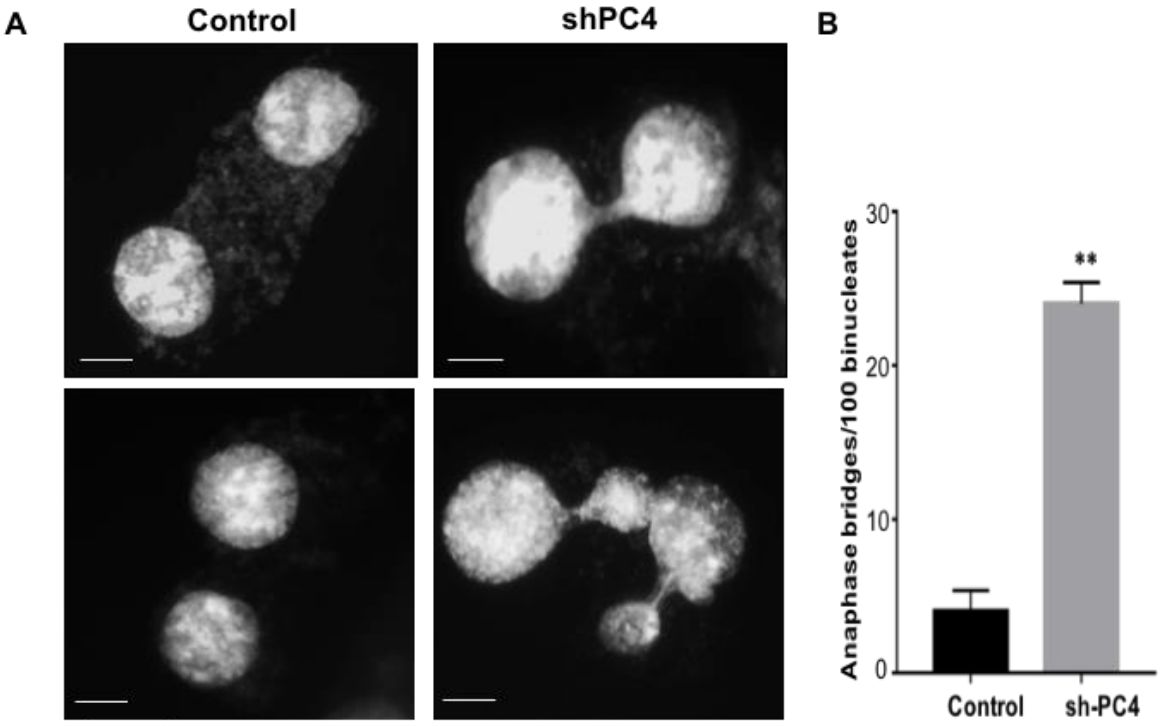

Figure 3.2.2 PC4 Knockdown leads to defects in the nuclear segregation process.(A) Nuclear division analyzed by binucleate analysis reveals irregular segregation and formation of Anaphase Bridges in the sh-PC4 cells compared to control cells. (B) Scale bar represents 1µm. Quantitative representation of number of anaphase bridges occurring per 100 nuclear divisions in control and sh-PC4 cells. n=100, N=2. Data are presented as means ± S.E.M. p** < 0.001, p*** < 0.0001.

To analyze the defects in segregation pattern at chromosomal level, we performed telomere PNA-FISH (Peptide nucleic acid fluorescence *in situ* hybridization). By assessing the PNA foci (fluorescent green signals) we can get a direct read of each chromosome during the segregation process. Control cells (HEK293 wildtype) showed equal number of PNA foci in the dividing nuclei, signifying equal distribution of chromosomes in two daughter nuclei (Figure 3.2.3A upper panel). In PC4 knockdown cells (sh-PC4) binucleates were observed with unequal number of PNA foci (Figure 3.2.3A lower panel). This unequal distribution of PNA foci was found to be statistically significant in the PC4 Knockdown cells as compared to the control cells (Figure 3.2.3B). This unequal distribution of chromosomes and the presence of anaphase bridges in the newly divided daughter nuclei of PC4 Knockdown cells could be attributed to segregation defects.

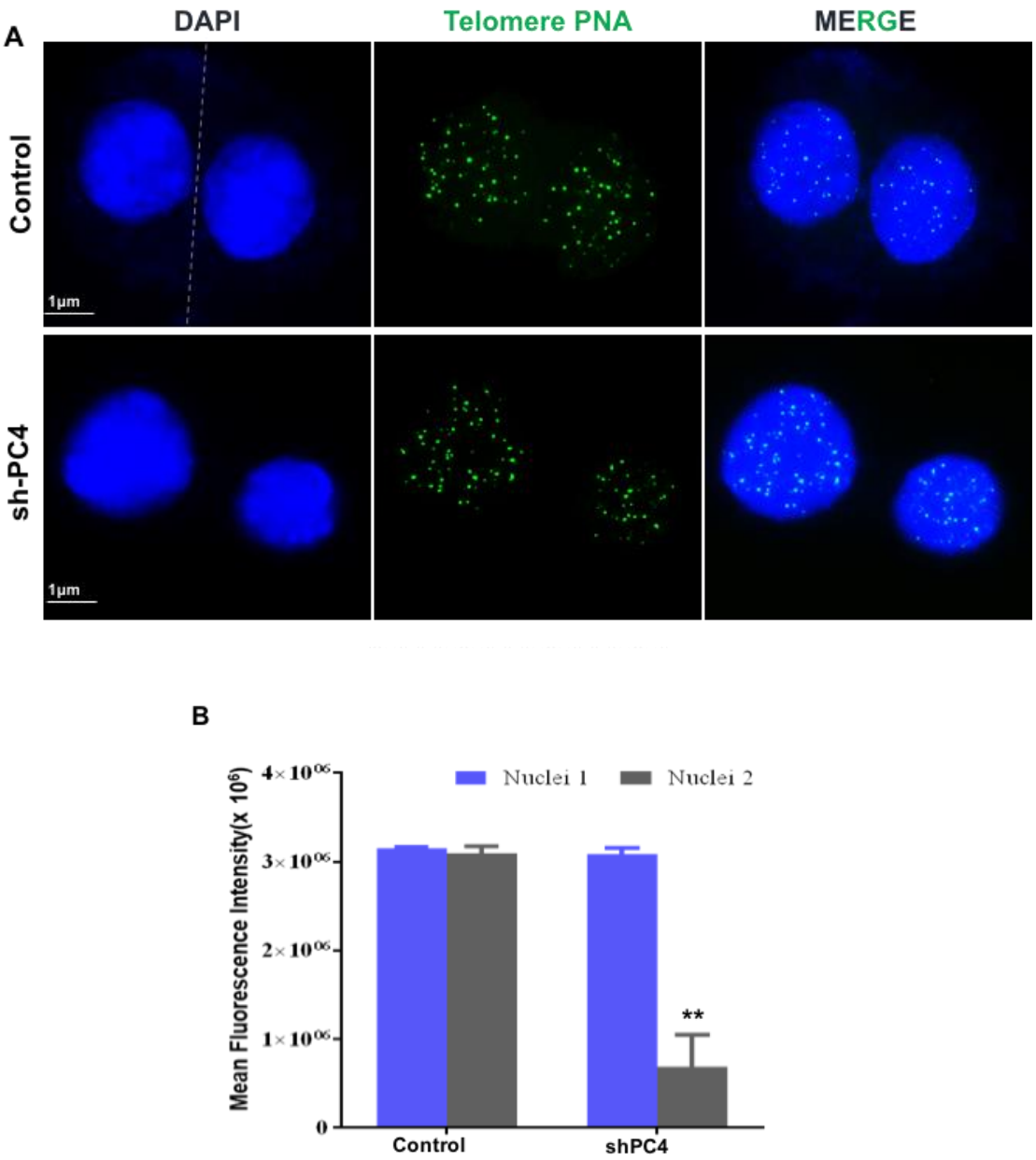

Figure 3.2.3 PC4 is critical for faithful chromosomal segregation process. (A) Telomere PNA-FISH analysis reveals irregular segregation pattern of chromosomes in sh-PC4 cells which is determined by the differing number of PNA foci in daughter nuclei as compared to control. Green fluorescence represents Telomere-PNA probe. The vertical dotted line denotes axis of cell division. Scale bar 1µm. (B) Quantitative representation of the PNA hybridization in daughter nuclei in terms of the mean fluorescence intensity in a.m.u. As shown, there is differing signal intensity in the daughter nuclei in sh-PC4 as compared to control cells. Data are presented as means ± S.E.M. (n = 50, N=2). p** < 0.001, p*** < 0.0001.

3.3. PC4 knockdown results in chromatin decompaction and alters the epigenetic status

To validate the role of PC4 as a chromatin organizer *in vivo,* we investigated the effect of PC4 repression on the compaction state of the chromatin by digesting the nuclei of the knockdown cells with micrococcal nuclease in a time dependent manner (Figure 3.3.A). The MNAse pattern from the PC4 knockdown cells showed high preponderance of mononucleosomes even at 0-time point establishing the decompacted state of chromatin in absence of PC4 (Figure 3.3.1). When nuclei from control cells were digested with equal units of MNase for similar time points as of 10 and 15 minutes, the presence of mono-, di-nucleosomes were much lesser as compared to the sh-PC4 cells (Fig. 3.3.1, compare lanes 3-4 versus lanes 7-8). Slow migrating higher molecular weight fragments were observed as smear in the control cells which was quite diminished in the chromatin obtained from PC4 Knockdown cells signifying that the resistance of chromatin from the control cells to MNAse digestion. It was also intriguing to observe that at 0 min time point of MNAse digestion (where the reaction was immediately stopped after addition of the enzyme), chromatin from sh-PC4 cells showed presence of mono-nucleosomes whereas the chromatin from the control cells showed no digestion pattern, as evident by the smear signifying higher molecular weight bands (Fig. 3.3.1, compare lane 1 vs lane 5). This result signifies the integral role of PC4 in chromatin organization and compaction in cells. Thus, knockdown of PC4 not only alters the nuclear and cellular architecture, it also leads to an open chromatin structure.

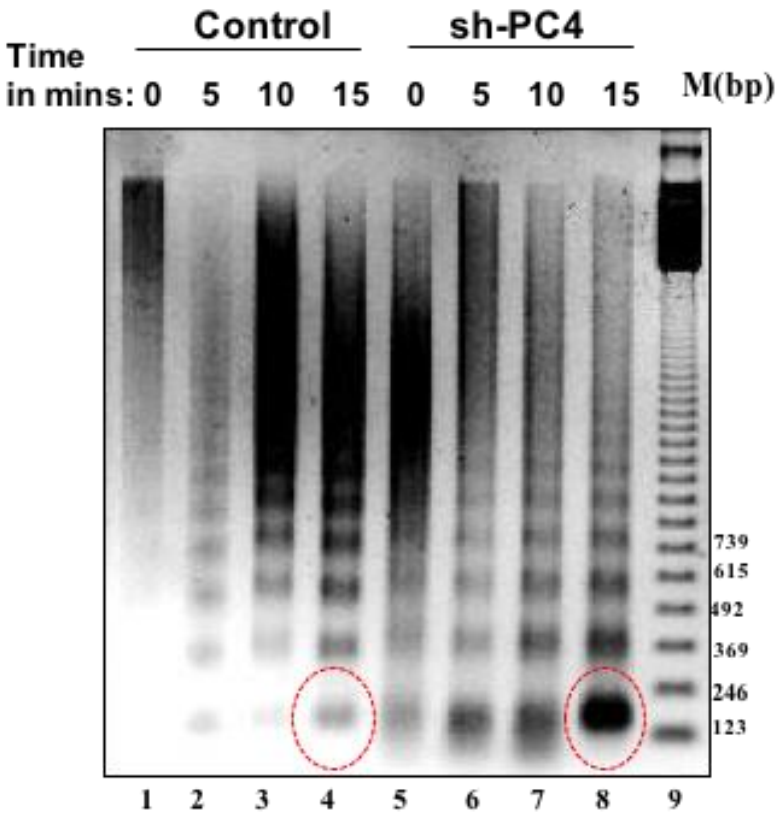

Figure 3.3.1 Absence of PC4 causes global chromatin decondensation. Micrococcal nuclease digestions were carried out at four different time points (0, 5, 10 and 15 mins) with the nuclei isolated from control cells (lanes 1 to 4) and from sh-PC4 cells (lanes 5 to 8). Red dotted circles highlight the presence of mononucleosomes.

Interestingly, in lieu with the decompacted state of chromatin, PC4 knockdown cells showed a distinct change in the epigenetic pattern particularly histone acetylation. Core histones were isolated from cells and their state of modifications was checked. PC4 knockdown cells showed higher H3K9, K18, K27 acetylation levels and also upregulation in H4K8, K12, K16 acetylation marks (Figure 3.3.2 lanes 1 vs 2). We also checked the methylation mark mediated by CARM1 enzyme and found that H3R17me2 to be upregulated in the PC4 knockdown cells. All these epigenetic markers were associated with the transcriptional activation phenomenon. Taken together, these data establish that stable knockdown of PC4 resulted in the change of the global chromatin state towards a more decompacted, and possibly transcriptionally amenable genome.

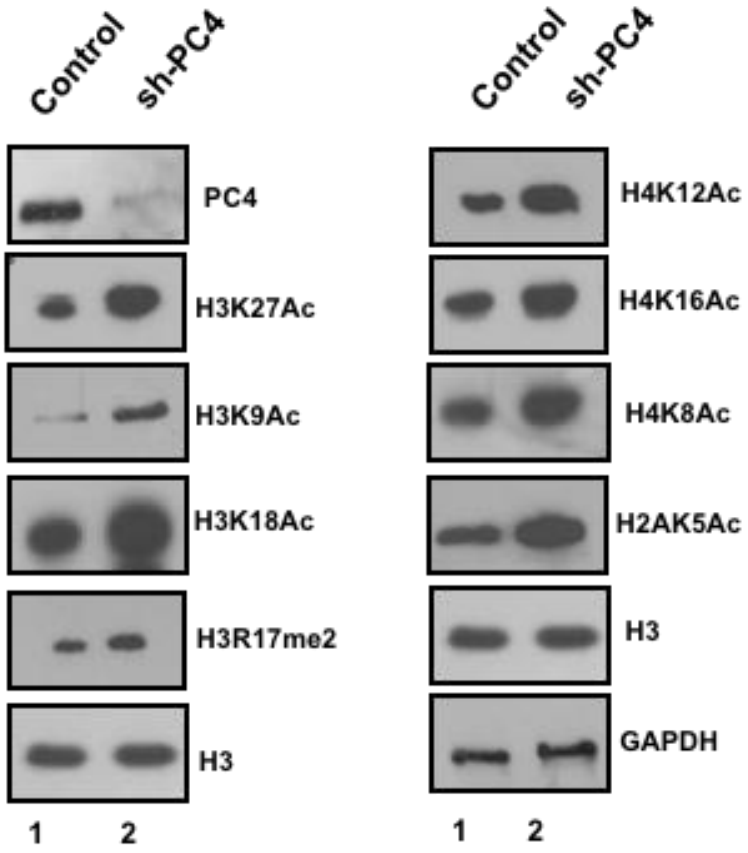

Figure 3.3.2 PC4 knockdown leads to the upregulation of active histone marks. Core histones were extracted from control cells and knockdown cells. Transcription activation associated histone modifications were examined by immunoblotting using specific antibodies as indicated. sh-PC4 cells showed enhanced levels of histone acetylation as well as methylation marks.

3.4. PC4 knockdown cells exhibit higher proliferation, migration and gamma irradiation resistance property

Although PC4 knockdown cells harbored several cell cycle and nuclear defects, interestingly we did not find inhibition in the growth pattern of these cells. They not only divided across multiple passages but also appeared to grow faster than the control HEK293 cells. To understand the rate of proliferation and growth pattern upon PC4 repression, we performed

clonogenic assay from equal number of cells from PC4 knockdown cells as well as control cells and monitored them after 10 days of growth. PC4 knockdown cells formed higher number as well as large colonies as compared to the control cells. We also checked the migratory property by wound healing assay. The rate of healing was found to be much faster in case of sh-PC4 when compared to control cells as complete closure of the wound was found in the sh-PC4 cells after 12 hours from the time of the scratch (Figure 3.4.1B). This faster healing of the wound could also be attributed to the higher growth rate of the PC4 knockdown cells. as compared to the control cells.

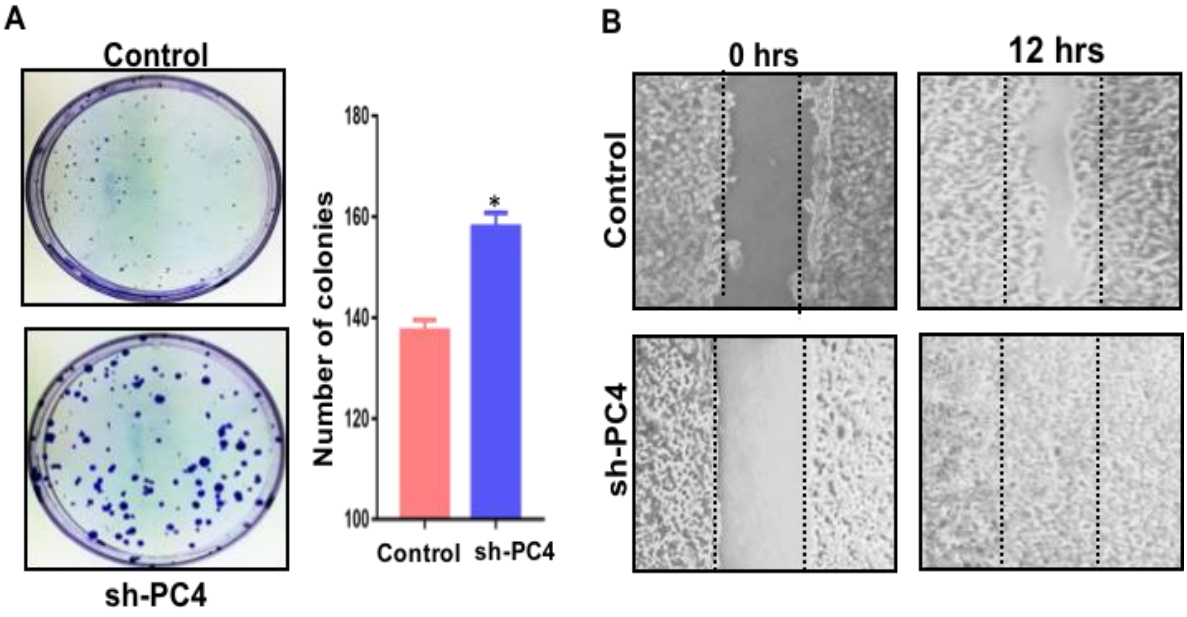

Figure 3.4.1 PC4 knockdown cells exhibit greater proliferation and migratory properties. (A) Representative image of the crystal violet stained colonies of control and sh-PC4 cells shows greater proliferation rate in sh-PC4 cells. Bar Graph depicts the quantitative comparison of proliferation rate in terms of number of colonies between control and sh-PC4 cells. Data are presented as means ± S.E.M. (N=2). p** < 0.001, p*** < 0.0001. (B) Microscopic images of wound healing assay performed for comparison of proliferation as well as migration rate between control and sh-PC4 cells. Wound was monitored until its closure at 12hours in the sh-PC4 cells.

Despite several defects the higher proliferation rate of PC4 knockdown cells was quite intriguing. We then further wanted to monitor the growth properties of the PC4 knockdown cells under the conditions of genotoxic stress or insult. We exposed the PC4 knockdown cells to increasing doses of gamma irradiation and monitored its proliferation as well as death rate. From the colony formation assay we find that PC4 knockdown cells survived more after the genotoxic insult mediated by gamma irradiation as compared to the control cells. Thus, PC4 knockdown cells exhibited the property of gamma irradiation resistance which is evidenced by the appearance of significantly greater number of live colonies after 10 days of exposure to gamma irradiation (Figure 3.4.2A and B).

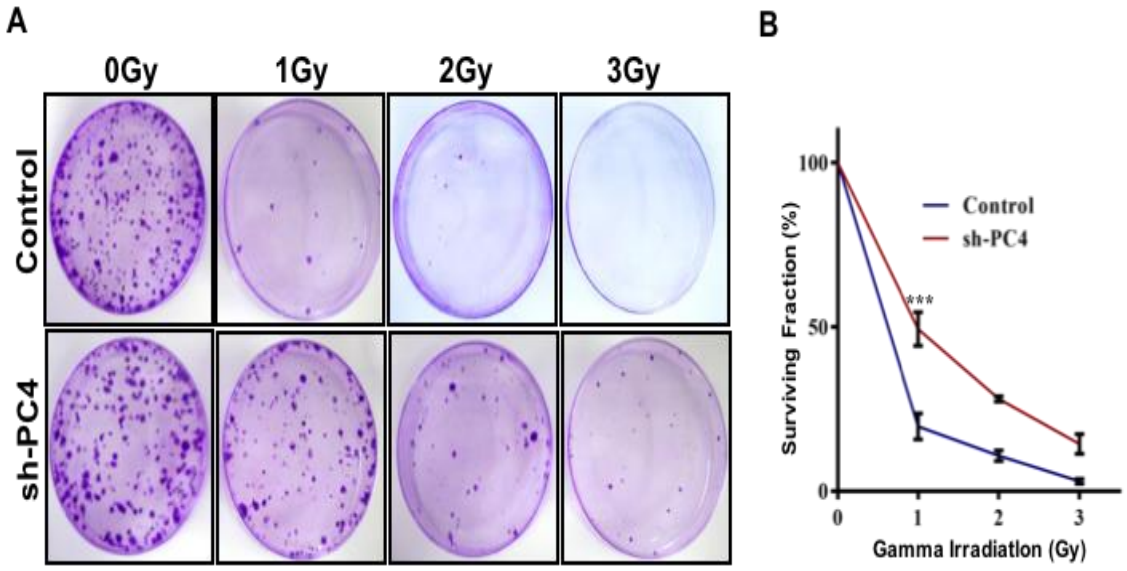

Figure 3.4.2 PC4 knockdown cells harbour gamma irradiation resistance property. (A) Representative image of the crystal violet stained colonies of control and sh-PC4 cells sustained after exposure to increasing doses of the gamma radiation (in Grey units) (B) Graph plot depicting surviving fraction in percentage against the doses of gamma irradiation. Data are presented as means ± S.E.M. (N = 3). p** < 0.001, p*** < 0.0001.

This result encouraged us to further investigate the property of gamma irradiation resistance of sh-PC4 cells through another experimental approach. We analyzed the apoptotic rate of the cells upon exposure to gamma irradiation (2 Grey Unit) by flow cytometry analysis using Annexin VCy3.18 dye. Annexin-Cy3.18 (AnnCy3) can form conjugates with the translocated phosphatidyl serine on the cell surface of apoptotic cells. This can be detected as red fluorescence which has been represented as blue in the upper quadrant (Figure 3.4.3 A upper panel). The live cells were pseudocolored as red. Since sh-PC4 cells harbored the stably expressing GFP containing shRNA plasmid (pGIPZ-shRNA for PC4 refer to materials and methods section) it emitted GFP fluorescence detected as green signal, in the lower quadrant of the sh-PC4 cells (Figure 3.4.3A lower panel). Staining of apoptotic cells after 6 hour of gamma irradiation using the Annexin V dye followed by flow cytometry, showed that sh-PC4 cells had significantly lesser apoptotic rate than the control cells (Figure 3.4.3). The control cells as expected showed significant apoptosis upon exposure to gamma irradiation (4.76% to 11.43%) while the percentage of apoptotic cells in sh-PC4 cell population showed no significant alteration in their population even after exposure to gamma irradiation (Figure 3.4.3 B). These results reinforce the fact that PC4 depletion confers radiation resistance to the cells.

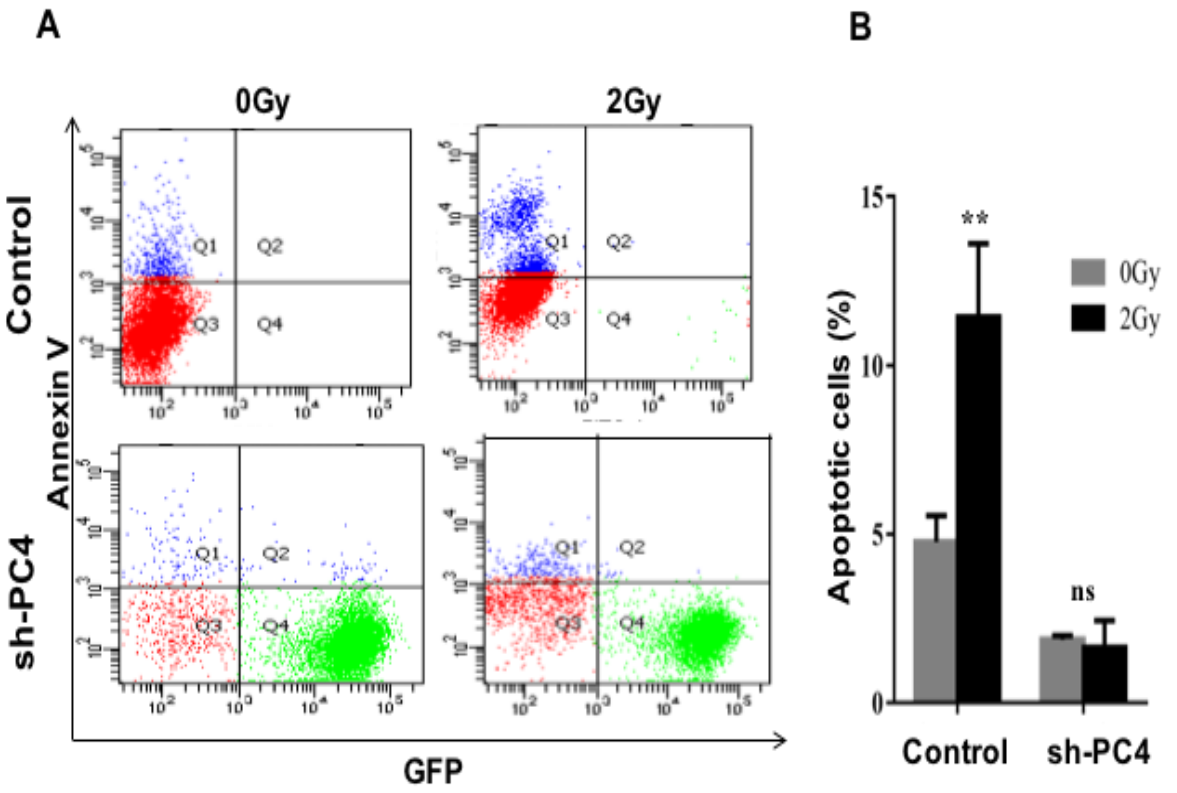

Figure 3.4.3 Gamma irradiation fail to induce apoptosis to PC4 knockdown cells : (A) Apoptosis analysis using Annexin V staining coupled with flow cytometry was performed in control vs sh-PC4 cells. Cells were irradiated at 2Gy and after 6hours of exposure cells were harvested and analyzed by FACS after staining the apoptotic cells with Annexin V. The upper right and left quadrant represents apoptotic cells. Since sh-PC4 cells harbour a GFP expressing shRNA plasmid, the upper left quadrant in sh-PC4 panel represents apoptotic GFP positive cells. (B) Total percentage of apoptotic cells were counted from the FACS analysis and represented in the bar graph. Data are presented as means ± S.E.M. (N = 3). p** < 0.001, p*** < 0.0001.

3.5. PC4 acts as a negative regulator of Autophagy

Knockdown of PC4 results in several cell segregation and nuclear defects. Despite such defects, the growth rate of PC4 knockdown cells was higher as compared to the control cells. More interestingly these cells showed gamma irradiation resistance. We thus wanted to elucidate the molecular mechanism of this property of enhanced proliferation and survival advantage of PC4 Knockdown cells. From our earlier observation, we found that PC4 knockdown cells failed to undergo apoptosis upon gamma irradiation, thus there might be any other cellular phenomenon which might be operating to enhance the proliferation and survival rate of cells upon PC4 repression. Autophagy, a well conserved, cellular degradative process is known to act as a potent survival mechanism for cells especially under stress or toxic conditions. Autophagy levels in cells were assayed by monitoring the levels of microtubule-associated protein light chain 3B (LC3) protein (an autophagy marker). Upon induction of autophagy LC3 is known to undergo lipidation, the lipidated LC3 (LC3II) can be monitored in a SDS-PAGE as it acquires differential mobility as compared to the non lipidated form (LC3 I). Western blotting analysis of cell lysates from PC4 knockdown and control cells show that in sh-PC4 cells the levels of LC3II (lipidated form of LC3) is significantly enhanced (approx. 3-fold) as compared to the control cells (Figure 3.5.1 A, compare lane 1 versus 2). We then induced autophagy by growing cells in a nutrient starved media for 2 hours. sh-PC4 cells showed further increase in the levels of LC3II (Figure 3.5.1A, lane 3 versus 4). This signifies that sh-PC4 cells exhibit elevated levels of LC3II at basal level which gets further enhanced upon starvation induced autophagy. To further confirm that the concomitant increase in LC3II levels directly results from enhanced autophagy and not due to the accumulation of autophagy vacuoles from a defective autophagic pathway we carried out a bafilomycin inhibition assay. Bafilomycin disrupts the autophagic flux by inhibiting the lysosomal proton pump V-ATPase, resulting in a defect in autophagosome-lysosome fusion. Cells were treated with increasing amount of bafilomycin inhibitor of 50nM and 100nM concentrations and the LC3II levels were monitored. We observe that there was an increase in the LC3II levels in the sh-PC4 cells over and above the induced LC3II levels (Figure 3.5.1 B, lane 4 versus 5 and 6). This data establishes the fact that the elevated LC3II level observed in the sh-PC4 cells is indeed due to enhanced autophagy which is abrogated in the presence of an inhibitor, bafilomycin. In control cells,

we observe the presence of LC3II only upon inhibition by Bafilomycin which further signify the inhibition of the autophagy pathway at the fusion stage.

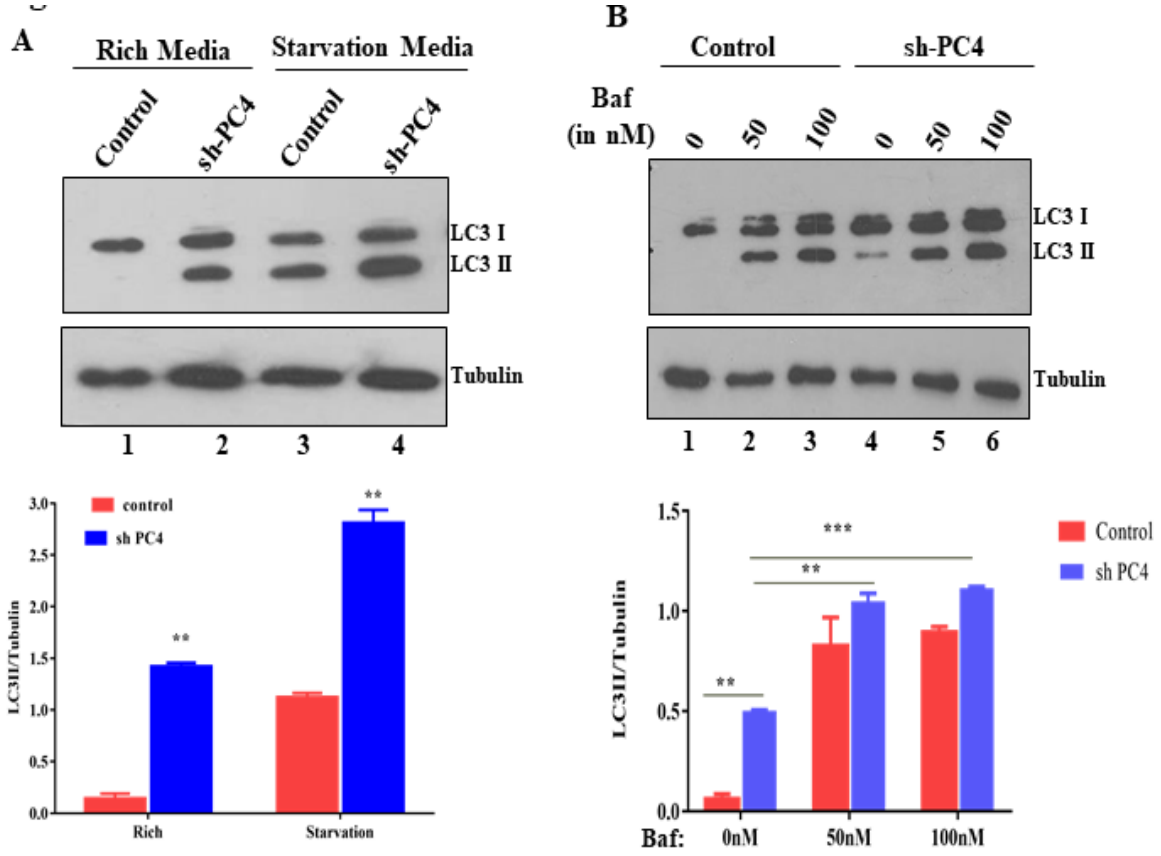

3.5.1 Absence of PC4 induces autophagy. (A) Induction of autophagy in sh-PC4 cells upon starvation: Control and sh-PC4 cells were starved for 2 hours in EBBS media. Cell lysates from both control and sh-PC4 cells in rich and starvation media were analyzed for LC3 I and LC3 II levels. Tubulin used as the loading control. Representative graph showing the change in LC3 II level upon PC4 knockdown both in rich and starvation media is shown. Data are presented as means ± S.E.M. (n = 2). p* < 0.01, p** < 0.001, p*** < 0.0001 (B) Effect of Bafilomycin (50 nM, 100nM) on control and sh-PC4 cells. Accumulation of LC3 II levels upon Bafilomycin treatment for 2 hours signify an inhibition in the process of autophagy. Corresponding, representative graph shows the change in LC3 II level upon Bafilomycin inhibition both in control as well as sh-PC4 cells. Data are presented as means ± S.E.M. (n = 2). p* < 0.01, p** < 0.001, p*** < 0.0001.

To validate the direct role of PC4 expression in regulation of autophagy, we rescued PC4 expression in the PC4 Knockdown cells (Figure 3.5.2 A) (harboring an shRNA which targets 3'UTR region of PC4) and then probed for LC3II levels. In accordance to the above results we found PC4 expression led to a decrease in the total LC3 levels in the cells (Figure 3.5.2 B lane 1 vs 2). Thus, PC4 expression in the knockdown cells rescued the enhanced levels of LC3II levels. This signifies the possible role of PC4 as a negative regulator of autophagy.

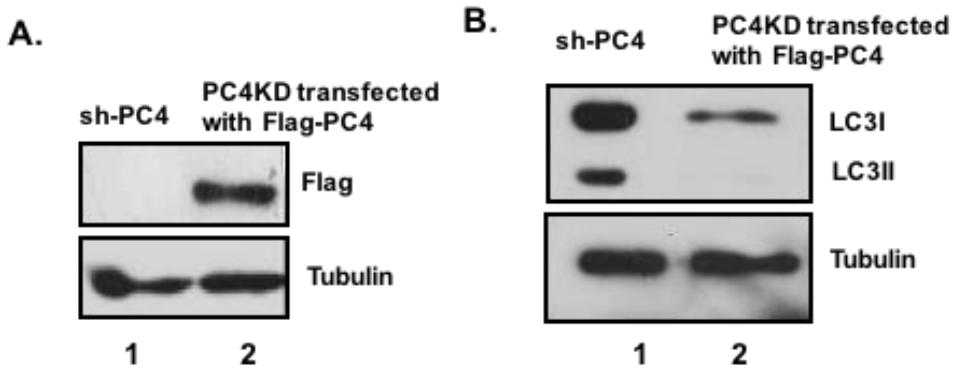

Figure 3.5.2 PC4 inhibits autophagy. (A) Flag PC4 was transiently expressed in PC4 knockdown cells and the expression was checked after 48hrs post transfection by immunoblotting with anti-Flag antibody. (B) LC3II levels were checked in PC4 Knockdown cells (lane 1) and PC4 Knockdown cells transfected with Flag PC4 (rescue) (lane 2).

To get a direct evidence of the enhanced autophagy in PC4 knockdown cells we resorted to electron microscopy to visualize the cellular signatures of the autophagy process. In agreement with the western data, the electron micrographs of the PC4 knockdown cells showed accumulation of large number of double membraned vesicles which are characteristics of autophagy vesicles (Figure 3.5.3, lower panel). We failed to observe in the control cells even after imaging several fields of electron micrographs (Figure 3.5.4, upper panel). The presence of double membraned vesicles in the cytosol of PC4 knockdown cells in basal condition without any stress or administration of autophagy inducers validate the fact that basal autophagy levels is elevated in the absence of PC4.

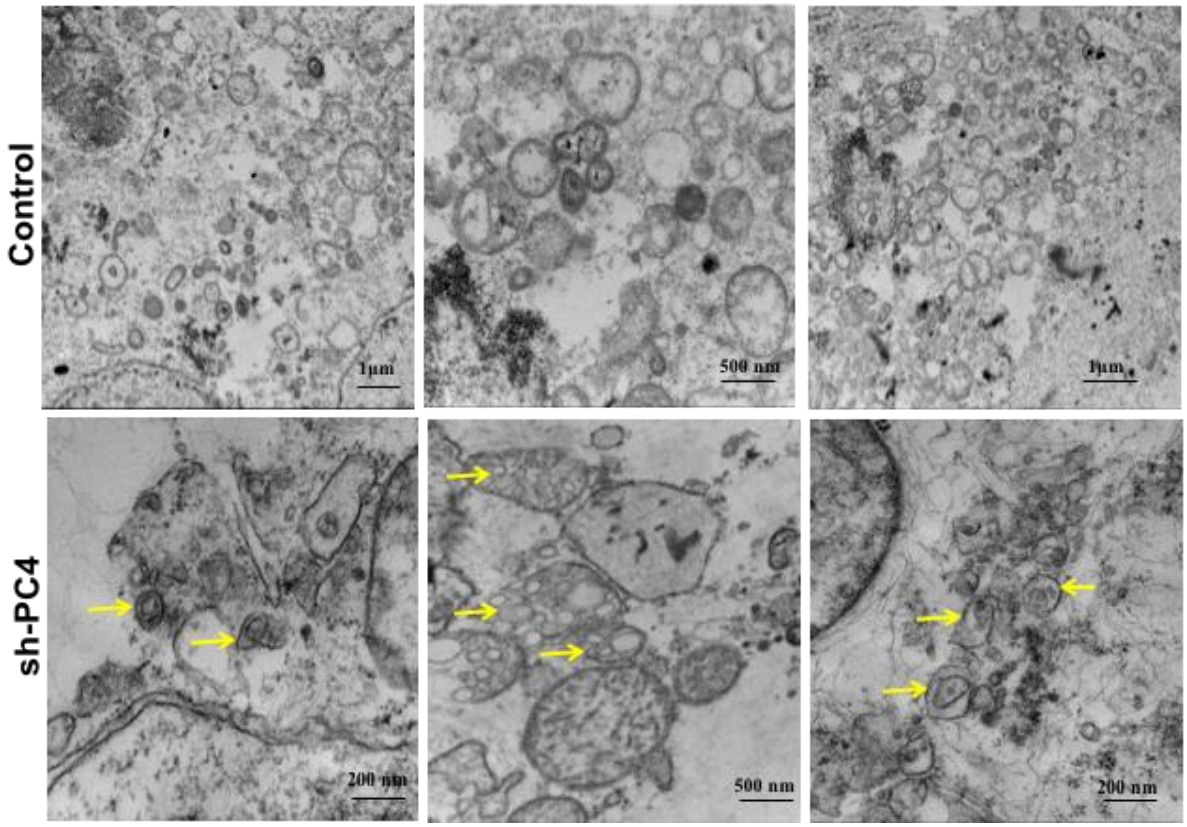

Figure 3.5.3 Cellular visualization of autophagy in PC4 knockdown cells. Electron micrographs of sh-PC4 cells (lower panel) show huge accumulation of double membraned vesicles which are characteristics of autophagy vacuoles. No such vacuoles were observed in control cells (upper panel). Scale bar as denoted in figure.

3.6. Enhanced autophagy in PC4 knockdown cells renders gamma irradiation resistance to the cells

sh-PC4 cells exhibit elevated levels of autophagy in their cell cytosol at basal level. This level is further enhanced upon starvation induced stress. To establish a relation between gamma irradiation resistance and elevated levels of autophagy in absence of PC4, we further analyzed autophagy levels upon gamma irradiation. For this purpose, both the control and sh-PC4 cells were exposed to increasing doses of gamma irradiation. Western blot analysis of cell lysates from sh-PC4 cells and control cells after 24 hours of gamma irradiation showed enhanced LC3II levels in sh-PC4 cells as compared to the control cells suggesting greater induction of autophagy in the PC4 depleted cells as compared to control cells (Figure 3.6.1

compare lanes 3 versus 4, 5 versus 6, and 7 versus 8, respectively). Thus, gamma irradiation induces a cellular stress condition that triggers further enhancement of autophagy levels in the PC4 depleted cells. In control cells, also we find an increase in the LC3II level which suggests the role of gamma irradiation as a potent inducer of autophagy.

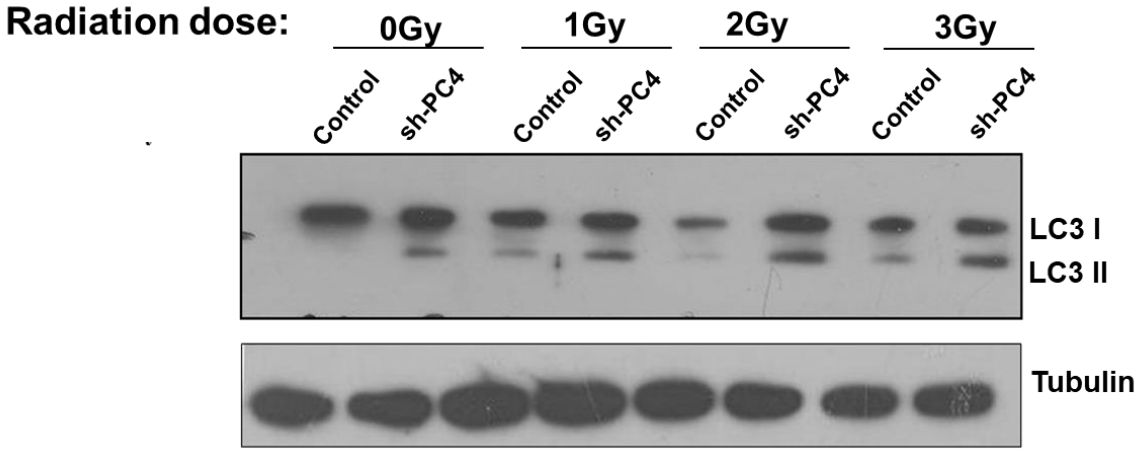

Figure 3.6.1 Induction of autophagy in sh-PC4 cells upon gamma irradiation. Control and PC4 knockdown sh-PC4 cells were irradiated with different doses of gamma rays as indicated. Cell lysates from both cell lines were harvested after 24 hours post irradiation and western blot analysis were carried out with specific antibodies. LC3 antibody was used to analyze the process of autophagy while tubulin was used as loading control.

To understand the role of autophagy in mediating gamma irradiation resistance in PC4 knockdown cells we evaluated the growth pattern of PC4 knockdown cells after gamma irradiation upon autophagy inhibition. We used two known chemical inhibitors of autophagy which inhibits the autophagy process at different stages (as described in Chapter 1). We pre-treated the cells with two known small molecule autophagy inhibitors, 3-Methyladenine (3-MA) and Bafilomycin (Baf) and then exposed to gamma irradiation, and then carried out colony formation assay to determine the survivability percentage of cells. Pre-treatment with both 3-Methyladenine and Bafilomycin led to significant decrease in the number of live sh-PC4 cells as compared to the control cell line. (Figure 3.6.2A and 3.6.3A). 3-Methyladenine being a PI3Kinase inhibitor its pretreatment showed reduction in the control cells as well which can be related to its autophagy independent function,

however comparatively sh-PC4 cells showed more sensitivity to 3-Methyladenine (Figure 3.6.2 A and B).

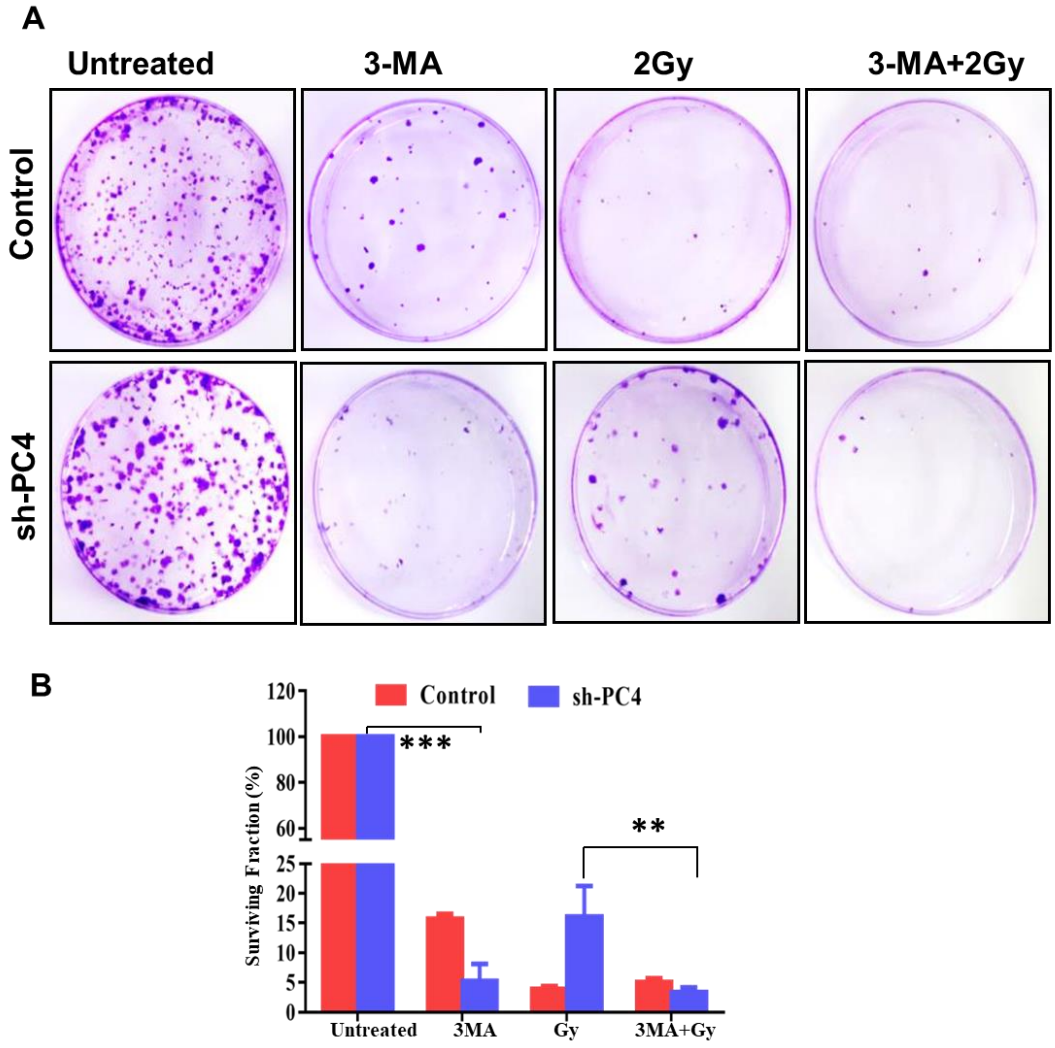

Figure 3.6.2 Autophagy inhibition sensitizes PC4 depleted cells to gamma irradiation. Control and sh-PC4 cells were treated with small molecule inhibitors of autophagy 10 mM 3-methyladenine (3-MA)) 2 hours prior to exposure to 2Gy of gamma irradiation. Cells were grown in the presence of the respective inhibitor for 24 hours post irradiation. Colonies were grown for 10 days. (A) Representative image of the crystal violet stained colonies of control and sh-PC4 cells sustained after treatment with 3MA and exposure to gamma irradiation. (B) Bar Graph depicting surviving fraction in percentage of the control and sh-PC4 cells after autophagy inhibition. Data are presented as means ± S. E. M. (N = 2). p* < 0.01, p** < 0.001, p*** < 0.0001.

Bafilomycin was further used as it was more specific and late stage inhibitor of autophagy. Pretreatment with Bafilomycin resulted in dramatic decrease in the proliferation of PC4 knockdown cells specifically and thus made it sensitive to gamma irradiation resistance (Figure 3.6.3A and B). Thus, administration of autophagy inhibitors also led to a significant decrease in the viability of sh-PC4 cells which were exposed to gamma irradiation (Figure 3.6.2B and 3.6.3B). Collectively the autophagy inhibition data suggests that autophagy might act as a critical factor to potentiate the advantageous survivability of PC4 knockdown cells over the control cells upon gamma irradiation.

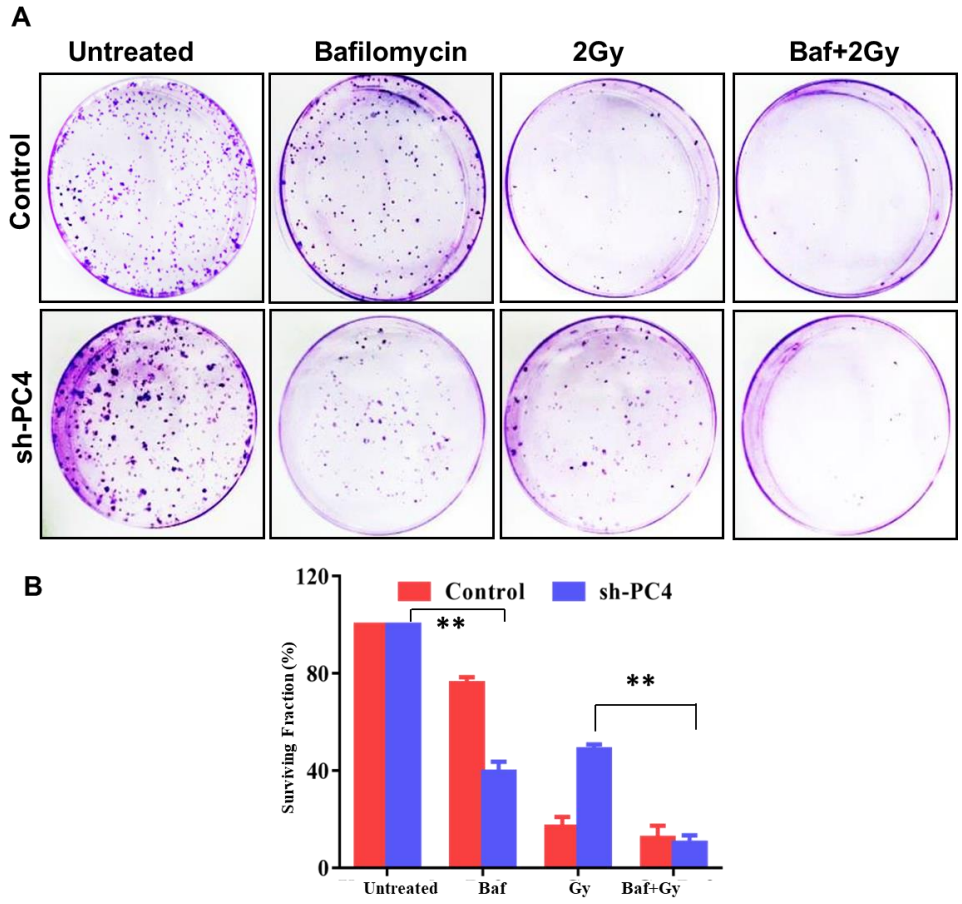

Figure 3.6.3 Bafilomycin treatment sensitizes PC4 knockdown cells to gamma irradiation. Control and sh-PC4 cells were treated with 100nM mM Bafilomycin (Baf) 2 hours prior to exposure to 2Gy of gamma irradiation. Cells were grown in the presence of the inhibitor for 24 hours post irradiation. Colonies were grown for 10 days. (A) Representative image of the crystal violet stained colonies of control and sh-PC4 cells sustained after treatment with Bafilomycin and exposure to gamma irradiation. B Bar Graph depicting surviving fraction in percentage of the control and sh-PC4 cells after autophagy inhibition. Data are presented as means ± S. E. M. (N = 2). p* < 0.01, p** < 0.001, p*** < 0.0001.

3.7. PC4 knockdown induces transcription of autophagy related genes

3.7.1. Inhibition of PC4 induces expression of autophagy related genes

Absence of PC4 leads to an open chromatin conformation state with concomitant increase in the transcriptionally favorable epigenetic or histone acetylation marks in the genome. This led us to further check that whether the induced autophagy in absence of PC4 is at the transcriptional level. We followed the possible gene expression pattern in PC4 knockdown cells both before and after exposure to gamma irradiation. Control and sh-PC4 cells were exposed to 2Gy of gamma irradiation. After 6 hours of irradiation, the live cells were sorted using Annexin V cy3 FACS analysis. The live cell population was sorted out from the positively stained apoptotic cell population (Annexin V cy3.18 positive) from both the control and sh-PC4 cells before and after gamma irradiation. RNA extraction was carried out from the above mentioned live cell population from control both the cell lines, both before and after gamma irradiation. This RNA was further subjected to qPCR analysis to investigate the differential gene expression signature between the control and sh-PC4 cells due to gamma irradiation. A set of genes taken from the autophagy array (details given in materials and methods) were taken to be analyzed. The result obtained for gene expression of each autophagy related genes as obtained from real time PCR analysis is summarized in the figure 3.7.1. Different color represents different autophagy genes, whereas each panel represents different cellular conditions. The first represents expression in control cells; the second is the fold change in gene expression of sh-PC4 cells. The third represents the fold change in gene expression after 6 hours of gamma irradiation (2Gy) in control cells and the fourth represents the same treatment but in sh-PC4 cells. RNA expression of live cell population was analyzed to ascertain the role of induced autophagy in mediating survivability in the PC4 knockdown cells. Correlating to the protein expression level of LC3II, we found that certain autophagy related genes like AMPKα1, AMPKα2, ULK1, ULK2, DRAM1 which are involved in the core machinery of the autophagosome formation was significantly upregulated in the PC4 knockdown cells(sh-PC4) as compared to the control cells. The transcript level of MAP1LC3B was also found to be upregulated, signifying that several genes which play key roles starting from the preinitiation stage to the completion stage (as described in chapter 1 section) were found to be upregulated in the

PC4 knockdown cells. We also followed the expression of the genes after gamma irradiation in both control and PC4 knockdown cells. We found that sh-PC4 cells after gamma irradiation showed further increase of the autophagy related genes. Other than the genes directly involved in the autophagy process, PTEN was also found to be significantly elevated in the PC4 knockdown cells upon gamma irradiation. PTEN is known to induce macroautophagy to get rid of unwanted proteins and organelles in the cell (ref). However, we also found upregulation of the autophagy related genes in the control cells as gamma irradiation induced autophagy in these cells as was evident in the LC3II western blotting in Figure 3.6. Collectively the gene expression analysis revealed induction of autophagy in the PC4 knockdown cells at the transcript level. Furthermore, it also revealed a possible AMPK-ULK1 axis mediated induction of autophagy. There were also some genes like GABARAPL1, GABARAPL2, which are also autophagy regulators whose expression was not significantly altered in the absence of PC4.

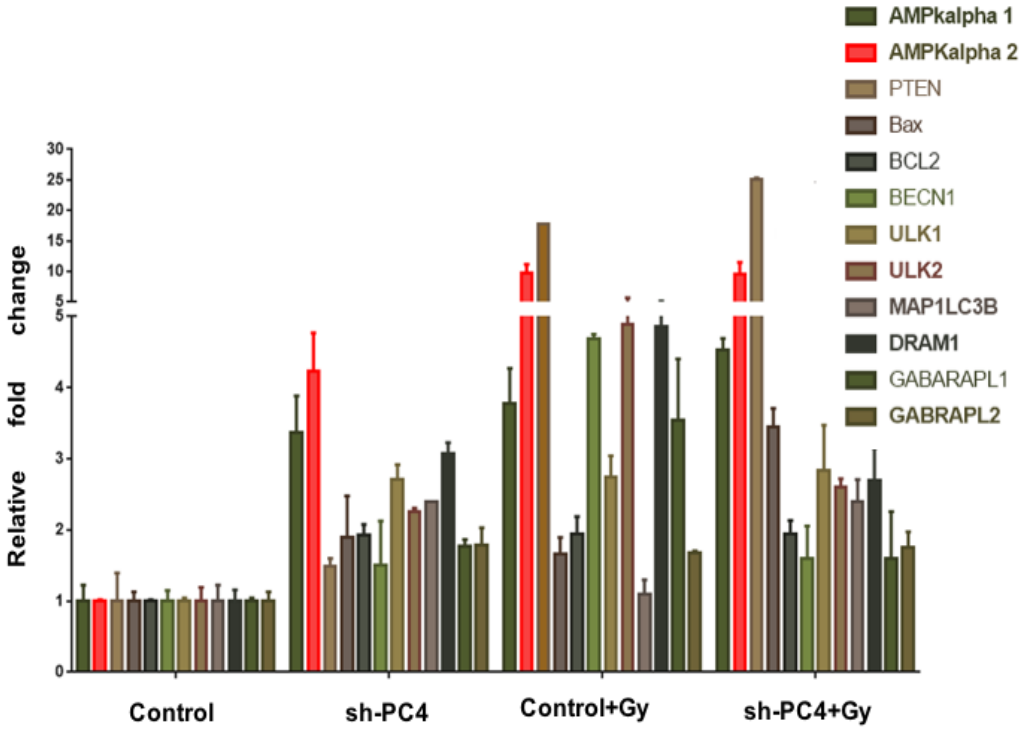

Figure 3.7.1 PC4 knockdown stimulates expression of autophagy genes. Alteration of autophagy related genes as determined by qPCR in ctrl versus sh-PC4 cells before and after gamma irradiation. Data are presented as means ± S.E.M. (n = 2). Actin is used as an internal control.

3.7.2. Knockdown of PC4 induces expression of autophagy related genes

Upregulation of autophagy related genes at the transcript level in PC4 knockdown cells further prompted us to analyze the molecular mechanism of this phenomenon. Inhibition of PC4 was shown to result in the global decompaction of the chromatin and upregulation of active histone acetylation marks. We here wanted to directly correlate the enhancement of active histone acetylation mark with the transcriptional output obtained in the previous section. The level of histone H3K9 acetylation (H3K9Ac) was analyzed on the promoter sites of different upregulated genes by chromatin immunoprecipitation assay using highly specific antibodies for H3K9Ac. Occupancy of the active histone H3K9Ac marks at the promoters of five critical autophagy related genes were checked both in the control as well as sh-PC4 cells. ChIP followed by qPCR with specific primers against the promoter region of each selected gene, showed enhanced occupancy of the H3K9Ac mark at the promoters of the autophagy genes in sh-PC4 cells as compared to the control cells (Figure 3.7.2B). The ChIP qPCR results are represented as the percent input; second bar for each individual colour coded gene represents enrichment in sh-PC4 cells while the first bar is representative of H3K9Ac occupancy in the control cells (Figure 3.7.2 B). The promoters of all the five autophagy genes that we tested (all the genes were transcriptionally upregulated in sh-PC4 cells) showed higher enrichment of H3K9Ac in the sh-PC4 cells as compared to the control cells. To check the specificity of this event we also analyzed the occupancy of the active H3K9Ac mark at the promoters of genes like GAPDH and HNF4a (genes non-related to autophagy pathway). The occupancy of this mark was unaltered at the promoters of these unrelated genes (Figure 3.7.2.B) signifying that the occupancy of the specific active mark is somewhat specific to only autophagy related genes. Overall these results suggest that the H3K9Ac mark which was highly upregulated in the sh-PC4 cells gets possibly enriched at specific promoter sites in the genome leading to an altered enhanced autophagic pathway. Thus, PC4 regulates the autophagy related genes possibly at the transcriptional level by epigenetically modulating their promoters.

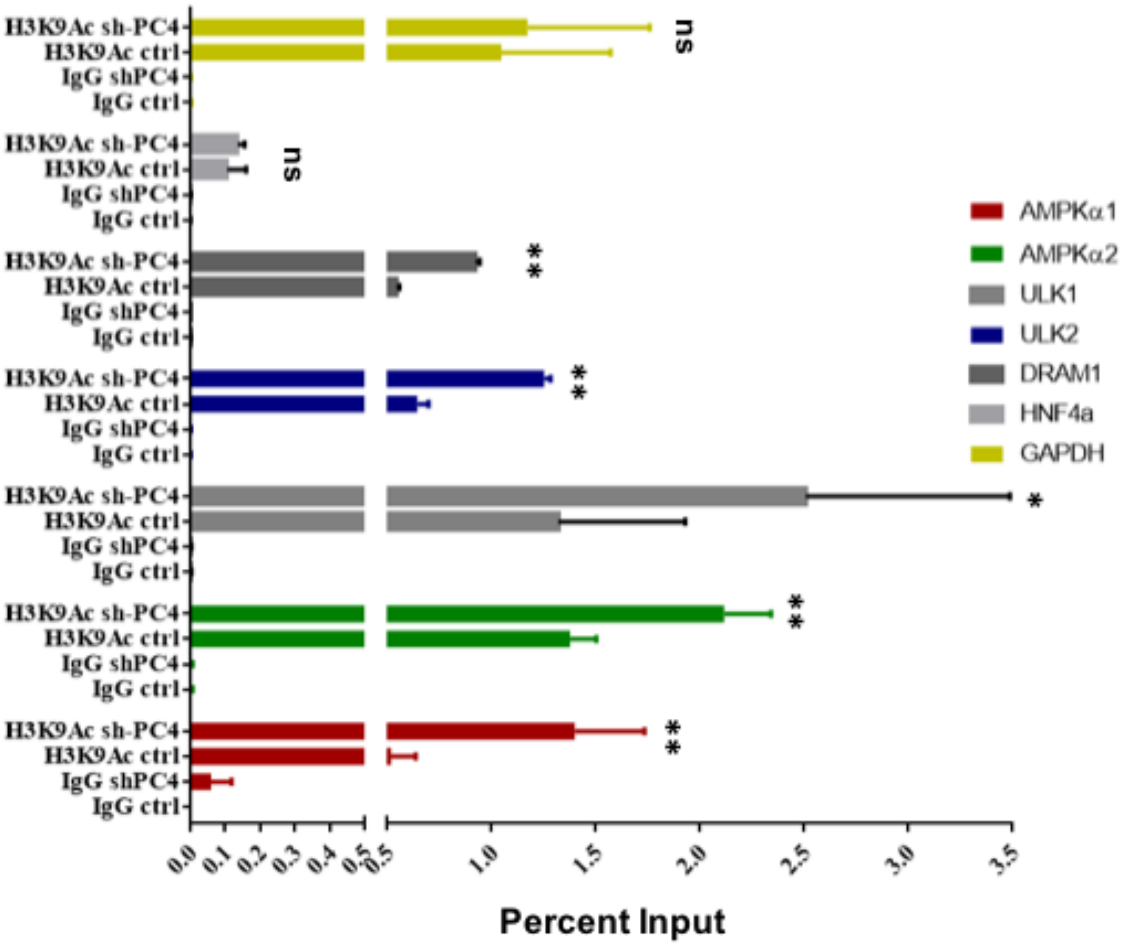

Figure 3.7.2 PC4 knockdown alters the epigenetic landscape of autophagy gene promoters. Occupancy of H3K9Ac at the promoters of selected autophagy related genes were assayed in both control and sh-PC4 cells. Percentage of enrichment of the mark at the selected promoters over the input was calculated. Data are presented as means ± S.E.M. (n = 2). p** < 0.001, p*** < 0.0001.

3.8. PC4 Knockdown enhances autophagy through the AMPK-ULK1 axis

3.8.1 Altered gene network upon PC4 downregulation

To gain an overview of the altered cellular phenomenon occurring in the PC4 knockdown cells, we resorted to an *in-silico* analysis of pathways regulated by the different altered genes (protocol described in chapter 2). For this analysis, we used two sets of genes, one gene set obtained from the altered transcriptome analysis (microarray) from PC4 Knockdown cells (reference) and the other was taken from the autophagy array. This network analysis of pathways interconnects several genes possibly altered by the downregulation of PC4, and thereby providing an insight to the cellular pathways which might get altered upon PC4 inhibition. Most of the genes to be altered belonged to the autophagy regulatory pathway referred in red circular nodes (Figure 3.8.1). From the analysis, it was found that downregulation of PC4 levels not only led to altered expression of autophagy genes, but also affected other essential cellular pathways for cell migration, proliferation, and homeostasis. The highly intertwined gene regulatory pathways show that in the cellular context, perturbation of one gene PC4 (Sub1 denoted as a green node) led to an alteration of several processes each signifying distinct phenotype. It is also to be noted that the alterations of several of these autophagy related genes were linked to other cellular processes, the characteristics of which was observed in the PC4 knockdown cells. As for example, ULK1 is critical for functioning of several cellular processes besides the autophagy machinery as mentioned like in cell motion, cell projection, etc. (Figure 3.8.1). Similarly, PTEN was found to regulate cell matrix adhesion, regulation of cell proliferation etc. besides its role in autophagy. The size of the nodes determines the number of pathways it is linked to. Larger the node, more is the number of pathways it regulates. Thus, in that context, BCL2, PTEN formed major pivotal nodes regulating various cellular processes. Conclusively, this network provides a detailed picture of the altered gene regulatory pathway upon repression of PC4, thus providing an insight to the phenotypic characteristics of the PC4 knockdown cells.

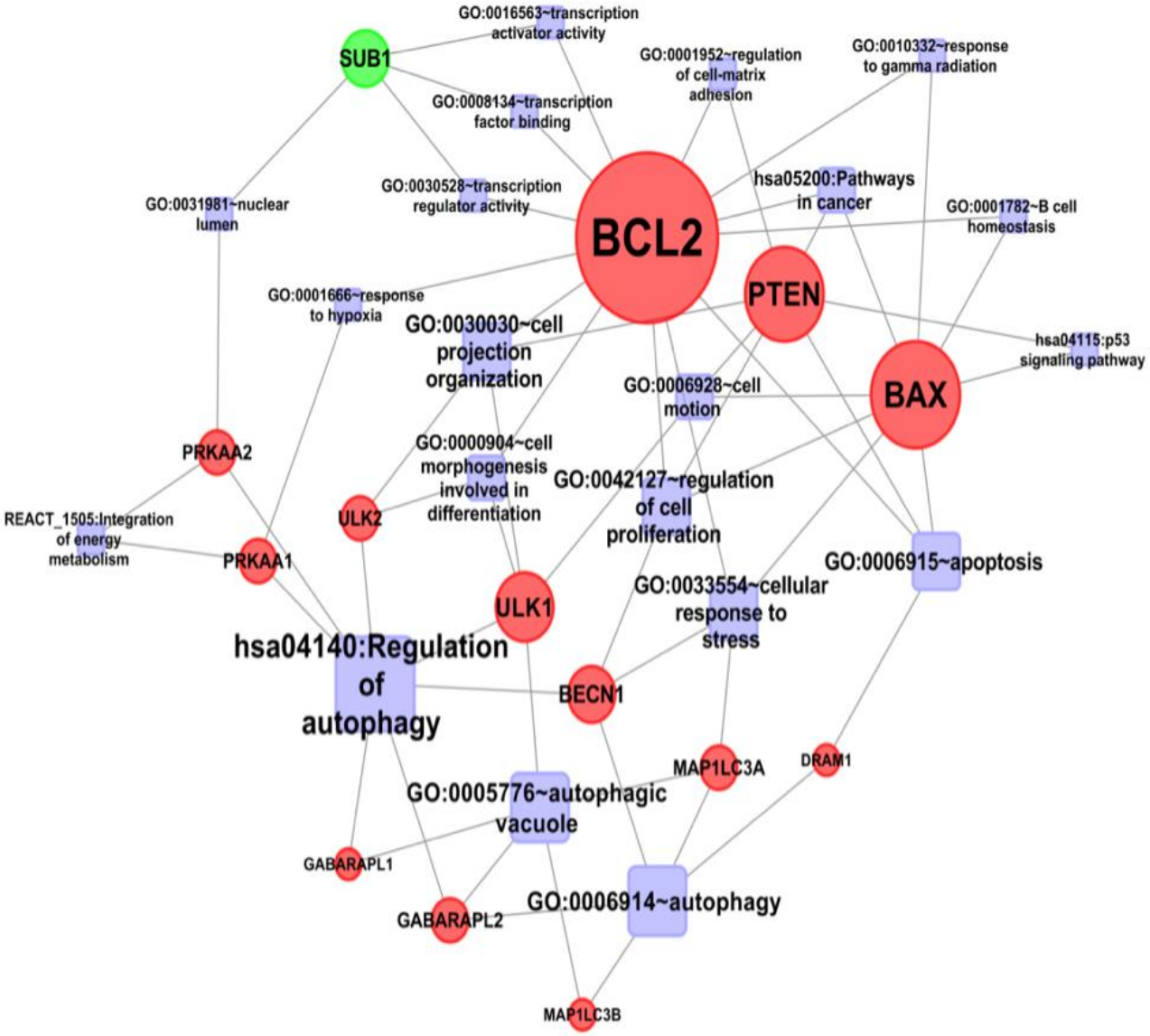

Figure 3.8.1 Altered gene network upon PC4 knockdown shows alteration in autophagy related genes and thereby the associated gene network. For generating the core network significantly enriched biological categories / gene ontology / pathways harbouring differentially expressed genes upon PC4 Knockdown as compared to the control cells were subjected to network identification using Bridgen Island Software, resulting in identification of key nodes and edges. Output of Bridge Island Software was used as input to CytoScape V 2.8. Force directed spring embedded layout under yFiles algorithm was used to visualize the network that encompasses biological categories, differentially expressed genes that were significantly enriched. All the genes in the network were color coded based on their fold change upon PC4 knockdown, compared to control *cells.*Down regulated gene is colour coded as green while genes showing upregulation is denoted as red.

3.8.2 PC4 Knockdown alters AMPK related genes

From the qPCR data mentioned in the above section, we analyzed that the AMPK pathway genes were majorly altered in the PC4 knockdown cells. We hypothesized that this might be the pathway operating in the knockdown cells which lead to the upregulation of the autophagy pathway. In order to further validate this observation, and to understand the specificity of the event, we checked expression of some genes which were neither involved in the autophagy process nor was involved in AMPK pathway. Significantly it was observed that expression of these genes, namely Glyceraldehyde 3-phosphate dehydrogenase (GAPDH), histone acetyltransferase p300, Synaptonemal complex protein (SCP1) do not change upon PC4 knockdown in contrast to the genes related to autophagy pathway (Figure 3.8.2)

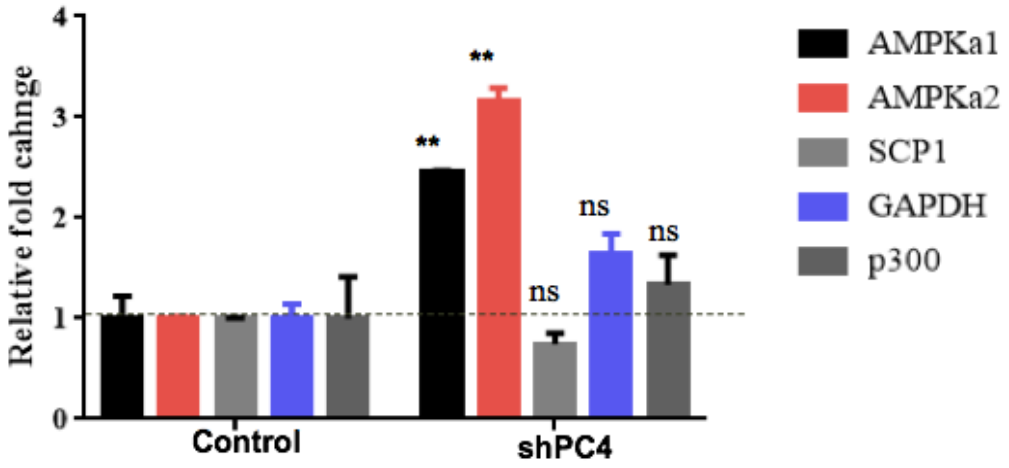

Figure 3.8.2 PC4 knockdown induces the AMPK pathway. Alteration of autophagy related genes along with other non-autophagy related genes as determined by qPCR in ctrl vs sh-PC4 cells. Data are presented as means ± S. E. M. (n = 2). Actin is used as an internal control.

3.8.3 Inhibition of autophagy by ULK1 knockdown in PC4 knockdown cells

To further validate that autophagy is critical for enhanced survivability of sh-PC4 cells and particularly through the AMPK-ULK1 axis, we resorted to genetic inhibition of autophagy pathway by administering cells with specific shRNA against ULK1 gene (Figure 3.8.3 C). ULK1 is known to act at the initiation of the autophagosome formation; its inhibition has been shown to dramatically abrogate the autophagy process in several cell lines. We observe that shRNA mediated knockdown of ULK1 drastically reduced the proliferation rate of the sh-PC4 cells in comparison to the control cells (Figure 3.8.3A and B). Collectively these data indicate that enhanced autophagy is one of the key mechanisms of better survivability and enhanced proliferation of PC4 depleted cells. Collectively, through the qPCR data and the inhibition assay, we also find that the AMPK–ULK1axis might be the critical pathway which induces autophagy in the PC4 Knockdown cells.

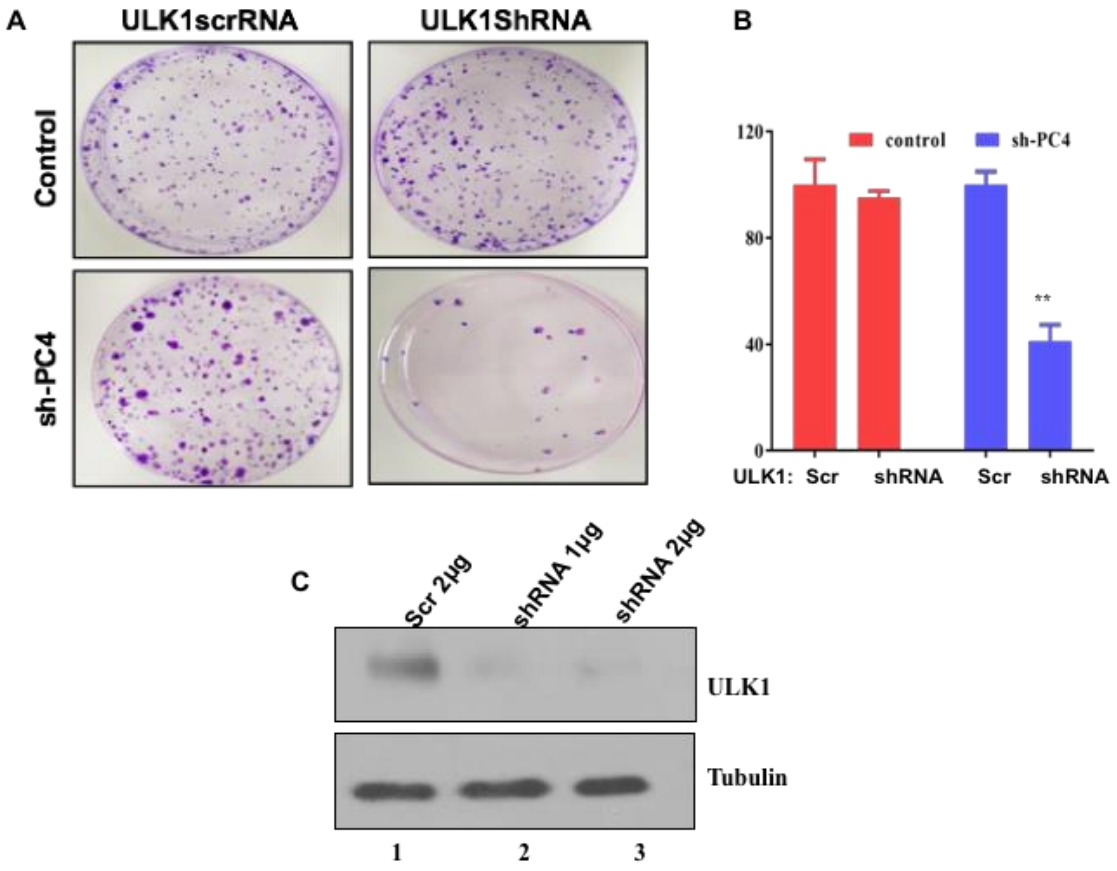

Figure 3.8.3 Autophagy inhibition by ULK1 knockdown reduces the proliferation rate of PC4 knockdown cells. (A) Control and sh-PC4 cells were transfected with 2 µg of shRNA for 48 hours, and then plated for colony formation assay. Representative images of the crystal violet stained colonies of control and sh-PC4 cells sustained after transfection of ULK1shRNA. (B) Bar Graph depicting surviving fraction in percentage of the control and sh-PC4 cells after autophagy inhibition. Data are presented as means ± S.E.M. (n = 2). p* < 0.01, p** < 0.001, p*** < 0.0001. (C) Western blotting to confirm ULK1 knockdown 48 hours post transfection with specific shRNA against ULK1 in increasing concentrations.

Summary

In this study we observe that

- Knockdown of PC4 alters the nuclear architecture as well as results in defects of chromosomal morphology
- PC4 depletion results in a decondensed chromatin with upregulation of histone activation marks.
- PC4 knockdown cells harbour cell segregation defects as is evidenced by the formation of anaphase bridges
- Despite the cellular defects, the PC4 knockdown cells show greater proliferation rate and resistance to gamma irradiation.
- Absence of PC4 induces autophagy both at the transcriptional and protein level
- Induction of autophagy genes in absence of PC4 is possibly due to the enriched histone acetylation (H3K9Ac) mark at the respective promoters of the gene
- Inhibition of autophagy by both chemical and genetic means leads to sensitization of PC4 knockdown cells to gamma irradiation.
- Autophagy in PC4 knockdown cells is possibly induced through the AMPK-ULK1 pathway.

Discussion

Human transcriptional coactivator, PC4 has been previously reported to be an integral component of the chromatin. Depletion of PC4 at cellular level alters global organization of the nucleus as well as leads to an open chromatin state establishing it as one of the most important chromatin architectural protein. The chromatin architecture is known to be intricately modulated by the physiological state of the cell, a well-organized chromatin in a compact nucleus is essential for maintaining cellular homeostasis. Here we establish a novel role of the chromatin associated protein PC4 in cell segregation, chromosomal morphology, and maintenance of the epigenetic state of the cell. PC4 depleted cells show abnormal cellular segregation, enhanced hyper acetylation of histones and distorted shaped chromosomes. Interestingly, despite harboring severe cellular defects, PC4 depleted cells shown higher proliferation rate than normal cells, and were also resistant to genotoxic stress like gamma irradiation, quite similar to the phenotype of an oncogenic transformed cells. To delineate the molecular mechanism of such a phenotype, we found that PC4 is a novel regulator of the well conserved cellular process of self-eating, called autophagy.

Autophagy levels were found to be highly elevated in absence of PC4. Electron micrographs of PC4 knockdown cells showed presence of various double membraned autophagy like vacuoles. Most of these vacuoles were found in close proximity to the irregularly shaped nucleus in PC4 knockdown cells. It was also interesting that PC4 depleted cells showed appearance of multivesicular bodies (large number of vacuoles engulfed in one vesicle). Appearance of multivesicular bodies has been reported in a particular type of autophagy process. Autophagy is a degradative pathway which plays an important role in maintaining protein homeostasis (proteostasis) as well as helps in the preservation of proper organelle function by selective removal of damaged organelles. The protective role of autophagy in maintaining cellular survival is mediated by the selective removal of dysfunctional mitochondria or other damaged organelles, which release pro-apoptotic factors and generate oxygen species. During autophagy, portions of cytosol are sequestered inside double-membraned vesicles (autophagosomes) that then fuse either with endocytic vesicles (as Multivesicular bodies) or lysosomes, which provide the hydrolytic enzymes that will degrade the content. The appearance of these multivesicular bodies and other double

membraned vesicles especially near the nucleus in PC4 depleted cells thus might be possibly an indication of a cellular cue which might be operating via the altered nuclear architecture to a cytosolic process like autophagy. The enhanced autophagy levels in the PC4 knockdown cells play a critical role in its survivability possibly by maintaining cellular homeostasis in an otherwise physiological chaotic state.

When the autophagy levels were depleted by administration of small molecule inhibitors or by knockdown of an essential autophagy gene ULK1, it highly compromised the survival rate of PC4 knockdown cells and upon gamma irradiation. This establishes the significant role of autophagy in attributing the property of enhanced growth rate to PC4 knockdown cells. Thus, PC4 depletion not only alters the nuclear architecture, chromatin compaction, epigenetic landscape but it also perturbs an important cytosolic event which in turn provides advantageous property to the otherwise abnormally transformed cells. We further investigated whether this phenomenon of enhanced autophagy is more specific to a loss of a chromatin condensing protein, PC4. PC4 knockdown significantly upregulated several autophagy related genes, like the AMPK and ULK genes which were previously reported to be prime regulators of the autophagy pathway. AMP-activated protein kinase (AMPK) is a well conserved energy sensing serine threonine kinase which is activated upon energy depleted or upon cellular stress conditions. This kinase further activates a cascade of proteins including the Unc-51-like kinase 1 and 2 (ULK1 and ULK2) which is an essential component in the formation and maturation of autophagosomes. We also find upregulation of MAP1LC3B gene in absence of PC4 which is involved in the final step of autophagosome maturation and thereby degradation. This signifies that PC4 knockdown in cells not only leads to just an enhanced initiation of the self-eating process but the degradative pathway is complete and functional up to its final step. When we complemented PC4 in the knockdown background, we found significant downregulation of LC3 at protein levels signifying its more direct role in regulation of autophagy.

We hypothesized that the phenomenon of enhanced autophagy in absence of PC4 might be occurring through the altered epigenetic state in PC4 depleted cells. The altered transcriptome in the PC4 depleted cells might be due to the modified epigenetic landscape which is now permissive to enhanced transcription. Thus PC4 knockdown alters the chromatin landscape at the autophagy related gene promoters, thereby upregulating

autophagy. This enhanced autophagy confers a survival advantage to the knockdown cells, making it to more resistant to stress conditions, like gamma irradiation. Inhibition of autophagy by small molecule inhibitors or genetic inhibition of autophagy greatly compromises the survivability and proliferative property of the knockdown cells. This signifies the critical role of autophagy for the survival advantage of PC4 knockdown cells.

Chapter 4: Role and Regulation of chromatin protein PC4 expression in Breast Cancer manifestation

This chapter describes the role of PC4 in Breast cancer progression. Here the consequence as well as the cause of PC4 downregulation in Breast cancer patient samples has been delved into in a detailed way. This part of the work also reinforces the role of enhanced autophagy upon down regulation of PC4 in mediating gamma irradiation resistance property to breast cancer cells.

Background

Our previous observation from PC4 knockdown cell line revealed atypical cellular signatures as that of a transformed cell line with oncogenic properties. PC4 knockdown cells harbour an open chromatin leading to an altered epigenetic landscape resulting in the induction of a different cascade of genes. Upon depletion of PC4 in human embryonic kidney cells, we observe several cellular segregation defects, abnormally shaped nuclei and altered chromosomal morphology. Regardless of all these cellular defects, PC4 knockdown cells exhibit a higher proliferation rate and was found to proliferate even upon exposure to gamma irradiation. Thus PC4 functions a critical factor for maintenance of genome integrity and cellular survivability. PC4 downregulation also alters the gene expression in the cells and might therefore alter the cellular phenotype. Like other chromatin associated proteins , PC4 has been associated with various types of cancer like lung cancer, lymph angiogenesis (Tao et al., 2015), astrocytoma (Chen et al., 2014), prostate cancer, (Chakravarthi et al., 2016) etc. In most of the cases PC4 was found to be upregulated signifying it positive role in the process of oncogenesis. However validating our observation in our cellular studies, we hypothesized that the downregulation of this highly abundant nuclear protein might play an important role in driving tumorigenesis as it rendered the chromatin open and the genome unstable. PC4 is also known to act as a putative tumor suppressor. It interacts with AP2 α and inhibits AP2 transcriptional interference in *ras* transformed cell line (Kannan and Tainsky, 1999). Its ability to interact and enhance the function of p53, a tumor suppressor protein, *in vivo* can also be interpreted as a tumor suppressor activity of PC4 (Banerjee et al., 2004).Not

only does the interaction of PC4 and p53 is critical for PC4-mediated activation of p53, but also the DNA bending ability of PC4 significantly contributes in the enhancement of DNA binding of p53 as well as its downstream function (Batta and Kundu, 2007). Genomics as well as cytogenetic studies in Breast cancer reveal that the cancer progression and its various molecular subtypes and hence the complexity arises due to the presence of large number of chromosomal aberrations and translocations.

In this particular study we therefore make an attempt to understand the expression pattern of PC4 in breast cancer tumor tissues surgically removed from patients considering various parameters like age, receptor status (ER positive/Triple negative) and tumor stage/grade. The studies were initiated to analyze the expression level of PC4 in the cancerous samples with respect to adjacent normal breast tissue from the same patient using immunohistochemistry (IHC). Initial studies indicated a difference in the expression of PC4 expression between cancer tissues as compared to normal counterpart (Kumari S, Thesis 2012). This data prompted us to investigate the role of the abundant non histone chromatin protein PC4 in the context of Breast cancer in more details. The molecular mechanisms which are responsible for its altered expression have also been investigated in the present study. Elucidating the expression pattern of chromatin associated protein PC4 in the process of oncogenesis brings forth the significance of chromatin dynamics in cancer progression. Alteration of chromatin organization and structure are associated with cancer manifestation. Chromosomal abnormalities like aneuploidy and translocations are regarded as hallmarks of malignancy. The abnormal expression of the non-histone proteins, which are also involved in the maintenance of the chromatin structure, might result in these chromosomal abnormalities as well as alteration in gene regulation during oncogenesis. Recent advances in the field of epigenetics suggest that oncogenic development could be closely associated with the altered epigenetic state of the genome. Such epigenetic changes involve aberrant DNA methylation, the alteration of chromatin components in DNA packaging (Ellis et al., 2009; Sharma et al., 2009) and also anomalous expression of noncoding RNAs like miRNAs. Chromatin alterations and DNA methylation cumulatively alter the epigenetic regulation of gene transcription in all the stages of tumor progression. Histone acetyltransferases and deacetylases are known to aberrantly express in Cancers, resulting in anomalous acetylation of histones as well as non-histone proteins. Thus both expression as well as the post

translational modifications of non-histone proteins might play determining roles in the onset of cancer and its progression. Microarray analysis from various tumor tissues has revealed the importance of miRNAs in the prediction, diagnosis and prognosis of tumor formation. **Oncogenic miRNAs (oncomiRs)** are usually overexpressed in cancers while tumor suppressive miRNAs are downregulated quite similar to their mRNA counterparts. When these oncomiRs or tumor suppressor miRNAs are repressed or stimulated, respectively, the oncogenic properties of a tumor cell is significantly reduced. Certain cancers become addicted to these oncomiR to such an extent that suppression of the oncomiR results in complete reduction of the tumor (Reddy, 2015) (Block et al., 2017). However, is intriguing to note that the miRNA expression pattern varies with cell tissue type as well as various tumors. A single miRNA can act as an oncogene for a certain type of cancer while portray tumor suppressive role in case of other cancer type. This diversity of effects might be due to the large number of genes influenced by a particular miRNA. Thus it is critical to understand the role of the intertwined network of miRNAs and their target mRNAs in a certain cancer type to elucidate the mechanism of onset and progression of oncogenesis.

4.1. Expression of PC4 in Breast cancer

4.1.1. PC4 expression in Breast Cancer cell lines

Our cell based study from HEK293 cells, prompted us to investigate the state of PC4 expression in other cell lines, especially the cancer cell lines. As Breast Cancer cell lines harboured specific features of genome instability, we explored the expression of PC4 in these cell lines. Breast cancer being a heterogeneous disease, the expression status of PC4 in different breast cancer cell lines exhibiting different molecular signatures, were studied . In a panel of thirteen breast cancer cell lines, having different origin and having different potential for invasion or migration property, the expression for PC4 was checked. Western blotting analysis across 13 breast cancer cell lines (Figure 4.1.1.A) exhibiting varied molecular subtypes revealed significant downregulation of PC4 in 3 cell lines, as compared to the expression of MCF10A (normal epithelial breast cell line which is non-tumorigenic). However, PC4 expression was relatively lower in MCF10A as compared to MCF7 (breast cancer cell line which is less invasive or migratory and is non-tumorigenic in absence of Estradiol treatment) (Figure 4.1.1B). All the other cancer cell lines used in this analysis, had greater oncogenic potential than MCF7 cells, thus PC4 expression in MCF7 was taken as a reference to distinguish up or downregulation. PC4 was found to be substantially downregulated in protein level in the 3 highly aggressive cell lines ZR-75-1, HCC38, HCC1806 whose properties and molecular signatures are described in details in Table 4.1. SKBR3 and MDAMB361 showed moderate downregulation in PC4 expression as compared to MCF7 cell lines. The other cell lines do not show any significant change while in T47D it was found to be upregulated. As mentioned in Chapter 1, Breast cancer although regarded as a single disease varies considerably in their molecular signatures and gene expression, similarly the panel of Breast cancer cell lines reflects these variability and thereby the expression of PC4. It was interesting to note that despite the variation, PC4 was significantly downregulated in most of the cell lines exhibiting higher invasive and migratory property, and also the property of radiation resistance as in case of ZR-75-1. This signifies the potential role of PC4 in the process of Breast cancer oncogenesis. This encouraged us to look into the PC4 expression pattern in Breast cancer patient samples described in the next section.

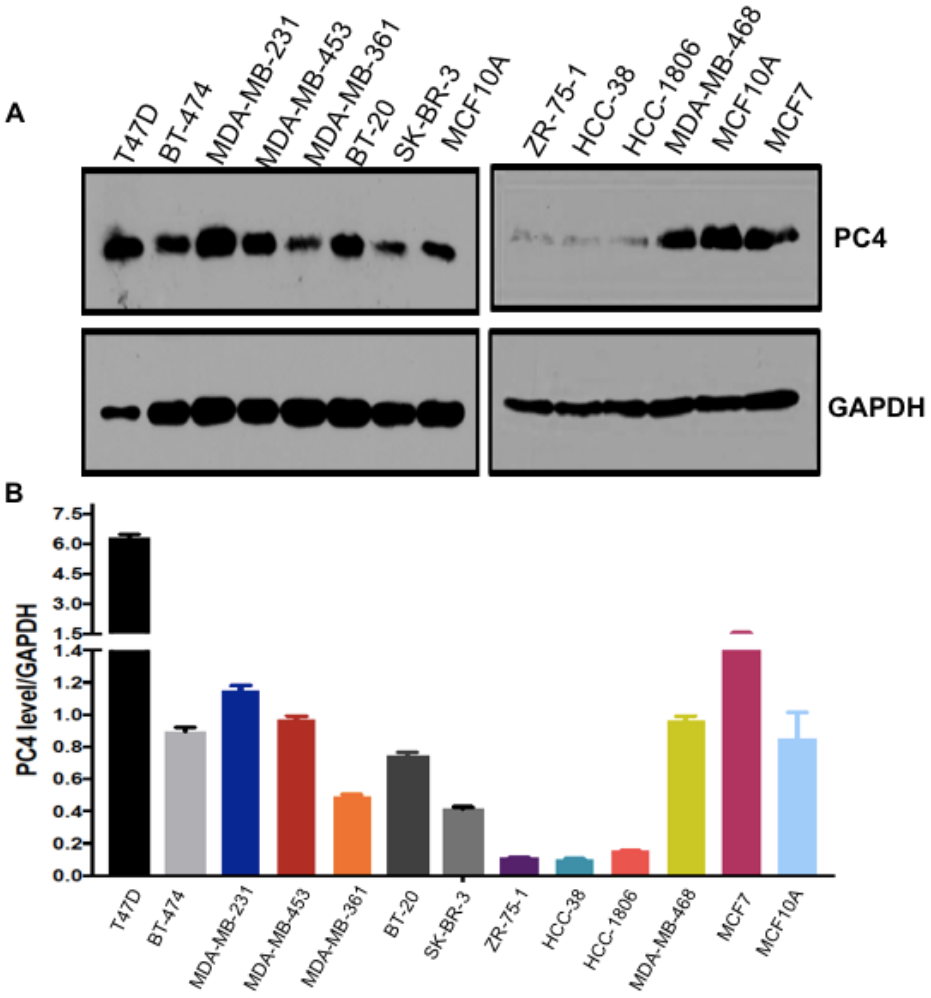

Figure 4.1.1. PC4 expression across different Breast Cancer cell lines. (A) Western Blot analysis of PC4 was done with lysates collected from different breast cancer cell lines. GAPDH was used as the loading control. (B) Densitometric analyses of protein bands were done. n=2. Data are presented as means ± S.E.M. p* < 0.01, p** < 0.001, p*** < 0.0001.

Cell line	Subtype #	ER *	PR*	ERBB2/ HER2*	Source	Tumor Type
HCC38	Basal B Subtype	-	-	-	primary tumor	ductal carcinoma
HCC1806	NA	-	-	-	primary tumor	Squamous Carcinoma
SKBR3	Luminal subtype	-	-	+	pleural effusion	adenocarcinoma
ZR751	Luminal	+	-	-	ascites fluid	invasive ductal carcinoma

Table No.1. Molecular characteristics of the Breast cancer cell lines harbouring low PC4 levels. The table summarizes the origin and receptor status of the cell lines which express low levels of PC4 both at transcript as well as protein level.

4.1.2. Expression of PC4 in Breast Cancer patient samples:

Taking cue from the observation obtained from the panel of Breast Cancer patient cell lines, we looked into the PC4 expression pattern from Breast cancer tumors obtained directly from patients. Immunohistochemistry analysis was carried out with a specific antibody against PC4. Adjacent normal tissues were taken as normal or control samples. Analysis of 20 pairs of Breast tumor tissues irrespective of the age, receptor status and stage revealed suggestive downregulation of PC4 at the protein level. This was in correlation with the expression analysis of PC4 as observed in the aggressive and invasive breast cancer cell lines. However in this IHC analysis, we find PC4 majorly downregulated in most of the tumor tissues. Correlation with stage or age or of the patient samples did not show any positive trend with PC4 downregulation. Thus downregulation of PC4 might not be affected due to the age, or the molecular signatures making it possibly a more universal phenomenon across different types of Breast Cancer. The details of the patient with their IDs are listed in Appendix 1.

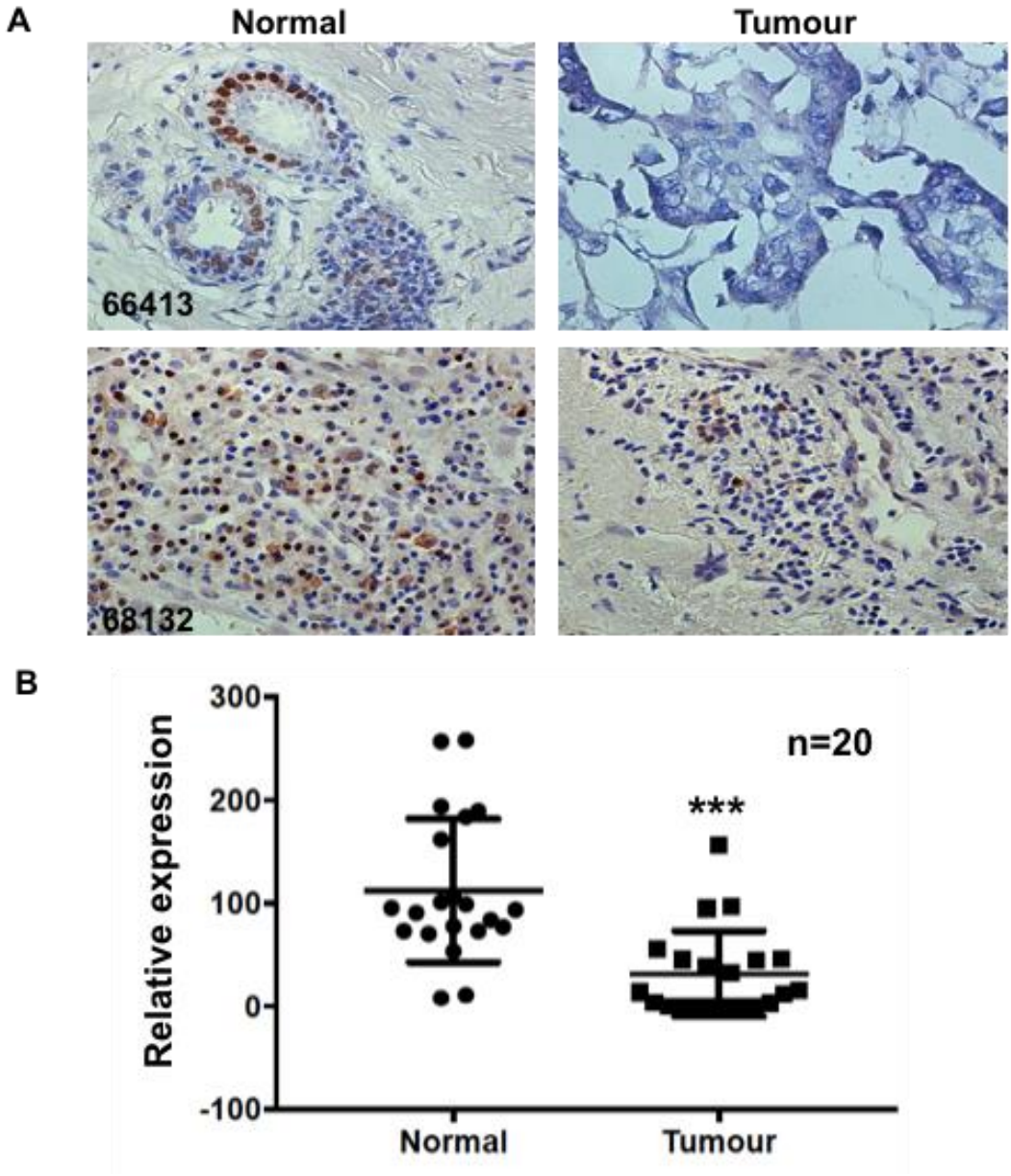

Figure 4.1.2: Immunohistochemistry of PC4 in Breast Cancer samples

(A) Representative images of PC4 expression in Normal tissue obtained from Adjacent to the tumor tissue and in Breast Cancer tumour tissue. (B) Data represents H-Scores from 20 pairs of Breast Cancer patient samples. . Data are presented as H-scores, p* < 0.01, p** < 0.001, p*** < 0.0001, n=20.

4.1.3. PC4 Expression is significantly downregulated at transcript level in Breast Cancer patient Samples

Taking cue from our Immunohistochemistry data, we wanted to further investigate whether this downregulation of PC4 is at the transcript level as well. RNA extracted from the tumour samples were subjected for PC4 expression analysis which was then compared to its expression in adjacent normal tissue (Figure 4.1.3 A). PC4 transcript levels were found to be significantly downregulated in Breast cancer tumours thus signifying the fact that the downregulation of PC4 observed is both at the transcript as well as protein level. We also correlated the PC4 expression in a large dataset of Breast cancer patient samples obtained from the **The Cancer Genome Atlas** (TCGA database). PC4 was found to be downregulated progressively across the different stages of Breast cancer (Figure 4.1.3.B).

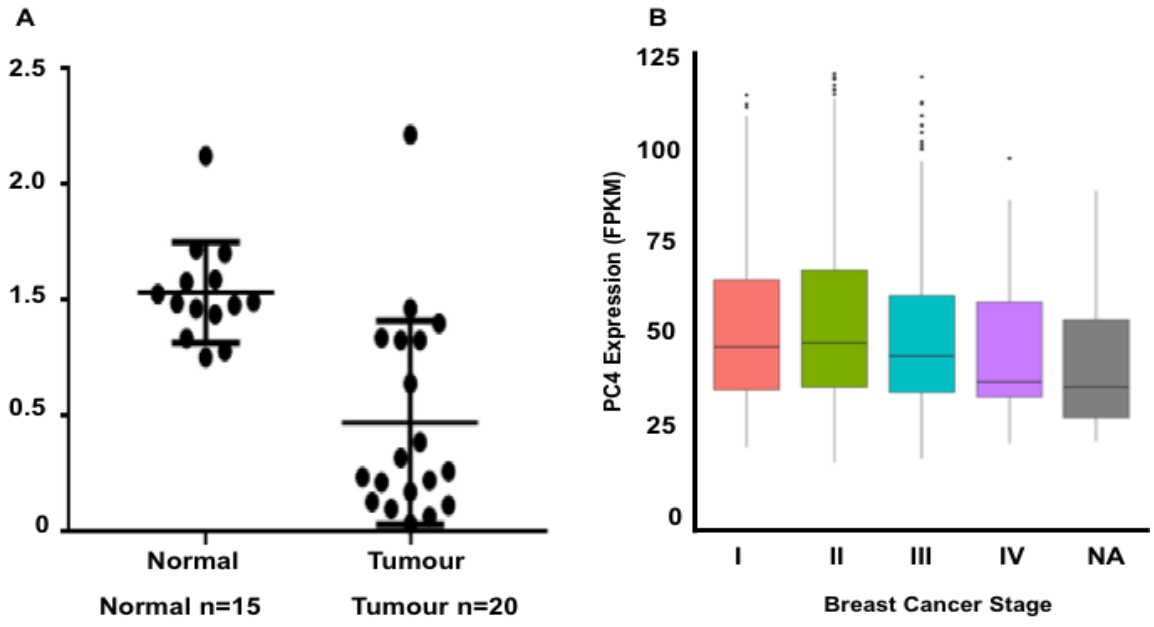

Figure 4.1.3 PC4 expression at transcript level in Breast Cancer patient samples: (A) PC4 transcript analysis from Breast cancer tumour samples as compared to the adjacent normal. PC4 expression was checked with gene specific primers. The fold change is calculated by the ΔΔCt method (see materials and methods). Actin specific gene primers are used for normalization. n=3, N=2. Data are presented as means ± S.E.M. p* < 0.01, p** < 0.001, p*** < 0.0001 (B) PC4 transcript analysis from 1029 patient samples obtained from TCGA database, stage wise.

4.2. Regulation of PC4 expression by miRNAs

The multifunctional chromatin protein PC4 is a highly abundant nuclear protein. Although a lot is known about its invivo functions, its expression status and its mode of regulation still remain to be elucidated. It is thus important to study the regulation of expression of such an important protein at the transcriptional level, especially in the conditions when it is differentially expressed. As mentioned earlier, an earlier study on the regulator of expression of PC4 reveals that it is a p53 responsive gene. Other factors regulating its expression are yet to be elucidated. PC4 is highly conserved across species. The PC4 gene is located in chromosome 5 which has five exons including one 5'-UTR (untranslated region). The 3'UTR region of PC4 was found to be almost 2kb long. Analysis of the 3'UTR region of PC4 by bioinformatics tools (refer Chapter 2) revealed several miRNA binding sites. MiRNAs are small non-coding RNAs 20-22 nucleotides long which on binding to the 3'UTR of genes mostly have an inhibitory effect on gene expression. Regulation of expression of PC4 by miRNAs has never been studied before, so this study might help in better understanding the significance of its role and abundance under normal physiological condition and how this homeostasis is perturbed in pathophysiological conditions. The bioinformatics miRNA prediction tools reveal a few high scoring miRNAs which might regulate PC4 gene expression through its 3'UTR. It is thus important to study these miRNAs in order to understand the regulation of PC4 gene under normal physiological conditions and also to address its altered expression under pathophysiological condition such as in Breast Cancer where as shown in the previous section it is downregulated.

4.2.1 PC4 3'UTR is a target of a specific set of miRNAs:

Upon analysis of the PC4 3'UTR, putative binding sites for miRNAs were found (Materials and Methods). Thus to experimentally validate the binding of miRNAs directly to the 3'UTR region of PC4, pMIR-REPORT luciferase vector containing the PC4 3'UTR sequence was used for this study. The 3' UTR of the luciferase gene contains a multiple cloning site for insertion of predicted miRNA binding targets or other nucleotide sequences. By cloning a predicted miRNA target sequence into pMIR-REPORT, the luciferase reporter is subjected to regulation that mimics the miRNA target. The 3'UTR region of PC4 is cloned into the MCS

region pMIR-REPORT luciferase vector. In order to address the binding of miRNAs to the PC4 3'UTR, miRNA (29a, 29b, and 29c) expressing constructs were also co transfected with the pMIR REPORT luciferase PC4 3'UTR plasmid. All the species of the miR29 family was found to repressed the luciferase gene containing the PC4 3'UTR sequence (Figure 4.2.1), thereby suggesting that it can bind to PC4 3'UTR and repress its expression in vivo.

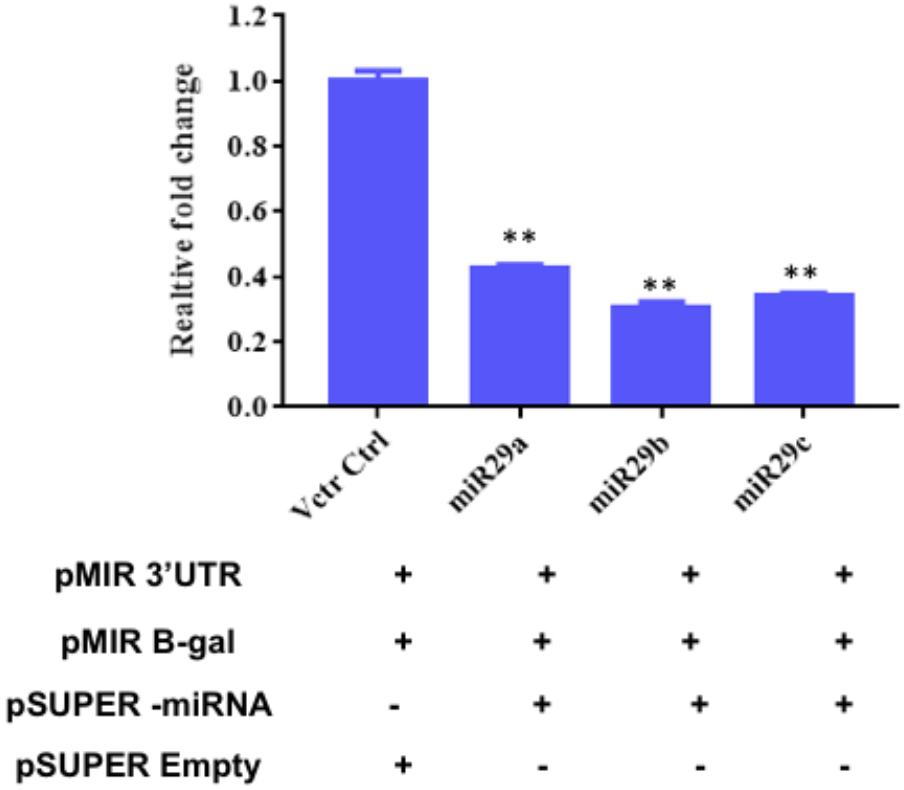

Figure 4.2.1. Regulation of PC4 3'UTR by miRNAs. HEK293 cells were transiently transfected with the PC4 3'UTR expression construct (500ng) along with miRNA expression plasmids. The 3'UTR region of PC4 is cloned into the MCS region pMIR-REPORT luciferase vector. Equivalent amount of control empty vector pSUPER was used to normalize the amount of transfected DNA. pMIR-βgal (500ng) was used as an internal control for all the transfection experiments to normalize luciferase activity. After normalization, relative fold change in luciferase activity was plotted (along y axis). n=3, N=2. Data are presented as means ± S.E.M. p* < 0.01, p** < 0.001, p*** < 0.0001.

4.2.2 Alteration of PC4 expression (mRNA level) by miRNAs

Taking cue from the 3'UTR luciferase miRNA experiment we further wanted to study the effect of PC4 expression at transcript level by Mir 29 family. Pre miR29a, miR29b, miR29c expressing plasmids were transiently transfected into HEK 293 cells. After 48hours of transfection PC4 expression at the transcript level was checked. Overexpression of miR29 significantly reduced expression of PC4 mRNA (Figure 4.2.2) thus verifying the potential role of miR29 as a negative regulator of PC4 expression.

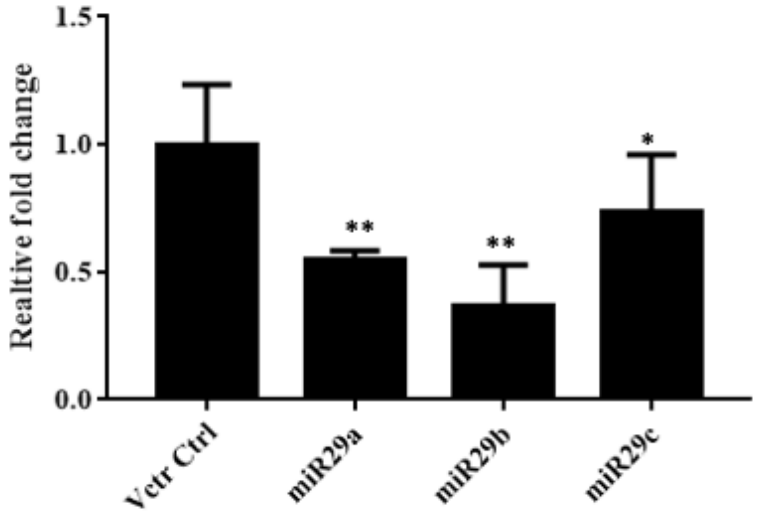

Figure 4.2.2 hsa-miR 29 regulates PC4 expression. PC4 expression was checked with gene specific primers after transfection of HEK293 cells for 48hrs with miR29 expressing vector. Empty pSUPER vector was transfected as vector control. The fold change is calculated by the ΔΔCt method (see materials and methods). Actin specific gene primers are used for normalization. n=3, N=2. Data are presented as means ± S.E.M. p* < 0.01, p** < 0.001, p*** < 0.0001.

4.2.3. miR29 downregulates PC4 protein expression

As the miRNAs were confirmed to bind to the 3'UTR of PC4 and inhibit PC4 expression at the mRNA level, the next approach was to look into alteration of the protein level upon miRNA overexpression. HEK293 cells were transiently transfected with miR29 and PC4 expression were analyzed at various time points. Western Blot analysis of PC4 was done with these samples to look into the alteration of endogenous PC4 level by these miRNAs. αTubulin was taken as an endogenous control. Consistent with the luciferase as well as the qRT-PCR data, overexpression of miRNAs in HEK293 cells showed a decrease in the endogenous level of PC4 at 96 hours. (Figure 4.2.3)

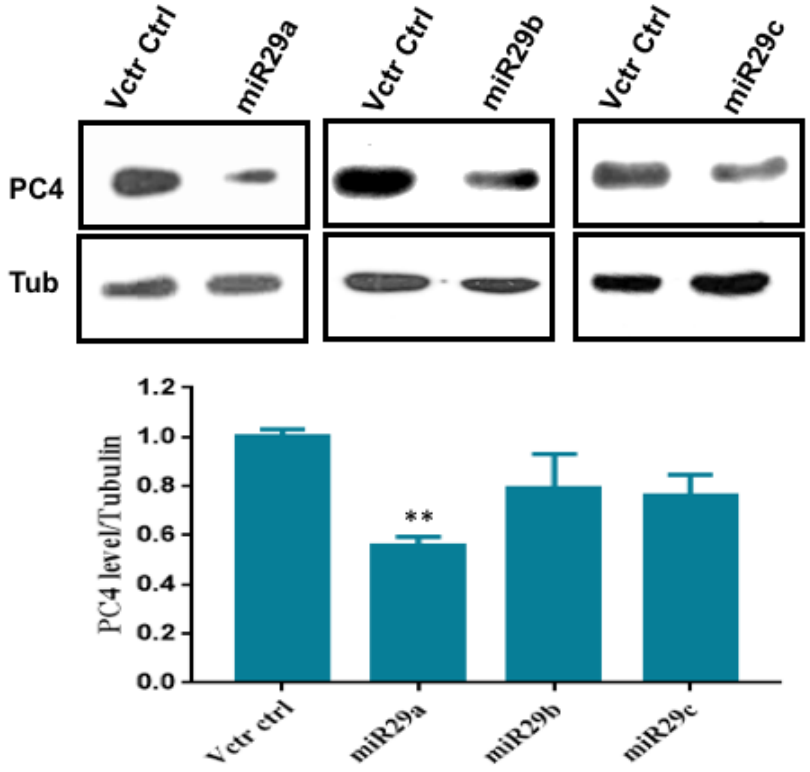

Figure 4.2.3 Ectopic expression of has-miR-29 downregulates PC4 expression in HEK293 cells. Western Blot analysis of PC4 was done after transfection with pSUPER empty vector (Vctr Ctrl) and miR29 at 96 hours. Here Tubulin was used as the loading control. Densitometric analyses of protein bands were done. n=3, N=2. Data are presented as means ± S.E.M. p* < 0.01, p** < 0.001, p*** < 0.0001.

4.3. Correlation of PC4 expression and miRNA in the context of Breast Cancer

MiR29 family was found to regulate PC4 expression in HEK293 cells. This prompted us to check that whether this miRNA is the potential regulator of PC4 expression in the context of Breast Cancer also. In the family of miR29 as miR29a showed significant downregulation of PC4 expression at protein level (Figure 4.2.4) we considered this miRNA in our Breast cancer study. As mentioned in the above section, PC4 expression was found to be downregulated at in large number of Breast cancer patient samples and also in some of the aggressive patient derived cell lines like ZR751, HCC388, HCC108, and SKBR3. To establish the potential role of miR29a in downregulating PC4 expression in Breast Cancer we analyzed the correlation of expression pattern of PC4 and miRNA29a in Breast cancer cell lines or patient samples We therefore checked expression of both PC4 mRNA as well as miRNA in those breast cancer cell lines in which PC4 was found to be low at protein level, as revealed by western blot analysis. qPCR analysis shows that cell lines ZR751,HCC388,HCC108,SKBR3 have high normalized Ct values as compared to MCF7 cells signifying that the level of PC4 mRNA was lower in these lines as compared to that in MCF7 cells.(Figure 4.3.1 A). Correspondingly we also checked the levels of miRNA 29a in these cell lines. MiR29a was found to be upregulated in all the cell lines where PC4 expression was found to be low (Figure 4.3.1 B). MDAMB361 and MDAMB453 were taken as control cell lines where PC4 expression was not found to be altered as compared to ZR751/HCC388. Correspondingly we see that miR29a levels were either downregulated or unaltered in these cell lines. This establishes an inverse correlation of PC4 expression and that of miR29a in the Breast cancer cell lines indicating that it could be acting as a regulator in the patient samples also.

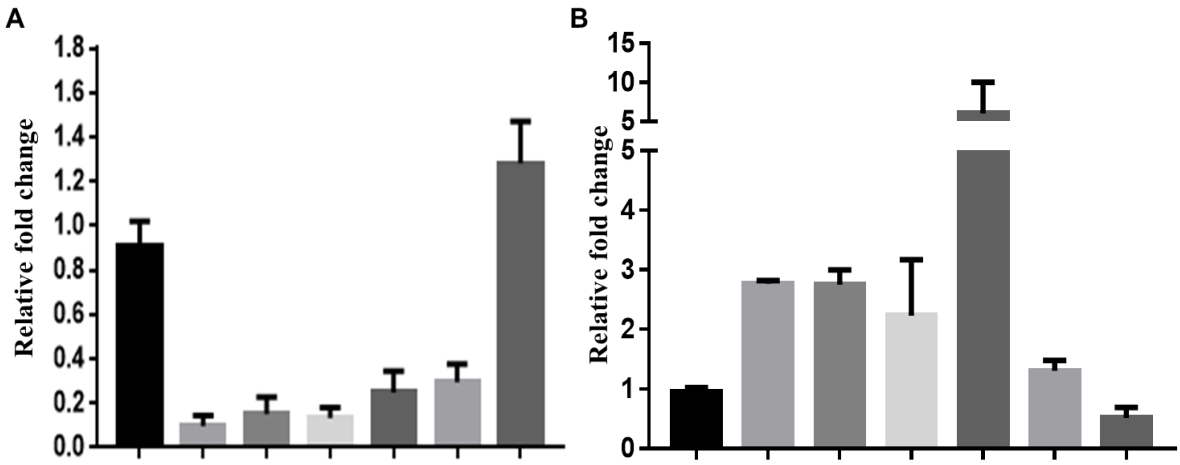

Figure 4.3.1 Correlation of PC4 and miR29a in Breast cancer cell lines. PC4 (A) and miR29a (B) expression was checked with gene specific primers in the panel of Breast cancer cell lines. The fold change is calculated by the ΔΔCt method (see materials and methods). Actin specific gene primers are used for normalization of mRNAs and U6 snRNA is used as a control for small RNAs. n=3. Data are presented as means ± S.E.M. p* < 0.01, p** < 0.001, p*** < 0.0001.

To further substantiate our hypothesis of miR29a downregulating PC4 expression in Breast cancer patient samples as well we carried out miRNA expression profiling of Breast Cancer patient samples which showed mostly downregulation of PC4 expression at protein level as analyzed by immunohistochemistry. Among the 25 pair of Breast cancer patient samples analyzed, we find there is indeed a negative correlation of PC4 expression and miR29a expression for a subset of 12 samples. This observation further validates that miR29a might be one of the prime factors that might be responsible for the downregulation of PC4 both at transcript and protein level in Breast cancer patient samples. However due to the existence of complex molecular subtypes of Breast Cancer we hereby do not negate the role of other factors that might be responsible for mediating the low expression status of Breast cancer. Correlating the expression data of miR29a in a large subset of Breast Cancer patient samples from TCGA database , we find that in stage IV miR29a expression was relatively high than the other stages(Stage II and III) (Figure 4.3.2B). This is in agreement to our PC4 expression

analysis from TCGA database where PC4 expression gradually decreased across different stages of Breast cancer the least being in Stage IV. Thus even at a larger subset of Breast cancer patient samples we do find a possible correlation of miR29a and PC4 expression validating miR29a as a negative regulator of PC4 expression and mediating its downregulation in Breast cancer patient samples.

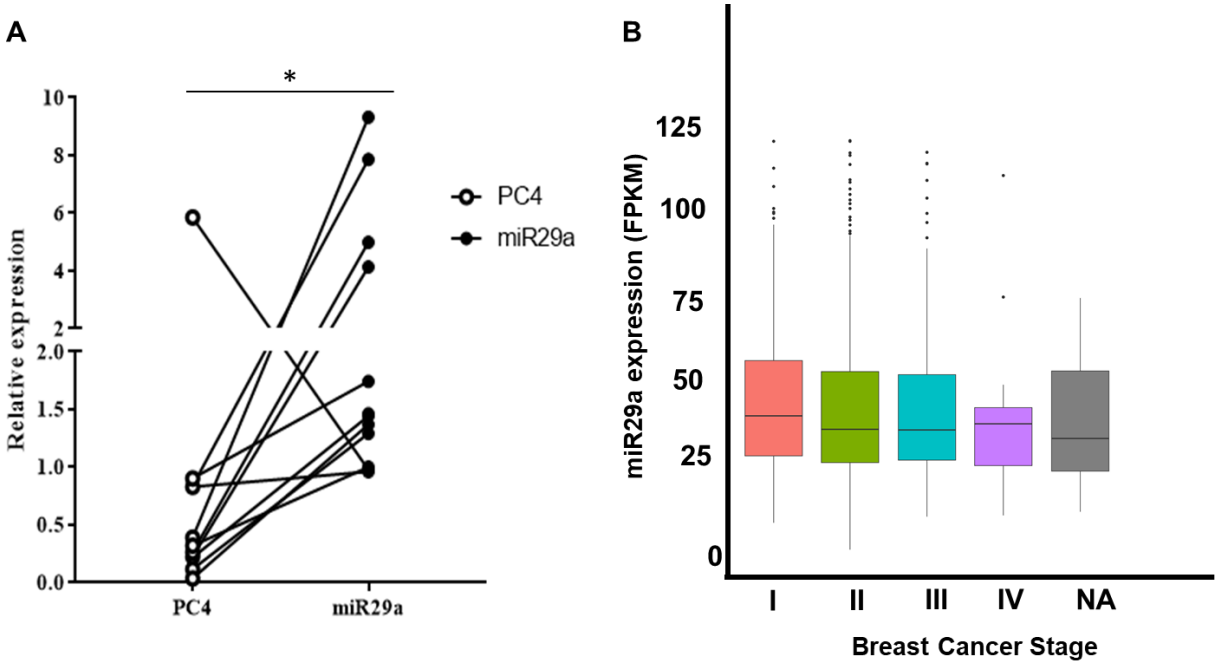

Figure 4.3.2 Correlation of PC4 and miR29a in Breast cancer patient samples. (A) PC4 and miR29a expression was checked with gene specific primers from RNA extracted from Breast cancer patient samples. The fold change is calculated by the ΔΔCt method (see materials and methods). Actin specific gene primers are used for normalization of mRNAs and U6 snRNA is used as a control for small RNAs. n=3. Data are presented as means ± S.E.M. p* < 0.01, p** < 0.001, p*** < 0.0001. (B) Transcript analysis of miR29a (Expression) from TCGA database stage wise.

4.4. miR29a regulates PC4 expression in Breast cancer cells

Our previous observations on the expression analysis of PC4 and miR29a prompted us to investigate the consequence of overexpression of miR29a in Breast cancer cells. Similar to the results obtained in HEK293 cells, we find that after 48 hours of miR29a overexpression in MCF7 cells results in decreased luciferase activity of PC4 3'UTR(Figure 4.4.A). MiR29a also led to the significant downregulation of PC4 mRNA (at 48 hours) (Figure 4.4.B) as well as protein level when overexpressed in MCF7 cells (at 96 hours) (Figure 4.4.C). Thus validating the role of miR29a as a post transcriptional regulator of PC4 expression in Breast cancer cells.

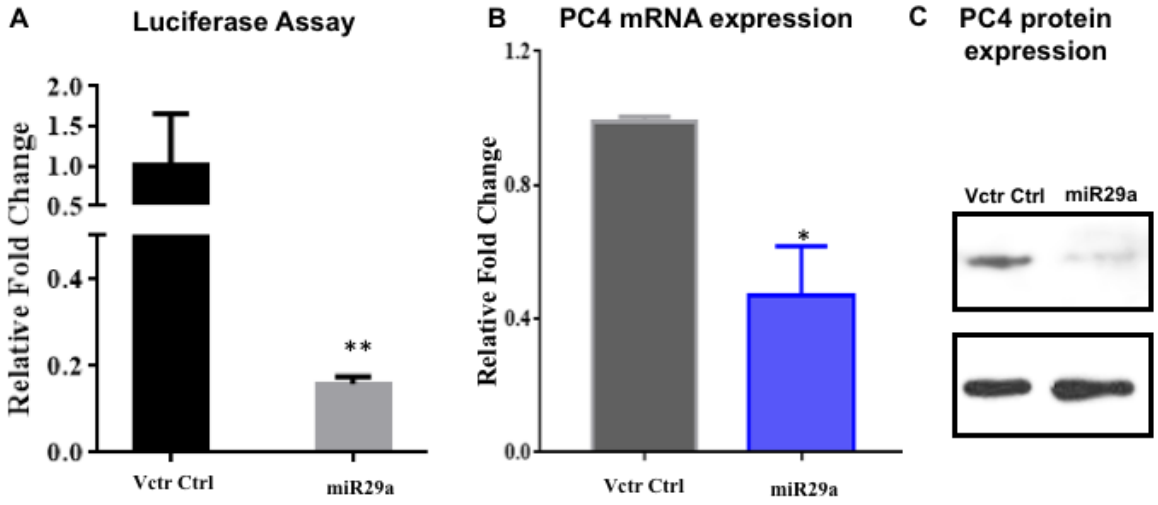

Figure 4.4. Regulation of PC4 expression in MCF7 cells by miR29a: (A) MCF7 cells were transiently transfected with the PC4 3'UTR expression construct along with miRNA expression plasmids. Equivalent amount of control empty vector pSUPER was used to normalize the amount of transfected DNA. pMIR-βgal was used as an internal control for all the transfection experiments to normalize luciferase activity. After normalization, relative fold change in luciferase activity after 48 hours of transfection was plotted (along y axis). n=3, N=2. Data are presented as means ± S.E.M. p* < 0.01, p** < 0.001, p*** < 0.0001. (B) PC4 expression was checked with gene specific primers after transfection of HEK293 cells for 48hrs with miR29 expressing vector. Empty pSUPER vector was transfected as vector control. The fold change is calculated by the ΔΔCt method (see materials and methods). Actin specific gene primers are used for normalization. n=3, N=2. Data are presented as means ± S.E.M. p* < 0.01, p** < 0.001, p*** < 0.0001. Western Blot analysis of PC4 was done after transfection with pSUPER empty vector (Vctr Ctrl) and miR29 at 96 hours. Here Tubulin was used as the loading control.

4.5. PC4 downregulation enhances cellular migration and invasive property of MCF7 cells

To understand the putative role of PC4 in Breast cancer progression, we wanted to analyse the significance of downregulation of PC4 in Breast Cancer cells. For this we established a stable knockdown of PC4 in MCF7 cells (refer materials and methods). To understand the physiological effect of PC4 knockdown in the context of cancer formation we looked into the migratory and invasive property of Breast cancer cells upon PC4 downregulation. Boyden chamber matrigel assay was carried out to measure the invasive property of the cells while the migratory property was assayed by monitoring the cells in the lower chamber of the Boyden transwell cup without the matrigel layer. Stable shRNA expressing cells were established using a less oncogenic and invasive cell line like MCF7 to assay the effect of downregulation of PC4 in the physiological characteristics of the cells. Downregulation of PC4 led to higher migration of MCF7 cells (Figure 4.5.A). MCF7 cells were also found to invade significantly the matrigel layer once PC4 is downregulated (Figure 4.5.B). Collectively, these data suggests that downregulation of PC4 harboured oncogenic properties to a lesser invasive Breast cancer cells (MCF7). This partially explains the cause of downregulation of PC4 in Breast cancer patient samples, and also the putative tumour suppressor role of PC4 in Breast cancer.

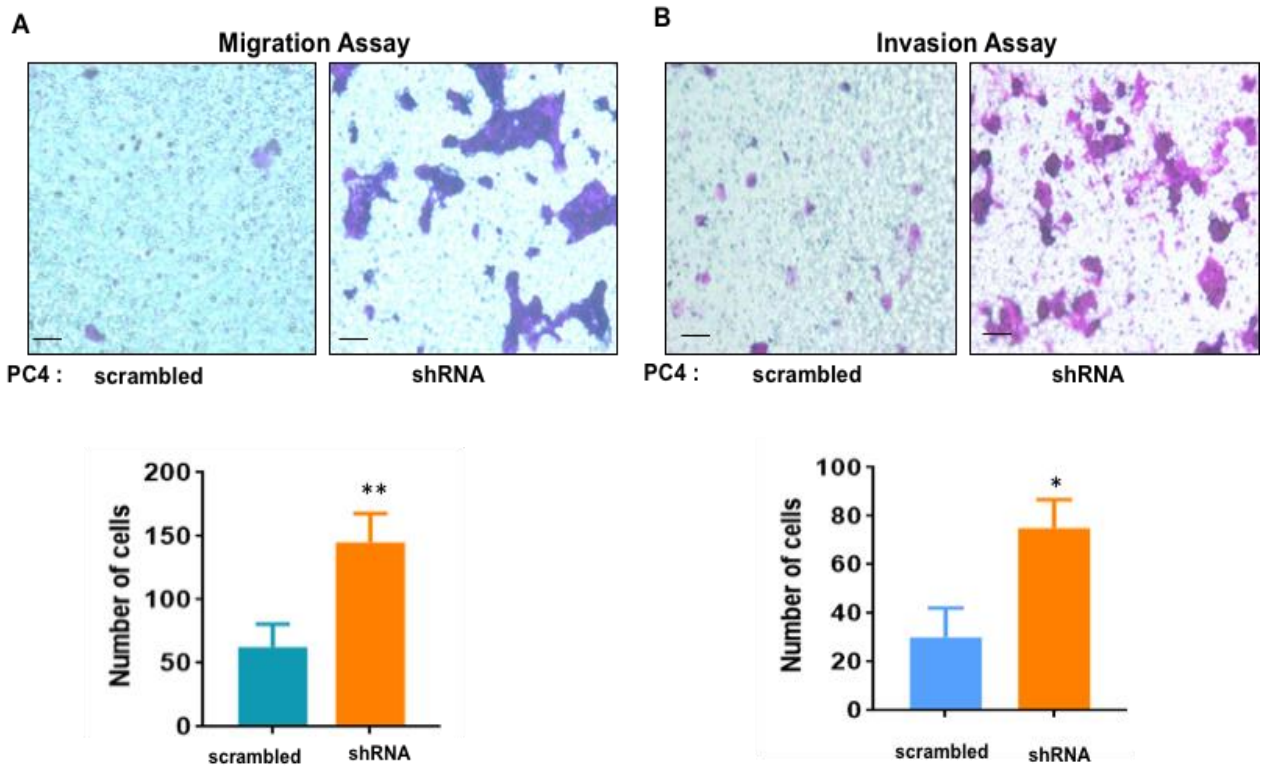

Figure 4.5. Enhanced migration and invasive property of MCF7 cells upon knockdown of PC4: Equal number of MCF7 cells harboring stably the scrambled shRNA as well as the PC4 shRNA was seeded in the upper chamber of the Boyden Chamber assay with or without matrigel. After 16hrs-24hours the cells in the lower chamber was stained with 10% Crystal Violet solution and then imaged for three independent fields. (A) Migration assay done with MCF7 stable scrambled shRNA as well as PC4 shRNA cell line. Number of cells which migrated to the lower chamber of the transwell cup was compared in between the two cell lines. Bar graph represents the quantitation of the migratory ability of the two cell lines. n=3,N=2. Data are presented as means ± S.E.M. p* < 0.01, p** < 0.001, p*** < 0.0001. (A) Invasion assay done with MCF7 stable scrambled shRNA as well as PC4 shRNA cell line. Number of cells which invaded to the lower chamber of the transwell cup in presence of the matrigel layer was compared in between the two cell lines. Bar graph represents the quantitation of the invasive ability of the two cell lines. n=3, N=2. Data are presented as means ± S.E.M. p* < 0.01, p** < 0.001, p*** < 0.0001.

4.6. Breast cancer cell lines harboring low levels of PC4 exhibit enhanced autophagy levels and is resistant to gamma irradiation.

Taking into account all the data as described above we infer that PC4 might play a tumor suppressive role in the context of Breast cancer. To further elaborate our hypothesis, we wanted to understand the molecular mechanism and further delve into the consequence of PC4 downregulation in Breast cancer cells. Our expression analysis from a milieu of breast cancer cell lines depicted that the highly invasive and oncogenic cell lines expressed low levels of autophagy. We chose two cell lines based on the expression pattern of PC4, MCF7 (less oncogenic cell line where PC4 is expressed) and ZR751 (a highly invasive cell line which harbored low levels of PC4 protein) and studied its various properties.

ZR751 is a luminal type ER+ Breast Cancer cell line. It is derived from a malignant ascitic effusion in a 63 year old female Caucasian with infiltrating ductal carcinoma. It was found to have depleted levels of PC4 and has high expression of miR29a (Figure 4.3.1B). In lieu to our previous observation, where PC4 was found to be a negative regulator of autophagy and mediating gamma irradiation resistance (Chapter 3), a short characterization in terms of its autophagy marker expression, wound healing assay and survivability upon gamma irradiation was studied. It was found that ZR751 showed high levels of LC3 II level as compared to MCF7 cells showing greater induction of autophagy (Figure 4.6.1A). To ascertain that this effect is due to the downregulation of PC4 we also analysed the expression pattern of LC3II, the autophagy marker in the MCF7 PC4 knockdown cells. There is indeed a greater induction of autophagy in absence of PC4 in MCF7 cells (Figure 4.6.1A). Thus the negative regulation of autophagy by PC4 holds true even in Breast Cancer cells and we indeed see a correlation of LC3II and PC4 expression in highly invasive ZR-75-1 cells. ZR-75-1 being a highly invasive cell line showed a faster healing property when compared to that of MCF7 cells (4.6.1B).

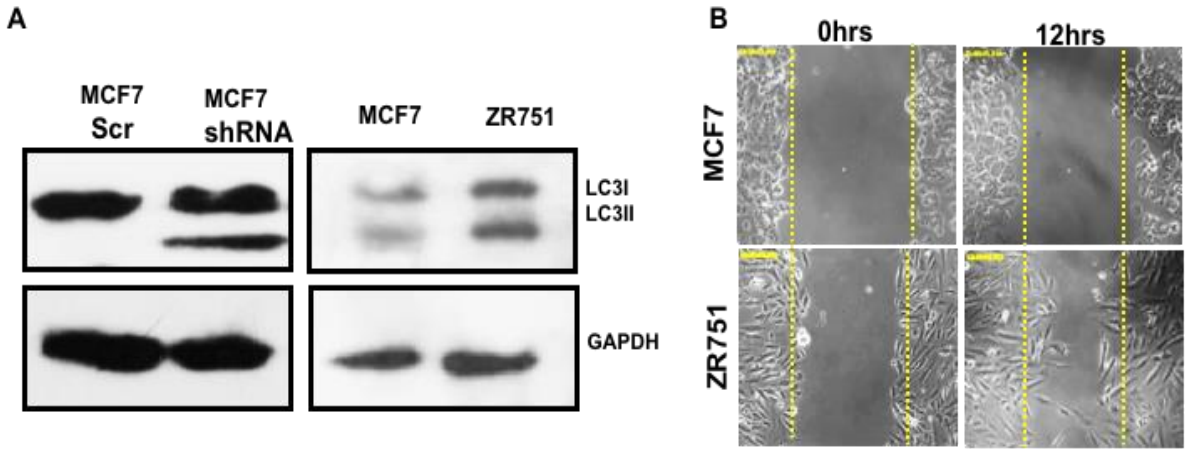

Figure 4.6.1. ZR-75-1 exhibit greater migratory ability and enhanced autophagy levels. (A) Autophagy levels were checked by immunoblotting for LC3II levels in MCF7 cells where PC4 was stably knocked down and also compared between MCF7 wildtype and ZR-75-1 cells. (B) Microscopic images of wound healing assay performed towards comparison of migration rate between MCF7 and ZR-75-1 cells. Equal wound created in both cell lines (0 hours) was monitored at regular time intervals till complete healing was achieved in either of the cells. Here at 12 hours' time point the extent of migration in both the cell lines are depicted.

From studies in HEK293 cells we have earlier observed that PC4 knockdown cells showed gamma irradiation resistance property. Correlating the results in Breast cancer cells we assayed the gamma irradiation sensitivity on the ZR-75-1 cells. ZR-75-1 cells which had endogenous low levels of PC4 indeed showed resistance to gamma irradiation induced cytotoxicity as is evidenced by the number of live colonies even after exposure to high doses of gamma irradiation (Figure 4.6.2A). We further wanted to validate that the gamma irradiation resistance property of ZR-75-1 cells is due to the enhanced autophagy levels mediated by the downregulation of PC4. Similar to the autophagy inhibition assay in the HEK293 cells, ZR751 cells were pretreated with Bafilomycin for 2 hours and 24 hours respectively followed by exposure to gamma irradiation. Bafilomycin treatment drastically reduced the number of live colonies in the ZR-75-1 cells in the presence of gamma

irradiation (Figure 4.6.2B). Thus the enhanced autophagy in the absence of PC4 might be the possible factor mediating the gamma irradiation resistance property of ZR-75-1 cells.

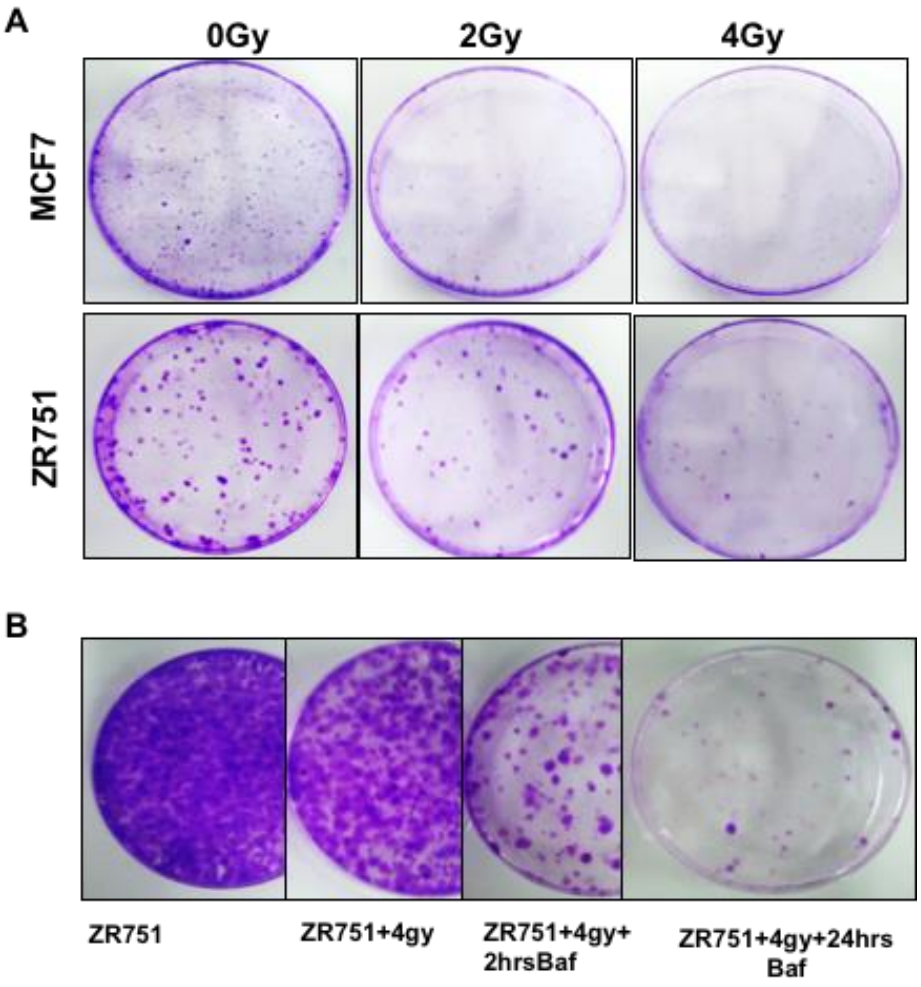

Figure 4.6.2 Autophagy inhibition sensitizes PC4 depleted breast cancer cells ZR-75-1 to gamma irradiation. (A) Representative image of the crystal violet stained colonies of ZR-75-1 cells sustained after exposure to increasing doses of the gamma radiation (in Grey units) (B) ZR-75-1 cells were treated with small molecule inhibitor, Bafilomycin 2 hours prior to exposure to 4Gy of gamma irradiation. Cells were grown in the presence of the respective inhibitor for 24 hours post irradiation. Colonies were grown for 10 days.

4.7. Restoration of PC4 expression in ZR-75-1 cells downregulates autophagy and also reduces its invasiveness and migratory ability

To validate the potential tumor suppressive role of PC4 we resorted to an approach of rescuing PC4 expression in the PC4 depleted Breast Cancer cells. Mammalian expression constructs of Flag tagged PC4 was transiently transfected into ZR-75-1 cells and the expression of PC4 was checked by immunoblotting with antiFlag antibody. We observed that restoration of PC4 expression in ZR-75-1 cells resulted in downregulation of autophagy as is evidenced by the reduced level of LC3II (Figure 4.7.A) as compared to ZR-75-1 cells transfected with the vector backbone (pCMV). This validates once again our previous observation of PC4 being a negative regulator of autophagy. Our observation of PC4 knockdown mediating higher migratory and invasive property to MCF7 cells, urged us to check these cellular properties upon expressing PC4 back in the knockdown background of ZR-75-1 cells. Expression of PC4 drastically reduced the migratory ability of the ZR-75-1 cells as is evidenced by the transwell migration assay after 48 hours of transfection of Flag PC4 constructs in ZR-75-1 cells (Figure 4.7.B upper panel). Supporting the migration data, the invasive property of ZR-75-1 cells was drastically reduced upon transfection of FPC4 at 48 hours' time point. This observation proves that PC4 directly regulates the migratory and invasive property of highly metastatic breast cancer cells validating its potential tumor suppressive role.

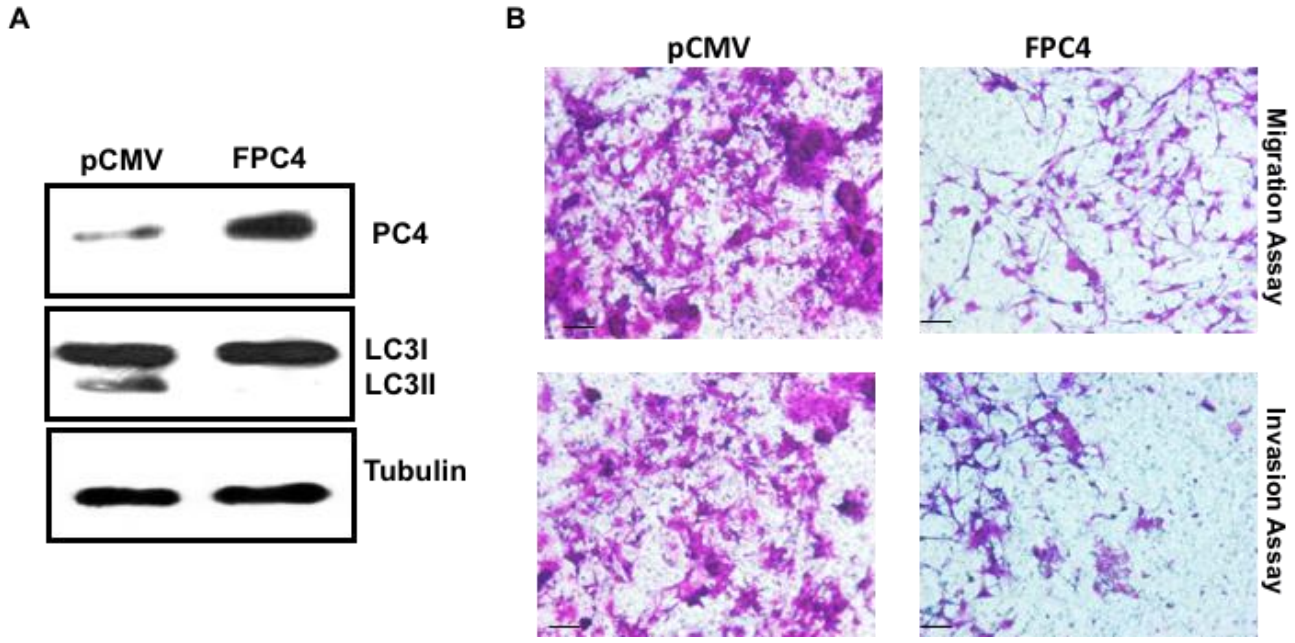

Figure 4.7. Restoration of PC4 expression in ZR-75-1 cells inhibits autophagy and the invasive property of the cells. Flag PC4 was transiently expressed in ZR-75-1 Breast Cancer cells and (A) the expression was checked after 48hrs post transfection by immunoblotting with anti-Flag antibody. LC3II levels were checked in ZR-75-1 cells transfected with vector control pCMV and ZR-75-1 cells transfected with Flag PC4. (B) Downregulation of migration and invasive property of ZR-75-1 cells upon transfection of PC4: Equal number of ZR-75-1 cells transfected either with pCMV or FPC4 was seeded in the upper chamber of the Boyden Chamber assay with or without matrigel. After 16hrs-24hours the cells in the lower chamber was stained with 10% Crystal Violet solution and then imaged for three independent fields. Migration assay done with the ZR-75-1 cells expressing PC4. Number of cells which migrated to the lower chamber of the transwell cup was compared in between the two cell lines. Invasion assay also done upon FPC4 expression in ZR-75-1 cells. Number of cells which invaded to the lower chamber of the transwell cup in presence of the matrigel layer was compared in between the two cell lines.

Summary

The major observations of this part of the study are summarized below:

- PC4 was found to be downregulated extensively in four breast cancer cell lines. Molecular characterization and physiological property suggests that most of the low PC4 expressing Breast cancer cells were more aggressive and invasive in nature.
- Expression study in tumour samples obtained from Breast cancer patients revealed downregulation of PC4 both at transcript and protein levels in majority of the Breast tumour tissues. Studying large cohorts of patient samples from the TCGA database showed similar trend of downregulation with increase in stage of the Breast Cancer disease.
- MiR29 binds to the 3'UTR region of PC4 and thereby downregulates its expression both at the mRNA and the protein level. Overexpression of this miRNA in Breast cancer cells also brought about inhibition of expression of PC4
- Expression analysis of miR29 in Breast cancer cell lines and patient samples where PC4 was found to be downregulated showed significant upregulation. This suggests a possible negative correlation of PC4 expression with that of miR29 especially to that of miR29a
- Stable knockdown of PC4 in Breast Cancer cells induces greater migration, invasion and proliferation property of the cells.
- PC4downregulation in Breast cancer cell line induces autophagy thereby rendering the gamma irradiation resistance property which is abrogated upon administration of autophagy inhibitors.
- Restoration of PC4 expression in a PC4 depleted Breast Cancer cell line ZR-75-1 inhibits its migratory and invasive properties.

Discussion

Global alteration of nuclear architecture as seen by loss of heterochromatin foci rendering nucleus more open in the absence of PC4, establishes it as one of the important chromatin architectural proteins. PC4 is essential for maintenance of chromatin as its knockdown resulted in an accessible chromatin conformation as revealed by enhanced histone acetylation modifications. Phenotypically, PC4 knockdown cell line demonstrated disruption of several cell cycle related events at different levels. Therefore, PC4 could be essential for guarding the genome against genotoxic insults and thereby prevent oncogenesis. The expression status of PC4 in Breast cancer patient samples correlated to our assumption of PC4 playing a tumor suppressive role. A large dataset of Breast cancer patient samples showed significant downregulation of PC4 both at protein as well as transcript level irrespective of its molecular signatures signifying the universal tumor suppressive role of PC4 across different subtypes of Breast cancer. In this study however we delve into the molecular mechanism of downregulation of PC4. We find that a specific set of miRNAs might play a critical role in modulating PC4 expression even in the breast cancer patient samples. It is revealed that hsa-miR29 directly target PC4 3'UTR and thereby down regulate its expression. Furthermore the downregulation of PC4 mRNA level and also of the endogenous protein level upon overexpression of miRNAs (as validated by qRT PCR data and western blot analysis) shows that PC4 might be a real target of this set of miRNAs. Aberrant expression of miRNAs targeting PC4 might regulate its expression in Breast Cancer cell lines**.** As is reported from an earlier study PC4 showed reduced expression both at transcript and protein level in breast cancer patient samples. Here in this study in a panel of breast cancer cell lines, up regulation of the validated miRNAs targeting PC4 was found corresponding to the downregulation of PC4 mRNA level. It is also observed that overexpression of one of the miRNAs; miR29a in MCF7 cells downregulates PC4 expression both at transcript and protein level.

Stable knockdown of PC4 expression in MCF7 cells reduced dramatically its migratory and invasive property. This signifies further the potential role of PC4 in inhibiting Breast cancer tumorigenesis. PC4 depleted breast cancer cell line also show enhanced autophagy levels and radiation resistance. ZR751, breast cancer cells has low endogenous PC4 levels. These cells were found to be highly invasive, have enhanced autophagy levels as is evidenced by higher

LC3II levels. In lieu to the previous observation in HEK293 sh-PC4 cells this Breast cancer cell line also showed gamma irradiation resistance which was abrogated in the presence of an autophagy inhibitor, Bafilomycin. Thus autophagy and the phenomenon of gamma irradiation resistance in absence of PC4 hold to be true in context of Breast Cancer also.

Restoring PC4 expression in the Breast cancer cell line depleted of PC4 reverted back the property of invasiveness and migration, also reducing the high autophagy levels intrinsically harbored by this cell line. This observation reveals that the importance of PC4 in mediating oncogenesis and tumorigenic properties. The repression of autophagy in Breast cancer cells by PC4 also ascertains the fact that PC4 acts as a negative regulator of autophagy not in a cell type specific manner. To reinforce the fact that PC4 might be acting as tumor suppressor in Breast Cancer, we carried out a preliminary *in vivo* mice model study. In this orthotropic mice model system, MDAMB231 cells silenced for PC4 was injected into the mammary fat pad tissue of mice, and then the tumor growth was monitored and measured. After 9 weeks, the PC4 knockdown cells showed a uniform tumor progression as compared to the vector control cells (Figure 4.8 B and C). This potentiates to the fact that PC4 indeed plays a tumor suppressive role as its knockdown results in tumor formation and progression even in Breast Cancer *in vivo* mice model.

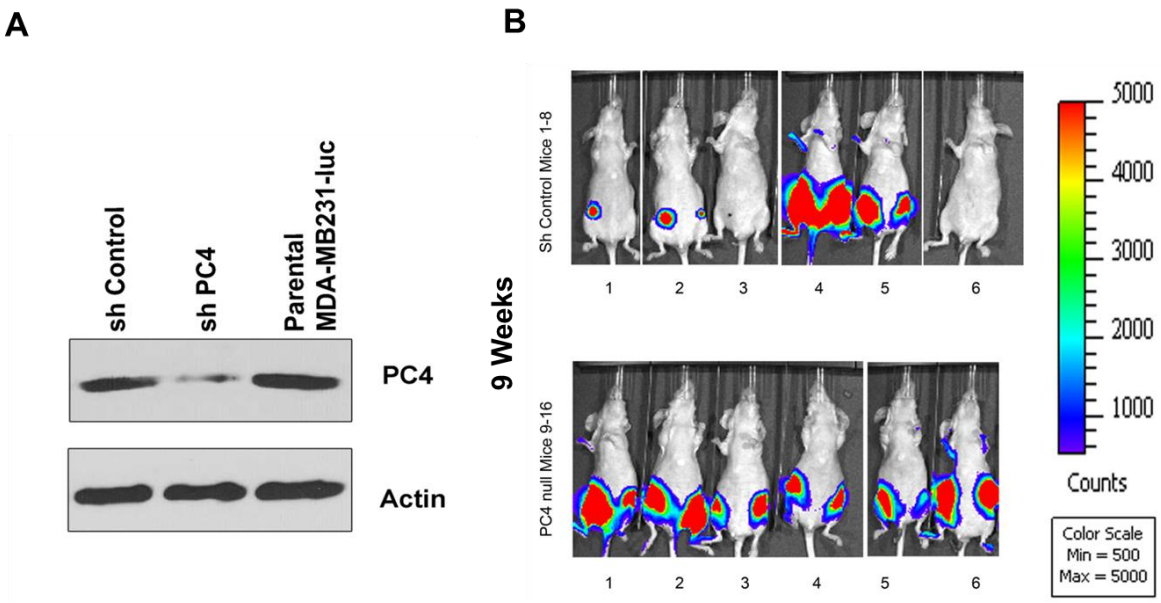

Figure 4.8. Absence of PC4 induces uniform tumour progression in orthotropic Breast cancer mice model. (A)MDAMB231 cells harboring an shRNA which targets PC4 was transfected and a stable knockdown cell line was established. Western blotting to confirm PC4 knockdown in MDAMB231 luc cells. (B) Mice imaged for luc expressing cells after 9 weeks from injection. Upper panel shows control mice, injected with MDAMB231 vector control cells which express PC4; lower panel represents set of mice where PC4 was knocked down.

Chapter 5: KAT5 (Tip60) mediated acetylation of PC4 is critical for maintenance of genomic stability

This chapter establishes PC4 as a novel substrate of the acetyltransferase Tip60. Here we find the exact site of acetylation in PC4 which is mediated by Tip60 and also elucidate its functional properties in vivo. Acetylation defective mutant of PC4 was further used to attribute the function of the Tip 60 acetylated form of PC4.

Background

The human genome is under constant threat from various genotoxic agents which can cause severe damage to our genetic material, DNA. Erroneous or inefficient repairing of the genome upon such genotoxic insults can cause changes in the DNA sequence itself which if not corrected can trigger genomic instability and thereby lead to harmful cellular environment or even untimely death. However as a safeguard mechanism cells counteract these adverse effects by activating the DNA damage response, which causes a synchronized series of events that regulates cell cycle progression and repair of DNA lesions (Broustas and Lieberman, 2014; Nair et al., 2017). The tight packaging of the genomic DNA very often poses a threat to the DNA repair pathway in living cells. Therefore cells modulate the chromatin structure at the site of damage by the help of various factors like post-translational histone modifications, ATP-dependent chromatin remodelers, to help the DNA repair machinery to access the DNA lesion.

In addition to the above mentioned factors, various non-histone proteins also play an important role either directly interacting with the DNA repair machinery proteins or by regulating the chromatin structure. Following a double strand break (DSB) in the euchromatin region, a number of heterochromatin associated proteins like KAP1 (KRAB-associated protein 1) and HP1 together with the H3K9 methyltransferase SUV39H1 are loaded onto the damage site facilitating the deposition of H3K9 tri-methylation mark. This in turn sends a cue to other protein complexes to bind through the HP1 binding to the H3K9me3 mark, which spreads to tens of kilobases from the lesion site. An important

DNA damage responsive histone acetyltransferase, Tip60 gets activated through its induced Tyr44 phosphorylation which promotes its binding to H3K9me3, thus facilitating ATM and histone H4 acetylation. The active acetylated ATM phosphorylates KAP1 resulting in the release of the complex from chromatin removing the repressive mark. It could be that H3K9 tri-methylation represents a transient shift to repressive chromatin that is required for TIP60 recruitment and ATM activation in more open regions of the chromatin. However, DSBs within heterochromatin undergo localized phosphorylation of KAP1 leading to retention of the protein into foci at sites of damage, a process that is dependent on the ATM effector protein, 53BP1. MRE11-NBS1 accumulation at late-repairing DSBs is augmented by 53BP1 in order to accumulate active ATM for enhanced localized pKAP1. KAP1 phosphorylation directly perturbs its interaction with the nucleosome remodeler, CHD3 (Chromodomain-helicase-DNA-binding protein 3) thereby dispersing CHD3 from heterochromatin and enabling relaxation for efficient repair (Hauer and Gasser, 2017; Nair et al., 2017).

Human positive coactivator 4, PC4 has been reported to get recruited early at DNA damage site (Mortusewicz et al., 2008). It has been shown to interact with the DNA repair protein XPG and gets recruited to DNA damage site (bubbled DNA). PC4 also prevents mutagenesis and killing by oxidative DNA damage repair by its ssDNA binding ability (Wang et al., 2004). Delving more into the molecular repair pathway it has been shown to enhance joining of Non-homologous end joining repair and double strand break repair activity (Batta et al., 2009) and also in homologous recombination repair (Mortusewicz et al., 2016). In this study, we pose the question that whether this DNA repair activity of PC4 is being modulated by any post translational modifications. Tip60 being a DNA damage responsive acetyltransferase which acetylates various effector proteins, like ATM,p53 to modulate the DNA repair pathway, we here attempt to understand the consequences of Tip60 mediated acetylation of PC4 in the context of chromatin and DNA repair.

5.1. PC4 is a substrate of KAT5 (Tip60) acetyltransferase

Owing to its role in DNA damage, we wanted to investigate PC4 as a substrate of the DNA damage responsive acetyltransferase, KAT5 (Tip60). PC4 was subjected to *in vitro* acetylation by both p300 and Tip60 (baculo expressed full length recombinant His tagged). As p53 was known to be a substrate of Tip60 it was taken as a positive non-histone protein control apart from the histone protein H3. The reaction mixtures containing equivalent activities of either p300 or Tip60 (as normalized by filter binding assay using Histone H3 and H4 respectively) and the indicated amount of proteins (Figure 5.1) were incubated with [^{3}H] acetyl-CoA for 30min at 30 °C. The products were analyzed by autoradiography of acetylated reaction products resolved on SDS-PAGE gel. From Figure 5.1. it was observed that PC4 was not only acetylated by p300 but also with equivalent activity of Tip60 (Figure 5.1, middle panel). Thus, p300 is not the only acetyltransferase which can acetylate PC4 *in vitro*. We thus show that like p53(right panel), PC4 might be a substrate of the acetyltransferase Tip60.

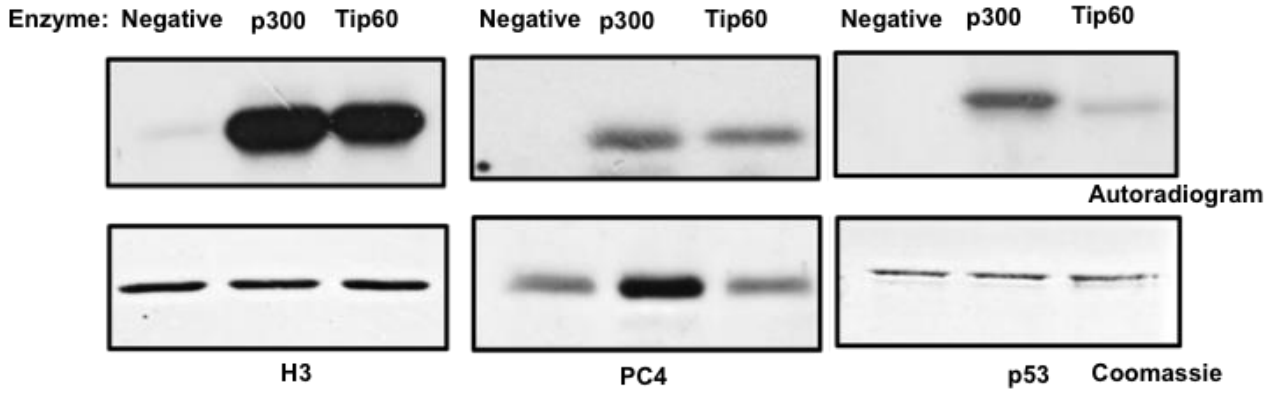

Figure 5.1. *In vitro* acetylation of PC4 by KAT5: Purified proteins were incubated with [^{3}H] acetyl-CoA for 30 min at 30 °C and then separated by SDS-PAGE (12%) and visualized by fluorography. 500ng of purified Histone H3(left panel) without any HAT (1st lane), with p300 (2nd lane), and with Tip60 (3rd lane) and bacterially expressed His-PC4 (middle panel) without any HAT (1st lane), with p300 (2nd lane), with Tip60 (3rd lane) p53 (right panel) without any HAT (lane 1) with p300 (lane 2), and with Tip60 (lane 3) were incubated.

5.2. Identification of specific acetylation sites in PC4 mediated by acetyltransferase KAT5

Once PC4 was established as a substrate of acetyltransferase of KAT5 (Tip60) by *in vitro* gel assay we next wanted to identify the specific acetylation sites through mass spectrometric analysis (as described in Chapter 2). PC4 was mass acetylated and then subjected to mass spectrometric analysis for identification of residues in PC4 which were post translationally modified. We here concentrated only on the acetylated lysine residues. Our mass spectrometric PTM analysis revealed confident acetylation sites in PC4. We narrowed down to 4 high scoring acetylated residues (represented in green) in the protein PC4 as given below (Figure 5.2. B). The table shows the change in the mass of the peptides due to an acetylated lysine residue obtained by mass spectrometric analysis.

A

Theoretical mass	Observed mass	Difference	Region	Site	Sequence
2030.020	2073.04822	43.02822	4-23	5	SkELVSSSSSGSDSDSEVDK
1224.275	1265.39839	41.12339	48-59	53	ALSSSkQSSSSR
913.11	956.59530	43.48	79-86	80	GkVLIDIR
2868.451	2908.22225	39.77	101-114	101	kGISLNPEQWSQLKEQISDIDDAVR

B

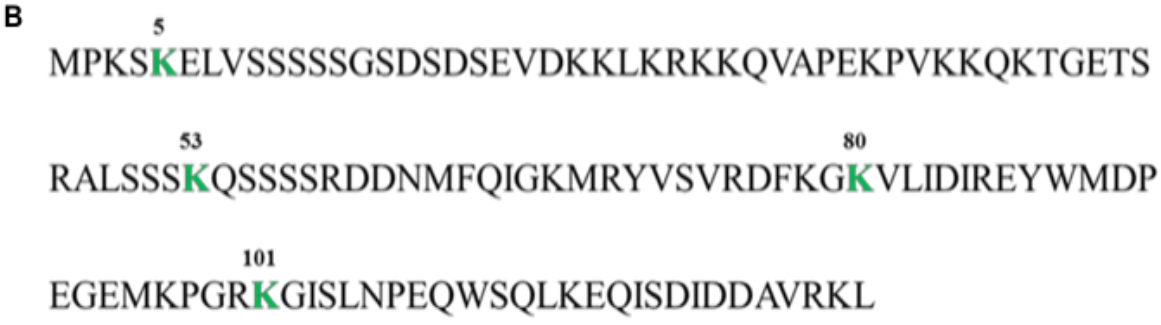

Figure 5.2. Identification of KAT5 mediated acetylation site of PC4. (A) Representative data from mass spectrometric analysis showing the change in mass of peptides containing a single acetylated lysine residue. The lysine residue which was found to be acetylated is represented in small font. (B) High scoring 4 acetylated lysine residue represented in the full protein sequence of PC4.

5.3. *In vitro V*alidation of acetylation site of PC4 by acetyltransferase KAT5

Taking cue from the mass spectrometric data we wanted to further validate the acetylation site in PC4 by generating acetylation defective mutants. Single site mutants were created for each of the lysine sites (changed to arginine) shown above, by site directed mutagenesis (described in chapter 2). In vitro acetylation assay with these mutants was carried out. Acetylation of PC4 K5R, K80R and K101R were highly compromised as compared to PC4 Wild type (WT) (Figure 5.3.1 lane 6vs 7,9 and 10). PC4 K53R showed no change in acetylation with Tip60 as compared to the wild type PC4. (Figure 5.3.1 lane 8). This proves that K53 might not be a major site of acetylation in PC4 mediated by Tip60. Mock acetylation controls were used (Figure 5.2.1 Lanes 1-5) where except the enzyme all components including protein were taken. This further signifies that the acetylation observed is specifically mediated by the enzyme Tip60.

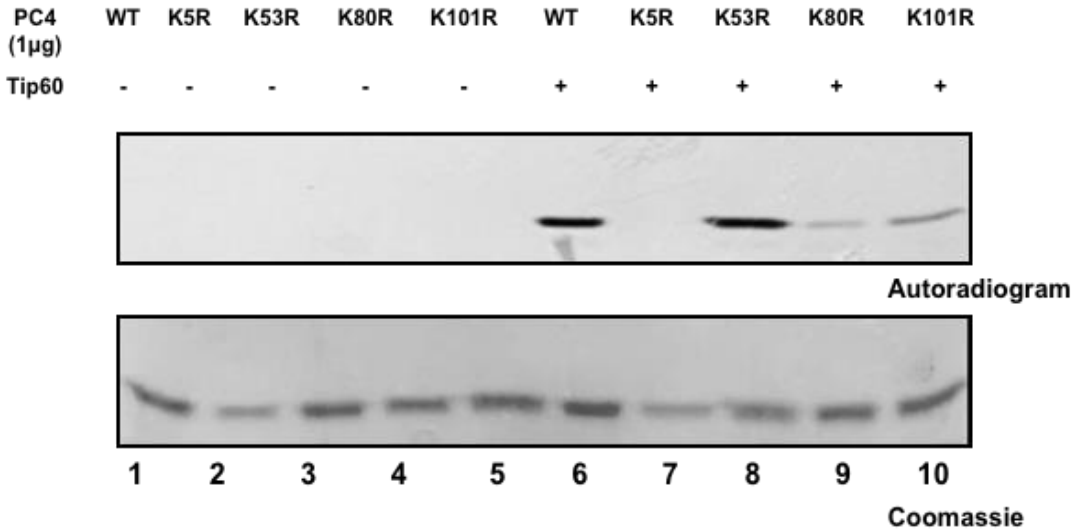

Figure 5.3.1. Acetylation of PC4 lysine mutants by KAT5 (Tip60). HAT assay was performed with 1µg PC4 wild type (WT) and 1µg of acetylation site mutants K5R, K53R, K80R and K101R in presence (lanes 6-10) or absence of Tip60 (lanes 1-5).

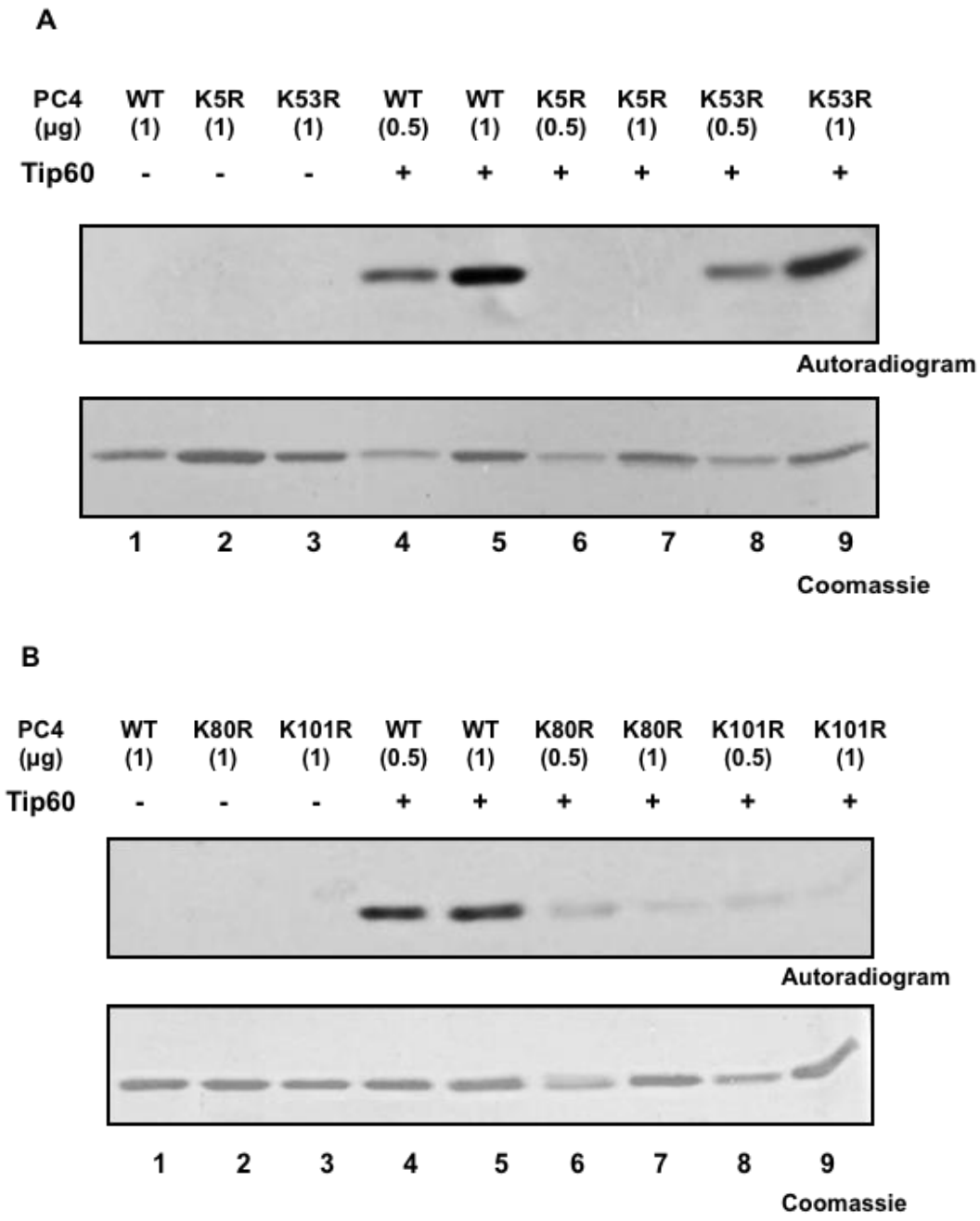

Figure 5.3.2 Tip60 mediated acetylation of lysine mutants of PC4 in a concentration dependent manner. HAT assay was performed with increasing concentrations of PC4 wild type (WT) (+ -500ng and ++ - 1µg) and with increasing concentrations of acetylation site mutants K5R, K53R (Panel A), K80R, K101R (Panel B) in presence (Panel A and B, lanes 4-9) or absence of Tip60 (Panel A and B, lanes 1-3).

In vitro HAT assay with PC4 acetylation defective mutants was carried out in a concentration dependent manner (Figure 5.3.2 A and B) to negate the effects of protein saturation and also to further confirm the mutants which was defective to acetylation by Tip60. Single mutation of lysine to arginine at 5^{th} amino acid position of PC4 (PC4K5R) completely abolished its ability to get acetylated even at higher concentration no band was observed. (Figure 5.3.2 A lane 6 and 7). PC4K80R and PC4K101R also showed compromised acetylation ability which was not affected by the different concentrations of the protein used (Figure 5.3.2 B lane 6, 7 and 8,9). Mutation at K53 to arginine did not affect the acetylation ability of PC4 by Tip60 (Figure 5.3.2A lane8, 9). Thus, lysine residues at 5, 80, and 101 appeared to be important for acetylation of PC4 by KAT5.

PC4 is also a substrate of acetyltransferase p300 (as shown in Figure 5.1). To further validate the lysine residues in PC4 identified as substrates of acetyltransferase Tip60 and not p300, HAT assay was done with each acetylation site mutants and p300. Comparing Figure 5.3.1 and 4.3.3, PC4 K5R showed reduction in acetylation by both p300 (Figure 5.3.3, lane 7) as well as Tip60 (Figure 5.3.1, lane 7) whereas PC4 K53R showed no drastic change in acetylation by either p300 (Figure 5.3.3, lane 8) or Tip60 (Figure 5.3.2, lane 8). PC4 K101R also showed compromised acetylation ability both by p300 (Figure 5.3.3, lane 10) and Tip60 (Figure 5.3.1, lane 10). However, PC4 K80R shows a drastic reduction in Tip60 mediated acetylation (Figure 5.3.1, lane 9) but when subjected to acetylation by p300 (Figure 5.3.3, lane 9) it showed considerable amount of acetylation. Thus, PC4 K80R might be a putative site of acetylation in PC4 specific for Tip60 only.

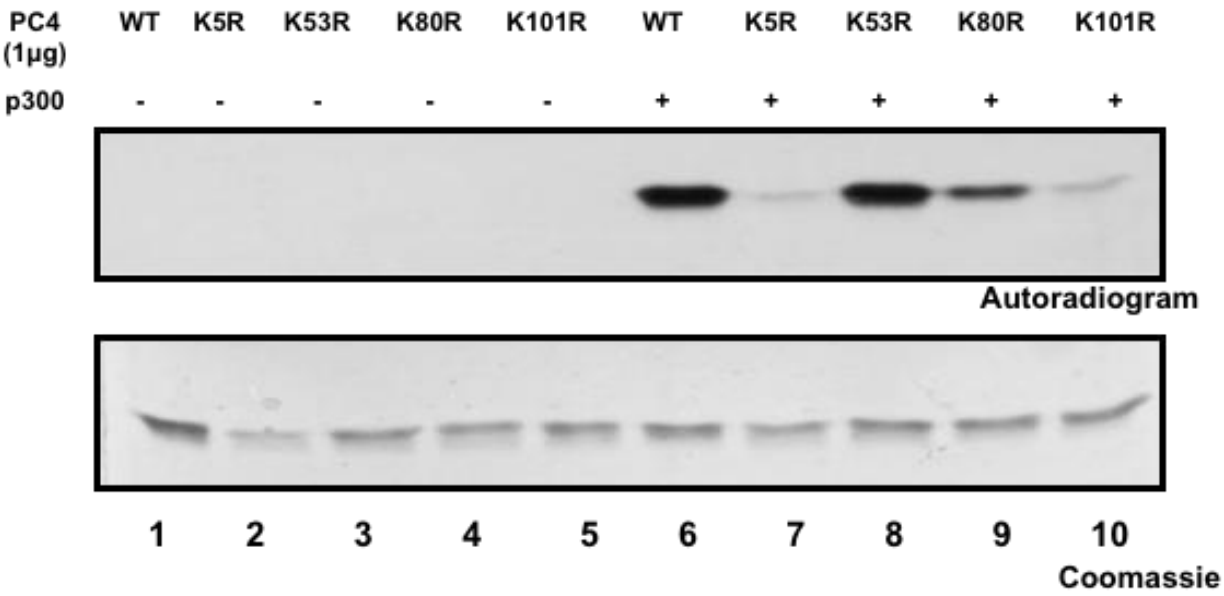

Figure 5.3.3. Acetylation of PC4 WT and PC4 acetylation site mutants by p300. HAT assay was performed with of PC4 wild type (WT) and with acetylation site mutants K5R, K53R, K80R, K101R in presence (lanes 6-10) or absence of p300 (lanes 1-5).

5.4. Acetylation of PC4 at K80 residue upon DNA damage conditions

To understand the physiological role of KAT5/Tip60 acetylated PC4, we raised a site specific (K80Ac) polyclonal antibody to detect the invivo acetylated PC4. The polyclonal antibody was tested for its specificity and sensitivity for Tip60 acetylated PC4 at K80 site as described in chapter 2. Considering its role particularly in DNA damage and repair has well been characterized (Ikura et al., 2000; Sapountzi et al., 2006), we looked for PC4 acetylation at K80 sites under conditions of HDACi treatment (Nicotinamide) and also upon Actinomycin D treatment. Actinomycin D is a DNA damage inducing agent which mostly forms DNA intercalation thereby producing radical oxygen species and thereby causing genotoxic insult to the DNA. It has also been shown to induce γ-H2Ax formation , and forms complex with DNA repair proteins, thereby leading to a DNA damaged condition inside cells (Mischo et al., 2005). Nicotinamide largely acts as Class III HDAC inhibitors but its role in mutagenesis and DNA damage is also known (Surjana et al., 2010). Thus, both the small molecules were

administered to provide a hyperacetylation as well as DNA damaging condition in cells. p53 expression was checked to validate the invivo conditions, as p53 was known to be upregulated upon DNA damage conditions. We find elevated expression of p53 as compared to GAPDH levels (used as an internal loading control). The i*nvivo* PC4 K80Ac mark is shown to be enhanced upon treatment with HDACi (Nicotinamide NAM) and also with DNA damaging agent Actinomycin D. **(**Figure 5. 4.1 Lane 1 vs Lane 2 and Lane 1 vs Lane 3**).** Anti PC4 blotting further reveals that with respect to the PC4 levels there is an upregulation in the acetylation level **(**Figure 5.4.1 PC4 panel compare across lanes 1, 2 and 3**).**

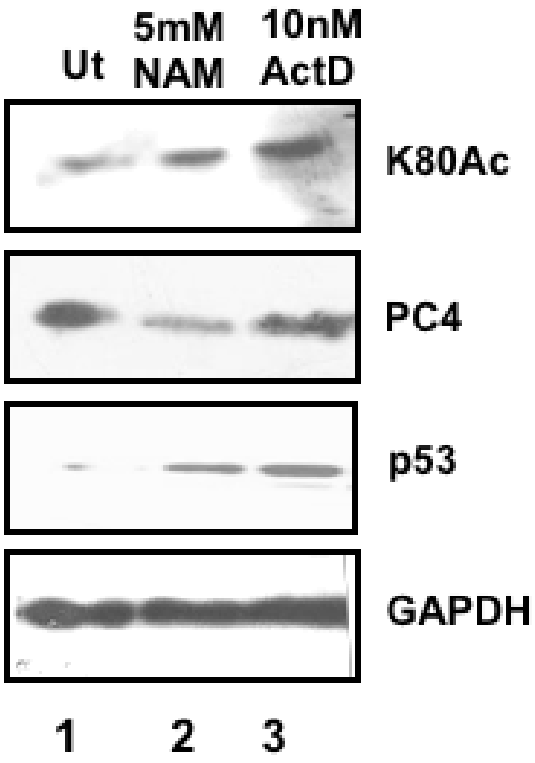

Figure 5.4.1 In vivo acetylation of PC4 at K80 site. HEK293 cells were treated with 5mM NAM (HDACi) and 10nM Actinomycin D (DNA damaging agent) for 6hrs and 12hrs respectively. RIPA lysates were made immunoblotting was done with the K80Ac Ab. Equal Volumes of RIPA lysates were electrophoresed on a 12%SDS gel and levels of PC4 was checked as a loading control. p53 levels were also checked with the same volume of the lysates and normalized against GAPDH.

To validate further our observation that PC4 might be playing a crucial role in DNA damage response in its acetylated form by Tip60, we chose to damage cells through two means. One by the administration of Actinomycin D, the other was exposure to gamma irradiation. We validated the extent of DNA damage upon these two treatments through the damage responsive histone marker γ-H2Ax (data shown in Chapter 2). Correlating with the western analysis, immunofluorescence with K80Ac specific PC4 antibody upon Actinomycin D and gamma irradiation condition also showed enhanced level of acetylation of PC4 at the particular site. (Figure 5.4.2) The PC4 levels were found to be unaltered. Visualizing the acetylation of PC4 upon irradiation or Actinomycin D induced DNA damage by staining with the K80Ac specific antibody led to the formation of distinct foci pattern which was completely absent in the untreated condition. Both the PC4 and AcPC4 showed nuclear localization signifying its nuclear role even upon DNA damage condition. This pattern of foci like staining was quite similar to that found for H2Ax gamma foci formation under similar DNA damage conditions (Chapter 2, figure). Collectively the western and the immunofluorescence data suggest that PC4 acetylation at K80 site is responsive to DNA damage condition. Considering the role of PC4 in DNA damage repair the acetylation might be critical for its repair activity.

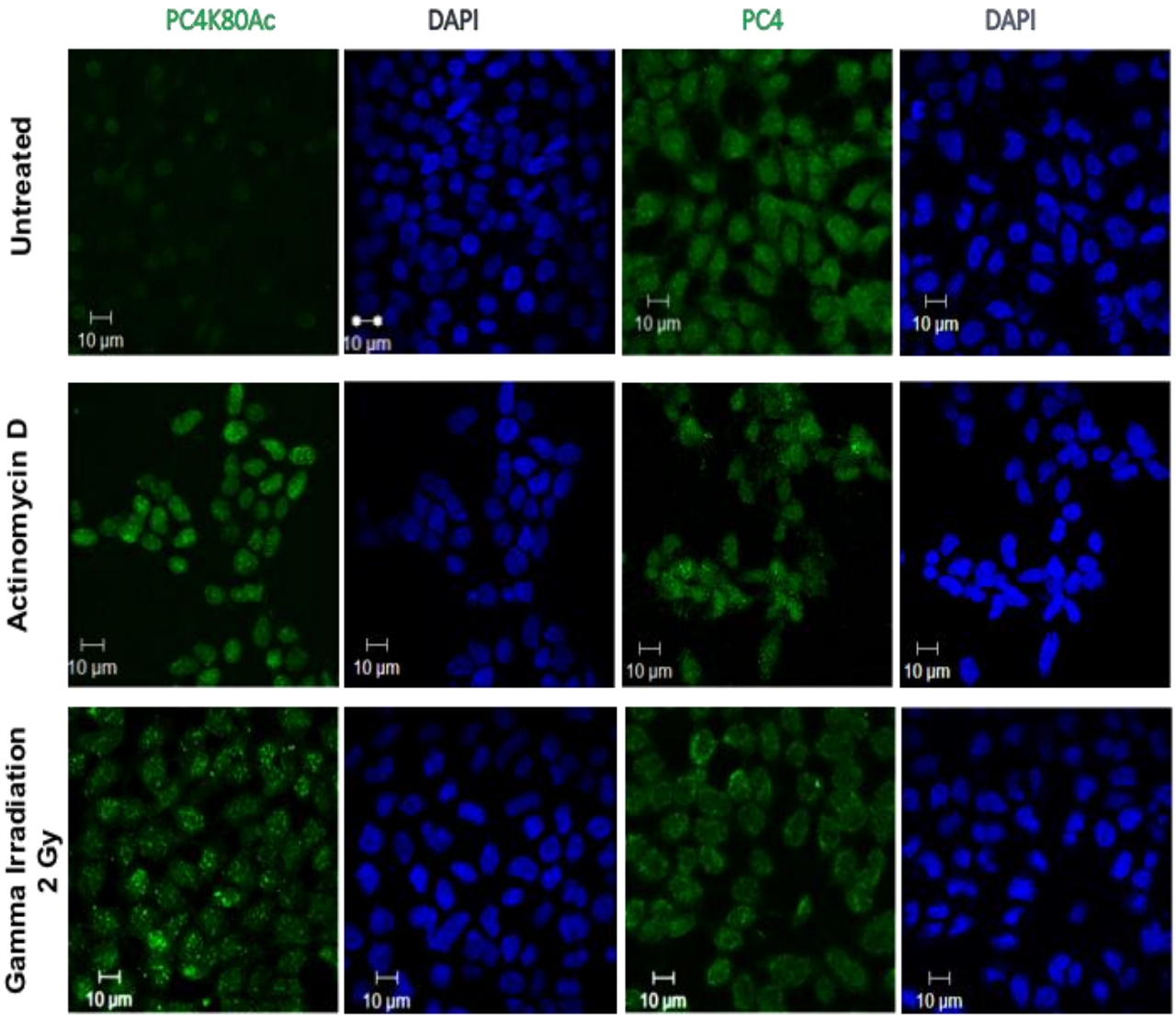

Figure 5.4.2 Immunofluorescence with K80 Ac specific antibody of PC4 under conditions of DNA damage. HEK293 cells were treated 10nM Actinomycin D for 12hours or irradiated with a dose of 2Grey units of gamma irradiation. Cells were stained after the aforementioned time point for Actinomycin D treatment and 6hours after Gamma irradiation. Staining with K80Ac PC4 antibody represented in the leftmost panel was used to detect the acetylation levels, while PC4 antibody was used to detect the unacetylated form as well.

5.5. Cellular function of Tip60 acetylated PC4

After establishing the cellular condition upon which PC4 gets acetylated at K80 site through the acetyltransferase Tip60 we wanted to investigate the functional consequence of this specific acetylation *in vivo*. Mammalian Flag tagged expression constructs of both the wild type and the acetylation defective mutant were created (described in Chapter 2). To check the expression and also their cellular localization, immunofluorescence studies were carried out. Flag constructs of both wild type and mutant PC4 were transfected in PC4 knockdown cells, to determine its *in vivo* localization. Mutation at K80 site to arginine did not perturb its cellular localization as both wild type and mutant protein showed similar nuclear localization (Figure 5.5.1).

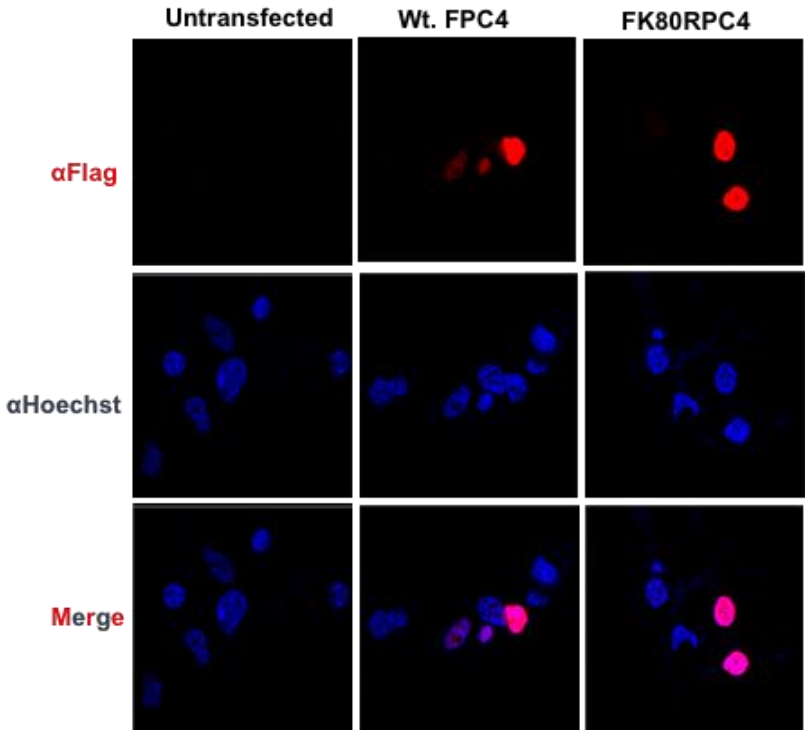

Figure 5.5.1: Cellular localization of acetylation defective mutant of PC4. Flag constructs of Wild type PC4 as well as acetylation defective mutant PC4 K80R was transfected in PC4sh8 KD cells and immunofluorescence was done with anti-flag antibody to check for its cellular localization. Hoechst was used for nuclear staining.

After confirming the expression pattern and determining the localization of both wild type and acetylation defective mutant of PC4, we wanted to elucidate the functional property of this acetylation of PC4. For this we resorted to a system where PC4 was already found to be absent so that exogenous expression of the flag constructs could help us monitor the functionality of both the wild type as well as the acetylation defective mutant. ZR-75-1 a breast cancer cell line which harbored low levels of PC4 as shown in Chapter 4 was used, particularly due to its oncogenic property and being a genomic instable system. Upon expression of the flag constructs, we first looked into the acetylation status, and in lieu to our previous observation we found that, wild type FPC4 showed acetylation at K80 site but the acetylation defective mutant failed to harbor any acetylation (Figure 5.5.2 lane 2 vs 3). This validated further the specificity of the acetylation specific antibody of PC4. PC4 western botting showed low levels in the vector backbone transfected lane versus the PC4 transfected lanes, both the Flag constructs were shown to express similarly.

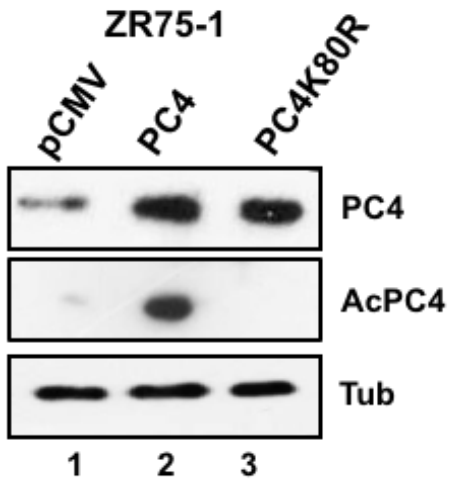

Figure 5.5.2. Determination of specificity of K80Ac PC4 antibody. Western blotting to detect acetylation levels at K80 site after transfection with flag constructs of Wild type PC4 as well as acetylation defective mutant PC4 K80R in ZR-75-1 cells. Tubulin is used as a loading control. PC4 and K80Ac PC4 antibodies were used to probe for the levels of PC4 and Tip60 acetylated PC4 respectively.

5.6. Regulation of Autophagy by Tip60 mediated acetylation of PC4

To establish the physiological consequence of Tip60 acetylated PC4 in the aspect of autophagy, we looked into the autophagy flux in ZR-75-1 cells upon transfection of wild type and acetylation mutant FPC4 constructs. ZR-75-1 which harbour high levels of autophagy, where shown to have reduced levels of LC3II when wild type PC4 was expressed (Figure 5.6. lane 1 vs 2). This was in coherence to the data we had previously observed in the rescue experiment in HEK293 PC4 knockdown cells. Thus PC4 acts as a negative regulator of autophagy even in Breast cancer cells. It was intriguing to observe that in presence of the acetylation mutant, the autophagy repression was relieved, which is signified by the higher LC3II levels (Figure 5.6 lane 2 vs 3). This signifies the importance of the Tip60 acetylation of PC4 in regulation of autophagy.

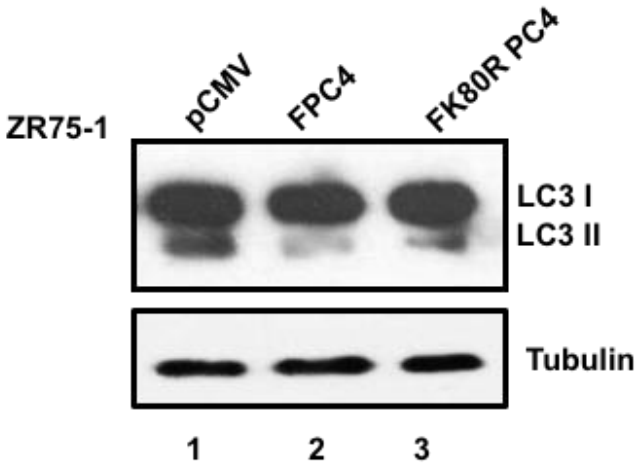

Figure 5.6. Role of acetylated PC4 in regulation of autophagy. Western blotting to detect autophagy levels after transfection with flag constructs of Wild type PC4 as well as acetylation defective mutant PC4 K80R in ZR75-1 cells. Tubulin is used as a loading control. Anti LC3B antibody was used to detect autophagy levels.

5.7. Function of Tip60 Acetylated PC4 in DNA damage

Considering the immense role of PC4 in DNA damage repair and also the appearance of the Tip60 acetylated PC4 under DNA damage conditions, we hypothesized whether the Tip60 mediated acetylation is playing a role in the DNA damage repair context. To assay the DNA damage repair we first looked into the phosphorylation status of H2Ax , a well-known marker for DNA damage. Following DNA double strand breaks, H2Ax gets phosphorylated which participates to form the DNA repair foci at the sites of DNA damage. ZR75-1, a Breast Cancer cell line with high levels of genome instability and endogenous gamma H2Ax, was transfected with wild type PC4 and acetylation defective mutant K80R. Upon FPC4 transfection, the phosphorylated γ-H2Ax levels decreased significantly (Figure 5.7.A lane 1 vs 2) while the acetylation defective mutant failed to decrease the phosphorylation of H2Ax (Figure 5.7.A lane 2 vs 3). This decrease in the phosphorylation level of H2Ax upon PC4 transfection in the ZR-75-1 cells could be attributed either to the DNA damage foci repair or due to the defective ATM signaling/repair pathways.

To further assay the consequence of Tip60 mediated acetylation of PC4, in DNA repair; we performed a comet assay using the same conditions of transfection in ZR75-1 cells. In a comet assay, the appearance of the nucleoid DNA structures from the DNA embedded in the agarose visualized by fluorescent dye gives an estimate of the extent of DNA damage in the cells. The intensity of the comet tail relative to the head suggests the number of DNA breaks. The likely explanation for this is that loops containing a break lose their supercoiling and become free to extend toward the anode. Thus estimation of the comet tail is a direct readout of the damaged DNA. ZR-75-1 cells as known, shows nucleoids with densely stained tail (Figure 5.7. B left hand panel vs middle panel), which completely abolishes once transfected with FPC4. Fascinatingly, such tailed nucleoid structure reappeared when transfected with a flag construct of PC4 which failed to undergo acetylation FK80R (right hand panel). This observation reinforces the fact that PC4 plays a possible role in DNA repair activity for which its acetylation by Tip60 at K80 site is crucial.

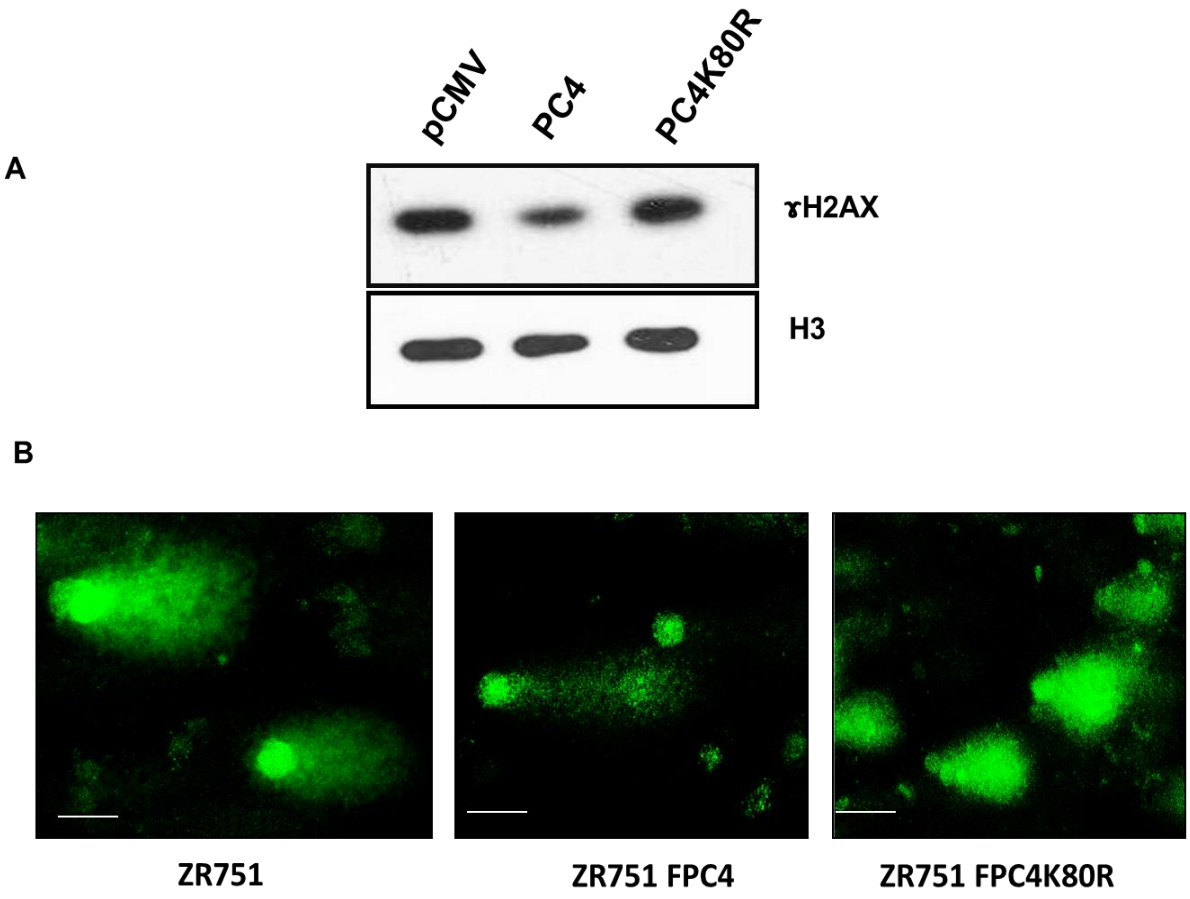

Figure 5.7. Acetylation of PC4 by Tip60 is critical for DNA repair activity: (A) Western blotting to detect γ-H2Ax levels after transfection with flag constructs of Wild type PC4 as well as acetylation defective mutant PC4 K80R in ZR-75-1 cells. H3 is used as the loading control. Cell lysates transfected with the Flag constructs were harvested after 48 hours of transfection and then used for immunoblotting. (C) Comet assay to detect nucleoids with head and tails. Representative image of the fields from comet assay obtained from DNA extracted from ZR75-1 cells, ZR75-1 cells transfected with FPC4 and FK80R. Comet assay was performed after 48 hours of transfection of wild type and acetylation defective mutant of PC4.

Summary:

The results from this chapter are summarized as follows:

- PC4 gets acetylated *in vitro* by KAT5, Tip60.
- Mass spectrometric analysis of KAT5 (Tip60) acetylated PC4 reveals 4 high scoring confident acetylation sites.
- Further *in vitro* gel assay with the PC4 lysine mutants specific for each site revealed that K80 might be a specific site of acetylation in PC4 by Tip60.
- A peptide based generation of polyclonal PC4 K80Ac antibody was done.
- Acetylation specific K80 antibody recognises wild type PC4 but not mutant K80R in vivo, signifying its sensitivity and selectivity for PC4 acetylated by Tip60
- Immunofluorescence data reveals the nuclear localization of acetylated PC4
- PC4 gets acetylated at K80 site in vivo upon DNA damage conditions.
- Complementation of PC4 depleted cell line with wildtype and acetylation defective mutant reveals the critical role of this acetylation in the context of autophagy and DNA damage repair
- Correlating with our previous observation, wild type PC4 could repress autophagy whereas the acetylation defective mutant failed to show similar inhibition to the process of autophagy.
- γ-H2Ax levels significantly reduced upon restoration of PC4 expression in a highly genetically unstable PC4 depleted cell line, ZR-75-1. This signifies the potential role of PC4 in DNA repair activity in an acetylation dependent manner.

Discussion:

KAT5/Tip60, an acetyltransferase, of the MYST family acetylates tumor suppressor p53, ATM kinase DNA repair enzyme and androgen receptor transcription factor other than histones. Due to its role in DNA repair and apoptosis Tip60 is reported to act as a tumor suppressor especially in Breast Cancer. Tip60 acts as a haplo-insufficient tumor suppressor whose expression decreases during breast cancer development and progression (Bassi et al., 2016). It has been also reported to stimulate the expression of tumor suppressor KAI. As has been reported earlier, PC4 also might have a tumor suppressive role whose expression decreases in Breast Cancer. Thus it was then looked whether PC4 might be a substrate for Tip60. From a previous study (Kumari S, et.al, Kundu TK unpublished), it has been shown that p300 might not be the only KAT acetylating PC4, as the KAT domains of Tip60 and MOZ acetyltransferases also acetylates it *in vitro*. In this study this phenomenon of acetylation of PC4 by Tip60 is investigated in further details. We observe that PC4 gets acetylated at a specific site by the acetyltransferase activity of KAT5 both *in vitro* and *in vivo*. As described in Chapter 1, KAT5 is a major enzyme that takes part in DNA repair pathway through acetylation of different substrates that mediate the repair of double strand breaks. The role of PC4 in DNA repair, especially that in case of double strand breaks is rather universal in terms of mediating DNA repair buy both the pathways namely NHEJ and HR. These contextual connections between Tip60 and PC4 prompted us to investigate the role of this acetylation upon DNA damage conditions. Indeed validating our hypothesis we find that PC4 alters the phosphorylation status of γ-H2Ax. To assign any functional property to the acetylated form of PC4, we took the mutant protein approach. PC4 acetylation defective mutant was complemented alongside the wild type protein in PC4 knockdown cell line which showed the property of genomic instability (ZR-75-1). Reduction of γ-H2Ax levels coupled with the DNA repair experiment (comet assay) revealed that PC4 might be mediating the DNA repair activity possibly through this critical acetylation site. PC4 has also been reported to get recruited very early at the DNA damage site. Thus it might modulate the chromatin structure at the DNA damage site, considering its role as chromatin protein, or might help in the recruitment of other DNA binding proteins which regulate the DNA repair

pathway. These molecular mechanisms in the context of its acetylation by KAT5 need to be further investigated. However these observations conclusively prove that PC4 might play a critical role in double strand break repair.

Macro autophagy is another regulatory pathway which mitigates the needs of the cell under DNA damage conditions by maintaining cellular homeostasis through the degradation of damaged organelles and cellular toxic agents. However interestingly, studies in this field have demonstrated the turnover of nuclear components such as nuclear lamina, chromatin, and DNA by autophagy thus signifying its importance in maintenance of genome stability (Vessoni et al., 2013). Loss or inhibition of autophagy resulted in decrease DNA repair activity thus accumulating cellular toxic agents leading to apoptosis. Autophagy is known to play a cytoprotective role under conditions of DNA damage, by regulating the dNTP pool levels, which are essential for DNA replication and repair. There have also been evidences that epigenetic modifications and thereby the chromatin state plays a critical role in altering the expression of key regulators of autophagy. Chromatin modulators like acetyltransferase, KAT5/TIP60 can be activated by GSK3 (glycogen synthase kinase-3) (Esa and Tor, 2012), which in turn directly acetylates ULK1 and induces autophagy. Thus there exists an underlying crosstalk of these two cellular events. PC4 being a key player in both these events, we investigated the role of KAT5 acetylated PC4 in regulation of autophagy. Earlier observation from this study showed that PC4 acts as a negative regulator of autophagy however this inhibition is alleviated in absence of K80 Acetylation of PC4 as evidenced by the LC3II levels. This opens up an intriguing arena in terms of regulation of autophagy by PC4. The acetylated form of PC4 on none hand facilitates DNA repair activity, but on the other might assist in the downregulation of autophagy. This might be a potential mechanism by which cells decide which pathway to act in upon DNA damage conditions. The molecular mechanisms and further deciphering of the role of KAT5 acetylated PC4 upon DNA damage response is thus of immense biological importance.

Chapter 6: Discussion

This chapter reviews the major outcomes of the present study. The results of the thesis are assessed in the perspective of the background study and the existing literature, accentuating on the highlights and its plausible outcomes.

6.1. Understanding the role of non-histone protein PC4 in nuclear architecture, chromatin organization, cellular segregation and maintenance of the epigenetic landscape of the cell

The ordered chromatin structure is maintained through the concerted activity of histones along with non-histone proteins, the DNA sequence and the non-coding RNA. Human positive coactivator 4 is an intrinsic component of the chromatin known to directly interact with the globular domains of histones H3 and H2B and inducing chromatin compaction (Das et al., 2006) leading to heterochromatinization of the genome (Das et al., 2010). Here in the present study we make an attempt to understand the physiological state of the cell in the absence of chromatin protein PC4. Knocking down PC4 in HEK293 cells resulted in a transcriptionally active chromatin conformation with an altered expression of histone acetylation marks (Figure 3.3.2). This observation reinforces the fact that PC4 acts as a global inducer of heterochromatinization absence of which leads to an open chromatin configuration (Figure 3.3.1) which allows the histones accessible to undergo post translational modifications, mostly acetylation which helps to maintain the active state of the chromatin (Figure 3.3.2). As evidenced from the structural features, the chromosomes from PC4 knockdown cells it appears to have an altered shape visually fluffy (Figure 3.2.1) owing to the decondensed chromatin state. Studies of histone H1 depletion reveals existence of elongated chromosomes and segregation defects (Maresca et al., 2005) possibly due to the global decompaction of the chromatin (Izzo and Schneider, 2016). As histone H1 is essential for maintaining the higher order organization of the chromatin, PC4 also appears to be one of the most important chromosomal architectural proteins through this present study. As is evidenced by the chromosomal FISH analysis, PC4 depletion results in irregular segregation

of nuclei and chromosomes (Figure 3.2.3). The defect in the segregation process resulted in the formation of anaphase bridge (Figure 3.2.2). Anaphase bridges are the common indicators of chromosomal instability. During the process of chromosomal segregation chromosomes are pulled simultaneously to the opposite poles of the microtubule spindle. Anaphase bridges mostly result from fusion of broken chromosome ends resulting in the formation of dicentric chromosomes which attach to both the spindle poles. These bridges were observed to break under stress from the mitotic apparatus and re-form in the next interphase, giving rise to breakage–fusion–bridge cycles (Hoffelder et al., 2004). Anaphase bridges can also be caused by abnormal shortening of the telomeres (de Lange 2002; Hande et al. 1999) or by persistent chromatid cohesion (Coelho et al. 2003; Haering and Nasmyth 2003). Thus depletion of PC4 also resulted in a genomically unstable condition in addition to the alteration of the chromatin architecture. It was also intriguing to observe the appearance of irregular shaped nuclei in the HEK293 PC4 knockdown cells (Figure 3.1) certifying its significant role also in preservation of the ordered nuclear architecture. Thus PC4 acts as a chromosomal architectural protein in maintaining the higher order organization of the chromatin, the epigenetic language, faithful cell segregation pattern and an organized nuclear shape.

6.2. Regulation of cellular survivability by chromatin protein PC4

To elucidate the physiological properties of a cell upon PC4 knockdown, we analyzed the cellular proliferation rate to understand the growth pattern of PC4 depleted cells. Despite harboring several cellular anomalies PC4 knockdown cells exhibited higher proliferation rate (Figure 3.4.1) and interestingly survived cellular stressful conditions like gamma irradiation (Figure 3.4.2). This was contrary to the previous observation (Li, 2010) which showed that knockout of PC4 expression in mouse embryonic stem cells led to lethality. However our study was based on a knockdown approach, and here the cellular scenario has been investigated not at the organismal level. Chromatin state plays an important and critical role in determining cellular fate and thereby its proliferation rate (Ma et al., 2015). Several chromatin remodelers alter the chromatin landscape mediating a change in the gene

expression pattern which in turn might regulate cellular proliferation and senescence (Garcia and Pereira-Smith, 2008). PC4 depletion alters the chromatin landscape drastically which also in turn alters the gene expression pattern of the cells. This subset of genes expressed in the absence of PC4 thus might be responsible for the enhanced proliferation pattern. However this phenomenon of enhanced proliferation and gamma irradiation resistance also reflects the properties of a transformed cell, which gains the oncogenic properties in order to survive under the conditions of stress with a milieu of differential gene expression. The significance of this observation is discussed in the forthcoming sections of this chapter.

6.3. PC4 as a regulator of autophagy

To delineate the molecular mechanism of higher proliferative rate of PC4 depleted cells we here establish the role of PC4 as a novel regulator of the well conserved cellular process of self-eating, called autophagy. Autophagy levels were found to be highly elevated in absence of PC4 (Figure 3.5.1). Electron micrographs of PC4 knockdown cells showed presence of various double membraned autophagy like vacuoles (Figure 3.5.3). Most of these vacuoles were found in close proximity to the irregularly shaped nucleus in PC4 knockdown cells. It was also interesting that PC4 depleted cells showed appearance of multivesicular bodies (large number of vacuoles engulfed in one vesicle). Appearance of multivesicular bodies has been reported in a particular type of autophagy process (Mizushima et al., 2008). Autophagy is a degradative pathway which plays an important role in maintaining protein homeostasis (proteostasis) as well as helps in the preservation of proper organelle function by selective removal of damaged organelles (Murrow and Debnath, 2013). The protective role of autophagy in maintaining cellular survival is mediated by the selective removal of dysfunctional mitochondria or other damaged organelles, which release pro-apoptotic factors and generate oxygen species. During autophagy, portions of cytosol are sequestered inside double-membraned vesicles (autophagosomes) that then fuse either with endocytic vesicles (as Multivesicular bodies) or lysosomes, which provide the hydrolytic enzymes that will degrade the content (Alerting, 2007). The appearance of these multivesicular bodies and other double membraned vesicles especially near the nucleus in PC4 depleted cells thus

might be possibly an indication of a cellular cue which might be operating via the altered nuclear architecture to a cytosolic process like autophagy. The enhanced autophagy levels in the PC4 knockdown cells play a critical role in its survivability possibly by maintaining cellular homeostasis in an otherwise physiological chaotic state. When the autophagy levels were depleted by administration of small molecule inhibitors or by knockdown of an essential autophagy gene ULK1, it highly compromised the survival rate of PC4 knockdown cells and upon gamma irradiation (Figure 3.6.2, 3.6.3, 3.8.3). This establishes the significant role of autophagy in attributing the property of enhanced growth rate to PC4 knockdown cells. Furthermore this study establishes a link of epigenetic regulation of autophagy genes which is mediated through the downregulation of PC4. Growing evidences in the field reflects the importance of specific epigenetic modifications in inducing autophagy. However the molecular mechanism still remains to be an enigma. This study connects directly the alteration of the nuclear architecture, change in the chromatin landscape and upregulation of a transcriptional active histone acetylation mark (H3K9Ac) at the promoters of the autophagy related genes, through the loss of an important non histone chromosome associated protein PC4.

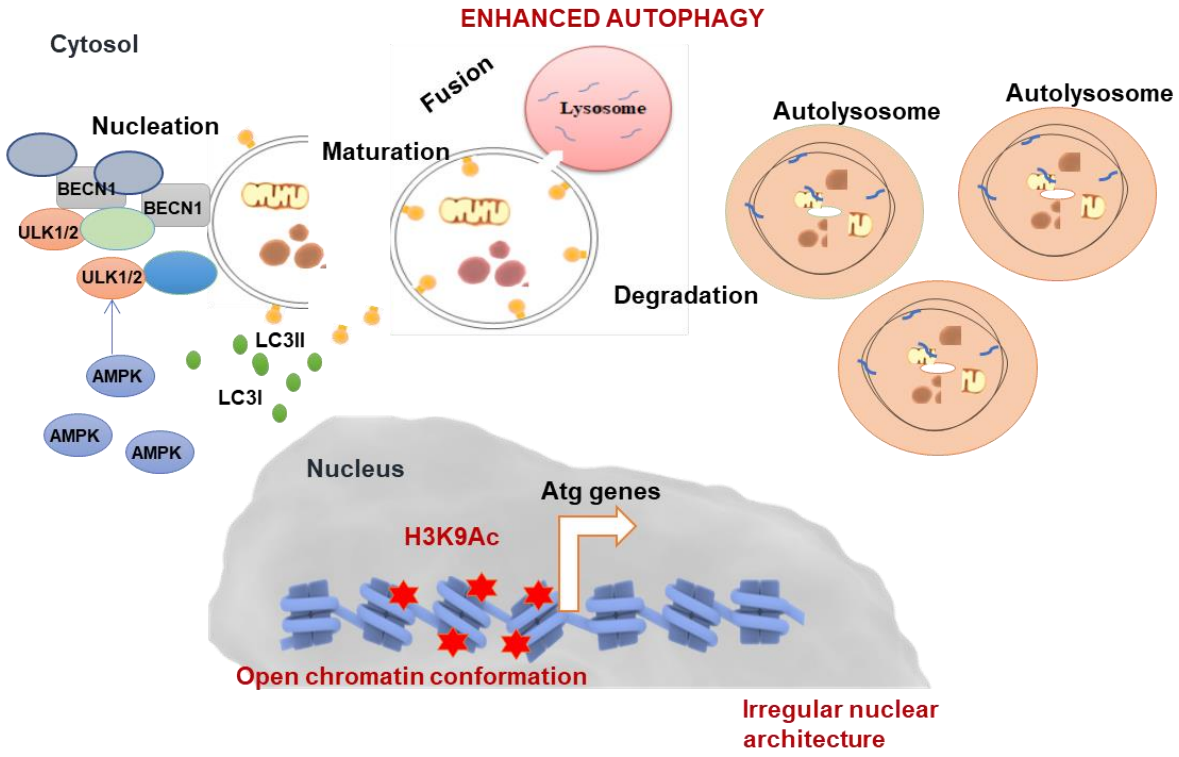

Figure 6.1. Model depicting the characteristics of PC4 HEK293 knockdown cells. PC4 knockdown cells exhibit an open chromatin structure (high H3K9Ac mark) and irregular nuclear shape. Besides the defects in the nucleus, the cytosol exhibit enhanced autophagy process.

6.4. Role of PC4 in Breast cancer

The cell based studies, HEK293 PC4 knock down cells, clearly points out the critical role of PC4 in maintaining genome stability and cellular homeostasis. Perturbation of PC4 expression resulted in a gross changes in the cellular physiology, like disrupted nuclear architecture, altered epigenetic language and cell segregation defects. Coupled to all these, we also find an upregulation of the autophagy process which is responsible for the survival

advantage and higher proliferative rate of PC4 knockdown cells. This study further enlightens the consequence of PC4 knockdown in Breast Cancer disease. PC4 was found to be downregulated in Breast Cancer patient samples both at transcript and protein level (Figure 4.1.2,4.1.3). This downregulation did not correlate with stage, age or any molecular classification of Breast Cancer. Contrary to the expression pattern of other non-histone proteins like PARP1 and HP1alpha (Green et al., 2015; Lee and Ann, 2015) PC4 showed downregulation in large number of patient samples analyzed. Upon analyzing the expression pattern among a panel of Breast Cancer patient derived cell lines, PC4 was found to be downregulated in the higher invasive cell lines (Figure 4.1.1). ShRNA mediated silencing of PC4 in Breast cancer MCF7 cell line increases its migratory as well as invasive properties (Figure 4.5), clear indicating the tumor suppressive property which PC4 harbors which is alleviated by its depletion possibly due to the formation of an unstable genome.

6.4. Regulation of PC4 by miR29 class of miRNAs: Implications in Breast cancer

To understand the molecular mechanism attributing to its downregulation in Breast cancer patient samples and cell lines, we resorted to analyze the 3'UTR region of PC4 to find any miRNA mediated regulation of the PC4 gene. Earlier studies have shown that PC4 is a p53 responsive gene and gets upregulated in a p53 dependent manner. A recent study revealed that PC4 3'UTR region can bind to miR101, thereby getting downregulated. This study further shows the association of this miRNA in the context of prostate cancer (Chakravarthi et al., 2016). However in our bioinformatics prediction, this miRNA did not appear in the high scoring miRNA targets, and also this miRNA was reported to be downregulated in Breast cancer patient samples (Guan et al., 2016). The PC4 3'UTR is 3kb long and contain multiple miRNA binding sites, which might regulate PC4 in a cell type and cancer specific manner. In this study we first report the regulation of PC4 expression by miR29 family, (miR 29a, 29b, 29c). Overexpression of miR29 led to the concomitant downregulation of PC4 both at transcript and protein level (Figure 4.2). Furthermore the importance of this downregulation is related to breast cancer cell lines and patient samples. There exists a distinct negative correlation of miRNA expression and PC4 expression in a number of Breast

cancer patient samples and also in the cell lines where PC4 was found to be downregulated (Figure 4.3). Upon overexpression of miR29a in breast cancer cells, MCF7 in addition to the downregulation of PC4 expression, it also induces the migratory properties of the cells (data not shown). This reinforces the earlier observation of PC4 knockdown inducing oncogenic properties to the cell. This study reflects the cause of the downregulation of this essential protein in Breast Cancer.

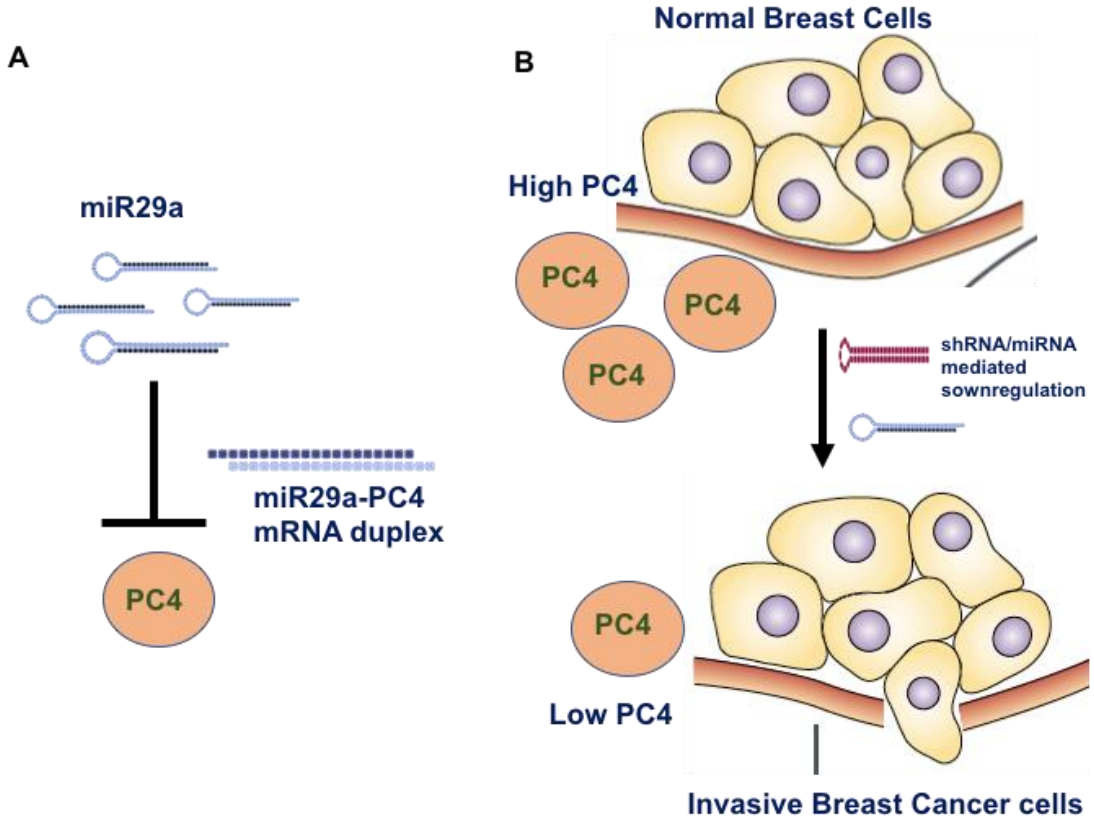

Figure 6.2. Regulation and role of PC4 expression in Breast cancer. (A) miR29a regulates PC4 expression by directly binding to its 3'UTR sequence thereby downregulating its expression. (B) Downregulation of PC4 in Breast cancer either by miRNA or its targeted shRNA enhances the invasiveness of Breast Cancer cells.

6.5. PC4 downregulation resulted in radiation resistance in Breast cancer cells which can be alleviated through the use of autophagy inhibitors

As observed in the HEK293 PC4 knockdown cells, downregulation of PC4 induced autophagy in breast cancer cells. Furthermore characterization of ZR751, breast cancer cells which harbored low levels of endogenous PC4 showed higher invasive property and enhanced autophagy levels as is evidenced by higher LC3II levels (Figure 4.6.1). In lieu to the previous observation in HEK293 sh-PC4 cells this Breast cancer cell line also showed gamma irradiation resistance which was abrogated in the presence of an autophagy inhibitor, Bafilomycin (Figure 4.6.2). Thus autophagy and the phenomenon of gamma irradiation resistance in absence of PC4 hold to be true in context of Breast Cancer also. Growing evidences in the field do attribute the property of enhanced autophagy to gamma irradiation resistance in various cancers (Green and Levine, 2014; Hu et al., 2016; Huang et al., 2017). However this is one of the first studies which connect the expression of a chromosomal protein to breast cancer, autophagy and gamma irradiation resistance.

6.6. KAT5 dependent acetylation of PC4 in Genome stability

PC4 besides being a chromatin condenser plays a crucial role in mediating genome stability by directly participating in the DNA repair pathway. In this study we elucidate the potential role of KAT5 acetylated PC4 in the process of autophagy as well as DNA repair. PC4 gets acetylated by KAT5/Tip60 both *in vitro* and *in vivo* at K80 residue (Figure 5.1). *In vivo* acetylation of PC4 at K80 is induced by DNA damage conditions. Acetylation of PC4 is crucial for the gamma-H2AX dynamics which plays a crucial role in sensing the DNA damage of cells as well as acts as a signalling component in the DNA repair pathway (Ikura et al., 2007). It was also intriguing to observe that KAT5 mediated acetylation of PC4 plays a significant role in the repression of autophagy. This raises greater questions on the biological significance of this acetylation as a mediator between two crucial cellular pathway responsible for maintaining genomic integrity and cellular homeostasis.

Multifunctional human chromatin protein PC4 is an integral part of the chromatin structure and plays vital roles in various DNA templated phenomenon signifying its importance in

cellular survivability and homeostasis. The role of PC4 in transcriptional coactivation has been elucidated extensively, which signifies its direct interaction with basal transcription factors as well as various activator proteins. Thus PC4 can modulate gene expression through the transcriptional machinery, including both RNA polymerase as well as RNA polymerase III. Although discovered as a transcriptional coactivator, we now understand that a significant fraction of the protein is tethered to the chromatin, thus mediating its condensation. Knockdown of PC4 alters the global chromatin landscape thus expressing genes which was otherwise silent/ dormant. Thus the alteration of gene expression by PC4 might be as a result of two distinct functions of PC4. In this study we make an attempt to understand the major physiological role of PC4 by knocking down in cell line. Quite contrary to the organismal level, PC4 knockdown facilitated cellular proliferation and gamma irradiation resistance property. To understand the molecular basis of this phenomenon we find PC4 negatively regulates autophagy. Thus the chaotic cellular environment created upon PC4 knockdown is controlled by the flux of autophagy genes. This phenomenon of enhanced autophagy confers radiation resistance and survival advantage to PC4 knockdown cells. The phenomenon of enhanced autophagy in absence of PC4 holds also true for Breast cancer where autophagy might be used to survive under stressful conditions. The PC4 knockdown study also elucidates the role of PC4 in maintaining the nuclear architecture and the cell segregation process. Several non-histone proteins like SMC, Cohesins, (described in Chapter 1) plays similar role in the cell division pathway. Elucidation of the phenotype of PC4 knockdown cells signifies that the major fraction of PC4 in the cell might be present associated with the chromatin bringing about its ordered organization inside the nucleus of the cell and thereby playing a critical role in genome stability and cellular survivability.

Chapter 7: Significance and Future Perspective of the study

Here the overall summary of the study is presented in the light of future studies to be conducted

To the best of our knowledge, this study provides the first evidence of association of any non-histone chromatin associated protein involved in the regulation of autophagy. The present finding opens up a new paradigm of autophagy regulation through chromatin associated protein. Even though the exact molecular mechanism of the enhancement of autophagy in absence of PC4 still remains to be deciphered, it is evidently clear that the altered genome organization and the epigenetic landscape profoundly affect the expression of genes responsible for autophagy induction. The pathway of the Autophagy induction by inhibition of PC4 might be through the ATP sensor kinase AMPK, but this needs further experimental demonstrations. It is also important to elucidate the function of PC4 in selective pathways of autophagy like nucelophagy etc. as this study is limited to macroautophagy.

The survival advantage due to enhanced autophagy in PC4 knockdown cells accentuates with its role in Breast cancer manifestation. Our serendipitous finding that almost 65% of breast cancer patient sample screen, there is a substantial downregulation of PC4 initiates a new axis of radiation resistance. Breast cancer incidence in which presumably the PC4 and autophagy are on the line with Breast cancer progression. This finding holds tremendous potential of implementing the concept of the regulation of autophagy in Breast Cancer therapeutics. Out of 13 different Breast Cancer cell line tested more than 1/3 rd cell line showed the dramatic downregulation of PC4 expression. Remarkably some of the cell lines were found to be radiation resistance but become sensitized after treatment with autophagy inhibitors. This observation opens up a realistic potential of our finding to take to the next level of understanding of chromatin function and its application in diagnostics and therapeutics of Breast Cancer.

In this study we also find a potential miRNA, miR29 which modulates the expression of PC4, also in the Breast cancer cells and tumour samples. However upon screening large

number of Breast Cancer tumour samples we do find heterogeneity in the expression of miRNAs, resulting in a non-perfect negative correlation between the expression of PC4 and miRNA. This is of immense biological significance as this might suggest that there might be other factors responsible for the downregulation of PC4 expression. Analysis of the genomic region of PC4 gene reveals the presence of strong stretches of CpG nucleotides which are prone to undergo extensive methylation. Our initial data suggests that abberant expression of DNA methyltransferases particularly in certain Breast Cancer patient samples where miR29 is not expressed might be an another additional epigenetic regulator of PC4 expression.

One of the acetyltransferase known to be critically involved in the DNA repair phenomenon, KAT5/Tip60 acetylates PC4 specifically at a distinct site. This acetylation of PC4 by Tip60 plays a very important role in the DNA repair phenomenon as well as the regulation of autophagy. It is thus critical to examine the molecular pathway by which the two critical pathways is regulated in conjunction with the acetylation of PC4.

Appendix I: Breast Cancer Patient Samples Details

Patient ID	Receptor status	Stage (TNM)	Tumor type
30040	ER +, PgR +, Her2/neu -	T2N0M0	IDC
52690	NA	T4N0M0	ILC
54890	TPN	pT2N0M0	IDC
55795	ER +, PgR +, Her2/neu -	T1N0M0	IDC
56110	ER +, PgR +, Her2/neu -	pT2N0M0	DCIS NOS type
56325	ER +, PgR -, Her2/neu -	T4N1M1	IDC
56919	ER +, PgR +, Her2/neu -	NA	NA
57864	ER +, PgR +, Her2/neu -	T2N0M0	IDC
58299	ER +, PgR +, Her2/neu -	T2N1	IDC
58336	ER +, PgR -, Her2/neu +	pT4bN3aMx	IDC, NOS type, NBR Score 8
58392	ER +, PgR +, Her2/neu -	T2N1	IDC
64171	ER +, PgR -, Her2/neu -	pT3N0	IDC
64405	ER +, PgR +, Her2/neu -	T2N3a	IDC
64570	ER +, PgR +, Her-2/neu -	T2N0M0	IDC
64813	ER -, PgR +, Her2/neu -	T2N1	IDC
64864	ER +, PgR +, Her-2/neu -	T4bN3a	IDC
66269	NA	pT2Nx	IDC, NOS type
66413	ER +, PgR +, Her-2/neu -	T2N1M0	IDC, DCIS
67709	ER +, PgR +, Her-2/neu +	T4N1M0	IDC, NOS type
68132	ER -, PgR -, Her2/neu +	pT2N1a	IDC
68424	ER +, PgR +, Her-2/neu -	T2N2M0	IDC
69541	ER +, PgR +, Her-2/neu -	T2N1M0	IDC
71402	ER +, PgR +, Her-2/neu -	T3N1M0	IDC, Mixed Ductal, NOS type
72946	ER +, PgR +, Her2/neu -	T2N2a	IDC
73002	TPN	T2N0	IDC

Appendix II: List of Abbreviations and Acronyms

3-MA	3 Methyl adenine
5-FU	5 Fluorouracil
AMPKα1	5'AMP-activated protein kinase catalytic subunit alpha-1
AMPKα2	5'AMP-activated protein kinase catalytic subunit alpha- 2
ATF4	Activating transcription factor 4 a
Baf	Bafilomycin A1
BCL2	Apoptosis regulator Bcl-2
BECN1	Beclin1
DCIS	ductal carcinoma in situ
DRAM1	DNA Damage Regulated Autophagy Modulator 1
EMT	Epithelial to mesenchymal transition
ER	Endoplasmic reticulum
FISH	Fluorescence in situ hybridization
GABARAPL1	Gamma-aminobutyric acid receptor-associated protein-like 1
GABARAPL2	Gamma-aminobutyric acid receptor-associated protein-like 2
HMG	High mobility group
HP1	Heterochromatin protein 1
IDC	invasive ductal carcinoma
IgG	Immunoglobulin G
IHC	Immunohistochemistry

IL	Interleukin
ILS	infiltrating lobular carcinoma
IR	Ionizing Radiation
KAT	Lysine (K) Acetyltransferase
MAP1LC3A	Microtubule-associated protein 1A light chain 3A
MAP1LC3B/LC3	Microtubule-associated protein 1B light chain 3B
MCl1	Induced myeloid leukemia cell differentiation protein
miR	microRNA
MMP	Matrix Metalloproteinase
mTOR	mammalian target of rapamycin
NFκB	Nuclear factor κB
Ni-NTA	Nickel-Nitrilotriacetic Acid
pri-miRNA	primary miRNA
PTEN	Phosphatidylinositol 3,4,5-trisphosphate 3-phosphatase and dual-specificity protein phosphatase
ROS	Reactive Oxygen Species
shRNA	Short hairpin RNA
TCL1	T-cell leukemia 1
Tip60	Tat-interacting Protein 60
ULK1	Unc-51 Like Autophagy Activating Kinase 1
ULK2	Unc-51 Like Autophagy Activating Kinase 2
UVRAG	UV Radiation Resistance Associated gene
YY1	Ying Yang 1

Publications

Research Paper:

Sweta Sikder, Sujata Kumari, Nisha Ramdas, Pallabi Mustafi, Arka Saha, Swatishree Padhi, Birendranath Banerjee, Ravi Manjithaya, Tapas K. Kundu*(2018). Non-histone human chromatin protein, PC4 is critical for genomic integrity and negatively regulates autophagy. **Uploaded in Biorxiv doi: https://doi.org/10.1101/266932**

Sweta Sikder, Sujata Kumari, Manoj Kumar, Sandeep Singh, TS Sridhar, Mukul Godbole, Amit Dutt, Sreekumar Chellappan, KS Gopinath, Gautam Sethi, Tapas K Kundu* (2018) Chromatin protein PC4 is downregulated in Breast Cancer to promote disease progression: Implications of miR29a. **(Manuscript under communication)**

Priya Mondal , Suraiya Saleem , **Sweta Sikder** , Tapas K Kundu ,Subhas Chandra Biswas, Siddhartha Roy*.(2018) Transcriptional coactivator PC4 Is of Paramount Importance in p53-dependent Genotoxic Stress Response. **(Manuscript under review)**

Sweta Sikder, Tapas K Kundu. (2018) Tip60 mediated acetylation of PC4 plays critical role in DNA repair**. (Manuscript under preparation)**

Book chapter:

Kumari S, Das C, Sikder S, Kumar M, Bachu M, Ranga U, **Kundu TK**° (2015) Identification and characterization of nonhistone chromatin proteins: human positive coactivator 4 as a candidate. ***Chromatin Protocols, Methods in Molecular Biology (Humana Press)***; 1288:245-*72*

References

Agresti, A., and Bianchi, M.E. (2003). HMGB proteins and gene expression. Curr. Opin. Genet. Dev. *13*, 170–178.

Alers, S., Loffler, A.S., Wesselborg, S., and Stork, B. (2012). Role of AMPK-mTOR-Ulk1/2 in the Regulation of Autophagy: Cross Talk, Shortcuts, and Feedbacks. Mol. Cell. Biol. *32*, 2–11.

Alerting, E. (2007). Autophagy : process and function. 2861–2873.

Aranda, S., Mas, G., and Di Croce, L. (2015). Regulation of gene transcription by Polycomb proteins. Sci. Adv. *1*, 1–16.

Babu, D., and Fullwood, M.J. (2015). 3D genome organization in health and disease: Emerging opportunities in cancer translational medicine. Nucleus *6*, 382–393.

Baek, S.H., and Kim, K. Il (2017). Epigenetic Control of Autophagy: Nuclear Events Gain More Attention. Mol. Cell *65*, 781–785.

Banerjee, S., Kumar, B.R.P., Tapas, K., and Kundu, T.K. (2004). General Transcriptional Coactivator PC4 Activates p53 Function General Transcriptional Coactivator PC4 Activates p53 Function. Society *24*, 2052–2062.

Bannister, A.J., and Kouzarides, T. (2011). Regulation of chromatin by histone modifications. Cell Res. *21*, 381–395.

Bánréti, Á., Sass, M., and Graba, Y. (2013). The emerging role of acetylation in the regulation of autophagy. Autophagy *9*, 819–829.

Barski, A., Cuddapah, S., Cui, K., Roh, T.Y., Schones, D.E., Wang, Z., Wei, G., Chepelev, I., and Zhao, K. (2007). High-Resolution Profiling of Histone Methylations in the Human Genome. Cell *129*, 823–837.

Barth, S., Glick, D., and Macleod, K.F. (2010). Autophagy: Assays and artifacts. J. Pathol. *221*, 117–124.

Bártová, E., Krejčí, J., Harničarová, A., Galiová, G., and Kozubek, S. (2008). Histone

modifications and nuclear architecture: A review. J. Histochem. Cytochem. *56*, 711–721.

Bassi, C., Li, Y.T., Khu, K., Mateo, F., Baniasadi, P.S., Elia, A., Mason, J., Stambolic, V., Pujana, M.A., Mak, T.W., et al. (2016). The acetyltransferase Tip60 contributes to mammary tumorigenesis by modulating DNA repair. Cell Death Differ. *23*, 1198–1208.

Batta, K., and Kundu, T.K. (2007). Activation of p53 Function by Human Transcriptional Coactivator PC4: Role of Protein-Protein Interaction, DNA Bending, and Posttranslational Modifications. Mol. Cell. Biol. *27*, 7603–7614.

Batta, K., Yokokawa, M., Takeyasu, K., and Kundu, T.K. (2009). Human Transcriptional Coactivator PC4 Stimulates DNA End Joining and Activates DSB Repair Activity. J. Mol. Biol. *385*, 788–799.

Bhaumik, S.R., Smith, E., and Shilatifard, A. (2007). Covalent modifications of histones during development and disease pathogenesis. Nat. Struct. Mol. Biol. *14*, 1008–1016.

Block, T.M., Rawat, S., Brosgart, C.L., and Francisco, S. (2017). HHS Public Access. *76*, 69–81.

Bonev, B., and Cavalli, G. (2016). Organization and function of the 3D genome. Nat. Rev. Genet. *17*, 661–678.

Brandsen, J., Werten, S., van der Vliet, P.C., Meisterernst, M., Kroon, J., and Gros, P. (1997). C-terminal domain of transcription cofactor PC4 reveals dimeric ssDNA binding site. Nat. Struct. Biol. *4*, 900.

Brinkman, A.B., Roelofsen, T., Pennings, S.W.C., Martens, J.H.A., Jenuwein, T., and Stunnenberg, H.G. (2006). Histone modification patterns associated with the human X chromosome. EMBO Rep. *7*.

Bristol, M.L., Emery, S.M., Maycotte, P., Thorburn, A., Chakradeo, S., and Gewirtz, D.A. (2013). Autophagy Inhibition for Chemosensitization and Radiosensitization in Cancer: Do the Preclinical Data Support This Therapeutic Strategy? J. Pharmacol. Exp. Ther. *344*, 544–552.

Broustas, C.G., and Lieberman, H.B. (2014). DNA Damage Response Genes and the Development of Cancer Metastasis. Radiat. Res. *181*, 111–130.

Catalanotto, C., Cogoni, C., and Zardo, G. (2016). MicroRNA in control of gene expression: An overview of nuclear functions. Int. J. Mol. Sci. *17*.

Chakradeo, S., Sharma, K., Alhaddad, A., Bakhshwin, D., Le, N., Harada, H., Nakajima, W., Yeudall, W.A., Torti, S. V., Torti, F.M., et al. (2015). Yet Another Function of p53--The Switch That Determines Whether Radiation-Induced Autophagy Will Be Cytoprotective or Nonprotective: Implications for Autophagy Inhibition as a Therapeutic Strategy. Mol. Pharmacol. *87*, 803–814.

Chakravarthi, B.V.S.K., Goswami, M.T., Pathi, S.S., Robinson, A.D., Cieślik, M., Chandrashekar, D.S., Agarwal, S., Siddiqui, J., Daignault, S., Carskadon, S.L., et al. (2016). MicroRNA-101 regulated transcriptional modulator SUB1 plays a role in prostate cancer. Oncogene *35*, 6330–6340.

Chen, L., Du, C., Wang, L., Yang, C., Zhang, J.R., Li, N., Li, Y., Xie, X.D., and Gao, G.D. (2014). Human positive coactivator 4 (PC4) is involved in the progression and prognosis of astrocytoma. J. Neurol. Sci. *346*, 293–298.

Chen, Y., Li, X., Guo, L., Wu, X., He, C., Zhang, S., Xiao, Y., Yang, Y., and Hao, D. (2015). Combining radiation with autophagy inhibition enhances suppression of tumor growth and angiogenesis in esophageal cancer. Mol. Med. Rep. *12*, 1645–1652.

Choi, K.S. (2012). Autophagy and cancer. Exp. Mol. Med. *44*, 109–120.

Cicchini, M., Karantza, V., and Xia, B. (2015). Molecular pathways: Autophagy in cancer-A matter of timing and context. Clin. Cancer Res. *21*, 498–504.

Codogno, P., and Meijer, A.J. (2005). Autophagy and signaling: Their role in cell survival and cell death. Cell Death Differ. *12*, 1509–1518.

Das, C., Hizume, K., Batta, K., Kumar, B.R.P., Gadad, S.S., Ganguly, S., Lorain, S., Verreault, A., Sadhale, P.P., Takeyasu, K., et al. (2006). Transcriptional coactivator PC4, a chromatin-associated protein, induces chromatin condensation. Mol. Cell. Biol. *26*, 8303–8315.

Das, C., Gadad, S.S., and Kundu, T.K. (2010). Human Positive Coactivator 4 Controls Heterochromatinization and Silencing of Neural Gene Expression by Interacting with REST/NRSF and CoREST. J. Mol. Biol. *397*, 1–12.

Dhanasekaran, K., Kumari, S., Boopathi, R., Shima, H., Swaminathan, A., Bachu, M., Ranga, U., Igarashi, K., and Kundu, T.K. (2016). Multifunctional human transcriptional coactivator protein PC4 is a substrate of Aurora kinases and activates the Aurora enzymes. FEBS J. *283*, 968–985.

Dinant, C., and Luijsterburg, M.S. (2009). The Emerging Role of HP1 in the DNA Damage Response. Mol. Cell. Biol. *29*, 6335–6340.

Dou, Z., Xu, C., Donahue, G., Shimi, T., Pan, J.A., Zhu, J., Ivanov, A., Capell, B.C., Drake, A.M., Shah, P.P., et al. (2015). Autophagy mediates degradation of nuclear lamina. Nature *527*, 105–109.

Ea, V., Baudement, M.O., Lesne, A., and Forné, T. (2015). Contribution of topological domains and loop formation to 3D chromatin organization. Genes (Basel). *6*, 734–750.

Easwaran, H.P., and Baylin, S.B. (2010). Role of nuclear architecture in epigenetic alterations in cancer. Cold Spring Harb Symp Quant Biol *75*, 507–515.

Eberharter, A., and Becker, P.B. (2002). Histone acetylation: A switch between repressive and permissive chromatin. Second in review on chromatin dynamics. EMBO Rep. *3*, 224–229.

Ellis, L., Atadja, P.W., and Johnstone, R.W. (2009). Epigenetics in cancer: Targeting chromatin modifications. Mol. Cancer Ther. *8*, 1409–1420.

Erkina, T.Y., Zou, Y., Freeling, S., Vorobyev, V.I., and Erkine, A.M. (2009). Functional interplay between chromatin remodeling complexes RSC, SWI/SNF and ISWI in regulation of yeast heat shock genes. Nucleic Acids Res. *38*, 1441–1449.

Esa, M., and Tor, T. (2012). GSK3-TIP60-ULK1 Signaling Pathway. *8*.

Fabbri, M., Garzon, R., Cimmino, A., Liu, Z., Zanesi, N., Callegari, E., Liu, S., Alder, H., Costinean, S., Fernandez-Cymering, C., et al. (2007). MicroRNA-29 family reverts aberrant methylation in lung cancer by targeting DNA methyltransferases 3A and 3B. Proc. Natl. Acad. Sci. *104*, 15805–15810.

Fischle, W., Wang, Y., and Allis, C.D. (2003). Histone and chromatin cross-talk. Curr. Opin. Cell Biol. *15*, 172–183.

Fukuda, A., Nakadai, T., Shimada, M., Tsukui, T., Matsumoto, M., Nogi, Y., Meisterernst, M., and Hisatake, K. (2004). Transcriptional coactivator PC4 stimulates promoter escape and facilitates transcriptional synergy by GAL4-VP16. Mol. Cell. Biol. *24*, 6525–6535.

Füllgrabe, J., Klionsky, D.J., and Joseph, B. (2014). The return of the nucleus: Transcriptional and epigenetic control of autophagy. Nat. Rev. Mol. Cell Biol. *15*, 65–74.

Galluzzi, L., Pietrocola, F., Bravo-San Pedro, J.M., Amaravadi, R.K., Baehrecke, E.H., Cecconi, F., Codogno, P., Debnath, J., Gewirtz, D.A., Karantza, V., et al. (2015). Autophagy in malignant transformation and cancer progression. EMBO J. *34*, 856–880.

Garavís, M., and Calvo, O. (2017). Sub1/PC4, a multifaceted factor: from transcription to genome stability. Curr. Genet. *63*, 1023–1035.

Garcia, S.N., and Pereira-Smith, O. (2008). MRGing chromatin dynamics and cellular senescence. Cell Biochem. Biophys. *50*, 133–141.

Ge, H., and Roeder, R.G. (1994). Purification, cloning, and characterization of a human coactivator, PC4, that mediates transcriptional activation of class II genes. Cell *78*, 513–523.

Ge, H., Zhao, Y., Chait, B.T., and Roeder, R.G. (1994). Phosphorylation negatively regulates the function of coactivator PC4. Proc. Natl. Acad. Sci. U. S. A. *91*, 12691–12695.

Gerlitz, G. (2010). HMGNs, DNA repair and cancer. Biochim. Biophys. Acta - Gene Regul. Mech. *1799*, 80–85.

Gonzalez-Sandoval, A., and Gasser, S.M. (2016). On TADs and LADs: Spatial Control Over Gene Expression. Trends Genet. *32*, 485–495.

Green, D.R., and Levine, B. (2014). To be or not to be? How selective autophagy and cell death govern cell fate. Cell *157*, 65–75.

Green, A.R., Caracappa, D., Benhasouna, A.A., Alshareeda, A., Nolan, C.C., Macmillan, R.D., Madhusudan, S., Ellis, I.O., and Rakha, E.A. (2015). Biological and clinical significance of PARP1 protein expression in breast cancer. Breast Cancer Res. Treat. *149*, 353–362.

Guan, H., Dai, Z., Ma, Y., Wang, Z., Liu, X., and Wang, X. (2016). MicroRNA-101 inhibits cell proliferation and induces apoptosis by targeting EYA1 in breast cancer. Int. J. Mol. Med.

37, 1643–1651.

Hartman, A.R., and Ford, J.M. (2003). BRCA1 and p53: Compensatory roles in DNA repair. J. Mol. Med. *81*, 700–707.

Hauer, M.H., and Gasser, S.M. (2017). Chromatin and nucleosome dynamics in DNA damage and repair. Genes Dev. *31*, 2204–2221.

He, C., and Levine, B. (2010). The Beclin 1 interactome. Curr. Opin. Cell Biol. *22*, 140–149.

Hoare, M., Young, A.R.J., and Narita, M. (2011). Autophagy in cancer: Having your cake and eating it. Semin. Cancer Biol. *21*, 397–404.

Hoffelder, D., Luo, L., Burke, N., Watkins, S., Gollin, S., and Saunders, W. (2004). Resolution of anaphase bridges in cancer cells. Chromosoma *112*, 389–397.

Holland, K.A. (2002). Chromosomes: Nonhistone Proteins. Encycl. Life Sci. 1–9.

Hu, L., Wang, H., Huang, L., Zhao, Y., and Wang, J. (2016). Crosstalk between autophagy and intracellular radiation response (Review). Int. J. Oncol. *49*, 2217–2226.

Huang, T., Kim, C.K., Alvarez, A.A., Pangeni, R.P., Wan, X., Song, X., Shi, T., Yang, Y., Sastry, N., Horbinski, C.M., et al. (2017). MST4 Phosphorylation of ATG4B Regulates Autophagic Activity, Tumorigenicity, and Radioresistance in Glioblastoma. Cancer Cell *32*, 840–855.e8.

Ikura, T., Ogryzko, V. V, Grigoriev, M., Groisman, R., Wang, J., Horikoshi, M., Scully, R., Qin, J., and Nakatani, Y. (2000). Involvement of the TIP60 Histone Acetylase Complex in DNA Repair and Apoptosis. Cell *102*, 463–473.

Ikura, T., Tashiro, S., Kakino, A., Shima, H., Jacob, N., Amunugama, R., Yoder, K., Izumi, S., Kuraoka, I., Tanaka, K., et al. (2007). DNA Damage-Dependent Acetylation and Ubiquitination of H2AX Enhances Chromatin Dynamics. Mol. Cell. Biol. *27*, 7028–7040.

Izzo, A., and Schneider, R. (2016). H1 gets the genome in shape. Genome Biol. 16–18.

Kannan, P., and Tainsky, M. a (1999). Coactivator PC4 mediates AP-2 transcriptional activity and suppresses ras-induced transformation dependent on AP-2 transcriptional interference. Mol. Cell. Biol. *19*, 899–908.

Karantza-Wadsworth, V., Patel, S., Kravchuk, O., Chen, G., Mathew, R., Jin, S., and White,

E. (2007). Autophagy mitigates metabolic stress and genome damage in mammary tumorigenesis. Genes Dev. *21*, 1621–1635.

Khan, S.N., and Khan, A.U. (2010). Role of histone acetylation in cell physiology and diseases: An update. Clin. Chim. Acta *411*, 1401–1411.

Kim, J.M., Kim, K., Schmidt, T., Punj, V., Tucker, H., Rice, J.C., Ulmer, T.S., and An, W. (2015). Cooperation between SMYD3 and PC4 drives a distinct transcriptional program in cancer cells. Nucleic Acids Res. *43*, 8868–8883.

King, M.-C. (2003). Breast and Ovarian Cancer Risks Due to Inherited Mutations in BRCA1 and BRCA2. Science (80-.). *302*, 643–646.

Klevos, G.A., Ezuddin, N.S., Vinyard, A., Ghaddar, T., Gort, T., Almuna, A., Abisch, A., and Welsh, C.F. (2017). A Breast Cancer Review: Through the Eyes of the Doctor, Nurse, and Patient. J. Radiol. Nurs. *36*, 158–165.

Klopf, E., Paskova, L., Sole, C., Mas, G., Petryshyn, A., Posas, F., Wintersberger, U., Ammerer, G., and Schuller, C. (2009). Cooperation between the INO80 Complex and Histone Chaperones Determines Adaptation of Stress Gene Transcription in the Yeast Saccharomyces cerevisiae. Mol. Cell. Biol. *29*, 4994–5007.

Kretzschmar, M., Kaiser, K., Lottspeich, F., and Meisterernst, M. (1994). A novel mediator of class II gene transcription with homology to viral immediate-early transcriptional regulators. Cell *78*, 525–534.

Kriegel, A.J., Liu, Y., Fang, Y., Ding, X., and Liang, M. (2012). The miR-29 family: genomics, cell biology, and relevance to renal and cardiovascular injury. Physiol. Genomics *44*, 237–244.

Kuma, A., Hatano, M., Matsui, M., Yamamoto, A., Nakaya, H., Yoshimori, T., Ohsumi, Y., Tokuhisa, T., and Mizushima, N. (2004). The role of autophagy during the early neonatal starvation period. Nature *432*, 1032–1036.

Kumar, B.R.P., Swaminathan, V., Banerjee, S., and Kundu, T.K. (2001). p300-mediated Acetylation of Human Transcriptional Coactivator PC4 Is Inhibited by Phosphorylation. J. Biol. Chem. *276*, 16804–16809.

Larsen, K.B., Lamark, T., ??vervatn, A., Harneshaug, I., Johansen, T., and Bj??rk??y, G.

(2010). A reporter cell system to monitor autophagy based on p62/SQSTM1. Autophagy *6*, 784–793.

Lazarou, M., Sliter, D.A., Kane, L.A., Sarraf, S.A., Wang, C., Burman, J.L., Sideris, D.P., Fogel, A.I., and Youle, R.J. (2015). The ubiquitin kinase PINK1 recruits autophagy receptors to induce mitophagy. Nature *524*, 309–314.

Lee, Y.-H., and Ann, D.K. (2015). Bi-phasic expression of Heterochromatin Protein 1 (HP1) during breast cancer progression: Potential roles of HP1 and chromatin structure in tumorigenesis. J. Nat. Sci. *1*, e127.

Levine, B., and Abrams, J. (2008). p53: The Janus of autophagy? Nat. Cell Biol. *10*, 637–639.

Li, N. (2010). Critical Role of Transcription Cofactor PC4 in Mammals.

Li, G., and Reinberg, D. (2011). Chromatin higher-order structures and gene regulation. Curr. Opin. Genet. Dev. *21*, 175–186.

Li, X., Xu, H., Liu, Y., An, N., Zhao, S., and Bao, J. (2013). Autophagy modulation as a target for anticancer drug discovery. Acta Pharmacol. Sin. *34*, 612–624.

LIANG, C., and yang, yongfei (2014). MicroRNAs : An Emerging Player In Autophagy. Sci. Res.

Liao, M., Zhang, Y., Kang, J.H., and Dufau, M.L. (2011). Coactivator function of Positive Cofactor 4 (PC4) in Sp1-directed Luteinizing Hormone Receptor (LHR) gene transcription. J. Biol. Chem. *286*, 7681–7691.

Lu, X., Wang, L., Yu, C., Yu, D., and Yu, G. (2015). Histone Acetylation Modifiers in the Pathogenesis of Alzheimerâ€™s Disease. Front. Cell. Neurosci. *9*, 623–644.

Ma, Y., Kanakousaki, K., and Buttitta, L. (2015). How the cell cycle impacts chromatin architecture and influences cell fate. Front. Genet. *5*, 1–18.

Maresca, T.J., Freedman, B.S., and Heald, R. (2005). Histone H1 is essential for mitotic chromosome architecture and segregation in Xenopus laevis egg extracts. J. Cell Biol. *169*, 859–869.

Mas, G., De Nadal, E., Dechant, R., De La Concepción, M.L.R., Logie, C., Jimeno-

González, S., Chávez, S., Ammerer, G., and Posas, F. (2009). Recruitment of a chromatin remodelling complex by the Hog1 MAP kinase to stress genes. EMBO J. *28*, 326–336.

Masumoto, H., Hawke, D., Kobayashi, R., and Verreault, A. (2005). A role for cell-cycle-regulated histone H3 lysine 56 acetylation in the DNA damage response. Nature *436*, 294–298.

Maycotte, P. (2014). Targeting autophagy in breast cancer. World J. Clin. Oncol. *5*, 224.

Meisterernst, M., Roy, a L., Lieu, H.M., and Roeder, R.G. (1991). Activation of class II gene transcription by regulatory factors is potentiated by a novel activity. Cell *66*, 981–993.

Mischo, H.E., Hemmerich, P., Grosse, F., and Zhang, S. (2005). Actinomycin D induces histone ??-H2AX foci and complex formation of ??-H2AX with Ku70 and nuclear DNA helicase II. J. Biol. Chem. *280*, 9586–9594.

Mizushima, N., Levine, B., Cuervo, A.M., and Klionsky, D.J. (2008). Autophagy fights disease through cellular self-digestion. Nature *451*, 1069–1075.

Mortusewicz, O., Roth, W., Li, N., Cardoso, M.C., Meisterernst, M., and Leonhardt, H. (2008). Recruitment of RNA polymerase II cofactor PC4 to DNA damage sites. J. Cell Biol. *183*, 769–776.

Mortusewicz, O., Evers, B., and Helleday, T. (2016). PC4 promotes genome stability and DNA repair through binding of ssDNA at DNA damage sites. Oncogene *35*, 761–770.

Murrow, L., and Debnath, J. (2013). Autophagy as a Stress-Response and Quality-Control Mechanism: Implications for Cell Injury and Human Disease. Annu. Rev. Pathol. Mech. Dis. *8*, 105–137.

De Nadal, E., Zapater, M., Alepuz, P.M., Sumoy, L., Mas, G., and Posas, F. (2004). The MAPK Hog1 recruits Rpd3 histone deacetylase to activate osmoresponsive genes. Nature *427*, 370–374.

Nair, N., Shoaib, M., and Sørensen, C.S. (2017). Chromatin dynamics in genome stability: Roles in suppressing endogenous DNA damage and facilitating DNA repair. Int. J. Mol. Sci. *18*, 1–21.

Polyak, K. (2007). Science in medicine Breast cancer : origins and evolution. Cell *117*,

3155–3163.

Qin, L., Wang, Z., Tao, L., and Wang, Y. (2010). ER stress negatively regulates AKT/TSC/mTOR pathway to enhance autophagy. Autophagy *6*, 239–247.

Reddy, K.B. (2015). MicroRNA (miRNA) in cancer. Cancer Cell Int. *15*, 4–9.

Rock, Kenneth L; Kono, H. (2008). The Inflammatory Response to Cell Death. Annu. Rev. Pathol. Dis. *3*, 67–97.

Sapountzi, V., Logan, I.R., and Robson, C.N. (2006). Cellular functions of TIP60. Int. J. Biochem. Cell Biol. *38*, 1496–1509.

Schneider, R., and Grosschedl, R. (2007). Dynamics and interplay of nuclear architecture , genome organization , and gene expression. 3027–3043.

Sharma, S., Kelly, T.K., and Jones, P.A. (2009). Epigenetics in cancer. Carcinogenesis *31*, 27–36.

Shin, H.J.R., Kim, H., Oh, S., Lee, J.G., Kee, M., Ko, H.J., Kweon, M.N., Won, K.J., and Baek, S.H. (2016). AMPK-SKP2-CARM1 signalling cascade in transcriptional regulation of autophagy. Nature *534*, 553–557.

Shivaswamy, S., and Iyer, V.R. (2008). Stress-Dependent Dynamics of Global Chromatin Remodeling in Yeast: Dual Role for SWI/SNF in the Heat Shock Stress Response. Mol. Cell. Biol. *28*, 2221–2234.

Smith, K.T., and Workman, J.L. (2012). Chromatin proteins: Key responders to stress. PLoS Biol. *10*, 7.

Squatrito, M., Gorrini, C., and Amati, B. (2006). Tip60 in DNA damage response and growth control: many tricks in one HAT. Trends Cell Biol. *16*, 433–442.

Stingl, J., and Caldas, C. (2007). Molecular heterogeneity of breast carcinomas and the cancer stem cell hypothesis. Nat. Rev. Cancer *7*, 791.

Struhl, K. (1998). Histone acetylation and transcriptional regulatory mechanisms. Genes Dev. *12*, 599–606.

Sun, Y., Jiang, X., Xu, Y., Ayrapetov, M.K., Moreau, L.A., Whetstine, J.R., and Price, B.D. (2009). Histone H3 methylation links DNA damage detection to activation of the tumour

suppressor Tip60. Nat. Cell Biol. *11*, 1376–1382.

Surjana, D., Halliday, G.M., and Damian, D.L. (2010). Role of Nicotinamide in DNA Damage, Mutagenesis, and DNA Repair. J. Nucleic Acids *2010*, 1–13.

Swaminathan, A., Delage, H., Chatterjee, S., Belgarbi-Dutron, L., Cassel, R., Martinez, N., Cosquer, B., Kumari, S., Mongelard, F., Lannes, B., et al. (2016). Transcriptional coactivator and chromatin protein PC4 is involved in hippocampal neurogenesis and spatial memory extinction. J. Biol. Chem. *291*, 20303–20314.

Talbert, P.B., and Henikoff, S. (2010). Histone variants ancient wrap artists of the epigenome. Nat. Rev. Mol. Cell Biol. *11*, 264–275.

Talbert, P.B., and Henikoff, S. (2017). Histone variants on the move: Substrates for chromatin dynamics. Nat. Rev. Mol. Cell Biol. *18*, 115–126.

Tanida, I., Ueno, T., and Kominami, E. (2004). LC3 conjugation system in mammalian autophagy. Int. J. Biochem. Cell Biol. *36*, 2503–2518.

Tao, S., Yu, J., Xu, Y., Deng, B., Sun, T., Hu, P., Wei, Z., Zhang, J., Wang, R., Shi, C., et al. (2015). PC4 induces lymphangiogenesis dependent VEGF-C/VEGF-D/VEGFR-3 axis activation in lung adenocarcinoma. Am. J. Cancer Res. *5*, 1878–1889.

Tsukada, M., and Ohsumi, Y. (1993). Isofation and characterization of autophagy-defective mutants of Saccharomyces cerevisiae. FEBS Lett. *333*, 169–174.

ur Rehman Kayani, M., Kayani, M.A., Malik, F.A., and Rani, F. (2011). Role of miRNAs in breast cancer. Asian Pacific J. Cancer Prev. *12*, 3175–3180.

Vessoni, A.T., Filippi-Chiela, E.C., Menck, C.F.M., and Lenz, G. (2013). Autophagy and genomic integrity. Cell Death Differ. *20*, 1444–1454.

Wang, Z., and Roeder, R.G. (1998). DNA topoisomerase I and PC4 can interact with human TFIIIC to promote both accurate termination and transcription reinitiation by RNA polymerase III. Mol. Cell *1*, 749–757.

Wang, C., Bian, Z., Wei, D., and Zhang, J. (2011). miR-29b regulates migration of human breast cancer cells. Mol. Cell. Biochem. *352*, 197–207.

Wang, J., Sarker, A.H., Cooper, P.K., and Volkert, M.R. (2004). The Single-Strand DNA

Binding Activity of Human PC4 Prevents Mutagenesis and Killing by Oxidative DNA Damage The Single-Strand DNA Binding Activity of Human PC4 Prevents Mutagenesis and Killing by Oxidative DNA Damage. *24*, 6084–6093.

Wei, F.Z., Cao, Z., Wang, X., Wang, H., Cai, M.Y., Li, T., Hattori, N., Wang, D., Du, Y., Song, B., et al. (2015). Epigenetic regulation of autophagy by the methyltransferase EZH2 through an MTOR-dependent pathway. Autophagy *11*, 2309–2322.

Werten, S., Stelzer, G., Goppelt, A., Langen, F.M., Gros, P., Timmers, H.T.M., Van Der Vliet, P.C., and Meisterernst, M. (1998). Interaction of PC4 with melted DNA inhibits transcription. EMBO J. *17*, 5103–5111.

Wright, R.H.G., Fernandez-Fuentes, N., Oliva, B., and Beato, M. (2016). Insight into the machinery that oils chromatin dynamics. Nucleus *7*, 532–539.

Yan, B., Guo, Q., Fu, F.J., Wang, Z., Yin, Z., Wei, Y.B., and Yang, J.R. (2015). The role of miR-29b in cancer: Regulation, function, and signaling. Onco. Targets. Ther. *8*, 539–548.

Yang, Z., and Klionsky, D.J. (2010). Mammalian autophagy: Core molecular machinery and signaling regulation. Curr. Opin. Cell Biol. *22*, 124–131.

You, L., Wang, Z., Li, H., Shou, J., Jing, Z., Xie, J., Sui, X., Pan, H., and Han, W. (2015). The role of STAT3 in autophagy. Autophagy *11*, 729–739.

Zhong, S., Li, W., Chen, Z., Xu, J., and Zhao, J. (2013). MiR-222 and miR-29a contribute to the drug-resistance of breast cancer cells. Gene *531*, 8–14.

Zhou, J., Zhang, W., Liang, B., Casimiro, M.C., Whitaker-Menezes, D., Wang, M., Lisanti, M.P., Lanza-Jacoby, S., Pestell, R.G., and Wang, C. (2009). PPAR-gamma activation induces autophagy in breast cancer cells. Int. J. Biochem. Cell Biol. *41*, 2334–2342.